APOE4 AFFECTS BASAL AND NMDAR MEDIATED PROTEIN SYNTHESIS IN NEURONS BY PERTURBING CALCIUM HOMEOSTASIS

A THESIS TO BE SUBMITTED TO

THE UNIVERSITY OF TRANS-DISCIPLINARY HEALTH SCIENCES AND TECHNOLOGY

FOR THE AWARD OF THE DEGREE OF

DOCTOR OF PHILOSOPHY

BY

SARAYU RAMAKRISHNA

UNDER THE GUIDANCE OF

DR. RAVI MUDDASHETTY

INSTITUTE FOR STEM CELL SCIENCE AND REGENERATIVE MEDICINE

GKVK POST, BELLARY ROAD, BENGALURU - 560065

JANUARY 2022

THE UNIVERSITY OF TRANS-DISCIPLINARY HEALTH SCIENCES AND TECHNOLOGY

Private University Established in Karnataka by ACT 35 of 2013

BENGALURU - 560064

DECLARATION BY THE CANDIDATE

I declare that this thesis entitled "**APOE4 affects basal and NMDAR mediated protein synthesis in neurons by perturbing calcium homeostasis**" submitted for the award of Doctor of Philosophy to THE UNIVERSITY OF TRANS-DISCIPLINARY HEALTH SCIENCES AND TECHNOLOGY, Bengaluru, is my original work, conducted under the supervision of my guide **Dr. Ravi Muddashetty** (and co-guide, **Dr. Dasaradhi Palakodeti**). I also wish to inform that no part of the research has been submitted for a degree or examination at any university. References, help and material obtained from other sources have been duly acknowledged

I hereby confirm the originality of the work and that there is no plagiarism in any part of the dissertation.

Sarayu R.

Place: Bengaluru **Signature of the Candidate**

Date: 05/01/2022

Name of candidate: Sarayu Ramakrishna

Reg. No: 21116030164

Month and Year of Admission: September 2018

THE UNIVERSITY OF TRANS-DISCIPLINARY HEALTH SCIENCES AND TECHNOLOGY

Private University Established in Karnataka by ACT 35 of 2013

BENGALURU - 560064

CERTIFICATE

This is to certify that the work incorporated in this thesis "**APOE4 affects basal and NMDAR mediated protein synthesis in neurons by perturbing calcium homeostasis**" submitted by **Sarayu Ramakrishna** was carried out under my supervision. No part of this thesis has been submitted for a degree or examination at any university. References, help and material obtained from other sources have been duly acknowledged. I hereby confirm the originality of the work and that there is no plagiarism in any part of the dissertation.

Research Supervisor

Date: 05/01/2022

Name, designation & address details: Dr. Ravi Muddashetty, Senior Fellow, Institute for Stem Cell Science and Regenerative Medicine, GKVK-Post, Bellary Road, Bengaluru - 560065

THE UNIVERSITY OF TRANS-DISCIPLINARY HEALTH SCIENCES AND TECHNOLOGY

Private University Established in Karnataka by ACT 35 of 2013

BENGALURU - 560064

CERTIFICATE

This is to certify that the work incorporated in this thesis "**APOE4 affects basal and NMDAR mediated protein synthesis in neurons by perturbing calcium homeostasis**" submitted by **Sarayu Ramakrishna** was carried out under my supervision. No part of this thesis has been submitted for a degree or examination at any university. References, help and material obtained from other sources have been duly acknowledged. I hereby confirm the originality of the work and that there is no plagiarism in any part of the dissertation.

Co-Supervisor

Date: 05/01/2022

Name, designation & address details: Dr. Dasaradhi Palakodeti, Associate Professor, Institute for Stem Cell Science and Regenerative Medicine, GKVK-Post, Bellary Road, Bengaluru - 560065

Plagiarism check report

Curiginal

Document Information

Analyzed document	Sarayu PhD thesis plagiarism check.docx (D123900863)
Submitted	2022-01-03T10:00:00.0000000
Submitted by	Giridharan R
Submitter email	registrar@tdu.edu.in
Similarity	6%
Analysis address	registrar.tdu@analysis.urkund.com

Sources included in the report

SA	**Thesis kappa + unpublished manuscripts_final_plagiarism check.pdf** Document Thesis kappa + unpublished manuscripts_final_plagiarism check.pdf (D121916559)	2
W	URL: https://www.pnas.org/content/103/15/5644 Fetched: 2021-12-02T20:17:54.9200000	1
W	URL: https://www.biorxiv.org/lookup/content/full/2020.12.10.418772v1 Fetched: 2022-01-03T10:00:47.6030000	8
W	URL: https://www.ncbi.nlm.nih.gov/pmc/articles/PMC4870502/ Fetched: 2022-01-03T10:01:21.6430000	1
W	URL: https://www.biorxiv.org/content/biorxiv/early/2020/12/16/2020.12.10.418772/DC1/embed/media-1.pdf?download=true Fetched: 2021-12-10T16:05:33.2330000	57
W	URL: https://portal.research.lu.se/en/publications/apoe4-affects-basal-and-nmdar-mediated-protein-synthesis-in-neurons-by-perturbing-calcium-homeostasis(95ee4ee8-380b-4af7-87a8-c1f3fd48acd8).html Fetched: 2022-01-03T10:01:12.5130000	1

Acknowledgements

My thesis would not have been possible without the support of many people. Firstly, I extend my gratitude to my PhD mentor Dr. Ravi Muddashetty. Along with being a supportive mentor, he has been a great friend and confidant. The thing I relish the most is the countless long, fun and intriguing discussions we had during the course of this work; it really kept my spirits high even during the toughest times. It made me realize science is as much about discussing numerous, sometimes even crazy possibilities and ideas, as it is about the experiments, analysis and interpretations. We had so many discussions especially with respect to calcium, it would go on for hours sometimes. And, at the end of it, we would feel more elated and refreshed, never exhausted. I had the most exciting time performing experiments for testing our wild calcium hypothesis which never made it to this thesis or the paper. Yet, we learnt so much, and more importantly I truly felt like the curious young scientist who had the freedom to experiment. I found a new meaning for the line by Polonius in Hamlet "Though this be madness, yet there is method in it". I cannot thank him enough for giving me this freedom. He taught me how to enjoy and cherish the process of doing science. I really hope to take forward his enthusiasm towards science, his rationality and his professional yet compassionate attitude towards his students.

I sincerely thank my thesis committee members Dr. Dasaradhi Palakodeti and Dr. Ravi Majithaya. Their suggestions and perspectives opened new thinking arenas for me and helped in directing my work towards what it is now. I extend my deepest thanks to our collaborators Dr. Kristine Freude, Dr. Gunnar Gouras and Dr. Poul Hyttel. I had the wonderful opportunity to spend couple of months in Dr. Kristine Freude's lab where I learnt neuronal and astrocyte differentiation of stem cells. Dr. Kristine was closely and constantly involved with the progress of this work, and has remained ever-encouraging professionally and personally. Specially, I thank Dr. Tina Christoffersen and Dr. Abhinaya Chandrashekar from Dr. Kristine's lab for their support and guidance during my visit to Copenhagen. Dr. Gunnar agreed to collaborate with us at the right time to validate our results with APOE astrocyte conditioned media which strengthened our work immensely. He was involved in helping me and guiding me throughout the progress of this work. I specially thank him for doing one of the most thorough reviews and editing of the manuscript. I also extend my gratitude to the other collaborators with whom I worked closely, learnt many things which broadened my outlook towards research – Dr. Deepak Nair, Dr. Akash Gulyani, Dr. Odity Mukherjee, Henriette Haukedal and Shekhar Kedia.

There are many people who contributed in different ways to the completion of this work. I sincerely thank Dr. Vijayalakshmi Nalavadi under whom I did my internship project. She is the one who taught the basics of how to go about reading papers, how to present papers, how to design experiments, how to hold a pipette, how to do cell culture, the importance of statistics, how to write a thesis; basically, every skill necessary for research. It would be impossible to finish this work without the foundation she gave me. Another person who provided me this foundation was Dr. Maki Murata Hori. She

taught me everything about stem cell culture, the technique which is the most critical and important one in my entire thesis. I also thank the teachers of all my course work, they all have influenced me in their own ways, they all have made my fundamentals stronger.

No number of words are sufficient to express my gratitude and love for my lab mates. I was lucky to have one of the most enriching lab environments where each one was co-operative and helpful, yet constructively critical which improved the quality of my work tremendously. I have learnt many things from each one of them and they contributed the most towards my development, as a researcher and as a person. I thank every lab mate, present and past – Preeti, Vishal, Sreenath, Sudhriti, Bharti, Michelle, Naveen, Vishwaja, Bindu, Sukanya, Sumita, Subhajit, Reena, Abhik and Nisa. Apart from work, we had some of the best times during our discussions over tea and lunch (literally about everything on this planet), movie nights, cooking sessions, parties, trips, eat outs and the list just goes on. The time I spent with them will be the best memories I will cherish always. I am also thankful to the wonderful opportunity I had to work with several trainees – Samantha, Sasha and Sandhya. Fortunately, due to the open lab system at inStem, I also got to closely interact with many members from CBDR. I am thankful to them and all other colleagues at NCBS-inStem for their timely support with respect to chemicals, technical help, and cordiality.

The timely completion of this work would be impossible without the central facilities at NCBS-inStem – the Central Imaging and Flow Cytometry (CIFF), Stem Cell Facility and Animal House. Along with catering to our research needs, each of the facility ensured that they trained us to be independent users. The training sessions were intense and now I can't be grateful enough for the skill and knowledge they have built in us. I thank each and every staff member of the facilities along with the members of canteen, lab kitchen, instrumentation, lab support, purchase, stores, securities, civil and electrical departments. The smooth functioning of the lab and my work would be impossible without them. I am extremely thankful to the members of the administrative team, academic unit and accounts unit at NCBS-inStem. They helped me with the activation of my fellowship, PhD registration with the university, activation of travel allowances and every other logistic need. During my stay at inStem, I had the wonderful opportunity to work with the Covid testing facility. I am thankful for this opportunity as it made me feel like I was using the skills I had gathered over these years to truly help in the times of need. Apart from this, I learnt innumerable things with this experience – the value of time, patience and meticulousness. I thank my team leaders Dr. Varadha and Dr. Anandi and my team mates Ansil, Radhika and Pilot for being so reassuring even during the toughest lockdown period.

I acknowledge all the funding sources which have generously supported my work. I thank DBT for providing my PhD fellowship for five years (DBT/2016/InStem/540) and for supporting this work through the Indo-Danish NeuroStem Grant (BT/IN/Denmark/07/RSM/2015-2016). I had the opportunity to attend several national and international conferences during my PhD which have expanded my outlook towards research. This would not have been possible without the travel grants I got – two of them from DMM (CTG-DMM2108532, 2021 and CTG-DMM2005499, 2020) and the

Brain Prize 2021 from FENS, IBRO-PERC. I also thank TDU for my PhD registration which made the completion of this work possible. I specially acknowledge Mr. Ravi Kumar, the academic coordinator at TDU, for being the point of contact and helping me with all the formalities at TDU. I extend my sincere gratitude to in the BLiSC (Bangalore Life Science Cluster) campus. It truly has one of the best environments for research where everyone is encouraged to think freely and discuss openly. The hierarchy-free culture, the encouraging peer group, the state-of-the-art facilities and opportunities makes it an ideal place for researchers.

I thank all my friends without whom I could have not maintained my sanity. I specially thank Sneha K M, Sanjana B S and Michelle for being there for me always, through thick and thin, on days of significance and non-significance. I am also lucky to have a bunch of amazing friends in and out of campus – Prajwal, Yojet, Nanjundeshwara, Pravallika, Sheetal, Prakruthi, Sujith, Sumukh, Vandana. They made sure that I had my share of fun and protected my crazy stupid side.

Finally, I thank my entire family and my in-laws for supporting me. I fail to express in words how fortunate and thankful I feel for the love, encouragement and motivation I get from my parents (Ramakrishna and Anuradha) and my brother (Saketh). My husband Shankar has been a pillar and a driving force for me throughout this journey. My parents, brother and husband have been the backbone for me, making sure I face no trouble, not only in this journey, but in every endeavor. This thesis would be impossible without their care and love, I dedicate it to them.

Table of Contents

List of Tables

Chapter 2

List of Figures

Chapter 1

Chapter 3

Chapter 4

Synopsis

Introduction *(Chapter 1 of the thesis)*

Alzheimer's disease (AD), the most common cause of dementia, is an irreversible progressive neurodegenerative disorder that leads to loss of memory and cognition (Hardy, 2006). Pathologically, AD is characterized by brain atrophy along with an accumulation of Aβ plaques and neurofibrillary tangles (Hardy, 2006). But the most robust correlation for the severity of dementia and staging of AD is with the extent of synapse loss (Shankar & Walsh, 2009). More than 90% of AD cases are sporadic with no known familial mutations in APP or PSEN genes (Tanzi, 2012). Beyond the familial mutations, many genetic factors significantly increase the risk of AD(Tanzi, 2012). Apolipoprotein isoform ε4 (APOE4) is the most well-established genetic risk factor which increases the frequency of AD occurrence and decreases the age of onset significantly (Kim et al., 2009; C. C. Liu et al., 2013). APOE has three major isoforms in humans - ε2 (APOE2), ε3 (APOE3) and ε4 (APOE4). But among them, only APOE4 is shown to increase the predisposition to AD by affecting the clearance of Aβ (Kim et al., 2009; C. C. Liu et al., 2013). However, many studies have reported that the presence of the APOE4 allele can cause synaptic defects independently. Reduction of neurite outgrowth, dendritic complexity, spine density, and loss of synaptic proteins is well reported in APOE4 mice models (Dumanis et al., 2009; Nathan et al., 1994; Rodriguez et al., 2013; Teter et al., 2002; Yong et al., 2014). Consequently, APOE4 mice of both younger and older age groups are reported to show defects in spatial learning and memory(Rodriguez et al., 2013). This supports the idea that APOE4 could have an impact on cognitive processes from early in life. In support of this, many studies have drawn correlations between APOE genotype and cognition in humans as well (de Jager et al., 2012; Reas et al., 2019; Small et al., 2004; Wisdom et al., 2011). One of the known mechanisms for APOE4 mediated synaptic defects is the interference of APOE4 with glutamate receptor signaling pathways (Chen et al., 2010), especially downstream of NMDARs (Bacskai et al., 2000; Nakajima et al., 2013; Sheng et al., 2008). Thus, upon binding to its cognate receptor, APOE not only performs the classical function of lipid transport, but it is also known to influence multiple signaling pathways in an isoform dependent manner (Hoe et al., 2005; Huang et al., 2017, 2019).

It is now well established that synapse loss is an early feature and a structural correlate of AD which occurs pre-symptomatically (Shankar & Walsh, 2009). Synapses are the sites where neuronal activity is interpreted, making them the fundamental functional units of learning and memory. Various stimuli can cause changes in the synaptic function, ultimately bringing about structural changes like induction, pruning, enlargement or shrinkage of spines (Kelleher et al., 2004; Sutton & Schuman, 2006). The re-modeling and maintenance of these structural and functional changes of synapses require the synthesis of new proteins which are tightly regulated spatio-temporally (Kelleher et al., 2004; Sutton & Schuman, 2006). Thus, activity mediated synthesis of new proteins and changes in the proteome play an important role in driving synaptic plasticity (Kelleher et al., 2004; Sutton & Schuman, 2006; Suzanne Zukin et

al., 2009). Though APOE4 is indicated to be one of the key factors influencing synaptic loss and cognitive defects in AD, the molecular mechanisms behind this are still unclear. Considering the importance of protein synthesis in synaptic functioning and its relevance to the synaptic loss in AD, investigating translation regulation becomes an important aspect in the context of APOE4 mediated defects as well. Hence, we studied the effect of APOE4 on basal and synaptic activity mediated translation in neurons, and tried to investigate the mechanism behind protein synthesis dysfunction, if any.

Hypothesis

APOE4 impairs synaptic protein synthesis regulation in neurons, and thus causes synaptic dysfunction.

Objectives

1. To investigate the effect of APOE on global protein synthesis in neurons
2. To investigate the effect of APOE on synaptic activity mediated protein synthesis in neurons
3. To examine the mechanism underlying the APOE mediated protein synthesis response

Model System

Rat primary cortical neurons and rat cortical synaptoneurosomes were the two primary model systems used in the study. They were treated with APOE from different sources at different time points.

Materials and methods *(Chapter 2 of the thesis)*

The materials and methods used in the study are published in "APOE4 Affects Basal and NMDAR-Mediated Protein Synthesis in Neurons by Perturbing Calcium Homeostasis" published in Journal of Neuroscience, October 20, 2021. DOI - 10.1523/JNEUROSCI.0435-21.2021.

Results

The results of the study are divided into 5 main chapters in the thesis. The results section here will be discussed as per the same thesis chapters –

Sources of APOE *(Chapter 3 of the thesis)*

We used 2 primary sources of APOE to treat the neurons or synaptoneurosomes – conditioned media from stem cells and recombinant APOE protein. Isogenic human stem cell lines expressing APOE3 or APOE4 or APOE KO were characterized for the expression and secretion of APOE. The amount of APOE secreted by the stem cells was quantified using ELISA, and equal amounts of APOE was used to treat the neurons. The final APOE concentration used for the treatments was 10-15nM. Phosphorylation of ERK was used as a readout to validate the APOE treatment (Hoe et al., 2005; Huang et al., 2017, 2019). APOE4 conditioned media or recombinant protein treatment for 20 minutes caused a significant increase in the phosphorylation of ERK, both in primary

neurons and synaptoneurosomes, thus validating that our APOE treatment paradigm was functional.

Figure 1

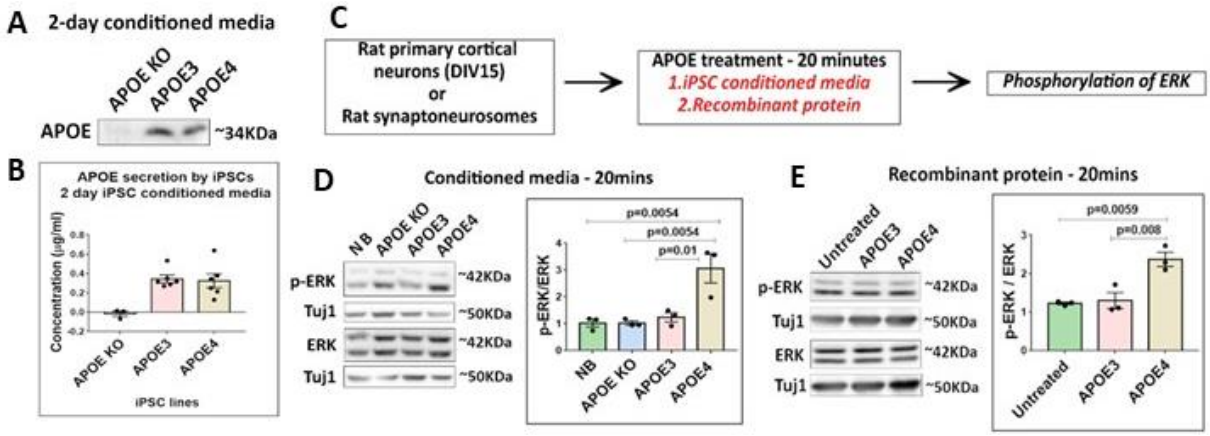

Figure 1 – Sources of APOE

A - Representative immunoblots showing the APOE secreted in 2-day iPSC conditioned media kept in culture conditions for 1 day.

B - The ELISA based measurements of the APOE concentrations in the 2-day iPSC conditioned media.

C – Experimental design for APOE treatment.

D – Representative immunoblots showing the levels of p-ERK, ERK and Tuj1 in rat primary cortical neurons after 20 minutes treatment with APOE conditioned media. The graph represents the ratio of p-ERK to ERK normalized to Tuj1 under different APOE conditions. Data is represented as mean +/- SEM. N=3, One-way ANOVA (p=0.0031) followed by Tukey's multiple comparison test.

E - Representative immunoblots showing the levels of p-ERK, ERK and Tuj1 in rat primary cortical neurons after 20 minutes treatment with APOE recombinant protein (10nM). The graph represents the ratio of p-ERK to ERK normalized to Tuj1 under different APOE conditions. Data is represented as mean +/- SEM. N=3, One-way ANOVA (p=0.0041) followed by Tukey's multiple comparison test.

Effect of APOE on regulation of protein synthesis *(Chapter 4 of the thesis)*

In order to investigate the effect of APOE on global protein synthesis, we used three different model systems – rat primary cortical neurons, rat synaptoneurosomes and human neurons derived from APOE KO iPSCs. The sources of APOE used were recombinant protein and stem cell conditioned media. The readouts used for global protein synthesis measurement were phosphorylation status of translation elongation factor eEF2 and FUNCAT (Fluorescent Non-Canonical Amino Acid Tagging). Increased phosphorylation of eEF2 reduces the translation elongation rates and hence inhibits global protein synthesis (Kaul et al., 2011). FUNCAT measures de-novo protein synthesis through incorporation of Methionine analog, and hence serves as a direct correlate for translation.

Interestingly, I observed that 1 minute treatment with both APOE3 and APOE4 caused a reduction of global protein synthesis. This was indicated by increased phosphorylation of eEF2 and decreased FUNCAT signal intensity. However, at 20-minute time point, only APOE4 caused an inhibition of global protein synthesis, whereas translation had recovered to basal levels in APOE3 treatment condition. The increased eEF2 phosphorylation (translation inhibition) caused by APOE4 at the 20-minute time point was validated in the all the three model systems mentioned. Further, we treated the neurons with APOE conditioned media for 1 minute, following which APOE was removed and recovery of 5mins, 10mins or 20mins was allowed. We observed that the recovery from the translation inhibition was significantly slower in case of APOE4 treatment, hence causing a longer and sustained increase in eEF2 phosphorylation. Additionally, APOE4 treatment for 20 minutes in the presence of APOE receptor antagonist RAP prevented the increased in eEF2 phosphorylation. Thus, we confirmed that the effect of APOE on translation was mediated through APOE receptors.

Figure 2

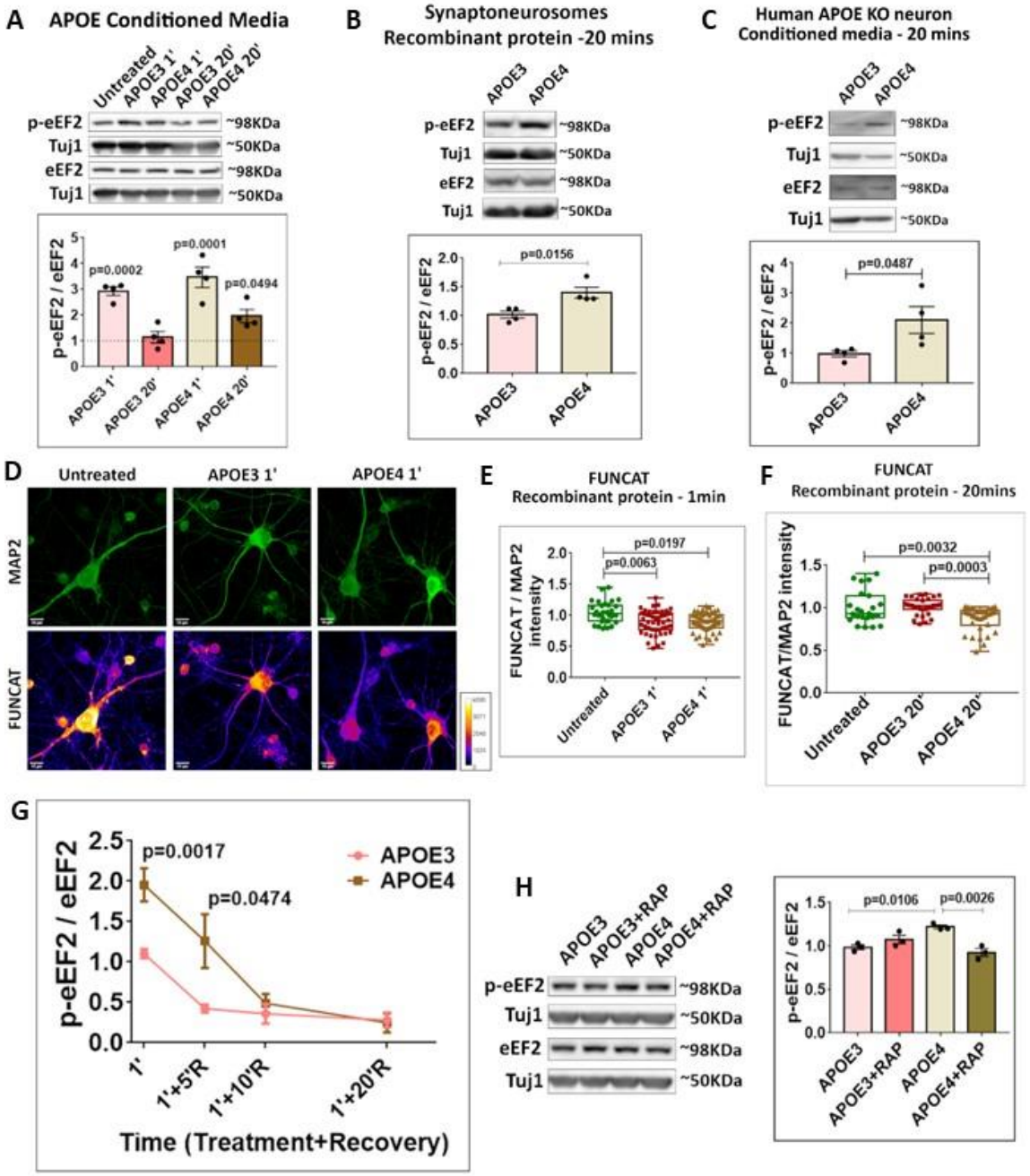

Figure 2 - Effect of APOE on regulation of protein synthesis

A - Representative immunoblots showing the levels of p-eEF2, eEF2 and Tuj1 in rat primary cortical neurons after 1 minute and 20 minutes treatment with APOE3 or APOE4 iPSC conditioned media. The graph represents the ratio of p-eEF2 to eEF2 normalized to Tuj1 under different APOE conditions. Data is represented as mean +/- SEM. Dotted line indicates the untreated condition. All the APOE treatments were normalized to untreated condition. N=4. One-way ANOVA ($p<0.0001$) followed by Dunnett's multiple comparison test.

B - Representative immunoblots showing the levels of p-eEF2, eEF2 and Tuj1 in rat cortical synaptoneurosomes after 20 minutes treatment with recombinant APOE protein. The graph represents the ratio of p-eEF2 to eEF2 normalized to Tuj1 under different APOE conditions. Data is represented as mean +/- SEM. N=4, Unpaired Student's t-test.

C – Representative immunoblots showing the levels of p-eEF2, eEF2 and Tuj1 in human APOE KO neurons after 20 minutes treatment with APOE3 or APOE4 iPSC conditioned media. The graph represents the ratio of p-eEF2 to eEF2 normalized to Tuj1 under different APOE conditions. Data is represented as mean +/- SEM. N=4, Unpaired Student's t-test.

D - The representative images for MAP2 and FUNCAT fluorescent signals in rat primary cortical neurons under untreated conditions or after 1 minute treatment with APOE3 / APOE4 recombinant protein (15nM) (Scale bar - 10µM).

E - The graph represents the quantification of the FUNCAT fluorescent intensity normalized to MAP2 fluorescent intensity under different APOE treatment conditions at 1-minute time point. N = 20-40 neurons from 4 independent experiments, One-way ANOVA ($p=0.0058$) followed by Tukey's multiple comparison test.

F - The graph represents the quantification of the FUNCAT fluorescent intensity normalized to MAP2 fluorescent intensity under different APOE treatment conditions at 20-minute time point. N = 20-40 neurons from 4 independent experiments, One-way ANOVA ($p=0.0001$) followed by Tukey's multiple comparison test.

G - The levels of p-eEF2, eEF2 and Tuj1 in rat primary cortical neurons after 1 minute treatment with APOE3 or APOE4 iPSC conditioned media followed by 5-minute, 10-minute and 20-minute recovery with pre-conditioned neurobasal media. The graph represents the ratio of p-eEF2 to eEF2 normalized to Tuj1 under different APOE conditions. The data from each recovery time point is normalized to its corresponding 1-minute APOE treated set. Data is represented as mean +/- SEM. For APOE3 1' and APOE4 1', N=8, Unpaired Student's t-test. For APOE 1' + 5'R, N=4, Unpaired Student's t-test. For APOE 1' + 10'R, N=5. For APOE 1' + 20'R, N=3.

H - Representative immunoblots showing the levels of p-eEF2, eEF2 and Tuj1 in rat primary cortical neurons after RAP pre-incubation (200nM) followed by 20 minutes treatment with APOE3 or APOE4 conditioned media. The graph represents the ratio of p-eEF2 to eEF2 normalized to Tuj1 under different APOE conditions. Data is represented as mean +/- SEM. N=5, One-way ANOVA ($p=0.003$) followed by Tukey's multiple comparison test.

Effect of APOE on NMDAR mediated translation response *(Chapter 5 of the thesis)*

In order to check the effect of APOE on activity mediated translation response, we chose stimulation of NMDA receptors as the activity paradigm. The reason for choosing NMDAR stimulation was that the interaction between NMDARs and APOE receptors

was previously reported, hence it is known that APOE mediated signaling influences the NMDAR mediated calcium influx and signaling pathways (Chen et al., 2010; D. S. Liu et al., 2015; Ohkubo et al., 2001; Qiu et al., 2003). The rat primary cortical neurons or synaptoneurosomes were treated with APOE for 20 minutes and stimulated with NMDA during the last 5 minutes. This was followed by the measurement of protein synthesis response using eEF2 phosphorylation and FUNCAT. The translation response of 5-minute NMDAR stimulation is well studied in our lab previously (Ghosh Dastidar et al., 2020; Kute et al., 2019). NMDAR stimulation for 5 minutes causes an increase in the phosphorylation of eEF2 and hence inhibition of global protein synthesis. In the background of the global translation inhibition, certain specific mRNAs like PTEN and PSD95 undergo translation upregulation (Kute et al., 2019). NMDAR stimulation in the APOE3 treated neurons and synaptoneurosomes showed a normal response – increased eEF2 phosphorylation, decreased FUNCAT signal, increased PTEN and PSD95 levels. However, in the background of APOE4 treatment, the neurons failed to elicit NMDAR mediated translation response. It is important to note that decreased FUNCAT signal and increased eEF2 phosphorylation, PTEN and PSD95 levels were observed with 20-minute APOE4 treatment alone, but NMDAR mediated increase was lost. Thus, the NMDA activity mediated protein synthesis response was perturbed by APOE4.

Intriguingly, the translation response with 20-minute APOE4 treatment seemed to resemble the translation response of 20-minute APOE3 treatment with 5-minute NMDAR stimulation. However, the puzzle was that the APOE4 treatment was for 20 minutes while the NMDAR stimulation was for 5 minutes. In order to make a better comparison of the translation profiles of APOE treatment and NMDAR stimulation, we performed NMDAR stimulation for 1-minute and 20 minutes (time points for which APOE translation response was established). We observed that 1-minute NMDAR stimulation caused an increase in eEF2 phosphorylation and global protein synthesis inhibition (decreased FUNCAT signal), similar to APOE3 and APOE4 treatment. However, 20-minute NMDAR stimulation caused a reduction of eEF2 phosphorylation and hence activation of global protein synthesis (increased FUNCAT signal). Thus, the 20-minute translation response was distinct for all 3 paradigms with NMDA causing reduction of eEF2 phosphorylation (translation upregulation), APOE3 causing no change in eEF2 phosphorylation (no change in translation) and APOE4 causing increased eEF2 phosphorylation (translation downregulation). Hence, we were able to establish the distinct temporal profiles of protein synthesis on NMDAR stimulation and APOE treatment.

Figure 3

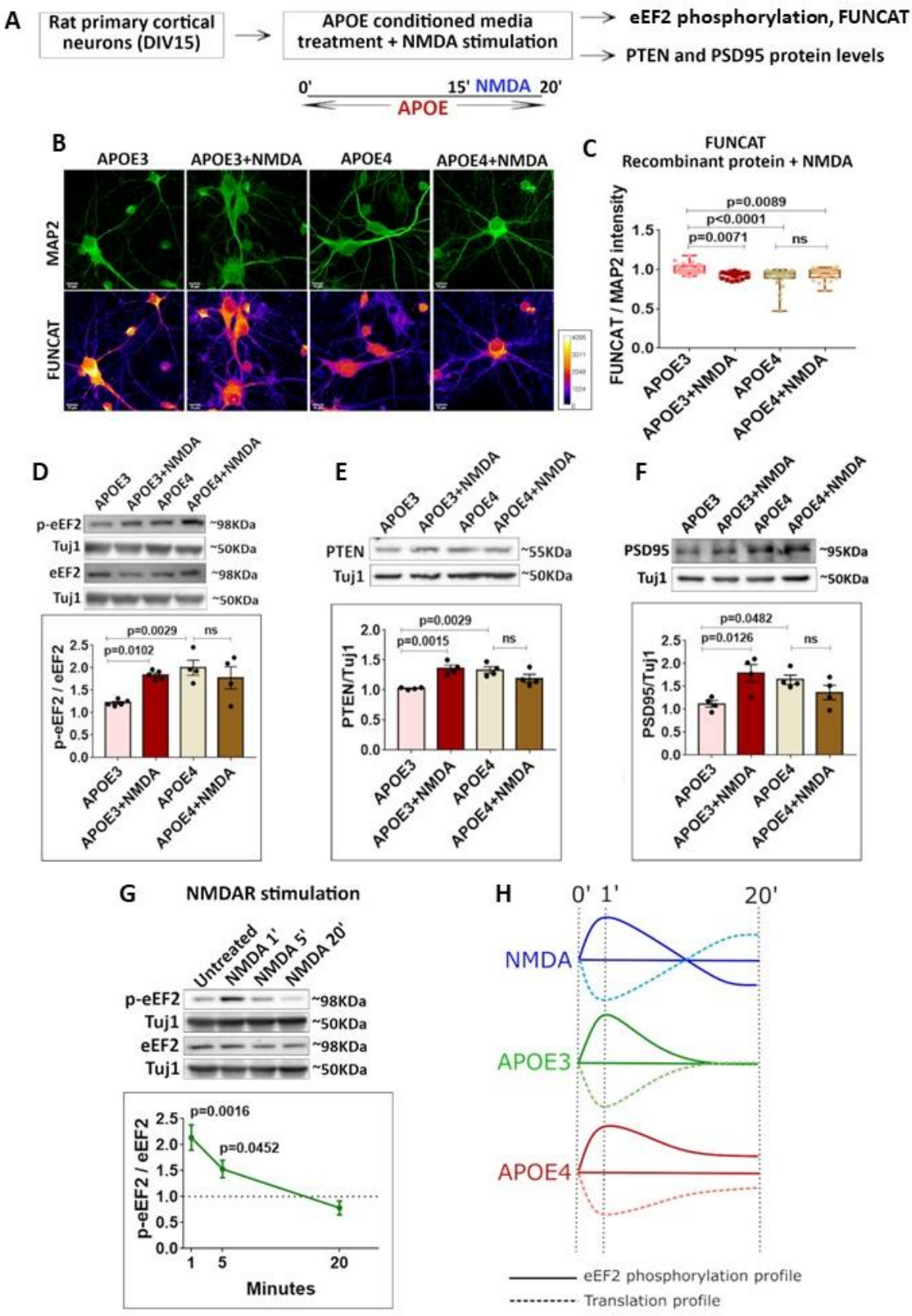
A
Rat primary cortical neurons (DIV15)
APOE conditioned media treatment + NMDA stimulation
eEF2 phosphorylation, FUNCAT
PTEN and PSD95 protein levels
0'
15' NMDA 20'
APOE
B
APOE3
APOE3+NMDA
APOE4
APOE4+NMDA
MAP2
FUNCAT
C
FUNCAT
Recombinant protein + NMDA
FUNCAT / MAP2 intensity
p=0.0089
p<0.0001
p=0.0071
ns
D
p-eEF2
Tuj1
eEF2
Tuj1
~98KDa
~50KDa
~98KDa
~50KDa
p-eEF2 / eEF2
p=0.0029
ns
p=0.0102
E
PTEN
Tuj1
~55KDa
~50KDa
PTEN/Tuj1
p=0.0029
p=0.0015
ns
F
PSD95
Tuj1
~95KDa
~50KDa
PSD95/Tuj1
p=0.0482
p=0.0126
ns
G
NMDAR stimulation
Untreated
NMDA 1'
NMDA 5'
NMDA 20'
p-eEF2
Tuj1
eEF2
Tuj1
~98KDa
~50KDa
~98KDa
~50KDa
p-eEF2 / eEF2
p=0.0016
p=0.0452
Minutes
H
0'
1'
20'
NMDA
APOE3
APOE4
eEF2 phosphorylation profile
Translation profile

Figure 3 - Effect of APOE on NMDAR mediated translation response

A – Experiment design for NMDAR stimulation following APOE conditioned media treatment of rat primary cortical neurons.

B - The representative images for MAP2 and FUNCAT fluorescent signals in rat primary cortical neurons treated with APOE3 / APOE4 recombinant protein (15nM) for 20 minutes along with NMDAR stimulation for 5 minutes (Scale bar - 10µM).

C - The graph represents the quantification of the FUNCAT fluorescent intensity normalized to MAP2 fluorescent intensity under different APOE treatment conditions along with NMDAR stimulation. N = 20-40 neurons from 2 independent experiments, One-way ANOVA ($p<0.0001$) followed by Tukey's multiple comparison test.

D - Representative immunoblots showing the levels of p-eEF2, eEF2 and Tuj1 in rat primary cortical neurons treated with APOE3 or APOE4 conditioned media for 20 minutes along with 5-minute NMDAR stimulation. The graph represents the ratio of p-eEF2 to eEF2 normalized to Tuj1. Data is represented as mean +/- SEM. N=4-5, One-way ANOVA ($p=0.0047$) followed by Dunnett's multiple comparison test.

E - Representative immunoblots showing the levels of PTEN and Tuj1 in rat primary cortical neurons treated with APOE3 or APOE4 conditioned media for 20 minutes along with 5-minute NMDAR stimulation. The graph represents the PTEN levels normalized to Tuj1. Data is represented as mean +/- SEM. N=4, One-way ANOVA ($p=0.002$) followed by Dunnett's multiple comparison test.

F - Representative immunoblots showing the levels of PSD95 and Tuj1 in rat primary cortical neurons treated with APOE3 or APOE4 conditioned media for 20 minutes along with 5-minute NMDAR stimulation. The graph represents the PSD95 levels normalized to Tuj1. Data is represented as mean +/- SEM. N=4, One-way ANOVA ($p=0.0216$) followed by Dunnett's multiple comparison test.

G - Representative immunoblots showing the levels of p-eEF2, eEF2 and Tuj1 in rat primary cortical neurons stimulated with NMDA (20µM) for 1 minute, 5 minutes and 20 minutes. The graph represents the ratio of p-eEF2 to eEF2 normalized to Tuj1. Data is represented as mean +/- SEM. N=3, One-way ANOVA ($p=0.0015$) followed by Tukey's multiple comparison test.

H – Model illustrating the temporal profiles of eEF2 phosphorylation and global protein synthesis on NMDAR stimulation, APOE3 treatment and APOE4 treatment.

Understanding APOE mediated translation response using polysome profiling *(Chapter 6 of the thesis)*

To obtain more mechanistic insights into the translation responses of APOE and NMDA, we performed polysome profiling assay. Briefly, the neurons treated with APOE or NMDA were subjected to density-based separation on 15-45% sucrose gradient. 11 fractions were collected from the gradient and probed for the distribution of ribosomal proteins. Puromycin treatment was used to identify actively translating ribosome fractions. Based on the shift of the ribosomal protein RPLP0 upon Puromycin treatment, fractions 7-11 were classified as actively translating ribosomes and fractions 1-6 were grouped as non-actively translating ribosomes. The ratio of the distribution of an mRNA or ribosomal protein in Fractions 7-11/Fractions 1-6 was calculated to understand the distribution in the translating pool/non-translating pool.

The neurons were subjected to NMDAR stimulation for 1, 5 and 20 minutes, subjected to polysome profiling and probed for the distribution of ribosomal protein RPLP0. At 1-minute NMDAR stimulation, there was no change in the RPLP0 distribution compared to basal conditions. However, at 5-minute NMDAR stimulation, there was a shift of ribosomes (detected through RPLP0) from the translating pool (fractions 7-11) to the non-translating pool (fractions 1-6) indicating an inhibition of protein synthesis. Conversely, at 20-minute NMDAR stimulation, the ribosomes shifted towards the actively translating pool (fractions 7-11) indicating translation upregulation. Thus, polysome profiling assay validated the NMDAR translation response observed previously through eEF2 phosphorylation and FUNCAT.

Further, we performed polysome profiling with APOE conditioned media treatment as well. 20-minute APOE3 treatment with 5-minute NMDAR stimulation caused a shift of ribosomes/RPLP0 towards the non-translating pool compared to APOE3 treatment indicating translation inhibition. Similarly, 20-minute APOE4 conditioned media treatment also caused a shift of ribosomes towards fractions 1-6/ non-translating pool. Along with RPLP0, we investigated the shift of PTEN and PSD95 mRNAs as well. As expected, APOE3+NMDA and APOE4 treatment caused a shift of the mRNAs towards the translating pool fractions 7-11 in the background of translation inhibition. However, control mRNAs such as β-actin and α-tubulin did not show any change, thus validating the translation activation of specific candidates.

Interestingly, 20-minute APOE4 treatment with 5-minute NMDAR stimulation led to a further shift of ribosomes towards the non-translating fractions 1-6 compared to APOE4 treatment, thus causing maximal inhibition of protein synthesis. In the previous assays of FUNCAT and eEF2 phosphorylation, APOE4+NMDA condition was similar to APOE4 treatment. This feature of APOE4+NMDA treatment causing maximal inhibition of translation was captured only with the polysome profiling assay. To investigate this further, we analyzed the non-translating fractions 1-6 only in all the conditions. The fractions 1-6 were grouped into fractions 1-3 and fractions 4-6. Fractions 1-3 constituted the mRNP pool due to the absence of ribosomal proteins in them. Fractions 4-6 formed the pool of ribosomal subunits 40S, 60S and monosomes 80S. The ratio of the mRNAs or proteins in Fractions 1-3/Fractions 4-6 determines their enrichment in the translationally inhibitory mRNP complex.

With the analysis of the fractions 1-6, we observed that all the mRNAs, irrespective of their specificity to NMDAR stimulation, showed a marked increase in fractions 1-3 or the mRNP pool. This corresponds with the maximal ribosomal shift of APOE4+NMDA condition, indicating a non-specific general translation inhibition. Since the mRNAs were accumulated in the mRNP pool, we hypothesized that the inhibition could be at the translation initiation stage. So, we investigated the phosphorylation status of translation initiation factor eIF2α which is a well-established marker for stress response (Wek, 2018). We observed that eIF2α phosphorylation increased only in the APOE4+NMDA condition. As a further validation, we observed that the RPS6 (small ribosomal subunit protein) had accumulated in Fractions 3-4 in APOE4+NMDA condition, which potentially correspond to the 48S pre-initiation complex. Thus, NMDAR stimulation in APOE4 background not only perturbs the NMDAR mediated

translation response, but it also causes a stress response phenotype by increasing the phosphorylation of eIF2α.

Figure 4

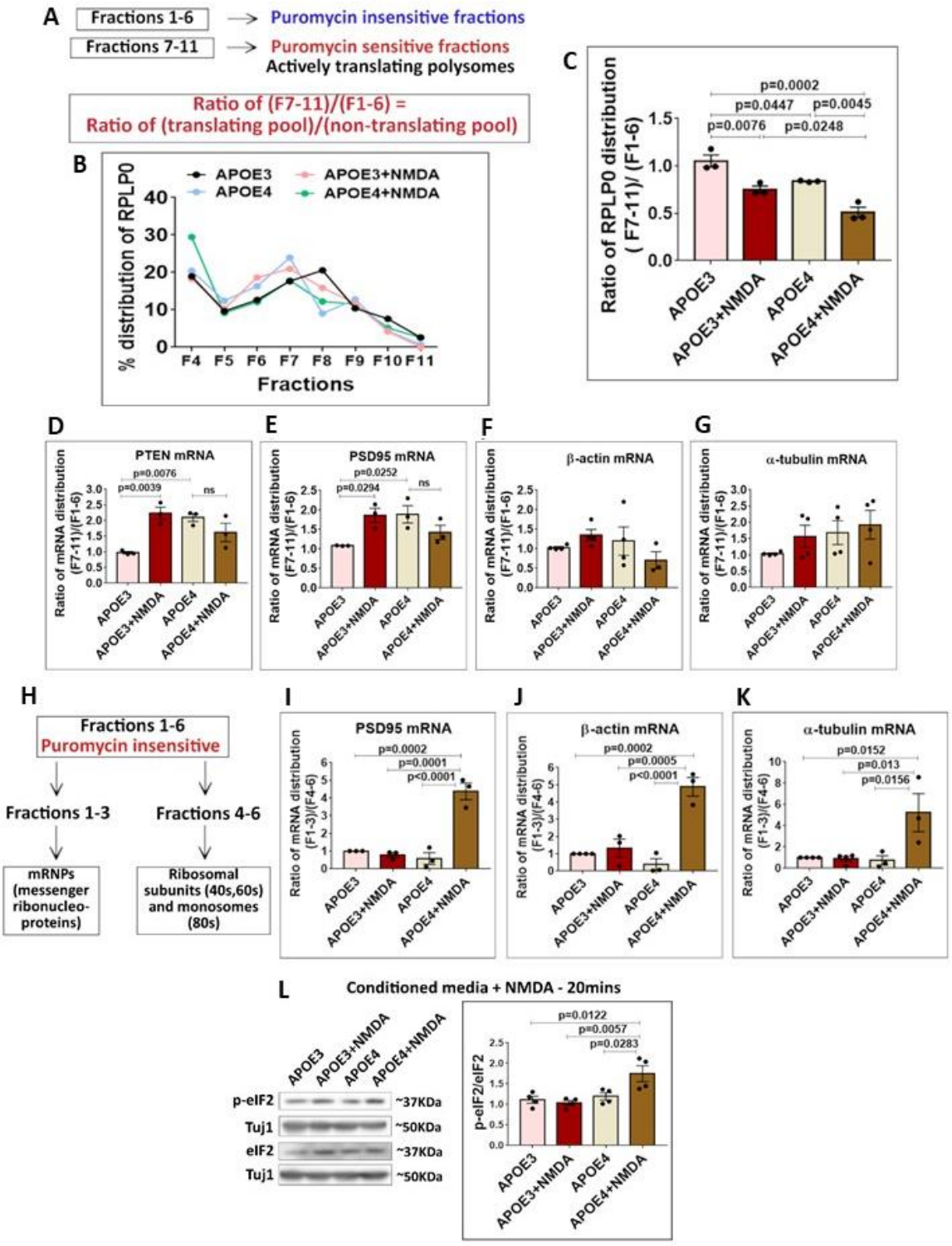

Figure 4 - Understanding APOE mediated translation response using polysome profiling

A – Grouping of fractions 1-6 as non-translating pool and fractions 7-11 as translating pool based on the puromycin sensitivity.

B - The percentage distribution of ribosomal protein RPLP0 in Fractions 4-11 on 20-minute APOE3 or APOE4 iPSC conditioned media treatment along with 5-minute NMDAR stimulation of rat primary cortical neurons.

C - The ratio of the percentage distribution of RPLP0 in the translating pool (F7-11) by non-translating pool (F1-6) on 20-minute APOE3 or APOE4 iPSC conditioned media treatment along with 5-minute NMDAR stimulation of rat primary cortical neurons. Data is represented as mean +/- SEM. N=3, One-way ANOVA ($p=0.0002$) followed by Tukey's multiple comparison test.

D - The ratio of the percentage distribution of PTEN mRNA in the translating pool (F7-11) by non-translating pool (F1-6) on 20-minute APOE3 or APOE4 iPSC conditioned media treatment along with 5-minute NMDAR stimulation of rat primary cortical neurons. Data is represented as mean +/- SEM. N=3, One-way ANOVA ($p=0.006$) followed by Dunnett's multiple comparison test.

E - The ratio of the percentage distribution of PSD95 mRNA in the translating pool (F7-11) by non-translating pool (F1-6) on 20-minute APOE3 or APOE4 iPSC conditioned media treatment along with 5-minute NMDAR stimulation of rat primary cortical neurons. Data is represented as mean +/- SEM. N=3, One-way ANOVA ($p=0.0286$) followed by Dunnett's multiple comparison test

F - The ratio of the percentage distribution of β-actin mRNA in the translating pool (F7-11) by non-translating pool (F1-6) on 20-minute APOE3 or APOE4 iPSC conditioned media treatment along with 5-minute NMDAR stimulation of rat primary cortical neurons. Data is represented as mean +/- SEM. N=3, One-way ANOVA (ns).

G - The ratio of the percentage distribution of α-tubulin mRNA in the translating pool (F7-11) by non-translating pool (F1-6) on 20-minute APOE3 or APOE4 iPSC conditioned media treatment along with 5-minute NMDAR stimulation of rat primary cortical neurons. Data is represented as mean +/- SEM. N=3, One-way ANOVA (ns).

H - Flowchart indicating the grouping of Fractions 1-6 into two pools – Fractions 1-3 (mRNPs) and Fractions 4-6 (Ribosomal subunits and monosomes). The ratio of percentage distribution of the mRNAs in Fractions 1-3 over Fractions 4-6 was considered for further analysis.

I - The ratio of the percentage distribution of PSD95 mRNA in the Fractions 1-3 (mRNPs) over Fractions 4-6 on 20-minute APOE3 or APOE4 iPSC conditioned media treatment along with 5-minute NMDAR stimulation of rat primary cortical neurons. Data is represented as mean +/- SEM. N=3, One-way ANOVA ($p<0.0001$) followed by Tukey's multiple comparison test.

J - The ratio of the percentage distribution of β-actin mRNA in the Fractions 1-3 (mRNPs) over Fractions 4-6 on 20-minute APOE3 or APOE4 iPSC conditioned media treatment along with 5-minute NMDAR stimulation of rat primary cortical neurons. Data is represented as mean +/- SEM. N=3, One-way ANOVA ($p<0.0001$) followed by Tukey's multiple comparison test.

K - The ratio of the percentage distribution of α-tubulin mRNA in the Fractions 1-3 (mRNPs) over Fractions 4-6 on 20-minute APOE3 or APOE4 iPSC conditioned media treatment along

with 5-minute NMDAR stimulation of rat primary cortical neurons. Data is represented as mean +/- SEM. N=3-4, One-way ANOVA (p=0.0079) followed by Tukey's multiple comparison test.

L - Representative immunoblots showing the levels of p-eIF2, eIF2 and Tuj1 in rat primary cortical neurons on 20-minute APOE3 or APOE4 iPSC conditioned media treatment along with 5-minute NMDAR stimulation. The graph represents the ratio of p-eIF2 to eIF2 normalized to Tuj1. Data is represented as mean +/- SEM. N=4, One-way ANOVA (p=0.0047) followed by Tukey's multiple comparison test.

The role of calcium in APOE mediated translation response *(Chapter 7 of the thesis)*

NMDARs are ionotropic glutamate receptors which cause the influx of calcium upon activation. The calcium influx controls multiple signaling pathways downstream of NMDARs, including the phosphorylation of eEF2 as eEF2 kinase is a calcium-calmodulin dependent kinase. Hence, we investigated the role of calcium in NMDAR and APOE translation profiles. When we performed NMDAR stimulation in the absence of extracellular calcium, the translation response was completely lost; neither the initial eEF2 phosphorylation increase nor the later phase p-eEF2 drop was observed. Similarly, when the primary cortical neurons were treated with APOE for 20 minutes in the absence of extracellular calcium, APOE4 mediated increase in eEF2 phosphorylation was absent, indicating that the translation inhibition caused by APOE4 was calcium dependent.

To identify the sources of calcium influx, we performed calcium imaging for 5 minutes using Fluo-4 AM dye for NMDAR stimulation and APOE treatment of rat primary cortical neurons. We tested for 2 major sources of extracellular calcium entry in the post-synapse NMDARs and L-type Voltage Gated Calcium Channels (L-VGCCs) using their respective antagonists MK801 and Nifedipine. As anticipated, we observed that NMDAR stimulation caused a robust influx of calcium in the neurons. MK801 completely blocked the NMDA mediated calcium influx, confirming the specificity of the drug. However, NMDAR stimulation in the presence of Nifedipine did not prevent the initial entry of calcium, but it significantly affected the sustenance of calcium in the neurons. Thus, upon NMDAR stimulation, NMDARs were the first and primary source of calcium influx. L-VGCCs were the secondary source responsible for the sustenance of calcium levels. Calcium imaging with APOE3 addition revealed that APOE3 caused a short burst of calcium in the neurons. We identified that NMDARs were the source of calcium influx and L-VGCCs were not involved in the case of APOE3. However, APOE4 led to a marked influx of calcium in the neurons, which was significantly higher than the APOE3 mediated calcium response. Even in the case of APOE4, NMDARs were the first and the primary source of calcium influx as MK801 pre-treatment completely blocked the APOE4 mediated calcium entry. However, L-VGCCs had a significant role in sustaining the calcium levels in the case of APOE4 treatment. Thus, both APOE3 and APOE4 activated NMDARs and caused calcium influx through it. Since the NMDAR mediated calcium influx was significantly higher in case of APOE4, it led to the activation of L-VGCCs which helps in sustaining the higher calcium levels in the presence of APOE4.

Once we identified the sources of calcium entry in each case, we investigated if the calcium channel antagonists could influence the translation profiles. Since APOE3 and APOE4 caused the initial burst of calcium through NMDARs, MK801 was able to prevent the APOE mediated increase in eEF2 phosphorylation and FUNCAT signal decrease at 1-minute. L-VGCCs had a role only in APOE4 mediated translation response at the 20-minute time point. Accordingly, Nifedipine was not able to block the APOE3 and APOE4 mediated eEF2 phosphorylation at 1-minute. However, Nifedipine was able to prevent the APOE4 mediated p-eEF2 increase and FUNCAT signal decrease at the 20-minute time point; whereas Nifedipine had no effect on the APOE3 translation response at 20 minutes. Thus, we were able to demonstrate that the distinct translation responses of APOE3 and APOE4 were closely linked to their calcium profiles.

Figure 5

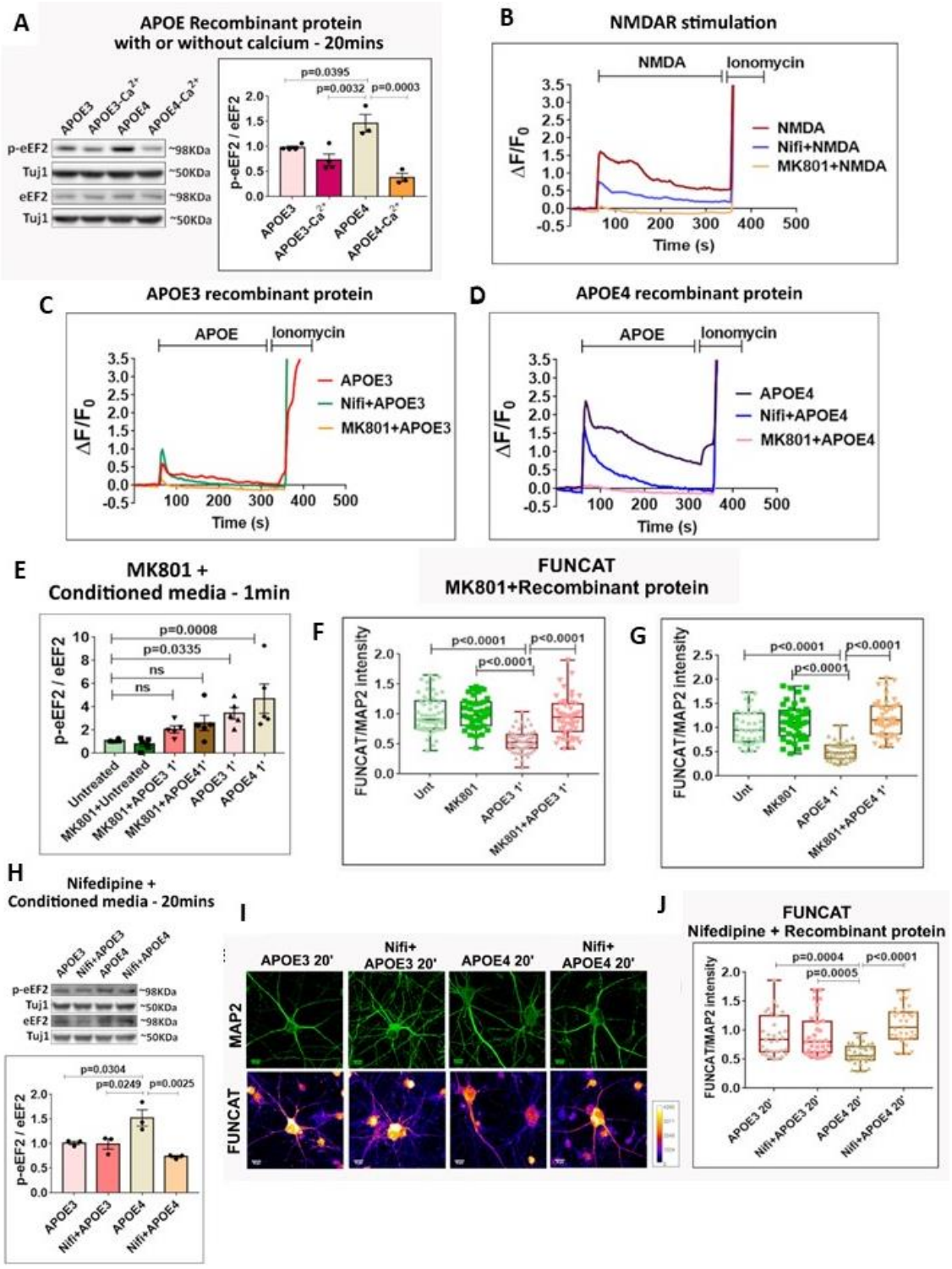

Figure 5 - The role of calcium in APOE mediated translation response

A - Representative immunoblots showing the levels of p-eEF2, eEF2 and Tuj1 in rat primary cortical neurons treated with APOE3 or APOE4 conditioned media for 20 minutes in the presence or absence of extracellular calcium. The graph represents the ratio of p-eEF2 to eEF2 normalized to Tuj1. Data is represented as mean +/- SEM. N=3-4, One-way ANOVA ($p=0.0004$) followed by Tukey's multiple comparison test.

Rat primary cortical neurons (DIV15) were subjected to calcium imaging for 7 minutes using Fluo-4AM dye. The graphs represent the time trace for the change in the fluorescence (Delta F/ F0) at a given time point compared with initial fluorescence (F0) under the following conditions –

B - NMDAR stimulation (20 µM), nifedipine (50 µM) pre-treatment followed by NMDAR stimulation (20 µM), and MK801 (25 µM) pre-treatment followed by NMDAR stimulation (20mM).

C - APOE3 treatment (15 nM), nifedipine (50 µM) pre-treatment followed by APOE3 addition (15 nM), and MK801 (25 µM) pre-treatment followed by APOE3 addition (15 nM).

D – APOE4 treatment (15 nM), nifedipine (50 µM) pre-treatment followed by APOE4 addition (15 nM), and MK801 (25 µM) pre-treatment followed by APOE4 addition (15 nM).

E - Representative immunoblots showing the levels of p-eEF2, eEF2 and Tuj1 in rat primary cortical neurons on 1-minute APOE3 or APOE4 iPSC conditioned media treatment along with MK801 (25 µM) pre-incubation. The graph represents the ratio of p-eEF2 to eEF2 normalized to Tuj1. Data is represented as mean +/- SEM, N = 5, One-way ANOVA ($p = 0.0006$) followed by Dunnett's multiple comparison test.

F - The graph represents the quantification of the FUNCAT fluorescent intensity normalized to MAP2 fluorescent intensity under different APOE3 and MK801 treatment conditions at 1-minute time point. Each data point represents an individual neuron. N=40–50 neurons from 4 independent experiments, One-way ANOVA ($p<0.0001$) followed by Tukey's multiple comparison test.

G - The graph represents the quantification of the FUNCAT fluorescent intensity normalized to MAP2 fluorescent intensity under different APOE4 and MK801 treatment conditions at 1-minute time point. Each data point represents an individual neuron. N=40–50 neurons from 4 independent experiments, One-way ANOVA ($p<0.0001$) followed by Tukey's multiple comparison test.

H - Representative immunoblots showing the levels of p-eEF2, eEF2 and Tuj1 in rat primary cortical neurons on 20-minute APOE3 or APOE4 iPSC conditioned media treatment along with Nifedipine (50 µM) pre-incubation. The graph represents the ratio of p-eEF2 to eEF2 normalized to Tuj1. Data is represented as mean +/- SEM, N=3, One-way ANOVA ($p = 0.0036$) followed by Tukey's multiple comparison test.

I - The representative images for MAP2 and FUNCAT fluorescent signals in rat primary cortical neurons treated with APOE3 or APOE4 recombinant protein (15 nM) for 20 minutes along with MK801 pre-incubation (50 µM) (Scale bar - 10µM).

J - The graph represents the quantification of the FUNCAT fluorescent intensity normalized to MAP2 fluorescent intensity under different APOE and Nifedipine treatment conditions at 20-minute time point. Each data point represents an individual neuron. N=20–30 neurons from 4

independent experiments, One-way ANOVA ($p<0.0001$) followed by Tukey's multiple comparison test.

Concluding Remarks *(Chapter 8 of the thesis)*

The primary finding of my work is that APOE4, a well-established risk factor for Alzheimer's disease affects global protein synthesis in neurons. We observe that the different APOE isoforms APOE3 and APOE4 have a distinct protein synthesis profile. APOE3 leads to a transient inhibition of global protein synthesis which eventually recovers to basal levels. However, APOE4 causes a larger and sustained inhibition of global protein synthesis which fails to recover to basal levels in 20-minute period.

The protein synthesis downstream of NMDAR stimulation has a distinct temporal profile with early phase translation inhibition and late phase translation activation. Though the initial translation response upon APOE3 and APOE4 treatment appears to mimic the early phase NMDAR translation inhibition, the protein synthesis profiles at the later phase is distinct. At 20-minute time point, NMDAR stimulation causes translation activation, APOE4 treatment causes translation inhibition and protein synthesis recovers to basal levels under APOE3 treatment. As a result of the distinct temporal profiles of translation, the neurons retain their physiological response to NMDAR stimulation in the background of APOE3 treatment. However, in the presence of APOE4, the translation response to NMDAR stimulation is perturbed. Interestingly, the phosphorylation of eIF2α increases only in the condition of APOE4 treatment along with NMDAR stimulation, implying the involvement of stress response.

Finally, the distinct profiles of protein synthesis are closely linked to calcium signatures. The stimulation of NMDARs causes an influx of calcium through NMDARs and L-VGCCs. APOE3 treatment causes a short burst of calcium influx through activation of NMDARs alone. However, APOE4 causes a larger and sustained influx of calcium through sequential activation of NMDARs followed by L-VGCCs. The sustained increase of calcium in the neurons on APOE4 treatment leads to the steady increase in eEF2 phosphorylation as well, thus causing an inhibition of global protein synthesis in APOE4 background. Thus, in summary, we propose the following model –

Figure 6

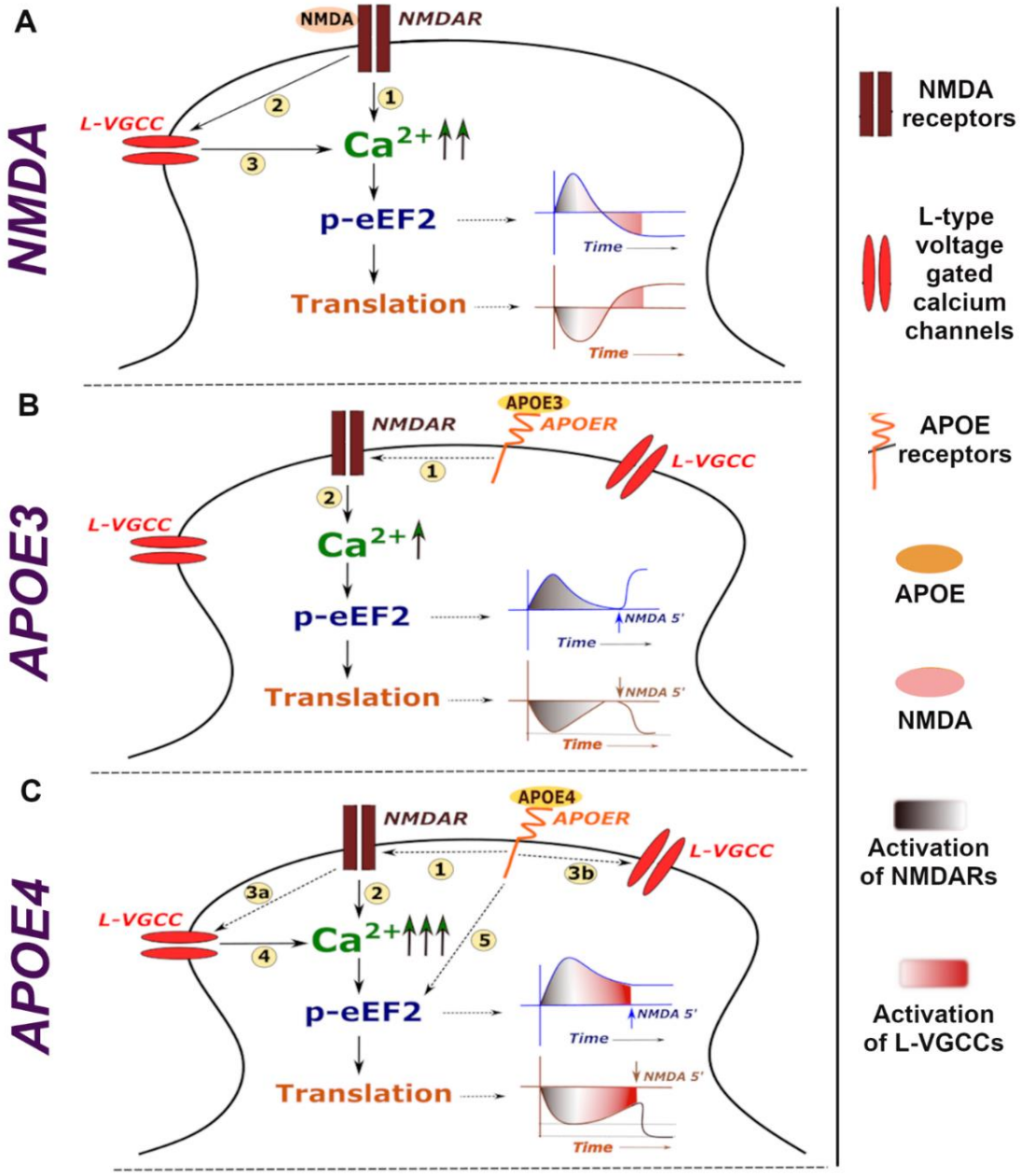

Figure 6 - Model illustrating calcium signature and corresponding protein synthesis regulation downstream of NMDAR stimulation and APOE treatment.

A - Stimulation of NMDA receptors lead to influx of calcium through NMDARs (1) which activates L-VGCCs (2). The influx of calcium through L-VGCCs further helps in sustaining the calcium levels on NMDAR stimulation (3). The calcium through NMDARs and L-VGCCs generates a specific temporal profile of eEF2 phosphorylation, causing an initial inhibition of global protein synthesis followed by translation activation in a later phase.

B - Exposure to APOE3 activates NMDARs through an unknown mechanism (1), leading to a short burst of calcium through it (2). This leads to an acute increase in eEF2 phosphorylation, primarily contributed by calcium influx through NMDARs, which recovers to basal levels. Global translation also follows a similar temporal profile of initial decrease followed by

recovery. Hence, the NMDA activity mediated translation response is unaffected in APOE3 treated neurons.

C - Exposure to APOE4 activates NMDARs through an unknown mechanism (1), causing higher influx of calcium through NMDARs (2) than APOE3 condition. The higher calcium influx through NMDARs could lead to L-VGCC activation in APOE4 condition (3a). Besides, APOE4 binding to APOE receptors could also directly regulate the sustained activation of L-VGCCs (3b). Overall, the L-VGCC activation under APOE4 treatment condition contributes to the huge and sustained increase in calcium levels (4). This leads to the sustained increase in eEF2 phosphorylation as well as global translation inhibition. There could also be a possibility of APOE4 activating signalling cascades which further contribute to the sustained increase in eEF2 phosphorylation (5). Hence, the NMDA activity mediated response is perturbed, potentially causing a stress-response phenotype in APOE4 treated neurons.

Future Directions

The mechanism by which APOE activates NMDARs is not addressed in the study. This would give more insights into the effect of APOE on glutamate receptor mediated signalling. The role of Aβ in APOE4 mediated protein synthesis response is another potential way to get the study forward. Studying the role of Aβ would help in understanding the role of protein synthesis dysregulation in familial AD models as well. The role of internal calcium sources in APOE mediated protein synthesis response is not explored. In our study, I have only focused on the role of extracellular sources of calcium influx. Since APOE4 is known to affect ER mediated calcium release, the role of intracellular calcium sources in APOE translation response would be interesting. This study draws attention to the idea of temporal regulation of protein synthesis by sequential activation of different calcium sources. This can be investigated further to delineate the effect of internal vs external calcium sources, spatial regulation of protein synthesis mediated by calcium and the mechanisms by which they regulate translation. Overall, the regulation of translation by calcium is the arena that the study opens up.

List of Publications

1. Chandrasekaran A, Dittlau KS, Corsi GI, Haukedal H, Doncheva NT, **Ramakrishna S**, Ambardar S, Salcedo C, Schmidt SI, Zhang Y, Cirera S, Pihl M, Schmid B, Nielsen TT, Nielsen JE, Kolko M, Kobolák J, Dinnyés A, Hyttel P, Palakodeti D, Gorodkin J, Muddashetty RS, Meyer M, Aldana BI, Freude KK. **Astrocytic reactivity triggered by defective autophagy and metabolic failure causes neurotoxicity in frontotemporal dementia type 3.** Stem Cell Reports. 2021 Nov 9;16(11):2736-2751. doi: 10.1016/j.stemcr.2021.09.013. Epub 2021 Oct 21. PMID: 34678206; PMCID: PMC8581052.

2. **Ramakrishna S**, Jhaveri V, Konings SC, Nawalpuri B, Chakraborty S, Holst B, Schmid B, Gouras GK, Freude KK, Muddashetty RS. **APOE4 Affects Basal and NMDAR-Mediated Protein Synthesis in Neurons by Perturbing Calcium Homeostasis.** J Neurosci. 2021 Oct 20;41(42):8686-8709. doi: 10.1523/JNEUROSCI.0435-21.2021.Epub 2021 Sep 2. PMID: 34475200; PMCID: PMC8528497.

3. Kute PM, **Ramakrishna S**, Neelagandan N, Chattarji S, Muddashetty RS. **NMDAR mediated translation at the synapse is regulated by MOV10 and FMRP.** Mol Brain. 2019 Jul 10;12(1):65. doi: 10.1186/s13041-019-0473-0. PMID: 31291981; PMCID: PMC6617594.

4. **Ramakrishna S**, Muddashetty RS. **Emerging Role of microRNAs in Dementia.** J Mol Biol. 2019 Apr 19;431(9):1743-1762. doi: 10.1016/j.jmb.2019.01.046. Epub 2019 Feb 7. PMID: 30738891.

5. Schmid B, Prehn KR, Nimsanor N, Garcia BIA, Poulsen U, Jørring I, Rasmussen MA, Clausen C, Mau-Holzmann UA, **Ramakrishna S**, Muddashetty R, Steeg R, Bruce K, Mackintosh P, Ebneth A, Holst B, Cabrera-Socorro A. **Generation of a set of isogenic, gene-edited iPSC lines homozygous for all main APOE variants and an APOE knock-out line.** Stem Cell Res. 2019 Jan; 34:101349. doi: 10.1016/j.scr.2018.11.010. Epub 2019 Jan 4. Erratum in: Stem Cell Res. 2020 Oct; 48:102005. PMID: 30660866.

Chapter 1

Introduction

1.0 Alzheimer's disease: History and Hallmarks

Alzheimer's disease (AD) is a progressive neurodegenerative disorder which causes brain atrophy leading to loss of memory and cognition[1]. It was first reported by Dr. Alzheimer in 1907 as a "Characteristic disease of the cerebral cortex", where he reported his observations on plaques (military foci) and neurofibrillary tangles (fibrils)[2]. Initially, a distinction was made between Alzheimer's disease and senile dementia (attributed to hardening of arteries or arteriosclerotic dementia). By 1970s, it was shown that majority of the cases which were classified as senile dementia had the hallmarks (plaques and tangles) of AD [3–5], thus making AD one of the most common causes of dementia in the world.

The biochemical composition of the lesions found in the AD brains were dissected out. In 1964, the ultra-structural studies of the neuritic plaques were conducted and its contents were identified as amyloid fibrils [6], now shown to be Aβ peptide. It was also predicted that the source of the fibril was a local cellular product and not a blood secretion [6]. Eventually, APP (Amyloid Precursor Protein) was identified as the genetic locus implicated in AD [7–11]. Genetic sequencing of Alzheimer's families helped in identification of mutations in APP, which were soon shown to affect the processing of APP [12–17]. In 1990s, Presenilin 1 and Presenilin 2 were identified as other genes whose mutations also increased amyloid plaques and caused early onset AD [18–23].

In 1963, the structure of the tangles was described as containing paired helical fragments (PHFs) [24]. By 1980s, it was identified that the tangles primarily consisted of the microtubule associated protein Tau [25–28]. Further, it was identified that the Tau protein in the tangles were hyperphosphorylated [29–33], which is shown to be the cause for the formation of the tangles [34–36]

1.1 Aβ pathology

Aβ, the primary component of the amyloid plaques, is generated as a result of the cleavage of the Amyloid Precursor Protein (APP). APP belongs to the class of type-I transmembrane proteins and it undergoes a sequential cleavage; first one by the α- or the β-secretase and second one by the ϒ-secretase [37,38]. The cleavage by α- or β-secretase results in the generation of the soluble APP fragment (sAPPα or sAPPβ) and the membrane tethered C-terminal fragment (APP-CTFα or APP-CTFβ) [37,38]. While the α-secretase cleaves APP within the Aβ domain (non-amyloidogenic pathway), the β-secretase cleaves right at the beginning of it (amyloidogenic pathway). The CTFs undergo a cleavage by the ϒ-secretase complex which cuts at the carboxy-end of the Aβ domain [37,38]. In case of CTFα, the ϒ-secretase cleavage results in the generation of a 3KDa peptide p3 and APP Intracellular Domain (AICD) [37,38]. In case of CTFβ, the ϒ-secretase cleavage results in the generation of Aβ peptide and APP Intracellular Domain (AICD) [37,38]. Among the α-secretases, zinc metalloproteinases ADAM10 and ADAM17 are the best characterized ones in mammals. Aspartyl protease BACE1 is the primary

β-secretase in neurons [37,38]. The ϒ-secretase is a complex which mainly contains the catalytic subunits Presenilins (Presenilin 1 and 2), Nicastrin, Anterior Pharynx Defective (APH1) and Presenilin enhancer (PEN2) [37–39]. ϒ-secretase catalyses three sequential cleavages in the Aβ domain of the APP protein – the ε-cleavage at Aβ 49, followed by the δ-cleavage at Aβ 46 and finally the ϒ-cleavage at the site Aβ 40 or Aβ 42, with Aβ 40 or Aβ 42 being the final products of the ϒ-secretase cleavage [40].

Figure 1.1 – Sequential processing of APP (Figure taken from Hui Zheng and Edward H Koo, Molecular Neurodegeneration, 2006)

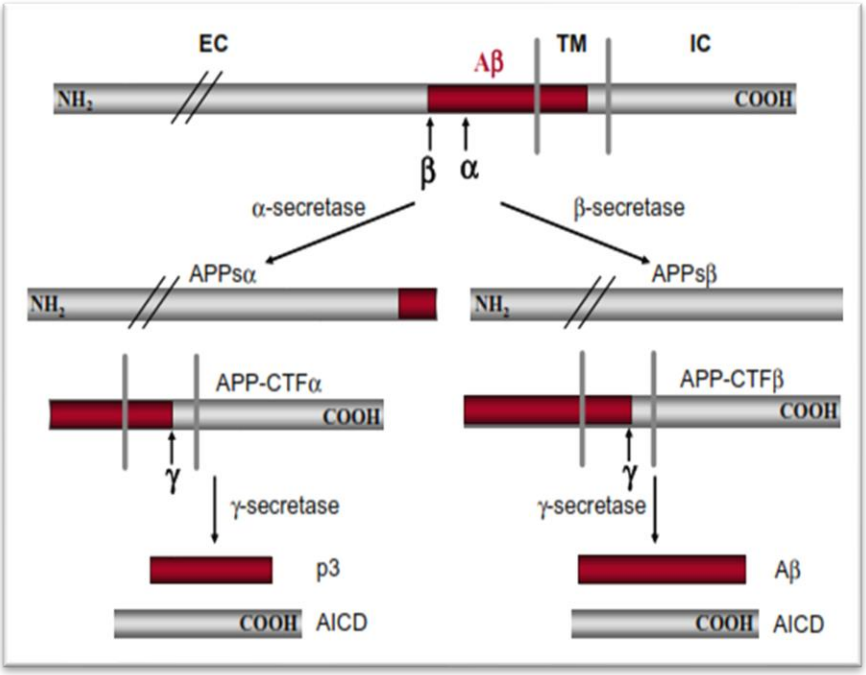

Over 20 AD-causing mutations have been identified in APP, where the mutations either increase the β-cleavage (shift the balance towards amyloidogenic pathway) or increase Aβ 42 levels [41]. The longer species Aβ 42 has a higher propensity to aggregate and form plaques, and hence considered as the more toxic one in AD pathology [42,43]. Thus, the deregulation of APP processing causes an increase in Aβ generation, particularly Aβ 42, which results in its aggregation and plaque formation [37,40]. This forms the basis of the amyloid cascade hypothesis which believes that Aβ accumulation is the primary event which drives AD pathology. There are over 200 mutations identified in the Presenilins (PSEN1 and PSEN2) which cause AD, where most of the mutations lead to increased production of Aβ 42 over Aβ 40 [44,45].

Now, it is clear that it is not just the aggregation of Aβ into plaques, but the intracellular soluble forms of Aβ are also toxic. This led to the Aβ oligomer hypothesis which proposes that the soluble Aβ oligomers initiate the AD pathogenesis rather than the plaques [46–48]. The Aβ oligomers were considered to be the intermediate form before the Aβ plaque generation [46–48]. However, many studies, including the ones using synthetic Aβ oligomers, have shown that the oligomers are necessary and sufficient to drive AD neurodegeneration [46–48]. Additionally, this has also led to the idea that the extracellular Aβ plaques could be the protective aggregates which sequester the toxic Aβ oligomers, thus reducing the intracellular defects caused by them [49].

1.2 Cellular defects in AD

1.2.1 Mitochondrial dysfunction

Mitochondrial dysfunction is reported extensively in AD and it is an established early feature in AD pathogenesis [50]. Impaired energy metabolism and reduced utilization of glucose (identified from PET imaging) is a key feature reported consistently in AD patients; and they are known to occur years before the onset of the disease [51–53]. Defects have been reported at multiple steps, starting from glucose transport to glucose metabolism [54]. Multiple transcriptomic and proteomic studies have shown genes/ proteins related to glycolysis, TCA cycle and oxidative phosphorylation being downregulated in AD [55–63], with OXPHOS being the most severely affected pathway [64]. Thus, a decrease in most of the complexes of ETC were reported [55,65], owing to an overall reduction in the ATP levels [50,66,67].

Increased oxidative stress is another well-established feature in AD [55,68]. Though Reactive Oxygen Species (ROS) are important signaling molecules, increased production of ROS by the mitochondria is shown to cause oxidative damage[55,68]. In case of AD, oxidative damage of cellular lipids (lipid peroxidation) [68,69], RNA/ DNA (8-hydroxyguanosine or 8-hydroxy de-guanosine) [70–72], proteins and sugars [73]are reported. In particular, the oxidation of several enzymes involved in energy metabolism is shown to affect their function and further contribute to the impaired metabolism [73]. Additionally, the increased oxidative stress is shown to cause mutations in mitochondrial DNA in the AD brain [55,74,75]. Along with this, alterations in mitochondrial fission-fusion dynamics are also reported in AD, titled more towards the fission process [76,77]. Particularly, Aβ is shown to stimulate the fragmentation of mitochondria, thus forming smaller dysfunctional mitochondria [77–79]. This gets further worsened by impaired mitophagy [80], thus leading to accumulation of damaged dysfunctional mitochondria.

Figure 1.2.1 – Mitochondrial dysfunction in AD (Figure modified from Wenzhang Wang et al, Molecular Neurodegeneration, 2020)

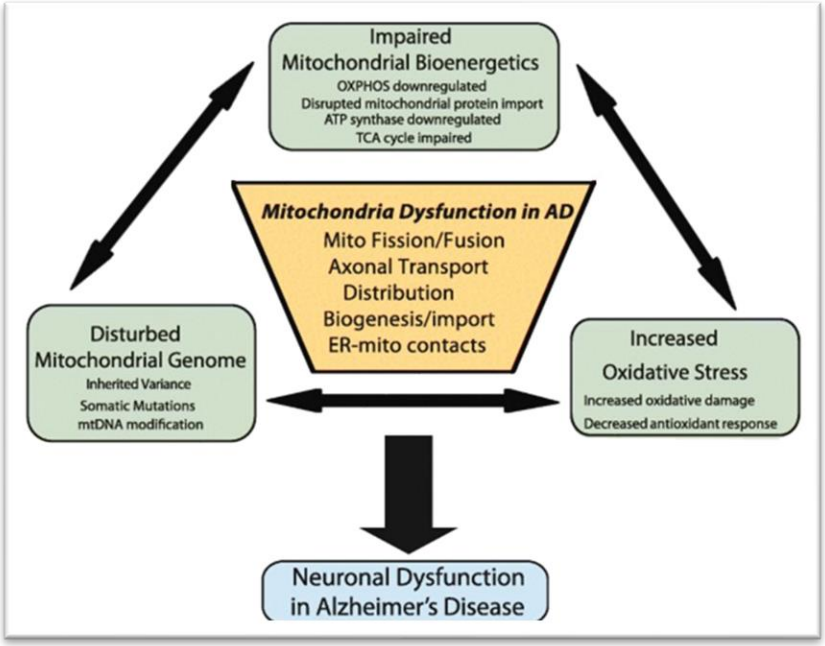

1.2.2 Synaptic dysfunction

Synapse loss is shown to occur pre-symptomatically in AD, much before plaque formation [81–83]. It is also shown to be the best correlate for the severity of dementia and staging of AD [81,82,84,85]. Loss of dendritic spines, pre- and post-synaptic proteins is reported in human AD brain samples and the transgenic mouse models of AD [81,84,86–92]. Even soluble Aβ oligomer treatment at low nanomolar to micromolar concentration is shown to affect synaptic plasticity and cognition in rats in vivo [93–96]. Additionally, the increased phosphorylation of Tau and disrupted microtubule network is shown to affect the axonal transport in AD neurons [97].

Long term potentiation and depression (LTP and LTD) are widely used as paradigms to study synaptic plasticity, memory and learning [82,98]. Both of them require the activation of glutamate receptors, influx of calcium which further regulates the kinase-phosphatase balance [82,98]. One of the consistent findings in AD is the impairment of long-term potentiation (LTP) by Aβ oligomers in the transgenic AD mouse models [95,96,99–103]. Some studies have also reported enhanced long-term depression (LTD) or weakening of synapses in the presence of Aβ [104–106]. This is further supported by studies which indicate increased internalization of post-synaptic glutamate receptors, particularly AMPARs [104], further contributing to the LTD exaggeration in AD. Ultimately, these result in behavioural, learning and memory deficits in the transgenic mouse model of AD.

Aβ is also proposed to activate many glutamate receptors at the post-synapse. One of the best-studied among them is NMDA receptors. Aβ is shown to cause calcium influx through NMDARs, hence affecting calcium homeostasis and causing excitotoxicity [107,108]. This is also proposed to cause the increased activation of the calcium dependent phosphatase calcineurin, thus enabling the dephosphorylation and internalization of AMPARs [104,109,110]. Additionally, the Aβ is also reported to activate extra-synaptic NMDARs; Aβ blocks synaptic NMDARs which causes glutamate spill over to activate extra-synaptic NMDARs [111]. The activation of extra-synaptic NMDARs is known to cause excitotoxicity and activate pro-death signalling in neurons [111]. The excitotoxicity is further worsened by the Aβ-mediated inhibition of the excess glutamate re-uptake by blocking Excitatory Amino Acid Transporters (EEATs) [112,113]. Metabotropic glutamate receptor 5 (mGluR5) is another proposed receptor candidate to which Aβ binds. Aβ is reported to affect the clustering and activation of mGluR5, thus affecting calcium dynamics downstream of it and leading to synaptic dysfunction [114,115]. Similarly, Aβ is also reported to bind to calcium permeable α-nicotinic acetylcholine receptors [116]. While one of the proposed mechanisms for synaptic dysfunction is the interaction between Aβ and neuronal receptors, the other potential mechanisms behind synaptic dysfunction in AD remain unexplored.

Figure 1.2.2 – Synaptic dysfunction in AD (Figure modified from Victoria Campos-Peña and Marco Antonio Meraz-Ríos, Chapter from InTech book series, 2014)

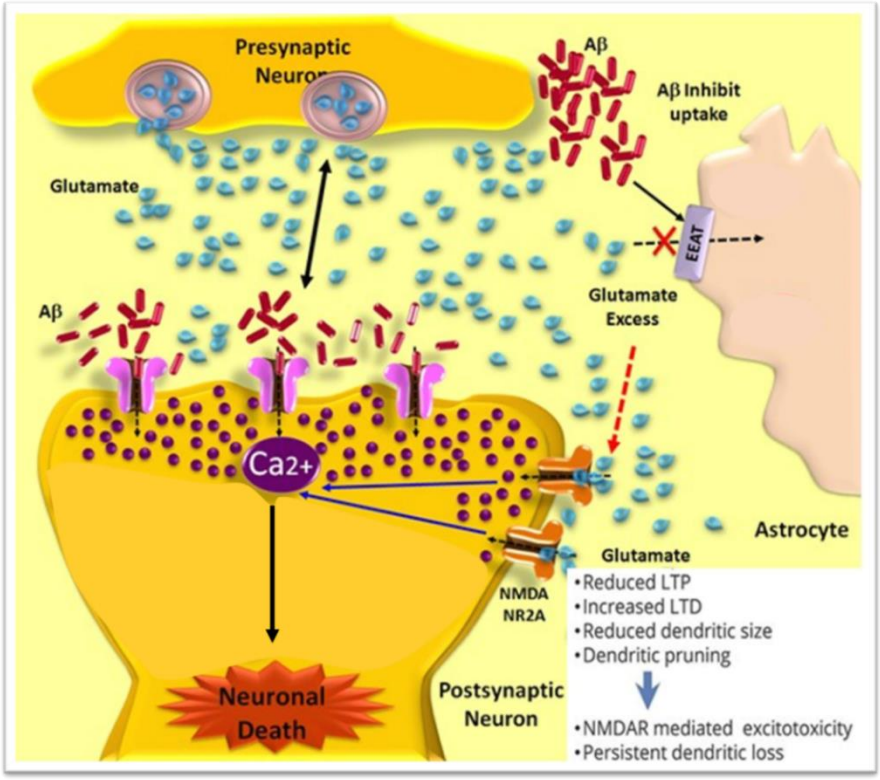

Apart from the mitochondrial and synaptic dysfunction which are well-established in AD, there are studies showing defects in lysosomes and Golgi apparatus as well. The process of autophagy is reported to be defective at multiple steps in AD – decreased levels of autophagosome regulator ATG7, failed maturation of lysosomes and impairment of auto-phagolysosomes [117,118]. With respect to Golgi, increased fragmentation of Golgi and defects in protein trafficking are reported [119].

1.2.3 Microglial and astrocyte dysfunction

Microglia plays a dual function in AD, where one part of it can be beneficial in Aβ clearance while the other part can worsen the AD phenotypes [120–122]. Classically, microglia are the macrophages of the CNS which get activated upon brain injury or infections. Several studies have indicated the presence of activated microglia around the Aβ deposits [123,124]. Additionally, microglia are also shown to physically interact with Aβ, hence enabling their phagocytosis and clearance [125–128]. On the other hand, excessive activation of microglia by Aβ leads to the release of pro-inflammatory cytokines which further worsen the process of neurodegeneration [124,129–132]. In support of this, aggravated microglial activation and impairment of microglial function is reported in AD which facilitates Aβ deposition and AD progression [120,121,129–133].

Astrocytes wrap around the pre- and post- synaptic compartments, providing critical support for synaptic functioning in terms of energy, ion and neurotransmitter homeostasis, growth factor secretion and oxidative stress regulation. Similar to microglia, astrocytes also have a dual role in AD pathology [121]. The astrocytes also play an important role in phagocytosis of Aβ deposits. They express a wide array of receptors

(RAGE and LRPs) which bind to Aβ and hence help in their clearance [132,134]. Additionally, astrocytes also express and secrete Aβ degrading proteolytic enzymes (Neprilysin, Insulin Degrading Enzyme) which further contribute to the clearance of Aβ [121,134,135]. However, Aβ mediated activation of astrocytes is also reported to promote neurodegeneration by secreting of pro-inflammatory cytokines [121,129,135]. Hence, similar to microglia, the Aβ load and the extent of activation become critical factors in determining the toxic/ trophic role of astrocytes. This is further compounded by the effect of Aβ on astrocyte functioning. Aβ is shown to disrupt the calcium homeostasis in astrocytes, particularly ER calcium regulation, and elevated astrocytic baseline calcium levels are observed in several AD model systems [136–139]. Aβ is reported to interact with several receptors (Metabotropic Glutamate Receptor 5, Nicotinic Acetylcholine Receptors, Purinergic Receptors P2Y1) which cause calcium influx in astrocytes [140–144]. Ultimately, this affects the glutamate uptake capacity of the astrocytes, hence exacerbating the glutamate excitotoxity and synaptic dysfunction in AD [135,145,146].

Figure 1.2.3 – Microglial and astrocytic dysfunction in AD (Figure taken from Marc Fakhoury, Current Neuropharmacology, 2018

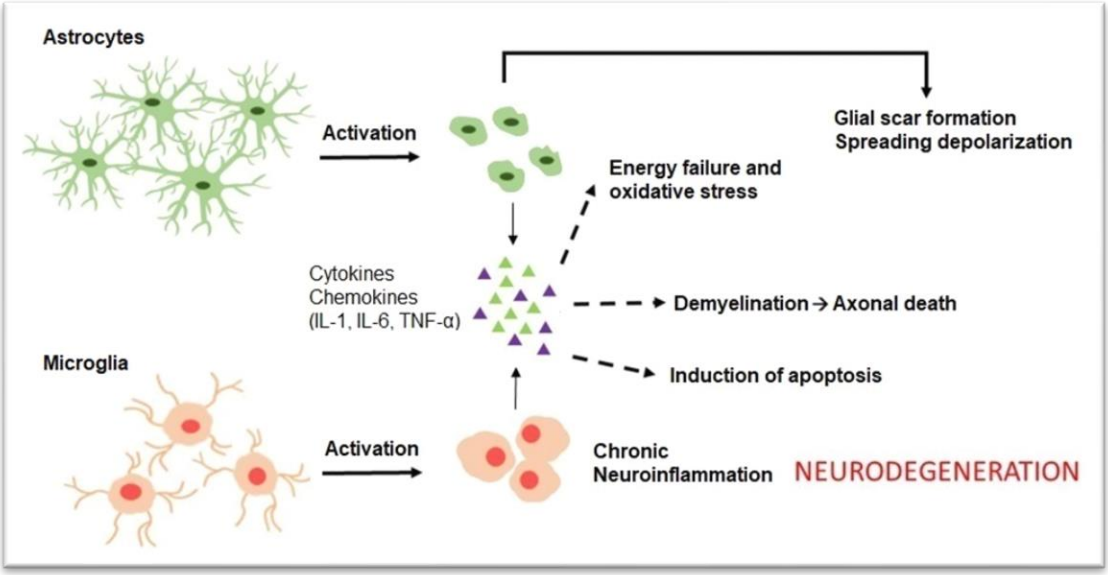

1.3 Risk factors of AD

AD is classified into early onset AD (EOAD) and late onset AD (LOAD) which occurs over 65 years of age. EOAD, contributing to about 5% of the total AD cases, is caused due to genetic mutations in either APP or PSEN genes leading to an increase in Aβ levels [1,147,148]. Though no known genetic mutations are established with sporadic or LOAD (which contributes to over 95% AD cases), certain genetic risk factors which increase the pre-disposition to AD are identified, the most well-established risk factor being ε4 isoform of Apolipoprotein E (APOE) [1,147–149]. The presence of APOE4, even in heterozygous condition, is shown to significantly increase the frequency of AD and reduce the mean age of clinical onset of AD [149]. The mechanistic insights about APOE are discussed in the upcoming sections.

The other reported genetic risk factor for AD is TREM2, a transmembrane receptor for lipoproteins in microglia [148,150]. It is also shown to act as a receptor for Aβ [148,150]. Though the mechanisms with regards to TREM2 are not well investigated, certain mutations of TREM2 are identified in AD patients, with R47H and R62H being the most well studied. The mutations were shown to affect the binding of Aβ to TREM2, hence altering the microglial clearance of Aβ and increasing the plaque associated neuronal loss [148,150]. Thus, deficiency in TREM2 function was shown to affect the protective barrier formed by the microglia around the plaques to enable their compaction. The amyloid plaques were more diffused, branched and covered larger surface area under conditions of TREM2 deficiency or mutations, hence increasing the risk of AD [148,150].

1.4 Apolipoprotein E (APOE) – cellular functions and isoforms

APOE is a lipoprotein primarily involved in the transport of cholesterol and other lipids by binding to its cognate receptors. Liver expresses the majority (about 75% of the total) of APOE, followed by the brain. In the brain, astrocytes are the primary cell types to express and secrete APOE [151–154]. The APOE expression in neurons is minimal and is reported to increase under stress conditions. It is a 299 aa protein having a receptor binding region (136-150 aa) in the N-terminal domain (1-167 aa) and a lipid binding domain (244-272 aa) in the C-terminal region (206-299 aa). Humans express three different isoforms of APOE (APOE2, APOE3 and APOE4) as a result of two single nucleotide polymorphisms (SNPs). Hence, the three APOE isoforms differ only at two amino acid positions 112 and 158. APOE2 has Cysteine residues at 112 and 158; APOE3 has Cysteine at 112 and Arginine at 158, while APOE4 has Arginine at both the positions [151–154]. APOE2 is the least common allele in the population (around 8%) and APOE3 is the most common one (around 77%). While APOE4 distribution in the population is around 14%, it is enhanced to 40% in AD patients, making it one of the most well studied risk factors of AD [151–154].

Apart from the distribution frequency, the isoforms also differ in their lipid binding preferences. While APOE2 and APOE3 show a preferential binding to high-density lipoproteins (HDLs), APOE4 is associated with low-density and very low-density lipoprotein complexes (LDLs and VLDLs) [151–154]. This difference is attributed to the 'domain interaction' which specifically occurs in APOE4. Due to the presence of Arg in 112th position of APOE4, there is an interaction between Arg 61 in the N-terminal domain with Glu 255 in the C-terminal domain which is termed as the 'domain interaction'. If the domain interaction is perturbed in APOE4 either by mutating Arg 61→Thr 61 or Glu 255→Ala 255, the lipid binding preference of APOE4 changes to HDL complexes [151–154]. Thus, the structural property of APOE4 distinguishes it from the other APOE isoforms with respect to its lipid binding and is implicated in increasing the pre-disposition to AD as well.

Figure 1.4 – Apolipoprotein E structural domains and isoforms (Figure modified from Takahisa Kanekiyo et al, Neuron, 2014).

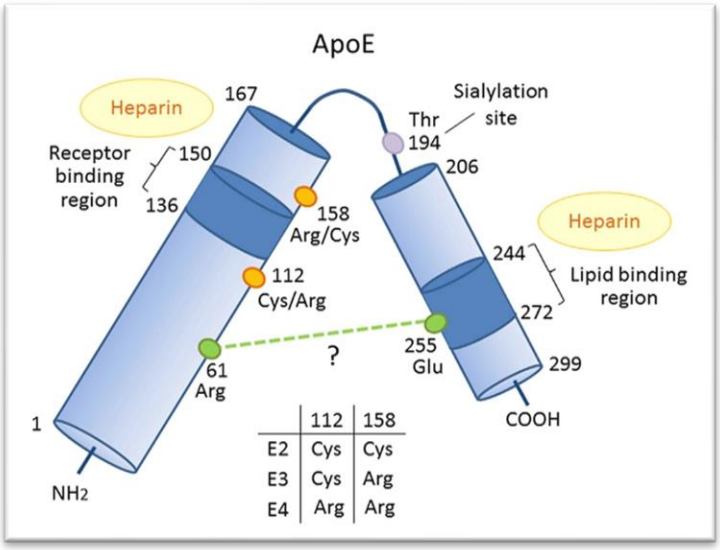

1.5 APOE receptors and receptor mediated signaling

APOE binds to family of type-1 single transmembrane receptors called LDLR family of receptors. The family contains over 10 different receptors each of them having the characteristic ligand binding repeats, EGF like repeats and YWTD motifs in the β-propellor domains [153,155]. Some of the receptors in the family include LDLR (Low Density Lipoprotein Receptor), VLDLR (Very-low Density Lipoprotein Receptor) and LRPs (LDLR related proteins). The receptor family binds to about 30 different ligands including APOE, Reelin, α2 macroglobulin and tissue type plasminogen activator [153,155]. Upon ligand binding, the receptors undergo a constitutive endocytosis to transport the ligands into the cell. Receptor Associated Protein (RAP) acts as an antagonist for the entire LDLR family of receptors [155–158].

Figure 1.5.1 – Apolipoprotein E receptors or LDLR family of receptors (Figure taken from Guojun Bu et al, Nature Reviews, 2009)

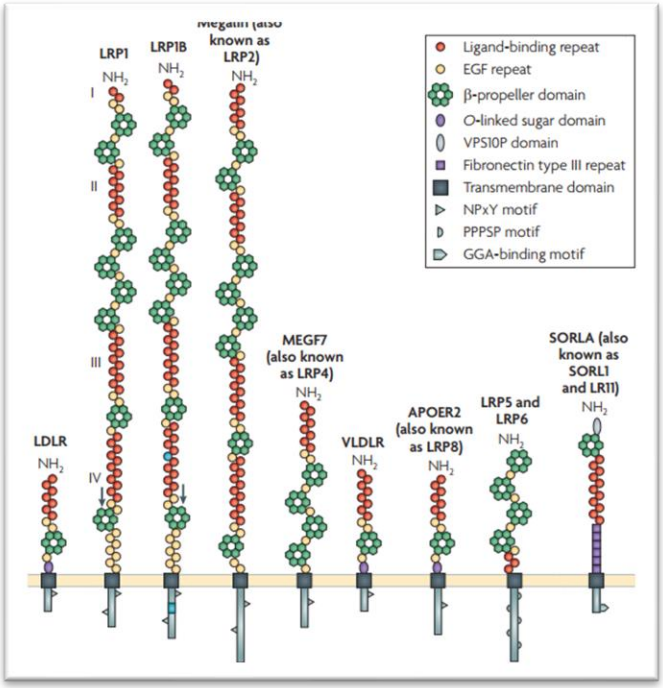

APOE is also shown to activate different signaling pathways upon binding to the APOE receptor. Three primary ones were the ERK pathway, Dab1-SFK pathway and PI3K-Akt pathway. ERK 1/2, Dab1 and Akt phosphorylation increased upon APOE treatment of neurons, and this was blocked by RAP indicating that the increase was receptor dependent [159]. Similarly, JNK 1/2 pathway was shown to be inhibited by APOE [159]. The isoforms of APOE are also known to have different affinities in binding to the receptor where APOE2 is shown to have the minimum affinity [151,155]. Hence, the signaling pathways downstream of APOE receptors are also activated with APOE4 causing the maximal activation of ERK 1/2 phosphorylation [160–162]. The ERK activation downstream of APOE treatment is shown to increase both c-fos and CREB phosphorylation, leading to transcriptional activation in an isoform dependent manner with APOE4 causing highest activation [160,161].

LDLR and LRP1 are the APOE receptors enriched in the brain. LRP1 is also shown to be present at the neuronal post-synaptic complexes, and influence synaptic signaling, especially downstream of NMDA receptors [153,161,163–165]. APOE receptors are shown to interact with NMDARs through PSD95 [166]; and internalized endosomes of APOE receptors are shown to contain NMDARs and AMPARs as well [167]. The activation of ERK pathway downstream of APOE is also shown to be dependent on NMDARs [159,162]. Along with RAP, even NMDAR antagonist MK801 was able to prevent the APOE mediated ERK phosphorylation, hence indicating that both APOE receptors and NMDARs were involved [159,162]. Studies have also indicated that APOE causes influx of calcium through NMDARs [164,165], but the mechanism of this remains unexplored. Hence, the binding of APOE to its cognate receptors activates multiple signaling pathways in an isoform-dependent manner.

Figure 1.5.2 – Signalling pathways regulated by APOE-APOE receptors (Figure taken from Hyang-Sook Hoe et al, Journal of Neurochemistry, 2005)

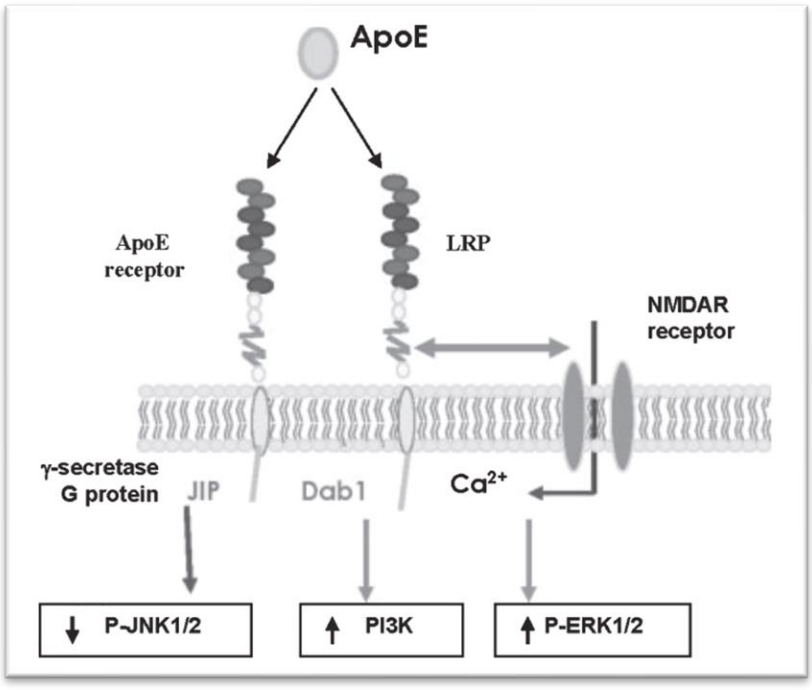

1.6 APOE and Alzheimer's disease

APOE was implicated in AD when it was found as one of proteins to be co-deposited with Aβ in the amyloid plaques [168]. Further, it was identified that the ε4 isoform of APOE increases the risk for AD. Several studies have suggested mechanisms through which APOE4 could increase the aggregation of plaques and decrease their clearance. The binding of APOE to Aβ depends on multiple factors, important ones being the isoform of APOE and its lipidation status. Aβ is shown to have two binding regions in APOE, one in N-terminal receptor binding domain between residues 144-148 and the other one in the lipid binding C-terminal domain of APOE [152,169]. Hence, the lipidation status of APOE influences where Aβ binds to APOE and its affinity. Experiments with the purified APOE protein or the recombinant APOE protein which is not lipidated suggest that APOE4 binds to Aβ with better affinity [169]. However, when cell-secreted lipidated APOE was used, APOE3 showed stronger interactions with Aβ as compared to APOE4 [170]. Thus, many studies have implicated the role of APOE in clearance of Aβ, where astrocyte secreted APOE3 can bind to Aβ better than APOE4 and clear it more efficiently.

There are three primary ways in which Aβ is cleared (proteolytic degradation, cellular clearance/lysosomal degradation, cerebro-vascular clearance/drainage pathway) and the role of APOE is implicated in all three mechanisms [152]. Firstly, APOE bound Aβ is shown to be more susceptible to the proteolytic degradation by enzymes such as NEP (Neprilysin) and IDE (Insulin Degrading Enzyme) [171]. The lipidated APOE3 which binds to Aβ better could facilitate the proteolytic degradation more than APOE4. Secondly, the cellular clearance of APOE3-Aβ complexes mediated through neuronal APOE receptors is better than the clearance of APOE4-Aβ complexes [152,172]. In case of APOE3, the receptor endocytosis of APOE-Aβ complex and the following lysosomal degradation is shown to be more efficient [152,172]. Additionally, the recycling of the APOE receptors back to the surface is also shown to be slower in case of APOE4, hence affecting the receptor availability for clearance [167]. Additionally, APOE is shown to promote the microglial phagocytosis for clearance of Aβ aggregates [173]. Even in this process, APOE3 is shown to induce microglial phagocytosis better than APOE4 [174,175]. Lastly, APOE-Aβ complexes are also cleared through the ISF drainage by binding to the APOE receptors on the brain vasculature or blood brain barrier [176,177]. Owing to the better binding of APOE3 to Aβ, even the clearance of Aβ through the blood brain barrier is more efficient in case of APOE3 than APOE4 [178–180].

Apart from the clearance of Aβ, many in-vitro studies have outlined the role of APOE with respect of aggregation of Aβ. APOE4 is shown to stabilize the Aβ peptide more than APOE3, and hence aid their oligomerization and aggregation [181,182]. Additionally, many recent studies have shown that APOE4 can increases the generation of Aβ itself. The activation of ERK pathway by APOE4 is shown to increase the transcription of APP mRNA, hence forming more APP protein and Aβ [183,184]. Thus, APOE4 can affect Aβ production, aggregation and clearance, rationalizing its strong association with AD pathogenesis.

Figure 1.6.1 – Role of APOE in Aβ pathogenesis (Figure taken from Sridevi Raman et al, Neurobiology of Disease, 2020)

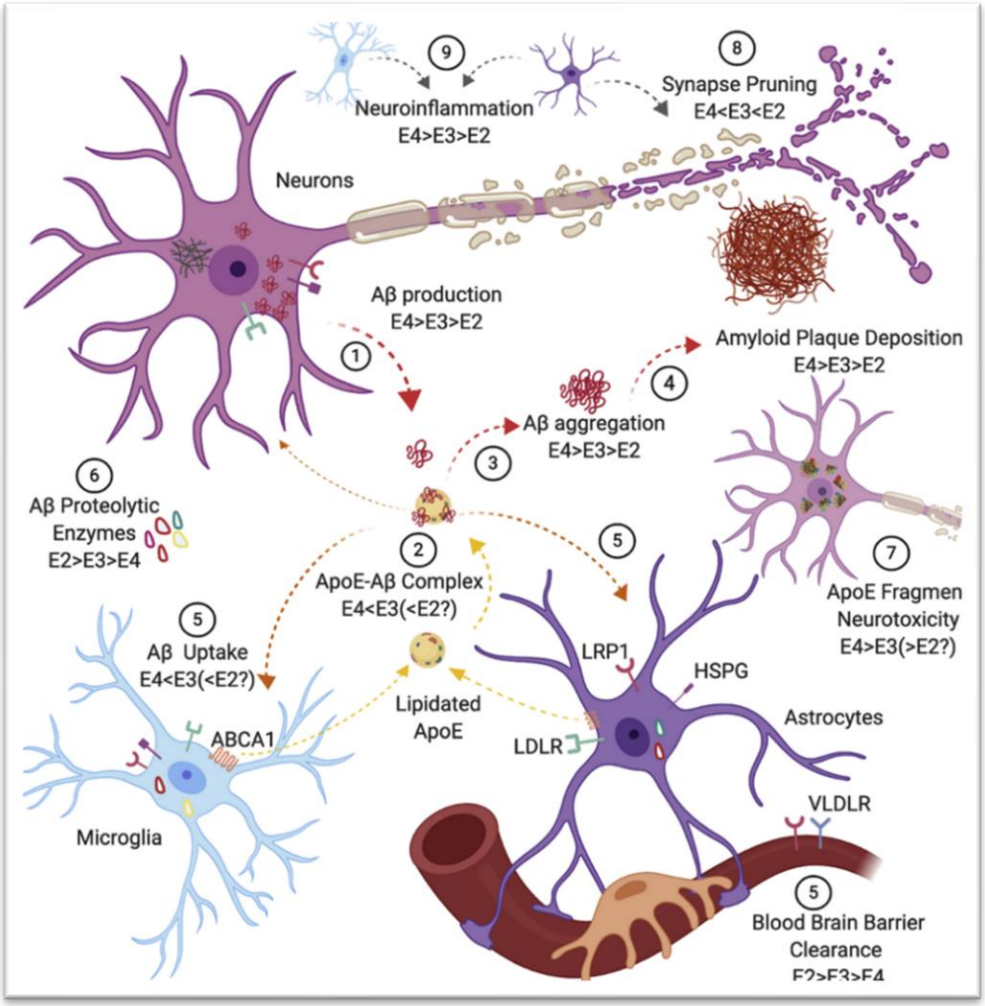

1.7 APOE and cellular defects

Along with their involvement in AD, many cellular defects are observed in APOE4 TR (targeted replacement) mice models and humans with APOE4 genotype, highlighting that presence of APOE4 alone could cause AD like phenotype.

1.7.1 Mitochondrial dysfunction

Similar to AD, defective uptake of glucose and impaired glucose metabolism is reported in APOE4 TR mice model as well [185]. Consecutively, cognitively normal APOE4 carriers (who have a risk for developing AD) were shown to have decreased glucose metabolism in the cerebrum [186,187]. In addition to glucose metabolism, reduced activity of mitochondrial ETC complex IV and altered expression of mitochondrial ETC enzymes is also reported in young adult APOE4 carriers [188,189]. However, transgenic APOE4 mice models showed defect in all ETC complexes and hence reduced mitochondrial respiration [190]. The PINK1-Parkin pathway was also shown to be affected in the neurons of APOE4 mice, hence leading to defects in mitochondrial fission and mitophagy [191]. The altered mitochondrial dynamics was observed in APOE4 expressing astrocytes as well [192].

One of the proposed mechanisms for APOE4 mediated mitochondrial defects is the domain interaction of APOE4. Cellular studies which have used APOE4 with disrupted domain interaction were able to rescue the mitochondrial defects, mainly the restored expression of mitochondrial ETC complexes [190]. The other proposed mechanism involves the intracellular cleavage of APOE4. APOE4 is shown to undergo a specific cleavage in neurons generating two fragments APOE4 1-272 and APOE4 272-299, both of which have been associated with mitochondrial defects. APOE4 fragment 1-272 is shown to interact with mitochondrial proteins of ETC complexes III and IV and impair their activity [193]. The APOE4 fragment 272-299 is shown to affect the ER-mitochondrial calcium homeostasis by increasing the mitochondrial calcium uptake [194]; hence causing mitochondrial dysfunction and eventual neurotoxicity.

1.7.2 Synaptic dysfunction

Initial studies reported that APOE4 carriers displayed cognitive deficits and reduction in hippocampal volume, decades before the development of dementia [186,195,196]. This supported the idea that APOE4 could have an impact on cognitive processes from early in life. Consequently, many studies have drawn correlations between APOE genotype and cognition in humans, where APOE4 carriers were shown to global cognitive functioning [197–200]. Accordingly, APOE4 mice of both younger and older age groups are reported to show defects in spatial learning and memory [201].

The memory defects are correlated with the multiple synaptic defects observed in the APOE4 mice model. Reduction of neurite outgrowth, dendritic complexity, spine density, and loss of synaptic proteins are well reported in APOE4 mice models [201–205]. Further, the APOE4 mice were also shown to affect the hippocampal long-term potentiation [167,206–208], thus impairing synaptic plasticity. APOE4 is also reported to interfere with glutamate receptor signaling pathways[167], especially downstream of NMDARs [163,165,209]. As discussed earlier, APOE receptors are shown to interact with NMDARs. The binding of APOE4 to APOE receptors is shown to activate NMDARs, cause excess calcium influx through NMDARs and initiate excitotoxic response [165,209–212]. The dysregulated calcium response mediated by APOE4 is proposed to be one of the ways by which APOE4 causes synaptic defects. Additionally, the internalized endosomes of APOE-APOE receptor are shown to contain the glutamate receptors NMDARs and AMPARs as well [167]. The recycling of the receptors back to the surface is shown to be slower in case of APOE4, hence reducing the surface availability of NMDARs and AMPARs [167]. This is another proposed mechanism through which glutamate mediated synaptic plasticity could be affected in the presence of APOE4.

1.8 Protein synthesis and AD – a link to synaptic dysfunction?

Synaptic dysfunction is one of the most well-established defects both in AD and APOE4 model system, and it is shown to occur decades before the onset of dementia. Yet the mechanisms behind synaptic defects are not well understood. We were interested in obtaining insights into the reason behind the synaptic failure in dementia; and hence explored protein synthesis dysregulation as a possible mechanism. It is now clear that protein synthesis is one of the key processes essential for synaptic plasticity, and in turn learning and memory. The changes in the synaptic strength are generally accompanied by changes in electrical properties or morphological changes in the synapses such as

pruning, induction, enlargement or shrinkage [213–215]. The re-modeling and maintenance of these structural and functional changes in the synapses requires the synthesis of new proteins, which are tightly regulated spatio-temporally[213–215]. Further, it is also well-established that many of these proteins are synthesized locally, in dendritic or axonal compartments, and in response to different synaptic stimulations [213–216]. Various synaptic stimuli, either in the form of neurotransmitters or neuromodulators, causes changes in the synaptic structure and function, often accompanying the synthesis of specific new proteins [213–216]. Thus, activity mediated synthesis of new proteins and changes in the proteome play an important role in driving synaptic plasticity; and could be a potential underlying mechanism behind the synaptic dysfunction in AD.

Multiple studies have shown the dysregulation of protein synthesis and its machinery in familial AD model systems. Dysregulation of de-novo protein synthesis is observed in AD [217,218] as well as in other forms of taupathies [219–223]. Along with basal translation, defects in synaptic activity mediated signaling and translation is also reported to occur pre-symptomatically in AD [217,224–226]. Intriguingly, ribosomes are also shown to be affected in AD with altered expression of rRNA and mRNAs coding for ribosomal proteins documented to occur pre-symptomatically [227–229]. Alterations in the amount, activity, and post-translational modifications of translation components like eIF2α, eEF1A, eIF4E, and p70 RPS6 kinase1 are also reported in AD [224,225,230–232].

Particularly, the role of translation initiation defects (eIF2α and its kinases) are well established in AD pathology. eIF2α and its phosphorylation is one of the major checkpoints regulating translation initiation. GTP bound eIF2α associates with Met-tRNA and 40s ribosomes to form the pre-initiation complex. On finding the start codon on the mRNA, the eIF2α dissociates through GTP hydrolysis [233–236]. The GDP-eIF2α is recharged with GTP through the interaction with the guanosine exchange factor (GEF) eIF2B [233–236]. The phosphorylation of eIF2α significantly hinders the interaction between eIF2α and eIF2B, hence causing an inhibition of translation initiation. The phosphorylation of eIF2α is mediated by four kinases (PERK, PKR, GCN2 and HRI), each of which act as sensors for stress signals (misfolded protein ER stress, viral infections, amino acid starvation and heme deficiency/ oxidative stress respectively) [233–236]. The translation inhibition mediated by eIF2α is accompanied by translation activation of specific candidates such as ATF4 which help in coping with the stress response and restoring translation to normal levels [233–236]. This entire process mediated by increased eIF2α phosphorylation is termed as integrated stress response (ISR).

Elevated phosphorylation of eIF2α is a consistent observation in AD, both in post-mortem human brain samples and in transgenic mouse models, indicating inhibition of protein synthesis in AD [225,234–241]. Interestingly, genetic or pharmacological suppression of eIF2α kinases PERK or GCN2 alleviated the plasticity and memory impairments of the transgenic AD mice model [225,239]. Hence, many therapeutic approaches have been designed targeting the eIF2α phosphorylation and the ISR. One such drug candidate is ISRIB (small molecule inhibitor of ISR) which alleviates the protein synthesis response, synaptic plasticity and memory defects in the AD mouse model [234,235,240]. Additionally, the BACE1 mRNA is shown to get translationally activated under the conditions of ISR due to its specialized 5'UTR, thus tilting the APP processing to the amyloidogenic

pathway [242]. This is also suggestive that protein synthesis defect could occur pre-symptomatically leading to the synaptic defects and Aβ accumulation.

Figure 1.8.1 – Role of eIF2α phosphorylation and integrated stress response in AD pathogenesis (Figure taken from Mauricio M Oliveira et al, Seminars in Cell and Developmental Biology, 2021)

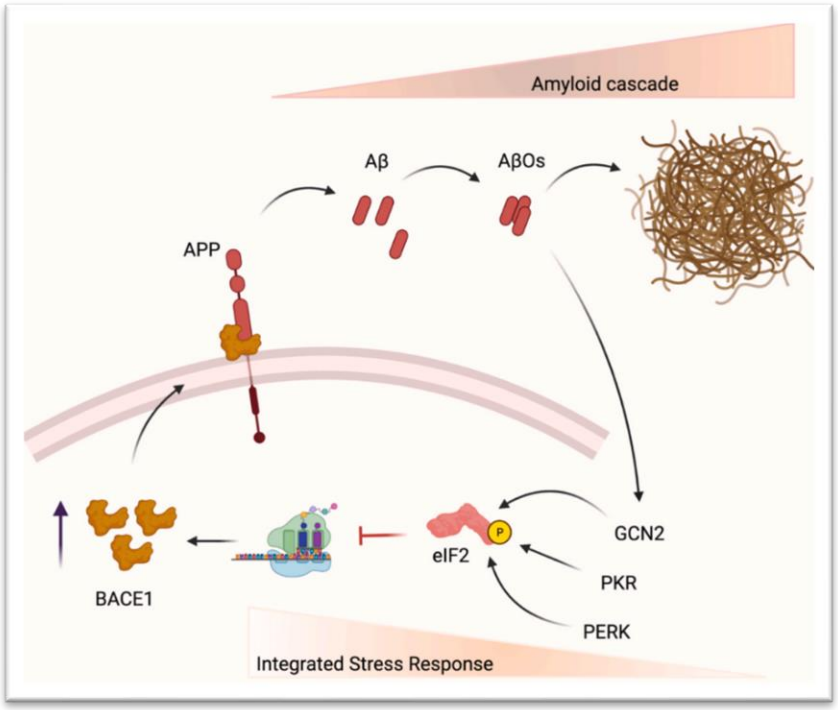

The other key step of translation regulation occurs at the stage of translation elongation, which is relatively less explored in the context of neurodegeneration. eEF2 and its phosphorylation is the checkpoint for the regulation of translation elongation. eEF2-GTP binds to the A-site on the ribosomes. Upon GTP hydrolysis, the ribosome undergoes a conformational change which enables the translocation of the ribosome on the mRNA, hence making the A-site available for the binding of the upcoming t-RNA during the translation elongation process [243]. The phosphorylation of eEF2 affects its binding to the A-site of the ribosome, hence reducing the ribosome translocation and translation elongation. The kinase which mediates the phosphorylation of eEF2 is the calcium-calmodulin kinase III or eEF2 kinase (eEF2K). Similar to eIF2α kinases which are sensitive to stress, eEF2 kinase is also activated upon energy deprivation, but it is also activated by calcium [243]. The calcium mediated regulation of eEF2K makes it important in the context of local translation regulation, especially upon synaptic stimulations which alter the calcium homeostasis in the neurons [244,245]. Unlike initiation, the role of translation elongation is not well explored in AD. Recently, there are some reports suggesting increased eEF2 phosphorylation in post mortem brain samples of AD patients and AD mouse models [243,246–248]. Additionally, reduction of eEF2K in the AD mouse model showed recovery of protein synthesis defects, spine morphology, post-synaptic density formation and finally synaptic long-term potentiation [246–248].

1.9 The gap in the knowledge or the missing links

1.9.1 APOE4 and protein synthesis

Though APOE4 is one of the most well-established risk factors for AD, and APOE4 TR mice mimics many of the AD phenotypes, the role of protein synthesis in the context of APOE4 is under explored. Considering - a) the synaptic dysfunction observed in the APOE4 model systems, b) the importance of protein synthesis for synaptic plasticity and c) the early defects of protein synthesis observed in familial AD model systems, protein synthesis regulation is likely to play a key role in APOE4 mediated synaptic pathology as well. Thus, investigating the defects of translation and their mechanisms in APOE4 model is critical, and a gap of knowledge in the field.

Although recent studies have shown the involvement of eEF2 in AD pathology, the mechanistic insights into this are minimal. The initiation step of translation can by-pass the dependency on eIF2α by adapting to cap-independent mechanisms. However, till date, eEF2-independent means of translation elongation are not known. Hence, I think that elongation would be a critical and fate-determining step for translation regulation. This was one of the reasons why we chose to investigate eEF2 mediated regulation of protein synthesis in APOE4 models. Additionally, I was also interested in exploring calcium as one of the possible connecting links between APOE4 and translation. Since calcium homeostasis is known to be disrupted in AD and calcium is a key factor regulating eEF2 kinase, we hypothesized that calcium could be an interesting link to provide mechanistic insights into APOE4 mediated defects.

Figure 1.9.1 – Cartoon depicting the proposed work – effect of APOE4 on protein synthesis

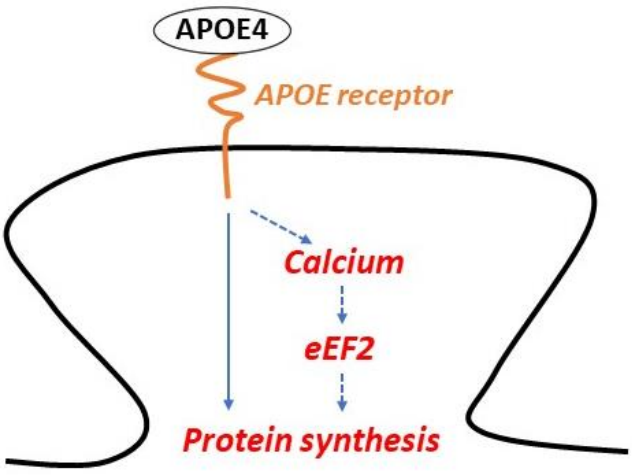

1.9.2 Aims, objectives and model system

With the above-mentioned ideas, we hypothesized that APOE4 would affect protein synthesis in neurons, and this could be one of the molecular mechanisms to explain APOE4 mediated synaptic dysfunction. Accordingly, we designed the following objectives for the study –

1. To investigate the effect of APOE4 on global protein synthesis in neurons, particularly on translation elongation

2. To investigate the effect of APOE4 on synaptic activity mediated protein synthesis in neurons
3. To examine the mechanism underlying the APOE4 mediated protein synthesis response

Since I was particularly interested in studying the effect on APOE on neuronal and synaptic protein synthesis, I chose rat primary cortical neurons (DIV15), rat cortical synaptoneurosomes and human iPSC derived neurons as the three model systems. The neurons or synaptoneurosomes were treated with APOE from different sources and evaluated for protein synthesis. The different sources of APOE and protein synthesis response are discussed in the results section.

1.10 References

Bibliography of the references in the introduction section is present at the end of the thesis in the references chapter.

Chapter 2

Materials and Methods

2.0 Ethics Statement

All rodent work was carried out with Sprague Dawley (SD) rats in accordance with the procedures approved by the Institutional Animal Ethics Committee (IAEC) and the Institutional Biosafety Committee (IBSC), InStem, Bangalore, India.

All the human stem cell work was carried out in accordance with and approval from the Institutional Human Ethics Committee, Institutional Stem Cell Committee, and Institutional Biosafety Committee at inStem, Bangalore, India. The proposal titled "Stem Cell Models for Discovery of RNA-mediated Regulation in Neurodegeneration" was given approval by the IC-SCR of inStem (Reference number – 017/SCR/IV-28.07.2015/RM-1).

2.1 Reagents used in the study

2.1.1 Antibodies used for Western blotting

Table 2.1

Protein	**Dilution**	**Catalog number, Company**
eEF2	1:1000	2332S, Cell Signaling Technologies
p-eEF2	1:2000	2331S, Cell Signaling Technologies
ERK	1:1000	9102, Cell Signaling Technologies
p-ERK	1:1000	9101, Cell Signaling Technologies
APOE	1:1000	NB110-60531, Novus Biologicals
Tuj1	1:4000	T8578, Sigma
RPLP0	1:4000	ab101279, Abcam
RPS6	1:3000	2217, Cell Signaling Technologies
PTEN	1:1000	9552S, Cell Signaling Technologies
PSD95	1:1000	P246, Sigma
α-tubulin	1:5000	T9026, Sigma
eIF2	1:1000	9722S, Cell Signaling Technologies
p-eIF2	1:1000	9721S, Cell Signaling Technologies
Secondary Rabbit HRP	1:5000	A0545, Sigma
Secondary Mouse HRP	1:5000	31430, Thermofisher Scientific

2.1.2 Antibodies used for Immunostaining

2.1.3 Drugs and dyes

Table 2.3

Drug	Concentration	Catalog number, Company
NMDA	20µM	0114, Tocris
RAP	200nM	553506-M, Sigma
Nifedipine	50µM	N7634, Sigma
MK801	25µM	0924, Tocris
Azidohomoalanine (AHA)	1µM	1066100, Click Chemistry tools
Cycloheximide	0.1mg/ml	C7698, Sigma
Puromycin	1mM	P8833, Sigma
Fluo-4AM	1µM	F14217, ThermoFisher Scientific
Fluo-8AM	2 µM	CAS 1345980-40-6, AAT Bioquest
Ionomycin	10µM	407950, Sigma

2.1.4 Neuronal Culture reagents

Table 2.4

Reagent	Catalog number, Company
Poly-L-Lysine	P2636, Sigma
Trypsin	15050057, ThermoFisher Scientific
MEM	10095080, ThermoFisher Scientific
FBS	12103C, Sigma
Neurobasal	21103049, ThermoFisher Scientific
B27	17504044, ThermoFisher Scientific
Glutamax	35050061, ThermoFisher Scientific

2.1.5 Stem Cell Culture and Neuronal Differentiation reagents

Table 2.5

Reagent	Catalog number, Company
mTeSr1	72232, Stem Cell Technologies
Matrigel	354277, Corning
Trypsin	15090046, ThermoFisher Scientific
Collagenase IV	17104019, ThermoFisher Scientific

Knock Out Serum Replacement	10828028, ThermoFisher Scientific
PBS	10010023, ThermoFisher Scientific
DMEM F12	21331020, ThermoFisher Scientific
Neurobasal	21103049, ThermoFisher Scientific
PenStrep	15140122, ThermoFisher Scientific
Glutamax	35050061, ThermoFisher Scientific
B27 without Vitamin A	12587–010, ThermoFisher Scientific
N2 supplement	17502–048, ThermoFisher Scientific
Poly-Ornithine	P4957, Sigma
Laminin	L2020, Sigma
SMAD Inhibitor SB431542	72232, Stem Cell Technologies
Noggin Analog LDN193189	72142, Stem Cell Technologies
EGF	AF-100-15, Pepotech
FGF	100-18C, Peprotech
DbcAMP	D0627, Sigma
BDNF	450-02, Peprotech
GDNF	450-10, Peprotech
L-Ascorbic Acid	A4403, Sigma
Rock Inhibitor	Y0503, Sigma
Accutase	A6964, Sigma

2.1.6 RNA isolation, cDNA synthesis and qPCR reagents

Table 2.6

Reagent	**Catalog number, Company**
Trizol LS	10296-028, ThermoFisher Scientific
Pellet paint	70748-3, Sigma
MMLV RT enzyme	M0253L, NEB
0.1 M dTT	707265ML, ThermoFisher Scientific
RNase Out	10777019, ThermoFisher Scientific
dNTPs	18427088, ThermoFisher Scientific
Random hexamer	N8080127, ThermoFisher Scientific

SYBR Green mix	RR420A, Takara

2.1.7 Primer sequences for qPCR

Table 2.7

mRNA	Forward Primer (5'→3')	Reverse Primer (5'→3')
PTEN	AGGACCAGAGATAAAAAGGGAGT	CCTTTAGCTGGCAGACCACA
PSD95	ATGGCAGGTTGCAGATTGGA	GGTTGTGATGTCTGGGGGAG
β - actin	GGCTCCTAGCACCATGAAGAT	AAACGCAGCTCAGTAACAGTC
α - tubulin	TATGCCAAGCGTGCCTTTGT	TGAAAGCAGCACCTTGTGAC

2.2 Buffer Compositions

2.2.1 Lysis Buffer

20mM Tris-HCl, 100mM KCl, 5mM $MgCl_2$, 1% Nonidet P-40 (NP40), 1mM Dithiothreitol (dTT), 1X Protease Inhibitor Cocktail, 40 units/ml RNase inhibitor, 1X Phosphatase Inhibitor, pH 7.4.

2.2.2 Gradient Buffer

20mM Tris-HCl pH (7.4), 100mM KCl, 5mM $MgCl_2$, 1% Nonidet P-40 (NP40), 1mM dTT, 1X Protease Inhibitor Cocktail, RNase inhibitor, 0.1mg/ml Cycloheximide.

2.2.3 Synaptoneurosome Buffer

118mM NaCl, 5mM KCl, 1.2mM $MgSO_4$, 2.5mM $CaCl_2$, 1.53mM KH_2PO_4, 212.7mM Glucose, 1X Protease Inhibitor Cocktail, pH 7.5.

2.2.4 Artificial Cerebro-Spinal Fluid (ACSF)

120mM NaCl, 3mM KCl, 1mM MgCl2, 3mM $NaHCO_3$, 1.25mM NaH_2PO_4, 15mM HEPES, 30mM glucose, with or without calcium (2mM $CaCl_2$), pH 7.4.

2.2.5 Resolving Gel Buffer – SDS PAGE

1.5mM Tris-HCl, pH 8.8.

2.2.6 Stacking Gel Buffer – SDS PAGE

1.0mM Tris-HCl, pH 6.8.

2.2.7 Running Buffer – SDS PAGE

25mM Tris-HCl, 190mM Glycine, 0.1% SDS, pH 8.3

2.2.8 Transfer Buffer – Western Blotting

25mM Tris-HCl, 190mM Glycine

2.2.9 TBST or Wash Buffer – Western Blotting

20mM Tris-HCl (pH 7.4), 150mM NaCl, 1% (v/v) Tween-20.

2.2.10 Blocking buffer – Western Blotting

5% Bovine Serum Albumin (BSA) prepared in 1X TBST.

2.2.11 Permeabilization buffer – Immunostaining

50mM Tris-HCl (pH 7.4), 150mM NaCl, 0.3% (v/v) Triton X-100.

2.2.12 $TBS_{50}t$ or Wash Buffer – Immunostaining

50mM Tris-HCl (pH 7.4), 150mM NaCl, 0.1% (v/v) Triton X-100.

2.2.13 Blocking buffer – Immunostaining

2% FBS and 2% BSA prepared in 1X $TBS_{50}t$.

2.2.14 Borate Buffer

40mM Boric acid, 10mM Borax, pH 8.5.

2.2.15 4X SDS loading buffer

250mM Tris-HCl (pH 6.8), 50% (v/v) Glycerol, 10% (w/v) SDS, 0.1% (w/v) Bromophenol Blue, 4% (v/v) β-mercaptoethanol.

2.3 Methods

2.3.1 Rat primary neuronal cultures

Preparation of the cell culture dishes - The dishes for neuronal cultures were coated for 5-6 hours at 37˚C with Poly-L-Lysine solution (0.2mg/ml) made in borate buffer (pH 8.5). Enough solution required to cover the surface of the dishes were added. After 5-6 hours, the excess solution was removed and washed thrice with autoclaved double distilled water, following which the plates were placed under UV for 2-3 hours. In case where coverslips were used, the coverslips were treated with nitric acid for 1 day, following which the excess nitric acid was washed with autoclaved water. Finally, the coverslips were autoclaved and used for coating with Poly-L-Lysine.

Neuronal cultures - Primary neuronal cultures were prepared from cerebral cortices of Sprague-Dawley rat embryos (E18.5) as previously published by our lab[1–3]. The cortex tissue was dissected from the embryos and trypsinized for 5 minutes at 37˚C using 0.25% trypsin. The trypsinized tissue was washed twice with 1X HBSS and homogenized in MEM media. The dissociated cells were counted with the help of tryphan blue using an automated cell counter. The cells were plated on pre-coated Poly-L-Lysine (P2636, Sigma) dishes at a density of 40000-50000 cells/cm^2 for biochemistry experiments and 30000-40000 cells/cm^2 for imaging-based experiments. For all the experiments, the neurons were initially plated on Minimum Essential Media (MEM, 10095080, ThermoFisher Scientific) supplemented with 10% FBS to aid their attachment. After 3 hours in MEM, the media was changed to Neurobasal (21103049, ThermoFisher Scientific) supplemented with B27 (17504044, ThermoFisher Scientific) and 1X Glutamax. Both MEM and Neurobasal complete media were subjected to filtration with 0.22µm filter before use. The neurons were maintained in culture for 15-

20 days at 37˚C, 5% CO_2 conditions by supplementing Neurobasal media every 5-6 days.

2.3.2 Synaptoneurosome preparation

Synaptoneurosomes were prepared from cortices of P30 male Sprague-Dawley rats as previously published[1,4,5]. The cortex tissue was dissected in chilled 1X PBS solution. The dissected cortices were homogenized on ice in 10 volumes of the synaptoneurosome buffer (118mM NaCl, 5mM KCl, 1.2mM $MgSO_4$, 2.5mM $CaCl_2$, 1.53mM KH_2PO_4, 212.7mM Glucose, 1X Protease Inhibitor Cocktail, pH 7.5). The homogenate was filtered through three 100µM nylon filters (NY1H02500, Merck Millipore) and one 11µM nylon filter (NY1102500, Merck Millipore). The filtrate was centrifuged at 1500 x g for 15 minutes at 4˚C. The pellet obtained was resuspended in 1.2ml synaptoneurosome buffer and used for APOE treatment.

2.3.3 iPSC maintenance and conditioned media collection

iPSC lines - The iPSCs (APOE KO, APOE 3/3, and APOE 4/4) were obtained from Bioneer A/S, Denmark. Briefly, the iPSCs from an 18-year old male of APOE 3/4 genotype were subjected to CRISPR-Cas9 gene editing to obtain isogenic iPSC lines of APOE KO, APOE 3/3, and APOE 4/4 genotypes[6].

iPSC culture - The iPSCs were maintained on hESC qualified Matrigel (354277, Corning) and cultured in mTeSR1 complete media (72232, Stem Cell Technologies) at 37˚C, 5% CO_2 conditions. CTK solution which is a mixture of 1mg/ml Collagenase IV (17104019, ThermoFisher Scientific), 0.25% Trypsin, 20% Knock-Out Serum (10828028, ThermoFisher Scientific), 1mM Calcium Chloride (made in PBS) was used to dissociate the iPSCs for passaging. The iPSCs were passaged once they reached about 80% confluency. The iPSCs were incubated with CTK solution for 5-6 minutes at 37˚C. After 5 minutes, the CTK solution was removed and the iPSCs were placed back in the incubator for 1 more minute. The colonies were collected in DMEM-F12 media supplemented with 10% KOSR and centrifuged at 1000rpm for 1-2 minutes. The pelleted cells were resuspended in fresh mTeSR1 media and plated on Matrigel coated dishes. The split ratio depended on the density of the iPSCs before the passage, but was usually maintained at 1→3.

Collection of conditioned media - Once the iPSCs reached about 50% confluency, the media was changed from mTeSR1 to Neurobasal supplemented with Glutamax. The iPSCs were washed once with Neurobasal before changing the media. The iPSCs were maintained in Neurobasal based media for 48 hours. After 48 hours, the conditioned media was collected, given a short spin at 1000 x g for 2 minutes to remove the cell debris and subjected to ELISA (ab108813, Abcam) to estimate the amount of APOE secreted by iPSCs.

2.3.4 Neuronal differentiation of iPSCs

The protocol for neural differentiation was adapted from Yichen Shi et al (Shi, Kirwan and Livesey, 2012) and Yu Zhang et al (Zhang et al., 2017) to differentiate iPSCs into forebrain glutamatergic neurons. The Neural Basic Media (NBM) for differentiation contained 50% DMEM F-12 (21331–020, ThermoFisher Scientific), 50% Neurobasal, 0.1% PenStrep, Glutamax, N2 (17502–048, ThermoFisher Scientific), and B27 without

Vitamin A (12587–010, ThermoFisher Scientific). Once the iPSCs reached 70-80% confluency on Matrigel-coated dishes, they were subjected to monolayer neural induction through Dual SMAD inhibition by changing the mTeSR1 media to Neural Induction Media (NIM). NIM is composed of NBM supplemented with small molecules SB431542 (10 µM, an inhibitor of TGFβ pathway) (72232, Stem Cell Technologies) and LDN193189 (0.1 µM, an inhibitor of BMP pathway) (72142, Stem Cell Technologies). The cells were subjected to neural induction for 12-15 days till a uniform neuroepithelial had formed. NIM was changed every day during the induction period. After the induction, the monolayer was dissociated using Accutase (A6964, Sigma). The dissociated cells were centrifuged at 1200 rpm for 3 minutes at room temperature. The pellet was resuspended in NIM and plated in NIM containing 10 µM ROCK inhibitor (Y0503, Sigma) overnight on pre-coated poly-L-ornithine/laminin dishes. These are considered as Passage 0 (P0) NSCs. Poly-L-Ornithine and Laminin coating was used for maintenance of neural progenitors and their terminal differentiation. Poly-L-Ornithine (1:10 dilution in 1X PBS) (P4957, Sigma) coating was performed at 37˚C for a minimum of 4 hours and maximum overnight. The excess Poly-L-Ornithine solution was removed and the plates were given 3 washes with 1X PBS. This was followed by overnight coating with Laminin (5 µg/ml diluted in 1X PBS) (L2020, Sigma) at 37˚C. The NSCs was maintained in Neural Expansion Media (NEM) which is composed of NBM supplemented with FGF (10 ng/ml) (100-18C, Peprotech) and EGF (10 ng/ml) (AF-100-15, Pepotech); and NSCs were passaged using dissociation reagent Accutase. NSCs beyond Passage 6 (P6) were not used for neuronal differentiation. Neuronal maturation and terminal differentiation were achieved by plating the neural stem cells at a density of 25,000-35,000 cells/cm2 in the Neural Maturation Media (NMM) composed of NBM supplemented with BDNF (20 ng/ml) (450-02, Peprotech), GDNF (10 ng/ml) (450-10, Peprotech), L-Ascorbic Acid (200 µM) (A4403, Sigma) and db-Camp (50 µM) (D0627, Sigma). The neurons were subjected to maturation for a period of 4-5 weeks by supplementing them with NMM every 4-5 days.

2.3.5 APOE treatment of neurons

The primary neurons or human iPSC derived neurons were treated with APOE from conditioned media or recombinant APOE protein (350-02, 350-04, Peprotech). For conditioned media treatment, the spent neuronal media was mixed with the APOE conditioned media in the ratio 1:1 such that the final APOE concentration used to treat the neurons was 8-10nM nM. In case of recovery, the conditioned media mixture was removed, and the spent neuronal media (neurobasal with B27 supplement) was added for recovery. For recombinant protein treatment, the neurons were treated with 15 nM of recombinant APOE3 or APOE4 protein in neurobasal media. In the experiments with no calcium in the external media, the neurons were treated with 15 nM recombinant APOE3 or APOE4 protein in Artificial Cerebrospinal Fluid (ACSF – 120 mM NaCl, 3 mM KCl, 1 mM $MgCl_2$, 3 mM $NaHCO_3$, 1.25 mM NaH_2PO_4, 15 mM HEPES, 30 mM glucose, pH 7.4) with or without calcium (2 mM $CaCl_2$). For stimulation of NMDAR receptors, 20 µM NMDA (0114, Tocris) was added in the neurobasal media for the required time periods. For NMDAR stimulation after APOE treatment, 20 µM NMDA was added during the last 5 minutes of the 20 minutes APOE treatment. For the pre-treatment with other drugs, Nifedipine (50 µM) (N7634, Sigma), MK801 (25 µM)

(0924, Tocris), or RAP (200 nM) (553506-M, Sigma) were added for 10 minutes before the addition of conditioned media mixture. After the treatment, the cells were lysed in buffer containing 20 mM Tris-HCl, 100 mM KCl, 5 mM $MgCl_2$, 1% Nonidet P-40 (NP40), 1 mM dTT, 1X Protease Inhibitor Cocktail, RNase inhibitor, 1X Phosphatase Inhibitor and centrifuged at 20000 x g, 4˚C for 20 minutes. The supernatant was either denatured in SDS-dye for Western blotting or in Trizol LS for RNA isolation.

2.3.6 APOE treatment of synaptoneurosomes

The resuspended synaptoneurosomes were treated with 20 nM recombinant APOE3 or APOE4 protein for 20 minutes at 37˚C with constant mixing at 350 rpm. For stimulation of NMDA receptors in the synaptoneurosomes, NMDA (40 µM) was added during the last 5 minutes of the 20 minutes treatment. For blocking APOE receptors, RAP (200 nM) was added 10 minutes before the addition of APOE. After the treatment, the synaptoneurosomes were given a short spin, the pellet was resuspended in lysis buffer (20 mM Tris-HCl, 100 mM KCl, 5 mM $MgCl_2$, 1% Nonidet P-40 (NP40), 1 mM dTT, 1X Protease Inhibitor Cocktail, RNase inhibitor, 1X Phosphatase Inhibitor) and centrifuged at 20000 x g, 4˚C for 20 minutes. The supernatant was denatured in SDS-dye and subjected to Western blotting.

2.3.7 Immunostaining

The APOE KO, APOE 3/3 and APOE 4/4 iPSCs grown on 4-well dishes were subjected to immunostaining of the pluripotency markers OCT4 and NANOG. The iPSCs were grown on coverslips and subjected to immunostaining once they reached 40-50% confluency. The iPSCs were fixed with 4% PFA for 10-15 minutes, which was followed by 3 washes with 1X PBS. This was followed by permeabilization with 0.3% Triton X-100 made in TBS_{50}. This was followed by 1 hour blocking with 2% BSA and 2% FBS prepared in $TBS_{50}T$. They were incubated with the primary antibody (prepared in blocking buffer) overnight at 4˚C. The details of the antibodies and their dilutions is mentioned in the material section. This was followed by 3 washes with $TSB_{50}T$ (approximately 10 minutes per wash) and 1-hour incubation with the secondary antibody (prepared in blocking buffer) at room temperature. The details of the antibodies and their dilutions is mentioned in the material section. After 3 washes with $TBS_{50}T$ following secondary antibody incubation (approximately 10 minutes per wash), the iPSCs were subjected to post-fixing with 4% PFA for 10-15 minutes. This was followed by 3 washes with 1X PBS and then mounting with Mowiol® 4-88 mounting media (81381, Sigma). The 4 well plates were imaged on Olympus IX73 inverted fluorescence microscope with 20X objective.

2.3.8 FUNCAT (Fluorescent non-canonical amino acid tagging)

For metabolic labeling, the existing neurobasal media of the DIV15 neurons was removed, and they were incubated in Methionine-free DMEM for 45 minutes. Following this, the neurons were treated with L-azidohomoalanine (AHA, 1 µM) (1066100, Click Chemistry tools) for 30 minutes in Met-free DMEM (21013024, ThermoFisher Scientific). They were then treated with 15 nM APOE3 or APOE4 recombinant protein in the same media (Met-free DMEM with AHA) for 1-minute or 20-minutes. For stimulation of NMDA receptors following APOE treatment, NMDA (20 µM) was added during the last 5 minutes of the 20 minutes treatment. For NMDA stimulation time point, 20 µM NMDA was added for 1,5 and 20 minutes. For FUNCAT

assays with MK801 (25 µM) pre-treatment, the drug was added during the last 20 minutes of AHA treatment. For FUNCAT assays with Nifedipine (50 µM) pre-treatment, the drug was added during the last 10 minutes of AHA treatment.

After the treatment, the coverslips were given one wash with 1X PBS and fixed with 4% PFA. After 15 minutes of fixing, they were washed thrice with 1X PBS. The neurons were permeabilized for 10 minutes with 0.3% Triton X-100 solution prepared in TBS_{50}. The permeabilized neurons were subjected to blocking for 1 hour with a mixture of 2% Bovine Serum Albumin (BSA) and 2% Fetal Bovine Serum (FBS) prepared in $TBS_{50}t$. After blocking, where the newly synthesized AHA incorporated proteins were tagged with an alkyne-fluorophore Alexa-Fluor 555 through click reaction for 2 hours at room temperature (C10269, CLICK-iT cell reaction buffer kit, Click Chemistry Tools). After 3 washes with $TBS_{50}t$ (approximately 10 minutes per wash), the neurons were stained with MAP2 antibody (prepared in blocking buffer) and incubated overnight at 4˚C. 3 washes with $TBS_{50}t$ (approximately 10 minutes per wash) were given after primary antibody incubation. This was followed by staining with secondary antibody (prepared in blocking buffer) against MAP2 for 1 hour at room temperature. 3 washes with $TBS_{50}t$ (approximately 10 minutes per wash) were given after secondary antibody incubation.

For FUNCAT experiments with 1-minute APOE treatment, 20-minute APOE treatment, APOE treatment + NMDA stimulation, primary antibody MAP2 (M9942, Sigma) and corresponding secondary antibody Alexa Flour 488 were used. For FUNCAT experiments with NMDA stimulation time points, MK801 +APOE treatment, Nifedipine + APOE treatment, primary antibody MAP2 (ab32454, Abcam) and corresponding secondary antibody Alexa Flour 647 were used.

The coverslips were mounted with Mowiol® 4-88 mounting media (81381, Sigma) and imaged on Olympus FV300 confocal laser scanning inverted microscope with 60X objective. The pinhole was kept at 1 Airy Unit and the optical zoom at 2X to satisfy Nyquist's sampling criteria in XY direction. The objective was moved in Z-direction with a step size of 1 µM (~8-9 Z-slices) to collect light from the planes above and below the focal plane. The image analysis was performed using FIJI software and the maximum intensity projection of the slices was used for quantification of the mean fluorescent intensities. The mean fluorescent intensity of the FUNCAT channel was normalized to the MAP2 channel for comparison between different APOE treatment conditions.

2.3.9 SDS PAGE and Western Blotting

The APOE treated neuron lysates or synaptoneurosome lysates denatured in 4X Laemmli buffer were run on SDS PAGE gels and subjected to western blotting analysis. The denatured lysates were run on 10% resolving and 5% stacking acrylamide/bis-acrylamide gels at a constant voltage of 75-80V. Once the samples reached the bottom, the gels were taken out and subjected to overnight transfer onto PVDF membrane at constant voltage of 20V. After transfer, the blots were stained with PonceauS to check for the transfer. The blots were also cut depending on the requirement of the proteins to be detected and their corresponding molecular weights. The blots were subjected to blocking for 1 hour at room temperature using 5% BSA prepared in TBST. This was followed by primary antibody (prepared in blocking buffer) incubation for 2-3 hours at

room temperature. HRP (Horseradish peroxidase) tagged secondary antibodies were used for primary antibody detection. The secondary antibodies (prepared in blocking buffer) were incubated with the blots for 1 hour at room temperature. Three washes of 5-10 minutes each were given after primary and secondary antibody incubation using TBST solution. The blots were subjected to chemiluminescent based detection of the HRP tagged proteins using the ECL mixture. The solution A and B of the ECL mixture was mixed in the ratio 1:1, incubated with the blots for 1-2 minutes, then removed and imaged in the ImageQuant/ GelDoc system.

All the western blot quantifications were performed using densitometric analysis on ImageJ software. For the analysis of eEF2 phosphorylation and ERK phosphorylation, the samples were run in duplicates where one set was used to probe for the phospho-proteins (p-eEF2 and p-ERK), and the other set was used to probe for the total proteins (eEF2 and ERK). In each set, the loading control used was Tuj1. In every set, eEF2 and ERK were probed on the same blot. Hence, the Tuj1 blot used to normalize the eEF2 and ERK blot was the same in a given set. Similarly, p-eEF2 and p-ERK were probed on the same blot for a given set. Hence, Tuj1 blot of the corresponding set was used to normalize the p-eEF2 and p-ERK blot of that set. Thus, for each sample, the ratios of p-eEF2/Tuj1 and eEF2/Tuj1 were obtained separately. Further, the ratio of p-eEF2/Tuj1 to eEF2/Tuj1 was calculated to get the final ratio of p-eEF2/eEF2. Similar analyses were done for calculating the ratios of p-ERK/ERK and p-eIF2/eIF2. For eIF2 phosphorylation analysis, the samples were run in duplicates (one set for phospho-protein, one set for total protein). Tuj1 was used as the normalizing control for each blot. For PTEN and PSD95 level analysis, the blots were cut; PTEN and PSD95 were probed on the same blot and Tuj1 was used as the normalizing control for each set. For RPLP0 and RPS6 distribution analysis, the individual polysome fractions were run and probed for the ribosomal proteins. The densitometric value was obtained for each fraction. The values from fractions 1-11 were summed up to get the total value. Further, the percentage distribution of the ribosomal protein in each fraction was calculated as *(densitometric value of the fraction/total densitometric value) *100*. When the distribution of the ribosomal protein in F1-6 or F7-11 or F3-4 were calculated, the sum of the percentages in the mentioned fractions were considered. The details of the antibodies used, and their dilutions are given in the table at the materials section.

2.3.10 RNA isolation

The neuron lysates were subjected to RNA isolation using the Trizol method. In case of total RNA levels measured from neurons, approximately 10% of the lysate prepared from 2 million neurons was used for RNA isolation. In case of polysome profiling samples, 200 µl was used from each fraction for RNA isolation. The lysates were mixed with 3 times more volume of Trizol LS solution. The samples were placed on the rotor for 5 minutes to enable proper mixing of lysates with Trizol LS. 0.2 ml Chloroform was added per 0.75 ml Trizol LS and incubated for 5 minutes. The samples were mixed once again and centrifuged at 12000g, 4˚C for 15 minutes. After the spin, the aqueous phase on the top was collected and transferred to another fresh tube. This was mixed with isopropanol solution (0.5 ml isopropanol was used per 0.75 ml Trizol LS solution) along with 2µl pellet paint and incubated at room temperature for 5-10 minutes. The samples were centrifuged at 12000g, 4˚C for 15 minutes. After the spin, the supernatant was

discarded and the 200µl of chilled 80% ethanol was added into each tube. The pellet was dislodged by giving a short vortex and centrifuged at 10000g, 4˚C for 10 minutes. The ethanol supernatant was discarded and the pellets were air dried till the ethanol evaporated. The dried pellets were resuspended in 10 µl of DEPC treated water. The extracted RNA was subjected to NanoDrop to measure the quantity and purity.

2.3.11 cDNA synthesis

The isolated RNA was subjected to reverse transcription to obtain the cDNA samples. In case of polysome samples, the entire RNA isolated from each fraction was subjected to cDNA synthesis. In case of total neuron lysate, 0.5-1 µg RNA was used for cDNA synthesis. The total volume of RNA was made up to 10 µl. Each RNA sample was mixed with 1 µl of Random Hexamer (50 µM) and 1 µl of dNTPs mix (10 mM each). This mixture was incubated at 65˚C for 5 minutes and then placed on ice for at least 1 minute. Master mix for the reverse transcription was prepared such that 10 µl of the master mix was added to each RNA sample. 10 µl of the master mix contained 2 µl of the 10X MMLV RT buffer, 2 µl of 0.1M dTT, 0.3 µl of the MMLV RT enzyme, 0.2 µl of RNase Out (RNase inhibitor). The RNA mix along with the master mix was incubated at 42˚C for 1 hour, followed by 75˚C for 10 minutes.

2.3.12 qPCR

The qPCR was performed for the required gene using SYBR green method. The details of the primers used for each candidate mRNA is mentioned in the material section. A master mix was prepared using 5 µl SYBR green master mix, 1 µl primer mix (10 µM mix of forward and reverse primer) and 3 µl water. 9 µl of the SYBR mix was added to each well on the qPCR plate. 1 µl of the required cDNA sample was added per well and subjected to qPCR amplification and detection. Primer against β-actin mRNA was used as the control. Ct value of the mRNA of interest and β-actin mRNA was noted. Copy number of mRNA of interest and β-actin was calculated and the ratio of this was considered for analysis. In case of polysome samples, the Ct value and copy number of the mRNA in each fraction was measured and percentage distribution was calculated.

2.3.13 Polysome profiling

The DIV15 neurons (~1.5 to 2 million cells) were treated with APOE3 or APOE4 iPSC conditioned media for 20 minutes. For stimulation of NMDARs, NMDA (20 µM) was added during the last 5 minutes of the 20 minutes treatment. After the treatment, the cells were lysed in about 1ml of lysis buffer containing 0.1 mg/ml Cycloheximide (C7698, Sigma) and centrifuged at 20000 x g, 4˚C for 20 minutes. The supernatant was loaded on 15%-45% linear sucrose gradient. 15% and 45% sucrose solutions were prepared in the gradient buffer and mixed with the gradient maker to prepare 10ml of 15-45% gradient. The gradients were loaded with approximately 900µl of the lysates and subjected to ultracentrifugation at 39000 rpm, 4˚C for 1.5 hours. After the spin, 60% sucrose was used to pump the separated factions of the gradient through the polysome profiler and 1ml fractions were collected (11 fractions in total). As the fractions were collected, they were passed through a UV spectrophotometer to obtain the absorbance profile at 254nm. The individual fractions were subjected to Western blotting to probe for ribosomal protein RPLP0 and RNA isolation/qPCR to probe for candidate mRNAs.

To identify actively translating polysomes, the cells were treated with 1 mM Puromycin (P8833, Sigma) and lysed in the buffer containing Puromycin instead of Cycloheximide. The Puromycin-sensitive fractions 7-11 were considered as the actively translating fractions whereas the Puromycin-insensitive fractions 1-6 were considered as the non-translating pool. The ratio was considered as shown –

Ratio of (Translating pool / Non-translating pool) = Ratio of (sum of percentage of mRNA or protein in fractions 7-11 / sum of percentage of mRNA or protein in fractions 1-6)

To further dissect the distribution of mRNAs/proteins in the non-translating pool, fractions 1-6 were further divided into fractions 1-3 (inhibitory complex) and fractions 4-6 (ribosomal subunits and monosomes). In this case, the percentage was calculated with respect to distribution in fractions 1-6 as total. The enrichment of the mRNAs/proteins in the inhibitory complex was calculated as –

Sum of percentage of mRNAs or proteins in fractions 1-3 / Sum of percentage of mRNAs or proteins in fraction 4-6

2.3.14 Calcium imaging

Calcium imaging was perfomed with DIV15 neurons plated on Nunc glass-bottomed imaging dishes. The imaging and washes were performed with ACSF media (120 mM NaCl, 3 mM KCl, 1 mM $MgCl_2$, 3 mM $NaHCO_3$, 1.25 mM NaH_2PO_4, 15 mM HEPES, 2 mM $CaCl_2$, 30 mM glucose, pH 7.4). The cells were washed once with ACSF and incubated at 37˚C with 1 ml of freshly prepared Fluo4-AM dye solution (1µM Fluo4-AM and 0.002% Pluronic acid in ACSF) (F14217, ThermoFisher Scientific) for 20 minutes. They were given two washes and incubated in ACSF at 37˚C for 10-20 minutes to enable the de-esterification of the dye. Further, the ACSF was removed and replaced with 800-900 µl of fresh ACSF before imaging. The drugs Nifedipine (50µM) and MK801 (25µM) were added during this de-esterification incubation step. During the drug treatment, all the washes were performed with ACSF containing the corresponding drug and imaged in ACSF containing the drug. The neurons were imaged using Olympus FV300 confocal laser scanning inverted microscope with 20X objective, illuminated with 488 nm lasers. The neurons were imaged for a total time of 7 minutes at a rate of 3 seconds per frame (140 frames in total). They were imaged in basal condition for 1 minute (20 frames). Following that, they were imaged for 5 minutes (100 frames) with addition of APOE recombinant protein (20 nM) or NMDA (20 µM). Finally, they were imaged for 1 minute (20 frames) with the addition of Ionomycin solution (10 µM Ionomycin with 10 mM $CaCl_2$) (407950, Sigma). The images obtained were analyzed using the Time-Series Analyzer plug-in on FIJI software. The average intensities were obtained for the selected ROIs (ROIs were drawn manually and the Ionomycin responsive cells were included). The change in fluorescent intensity at each frame was normalized to the initial fluorescent intensity of the first frame (F0) for each ROI. The normalized change in fluorescent intensity ($\Delta F/F0$) was plotted along the time axis and used for statistical analysis as well. For calculation of changes at 1-minute and 2-minutes after APOE addition, sum of the intensities before APOE addition (F0) and sum of the intensities after 1-minute or 2-minutes of APOE addition (F) was calculated. The summed values were used to calculate the $\Delta F/F0$ value or $(F-F0)/F0$ value.

2.3.15 Statistical analyses

All statistical analyses were performed using Graph Pad Prism software. The normality of the data was checked using the Kolmogorov-Smirnov test. For experiments with less than 5 data points, parametric statistical tests were applied. Data were represented as mean ± SEM in all biochemical experiment graphs. FUNCAT and calcium imaging data was represented as boxes and whiskers with all the individual data points. Statistical significance was calculated using Unpaired Student's t-test (2 tailed with equal variance) in cases where 2 groups were being compared. One-way ANOVA was used for multiple group comparisons, followed by Tukey's multiple comparison test or Dunnett's multiple comparison test. P-value less than 0.05 was considered to be statistically significant.

2.4 References

1. Kute, P. M., Ramakrishna, S., Neelagandan, N., Chattarji, S. & Muddashetty, Ravi. S. NMDAR mediated translation at the synapse is regulated by MOV10 and FMRP. *Molecular Brain* **12**, 65 (2019).

2. Ghosh Dastidar, S. *et al.* Distinct regulation of bioenergetics and translation by group I mGluR and NMDAR. *EMBO reports* (2020) doi:10.15252/embr.201948037.

3. Ravindran, S., Nalavadi, V. C. & Muddashetty, R. S. BDNF induced translation of limk1 in developing neurons regulates dendrite growth by fine-tuning cofilin1 activity. *Frontiers in Molecular Neuroscience* (2019) doi:10.3389/fnmol.2019.00064.

4. Muddashetty, R. S., Kelić, S., Gross, C., Xu, M. & Bassell, G. J. Dysregulated metabotropic glutamate receptor-dependent translation of AMPA receptor and postsynaptic density-95 mRNAs at synapses in a mouse model of fragile X syndrome. *Journal of Neuroscience* (2007) doi:10.1523/JNEUROSCI.0937-07.2007.

5. Paul, A. *et al.* Differential regulation of syngap1 translation by FMRP modulates eEF2 mediated response on NMDAR activity. *Frontiers in Molecular Neuroscience* (2019) doi:10.3389/fnmol.2019.00097.

6. Schmid, B. *et al.* Generation of a set of isogenic, gene-edited iPSC lines homozygous for all main APOE variants and an APOE knock-out line. *Stem Cell Research* (2019) doi:10.1016/j.scr.2018.11.010.

Chapter 3

Sources of APOE

3.0 Introduction

Apolipoprotein E (APOE) belongs to the family of lipoproteins well characterized for their function of lipid transport, highly expressed in the liver [1,2]. APOE is the most abundant lipoprotein expressed in the central nervous system (CNS) [3]. In the CNS, astrocytes are the primary cell types which largely express APOE [2–5], whereas neurons are known to express APOE under conditions of stress[2,5–7]. ABCA1 (ATP-binding cassette protein) interacts with APOE and transports cholesterol, thus making the astrocyte secreted APOE lipidated in nature[8]. The lipidation status of APOE is shown to create differences in the binding of APOE to Aβ[9], thus influencing the clearance of Aβ. However, the lipidation of APOE does not seem to affect the signaling pathways activated by the binding of APOE to its cognate receptors in neurons[10,11].

In order to study the effect of APOE on neuronal protein synthesis, we decided to use APOE from two major sources – the cell secreted APOE which is lipidated in nature and the recombinant APOE protein which is not lipidated. The use of recombinant protein helps in achieving APOE treatment of uniform concentration across batches. Previously, studies have reported the use of APOE secreted from astrocytes or cell lines overexpressing different isoforms of APOE[5,10,12–16]. However, the limitation of using cell lines overexpressing different APOE isoforms would be that the cell lines have the endogenous APOE expressed and secreted as well. This could also influence the expression and secretion of the over-expressed APOE isoforms. To our advantage, we had the availability of isogenic iPSC lines expressing different isoforms of APOE (APOE 3/3, APOE 4/4 and APOE KO) obtained from the CRISPR-Cas9 editing of the original line APOE 3/4. We also had the understanding that stem cells express and secrete abundant amounts of APOE[12]. Based on this, we thought that the iPSCs could be an apt source for APOE as we had isogenic iPSCs endogenously expressing different isoforms of APOE. Hence, we used the stem cell secreted medium as the primary source for APOE, which we propose is better than using conditioned media from APOE over-expressing cell lines. We have also used the recombinant APOE protein as an additional source to validate the results from the conditioned media.

Results

3.1 Characterization of the APOE isogenic iPSC lines

In order to use the APOE secreted by stem cells as a source, we began by performing a thorough characterization of the iPSCs expressing different APOE isoforms. APOE 3/4 was the primary iPSC line obtained from the fibroblasts of an 18-year-old healthy male[17,18]. APOE 3/4 iPSC line was subjected to CRISPR/Cas9 based gene editing to obtain the other isogenic iPSC lines expressing different isoforms APOE 3/3, APOE 4/4 and APOE KO[17,18]. We did not use the conditioned media from the heterozygous APOE 3/4 iPSC line as the proportion of expression and secretion of the individual

isoforms (APOE3 and APOE4) remains unclear, which would make the analysis inconclusive.

APOE KO, APOE 3/3 and APOE 4/4 iPSCs showed the expression of the pluripotency markers OCT4 and Nanog (Fig 3.1 A). OCT4 and Nanog expression was nuclear, as characterized by the use of nuclear marker DAPI (Fig 3.1 A). All the three iPSC lines showed normal karyotyping profile (Fig 3.1 B). APOE 3/3 and APOE 4/4 iPSCs expressed similar and substantial amounts of APOE while there was absence of APOE expression in the APOE KO iPSC lines (Fig 3.1 C).

Figure 3.1

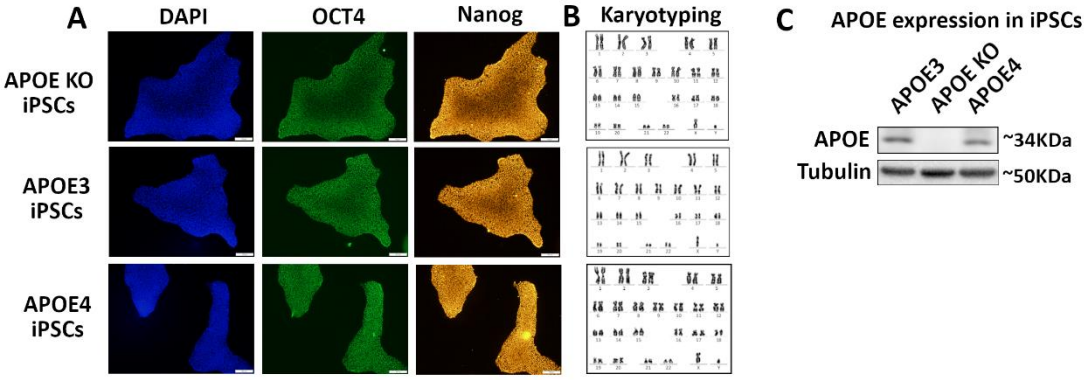

Figure 3.1 – Characterization of APOE isogenic iPSC lines

A – Representative images of APOE KO, APOE 3/3 and APOE 4/4 iPSCs subjected to immunostaining for nuclear marker (DAPI) along with pluripotency markers OCT4 (green) and Nanog (gold). Scale bar - 100µM.

B – Karyotyping profiles of APOE KO, APOE 3/3 and APOE 4/4 iPSCs

C – Representative immunoblots indicating the expression of APOE and loading control α-tubulin in APOE KO, APOE 3/3 and APOE 4/4 iPSCs.

3.2 APOE secretion by iPSCs

In order to estimate the amount of APOE secreted by the iPSCs, the iPSCs were first subjected to a media change from stem cell media mTeSR1 to Neurobasal once they reached 50% confluency. This step was carried out to ensure that the APOE treatment of the neurons was performed in Neurobasal based conditioned media rather than mTeSR1 based conditioned media. The iPSCs were maintained in Neurobasal for 48 hours. The 2-day conditioned media had significant amount of APOE secreted into it as detected by Western Blotting (Fig 3.2 A). The secreted APOE in the 2-day conditioned media was also stable for up to 24 hours when kept in culture conditions (37˚C, 5% 0_2) (Fig 3.2 B). The amount of APOE in the 2-day conditioned media was estimated using ELISA (Fig 3.2 C). The APOE concentration in 2-day conditioned media was approximately 0.3µg/ml (Fig 3.2 D). This was comparable between APOE3 and APOE4 conditioned media while APOE KO iPSCs did not show any APOE secretion.

Figure 3.2

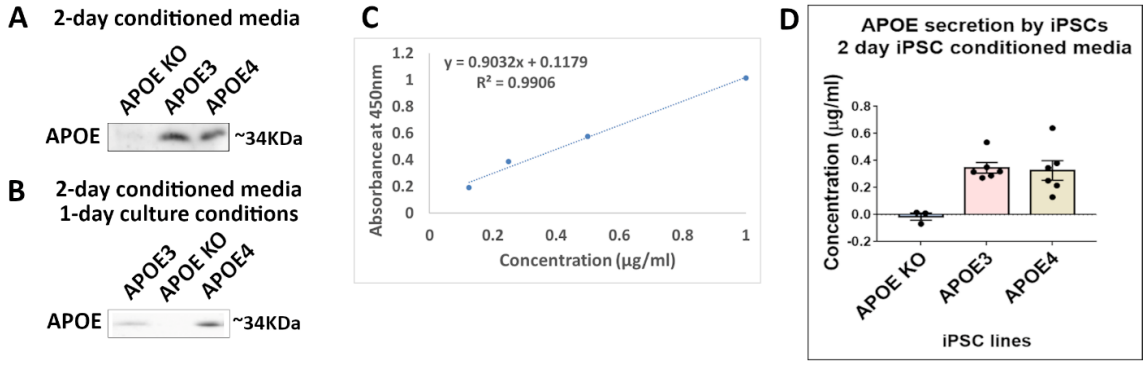

Figure 3.2 - APOE secretion by iPSCs

A – Representative immunoblots showing the APOE secreted in 2-day iPSC conditioned media.

B - Representative immunoblots showing the APOE secreted in 2-day iPSC conditioned media kept in culture conditions for 1 day.

C – Standard curve for APOE ELISA.

D – The ELISA based measurements of the APOE concentrations in the 2-day iPSC conditioned media.

3.3 Validation of APOE treatment paradigm

Primary cortical neurons (DIV15) obtained from the cortices of the Sprague-Dawley rat embryos (E18.5) were used for the validation of the APOE treatment paradigm (Fig 3.3 A). The iPSC conditioned media was mixed with the existing neuron media to obtain the APOE concentration of 8-10nM. Along with conditioned media, we used recombinant APOE protein as another source of APOE. Previously, many studies have reported the activation of ERK signaling pathway downstream of APOE treatment [10–12,19]. APOE mediated increase in ERK phosphorylation was also shown to be isoform-dependent, with APOE4 causing the maximal phosphorylation of ERK [10,12]. Hence, we used this well-established readout of ERK phosphorylation to validate our treatment paradigm and APOE sources.

Previous studies have reported that the ERK phosphorylation in neurons increased with around 15-minute APOE treatment and remained high for up to 2 hours treatment, following which the p-ERK recovered to basal levels[10,11]. Hence, we looked at the phosphorylation of ERK in primary neurons after 20-minute treatment with APOE conditioned media, as it was the earliest time point at which the ERK phosphorylation was increased. As reported previously, APOE4 conditioned media treatment for 20 minutes caused the maximal increase in ERK phosphorylation (Fig 3.3 B), whereas APOE3 and APOE KO conditioned media treatment was similar to control conditions (Fig 3.3 B). Similarly, APOE4 recombinant protein treatment (15nM) for 20 minutes also caused a marked increase in ERK phosphorylation, thus validating that the APOE mediated signaling effects are independent of lipidation status (Fig 3.3 C). Further, we conducted the APOE treatment experiments in rat cortical synaptoneurosomes

(biochemically isolated synaptic compartments) to verify if the APOE mediated signaling effects are synaptic. APOE4 recombinant protein treatment (15nM) for 20 minutes caused an increase in ERK phosphorylation in the synaptoneurosomes as well (Fig 3.3 D). To confirm the specificity of APOE mediated ERK activation, we pre-incubated the neurons with APOE receptor antagonist RAP, followed by the APOE conditioned media treatment for 20 minutes. RAP treatment blocked the APOE4 mediated increase in ERK phosphorylation validating that the signaling was mediated by APOE binding to its cognate receptors in the neurons (Fig 3.3 E).

Figure 3.3

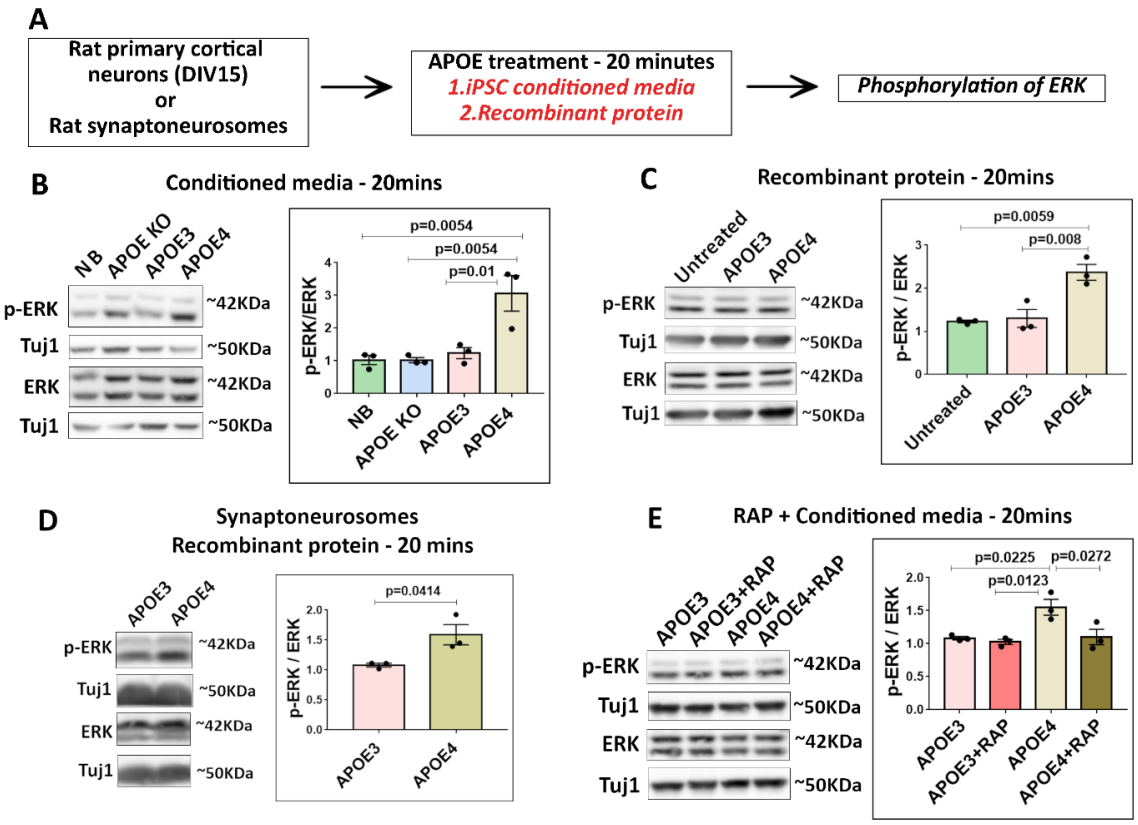

Figure 3.3 - Validation of APOE treatment paradigm

A – Experimental design.

B – Representative immunoblots showing the levels of p-ERK, ERK and Tuj1 in rat primary cortical neurons after 20 minutes treatment with APOE conditioned media. The graph represents the ratio of p-ERK to ERK normalized to Tuj1 under different APOE conditions. Data is represented as mean +/- SEM. N=3, One-way ANOVA (p=0.0031) followed by Tukey's multiple comparison test.

C - Representative immunoblots showing the levels of p-ERK, ERK and Tuj1 in rat primary cortical neurons after 20 minutes treatment with APOE recombinant protein (15nM). The graph represents the ratio of p-ERK to ERK normalized to Tuj1 under different APOE conditions. Data is represented as mean +/- SEM. N=3, One-way ANOVA (p=0.0041) followed by Tukey's multiple comparison test.

D - Representative immunoblots showing the levels of p-ERK, ERK and Tuj1 in rat cortical synaptoneurosomes after 20 minutes treatment with APOE recombinant protein (15nM). The graph represents the ratio of p-ERK to ERK normalized to Tuj1 under different APOE conditions. Data is represented as mean +/- SEM. N=3, Unpaired Student's t-test.

E - Representative immunoblots showing the levels of p-ERK, ERK and Tuj1 in rat primary cortical neurons after RAP pre-incubation (200nM) followed by 20 minutes treatment with APOE conditioned media. The graph represents the ratio of p-ERK to ERK normalized to Tuj1 under different APOE conditions. Data is represented as mean +/- SEM. N=3, One-way ANOVA (p=0.0097) followed by Tukey's multiple comparison test.

3.4 Summary and discussion

In summary, we have characterized the APOE iPSCs for their pluripotency markers, karyotype profile and APOE expression. We have quantified the APOE secretion by iPSCs and optimized the APOE iPSC conditioned media treatment paradigm for primary cortical neurons and synaptoneurosomes. The use of synaptoneurosomes showed that the effect of APOE signaling was synaptic as well. This was consistent with the findings that APOE receptors LRP1 and ApoEr2 are present at the post-synapse[13,20,21]. We have validated the treatment by probing for ERK phosphorylation, a previously established readout for APOE treatment. Importantly, we did not observe any changes in ERK phosphorylation depending on the APOE source, as APOE from conditioned media and recombinant protein showed comparable results. This was consistent with other studies which have shown that the signaling effect of APOE does not depend on the source[10]. Hence, we decided to use APOE from both sources for our future experiments related to protein synthesis analysis as well. I would like to bring to notice that while APOE concentration in conditioned media came up to 8-10nM, recombinant APOE protein was used at 15nM. We initially began our experiments using 15nM as the APOE concentration based on ERK phosphorylation and previous literature. But, since APOE secreted by iPSCs is not constant and we dilute APOE iPSC conditioned media with neurobasal in the ratio 1:1, we did not get 15nM of APOE every time from iPSCs. Hence, the concentration of APOE in iPSC conditioned media ranged from 8-15nM while we used recombinant protein at 15nM.

Further, we have verified that the ERK activation was specific to APOE binding to its receptors in the neurons by using APOE receptor antagonist RAP. The control experiments using RAP and APOE KO conditioned media validated that the results we observed were APOE specific. A major concern in the field of APOE has been regarding the concentrations of the APOE protein used in the experiments. The concentration of APOE in the mouse brain interstitial fluid and human cerebrospinal fluid is in the low nanomolar range [22,23]. Hence, the APOE concentrations we have used in the study are quite comparable to physiological concentrations of low nanomolar range, as opposed to the many studies which have used APOE concentrations of high micromolar range [10,12,13]. Thus, we have established stem cell secreted APOE as a valid source and optimized our treatment paradigm with two different sources of APOE at physiologically relevant concentrations.

3.5 References

1. Martínez-Martínez, A. B. *et al.* Beyond the CNS: The many peripheral roles of APOE. *Neurobiology of Disease* vol. 138 (2020).

2. Xu, Q. *et al.* Profile and regulation of apolipoprotein E (ApoE) expression in the CNS in mice with targeting of green fluorescent protein gene to the ApoE locus. *Journal of Neuroscience* **26**, (2006).

3. Mahley, R. W. Central Nervous System Lipoproteins. *Arteriosclerosis, Thrombosis, and Vascular Biology* **36**, (2016).

4. Boyles, J. K., Pitas, R. E., Wilson, E., Mahley, R. W. & Taylor, J. M. Apolipoprotein E associated with astrocytic glia of the central nervous system and with nonmyelinating glia of the peripheral nervous system. *Journal of Clinical Investigation* **76**, (1985).

5. Harris, F. M. *et al.* Astroglial regulation of apolipoprotein E expression in neuronal cells: Implications for Alzheimer's disease. *Journal of Biological Chemistry* **279**, 3862–3868 (2004).

6. Boschert, U., Merlo-Pich, E., Higgins, G., Roses, A. D. & Catsicas, S. Apolipoprotein E expression by neurons surviving excitotoxic stress. *Neurobiology of Disease* **6**, (1999).

7. Pu-Ting, X. *et al.* Specific regional transcription of apolipoprotein E in human brain neurons. *American Journal of Pathology* **154**, (1999).

8. Wahrle, S. E. *et al.* ABCA1 is required for normal central nervous system apoE levels and for lipidation of astrocyte-secreted apoE. *Journal of Biological Chemistry* **279**, (2004).

9. Tokuda, T. *et al.* Lipidation of apolipoprotein E influences its isoform-specific interaction with Alzheimer's amyloid β peptides. *Biochemical Journal* **348**, (2000).

10. Huang, Y. W. A., Zhou, B., Wernig, M. & Südhof, T. C. ApoE2, ApoE3, and ApoE4 Differentially Stimulate APP Transcription and Aβ Secretion. *Cell* **168**, 427-441.e21 (2017).

11. Ohkubo, N. *et al.* Apolipoprotein E4 Stimulates cAMP Response Element-binding Protein Transcriptional Activity through the Extracellular Signal-regulated Kinase Pathway. *Journal of Biological Chemistry* **276**, 3046–3053 (2001).

12. Huang, Y. W. A., Zhou, B., Nabet, A. M., Wernig, M. & Südhof, T. C. Differential Signaling Mediated by ApoE2, ApoE3, and ApoE4 in Human Neurons Parallels Alzheimer's Disease Risk. *Journal of Neuroscience* **39**, 7408–7427 (2019).

13. Chen, Y., Durakoglugil, M. S., Xian, X. & Herz, J. ApoE4 reduces glutamate receptor function and synaptic plasticity by selectively impairing ApoE receptor recycling. *Proceedings of the National Academy of Sciences of the United States of America* **107**, (2010).

14. Morikawa, M. *et al.* Production and characterization of astrocyte-derived human apolipoprotein E isoforms from immortalized astrocytes and their interactions with amyloid-β. *Neurobiology of Disease* **19**, (2005).

15. Qi, G. *et al.* ApoE4 Impairs Neuron-Astrocyte Coupling of Fatty Acid Metabolism. *Cell Reports* **34**, (2021).

16. Du, J., Chang, J., Guo, S., Zhang, Q. & Wang, Z. ApoE 4 reduces the expression of Aβ degrading enzyme IDE by activating the NMDA receptor in hippocampal neurons. *Neuroscience Letters* **464**, (2009).

17. Poon, A. *et al.* Generation of a gene-corrected isogenic control hiPSC line derived from a familial Alzheimer's disease patient carrying a L150P mutation in presenilin 1. *Stem Cell Research* **17**, 466–469 (2016).

18. Schmid, B. *et al.* Corrigendum to "Generation of a set of isogenic, gene-edited iPSC lines homozygous for all main APOE variants and an APOE knock-out line" [Stem Cell Res. 34/1873–5061 (2019) 101349–55] (Stem Cell Research (2019) 34, (S1873506118302794), (10.1016/j.scr.2018.11.010)). *Stem Cell Research* vol. 48 (2020).

19. Qiu, Z., Hyman, B. T. & Rebeck, G. W. Apolipoprotein E receptors mediate neurite outgrowth through activation of p44/42 mitogen-activated protein kinase in primary neurons. *Journal of Biological Chemistry* **279**, 34948–34956 (2004).

20. Nakajima, C. *et al.* Low density lipoprotein receptor-related protein 1 (LRP1) modulates N-methyl-D-aspartate (NMDA) receptor-dependent intracellular signaling and NMDA-induced regulation of postsynaptic protein complexes. *Journal of Biological Chemistry* **288**, (2013).

21. Hoe, H. S. *et al.* Apolipoprotein E receptor 2 interactions with the N-Methyl-D-aspartate receptor. *Journal of Biological Chemistry* **281**, (2006).

22. Ulrich, J. D. *et al.* In vivo measurement of apolipoprotein e from the brain interstitial fluid using microdialysis. *Molecular Neurodegeneration* **8**, (2013).

23. Wang, C. *et al.* Gain of toxic apolipoprotein E4 effects in human iPSC-derived neurons is ameliorated by a small-molecule structure corrector article. *Nature Medicine* **24**, (2018).

Chapter 4

Effect of APOE on regulation of protein synthesis

4.0 Introduction

APOE4 is associated with AD as a risk factor due to its role in Aβ clearance[1–4]. However, many studies have shown that the presence of APOE4 alone is sufficient to increase the Aβ load, implying APOE4 as a causative factor for AD[5,6]. Additionally, there are increasing evidences suggesting the independent role of APOE4 in causing cognitive defects. Several studies and meta-analysis of studies have shown that adult APOE4 carriers (with no AD pathology) perform significantly worse in measures of episodic memory, executive functioning, and global cognitive ability compared to APOE4 non-carriers[7–10]. APOE4 carriers with Mild Cognitive Impairment (MCI) showed an accelerated cognitive decline compared to non-carriers of APOE4, reflecting early signs of AD pathology as well [11]. In corroboration, APOE4 knock-in mice model also show defects in spatial learning and memory[12,13]. In fact, the learning and memory deficits were observed in younger APOE4 mice (3 months old) and it persisted in older adults (18 months) as well[12]. Correspondingly, there was a reduction of spine density, dendritic length and arborization in the entorhinal cortex of the 3-month-old APOE4 mice[12]. Several other studies have also reported reduction of neurite outgrowth, dendritic complexity and spine density in the cortex of APOE4 mice models[13–20], as early as 1-month as well[21]. The loss of synaptic proteins, particularly in an age-dependent manner, is also well-reported in APOE4 mice models[13,22].

However, the mechanisms behind APOE4 mediated synaptic defects are poorly understood. Though dysregulation of protein synthesis is implicated in familial models of AD [23–25], the role of translation is not studied in the context of APOE4. As I have explained earlier in the introduction, protein synthesis is an integral process important for synaptic structure and function. Hence, we decided to investigate the effect of APOE on protein synthesis regulation, as a possible mechanism to understand APOE4 mediated synaptic and cognitive defects.

Results

4.1 APOE4 treatment for 20 minutes increases eEF2 phosphorylation in rat neurons and synaptoneurosomes

In order to study the effect of APOE on protein synthesis, we treated rat primary cortical neurons (DIV 15) or rat synaptoneurosomes with APOE for 20 minutes, a time point which we have validated previously using ERK phosphorylation. We used APOE from iPSC conditioned media (8-10nM) and recombinant APOE protein (15nM) as the two sources of APOE (Fig 4.1 A). One of the primary readouts we used to assess protein synthesis response was phosphorylation status of eukaryotic translation elongation factor 2 (eEF2) (Fig 4.1 A). eEF2 is a GTP-dependent translocase which catalyzes the step of ribosome translocation during protein synthesis [26]. eEF2 is regulated by phosphorylation at the site of Threonine 56 (T56) in the GTP binding domain, which

hinders the association of eEF2 with the ribosome [27–30]. Hence, increased eEF2 phosphorylation is a readout for global reduction of protein synthesis [26,30–32].

The neurons treated with APOE4 conditioned media for 20 minutes showed a significant increase in eEF2 phosphorylation compared to APOE3 conditioned media, APOE KO conditioned media and neurobasal conditions (Fig 4.1 B). APOE3 or APOE KO conditioned media treatment had no effect on neuronal translation upon 20-minute exposure (Fig 4.1 B). This indicated that APOE4 conditioned media treatment for 20 minutes caused a global reduction of protein synthesis. The same effect was observed with recombinant APOE protein treatment as well. While 20-minute treatment with APOE4 recombinant protein caused an increase in eEF2 phosphorylation, APOE3 recombinant protein treatment for 20 minutes did not affect eEF2 phosphorylation compared to control conditions (Fig 4.1 C). Additionally, synaptoneurosomes treated with recombinant APOE4 protein also showed an increase in eEF2 phosphorylation compared to APOE3 treatment, verifying that the effect of APOE4 on protein synthesis is synaptic as well (Fig 4.1 D). Thus, 20-minute treatment with APOE4 (conditioned media or recombinant protein) caused an increase in eEF2 phosphorylation, both in neurons and synaptoneurosomes preparations, implying an inhibitory effect of APOE4 on global protein synthesis.

Figure 4.1

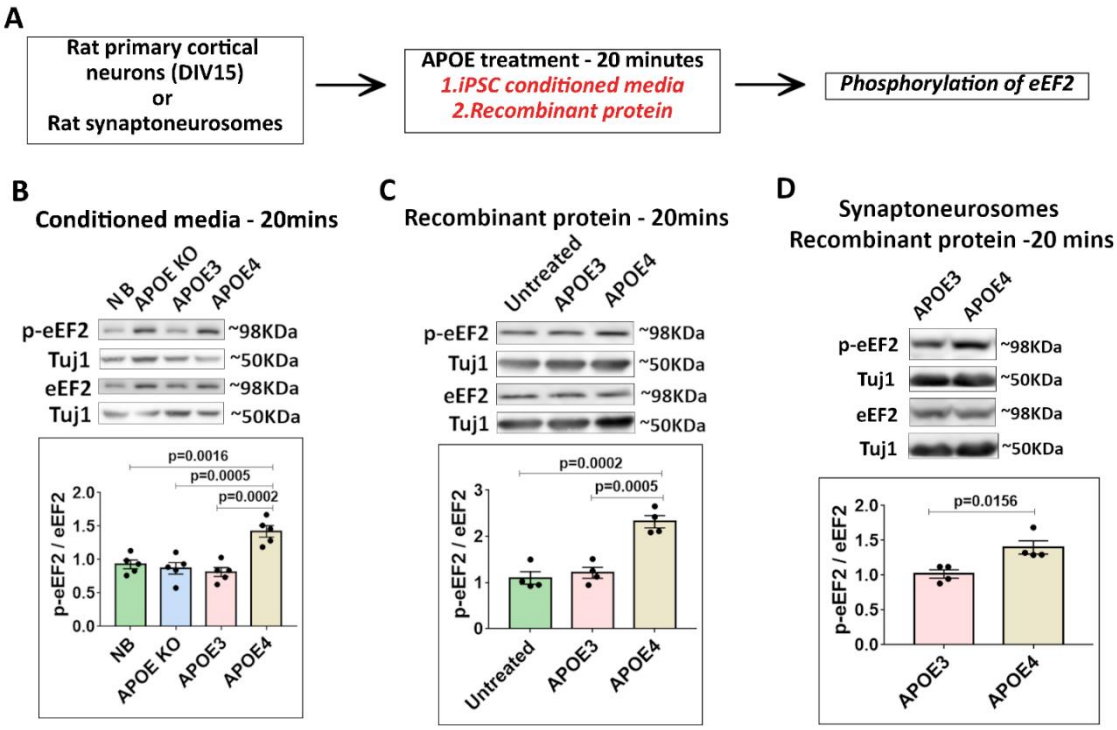

Figure 4.1 - APOE4 treatment for 20 minutes increases eEF2 phosphorylation in rat neurons and synaptoneurosomes

A – Experimental design

B - Representative immunoblots showing the levels of p-eEF2, eEF2 and Tuj1 in rat primary cortical neurons after 20 minutes treatment with APOE iPSC conditioned media. The graph represents the ratio of p-eEF2 to eEF2 normalized to Tuj1 under

different APOE conditions. Data is represented as mean +/- SEM. N=5, One-way ANOVA (p=0.0001) followed by Tukey's multiple comparison test.

C - Representative immunoblots showing the levels of p-eEF2, eEF2 and Tuj1 in rat primary cortical neurons after 20 minutes treatment with recombinant APOE protein. The graph represents the ratio of p-eEF2 to eEF2 normalized to Tuj1 under different APOE conditions. Data is represented as mean +/- SEM. N=4, One-way ANOVA (p=0.0002) followed by Tukey's multiple comparison test.

D - Representative immunoblots showing the levels of p-eEF2, eEF2 and Tuj1 in rat cortical synaptoneurosomes after 20 minutes treatment with recombinant APOE protein. The graph represents the ratio of p-eEF2 to eEF2 normalized to Tuj1 under different APOE conditions. Data is represented as mean +/- SEM. N=4, Unpaired Student's t-test.

4.2 APOE4 mediated increase in eEF2 phosphorylation is dependent on APOE receptors

In order to ensure the robustness of the effect of APOE4 on protein synthesis, we validated our results in human iPSC derived neuron system. We subjected APOE KO iPSCs to neuronal differentiation to obtain forebrain glutamatergic neurons. Human APOE KO neurons (1 month into neuronal maturation) were treated with APOE3 or APOE4 iPSC conditioned media for 20 minutes (Fig 4.2 A). As observed previously, the neurons treated with APOE4 conditioned media showed an increase in eEF2 phosphorylation compared to APOE3 treated neurons (Fig 4.2 B). Thus, we validated the inhibitory effect of APOE4 on global protein synthesis in human neurons as well as in mouse neurons treated with astrocyte secreted APOE.

Further, to confirm the specificity of the effect of APOE on eEF2 phosphorylation, rat primary cortical neurons were treated with APOE3 or APOE4 iPSC conditioned media in the presence of APOE receptor antagonist RAP (Fig 4.2 C). RAP abolished the APOE4 mediated increase in eEF2 phosphorylation, while it had no effect in the presence of APOE3 conditioned media (Fig 4.2 C) or APOE KO conditioned media (Fig 4.2 D). RAP prevented the APOE4 mediated increase in eEF2 phosphorylation in the synaptoneurosomes as well (Fig 4.2 E), while it had no effect upon APOE3 treatment (Fig 4.2 E). Synaptoneurosomes treated with RAP in the absence of APOE did not show any change in eEF2 phosphorylation (Fig 4.2 F), confirming the specificity of APOE4 response. Thus, similar to ERK phosphorylation, the effect of APOE4 on eEF2 phosphorylation was also dependent on APOE binding to its cognate receptors in neurons and signaling downstream of APOE receptors.

Figure 4.2

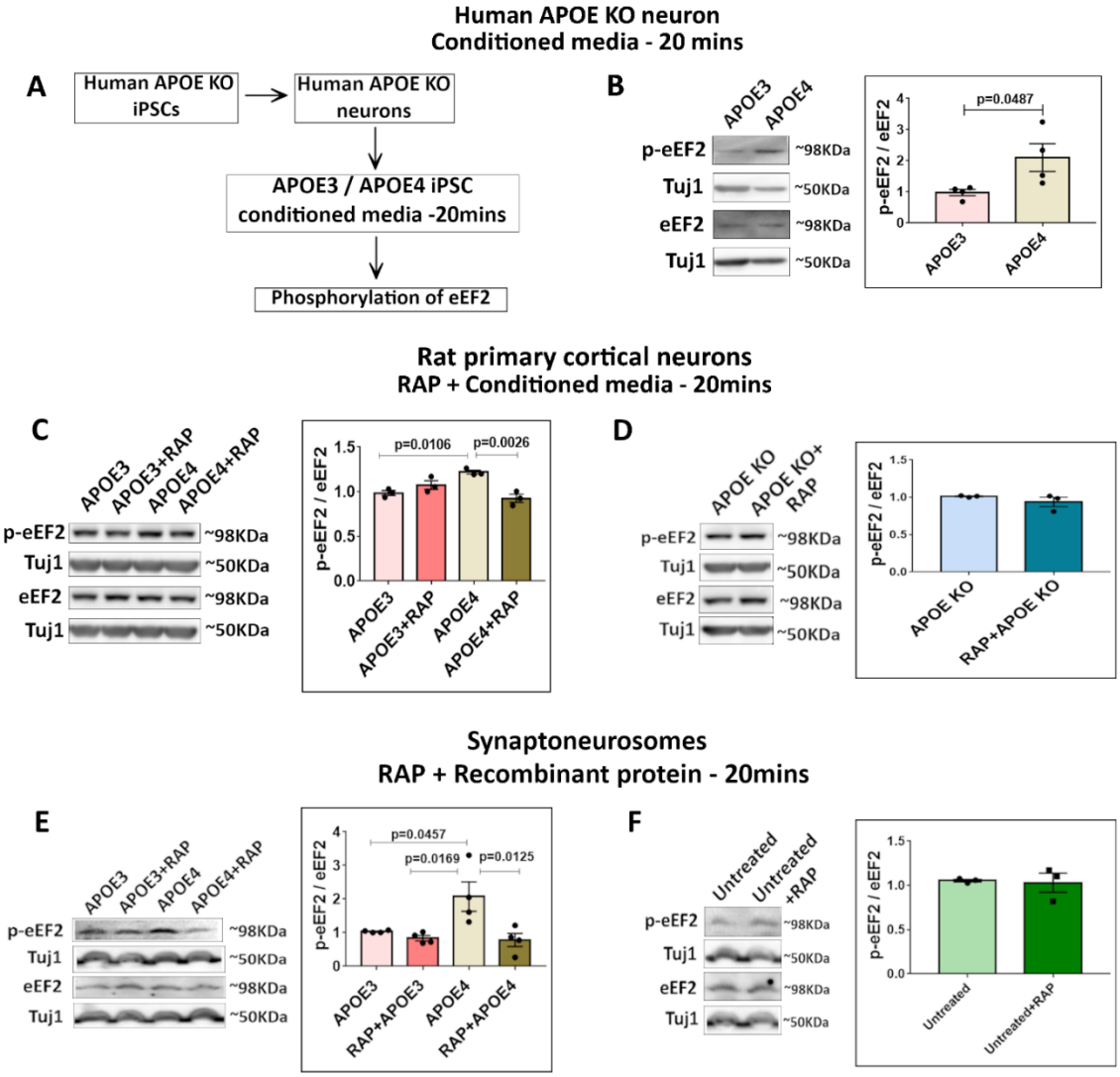

Figure 4.2 - APOE4 treatment for 20 minutes increases eEF2 phosphorylation in mouse neurons and human neurons

A - Experimental design for APOE treatment of human iPSC derived neurons

B – Representative immunoblots showing the levels of p-eEF2, eEF2 and Tuj1 in human APOE KO neurons after 20 minutes treatment with APOE3 or APOE4 iPSC conditioned media. The graph represents the ratio of p-eEF2 to eEF2 normalized to Tuj1 under different APOE conditions. Data is represented as mean +/- SEM. N=4, Unpaired Student's t-test.

C - Representative immunoblots showing the levels of p-eEF2, eEF2 and Tuj1 in rat primary cortical neurons after RAP pre-incubation (200nM) followed by 20 minutes treatment with APOE3 or APOE4 conditioned media. The graph represents the ratio of p-eEF2 to eEF2 normalized to Tuj1 under different APOE conditions. Data is represented as mean +/- SEM. N=5, One-way ANOVA (p=0.003) followed by Tukey's multiple comparison test.

D - Representative immunoblots showing the levels of p-eEF2, eEF2 and Tuj1 in rat primary cortical neurons after RAP pre-incubation (200nM) followed by 20 minutes treatment with APOE KO conditioned media. The graph represents the ratio of p-eEF2 to eEF2 normalized to Tuj1 under different APOE conditions. Data is represented as mean +/- SEM. N=3, Unpaired Student's t-test (ns).

E - Representative immunoblots showing the levels of p-eEF2, eEF2 and Tuj1 in rat cortical synaptoneurosomes after RAP pre-incubation (200nM) followed by 20 minutes treatment with APOE3 or APOE4 recombinant protein. The graph represents the ratio of p-eEF2 to eEF2 normalized to Tuj1 under different APOE conditions. Data is represented as mean +/- SEM. N=4, One-way ANOVA (p=0.0088) followed by Tukey's multiple comparison test.

F - Representative immunoblots showing the levels of p-eEF2, eEF2 and Tuj1 in rat cortical synaptoneurosomes after RAP incubation (200nM) in the absence of APOE treatment. The graph represents the ratio of p-eEF2 to eEF2 normalized to Tuj1 under different APOE conditions. Data is represented as mean +/- SEM. N=3, Unpaired Student's t-test (ns).

4.3 Both APOE3 and APOE4 inhibit global protein synthesis at 1-minute, while only APOE4 is inhibitory at 20 minutes

In order to obtain a more profound understanding of the effect of APOE on protein synthesis, we decided to investigate an earlier treatment time point. Since the effect of APOE on protein synthesis was receptor mediated, we hypothesized that we would be able to capture this earlier than 20-minutes as well. Hence, we treated the rat primary cortical neurons with APOE3 or APOE4 iPSC conditioned media at two different time points – 1 minute and 20 minutes. Interestingly, at 1-minute time point, both APOE3 and APOE4 conditioned media treatment caused an increase in eEF2 phosphorylation compared to control conditions (Fig 4.3 A). However, by 20-minute time point, eEF2 phosphorylation had recovered to basal levels in APOE3 treated conditions, while it continued to remain high in APOE4 treated neurons (Fig 4.3 A). These results indicated that both APOE3 and APOE4 treatment for 1-minute caused a global inhibition of protein synthesis, whereas only APOE4 treatment caused translation inhibition at 20-minute.

Though eEF2 phosphorylation is a robust readout for translation status, it is also a correlative one. Hence, we validated the results using a more direct readout for protein synthesis such as FUNCAT (Fluorescent Non-Canonical Amino-acid Tagging). Briefly, the neurons were subjected to Methionine deprivation for 45 minutes followed by the incorporation of Methionine analog AHA for 30 minutes (Fig 4.3 C). The AHA incorporated in the de-novo synthesized proteins was detected using a fluorescent tag attached to it through click chemistry (Fig 4.3 C). The assay was validated using the control condition of Methionine deprivation without AHA incorporation, but followed by click chemistry reaction. Under this condition, the fluorescent FUNCAT signal following click chemistry was absent, indicating that the FUNCAT signal was indeed from the AHA incorporated de-novo synthesized proteins only (Fig 4.3 B). We also performed MAP2 immunostaining following the FUNCAT reaction to detect the neurons and normalize the FUNCAT signal.

We conducted the FUNCAT assay with APOE treatment conditions where the neurons were exposed to APOE after the AHA incorporation step (Fig 4.3 C). At 1-minute, treatment with both APOE3 and APOE4 recombinant protein (15nM) showed a reduction in the FUNCAT signal compared to untreated conditions, indicating a reduction of global protein synthesis (Fig 4.3 D and E). However, at 20-minutes, only APOE4 treated neurons showed a significant reduction in the FUNCAT signal, whereas the FUNCAT signal of APOE3 treated neurons was similar to untreated conditions (Fig 4.3 F and G). The results with the FUNCAT assay corroborated the eEF2 phosphorylation results. In summary, both APOE3 and APOE4 inhibited global protein synthesis at 1-minute. While APOE3 treated neurons recovered, APOE4 continued to inhibit protein synthesis at 20-minute time point as well.

Figure 4.3

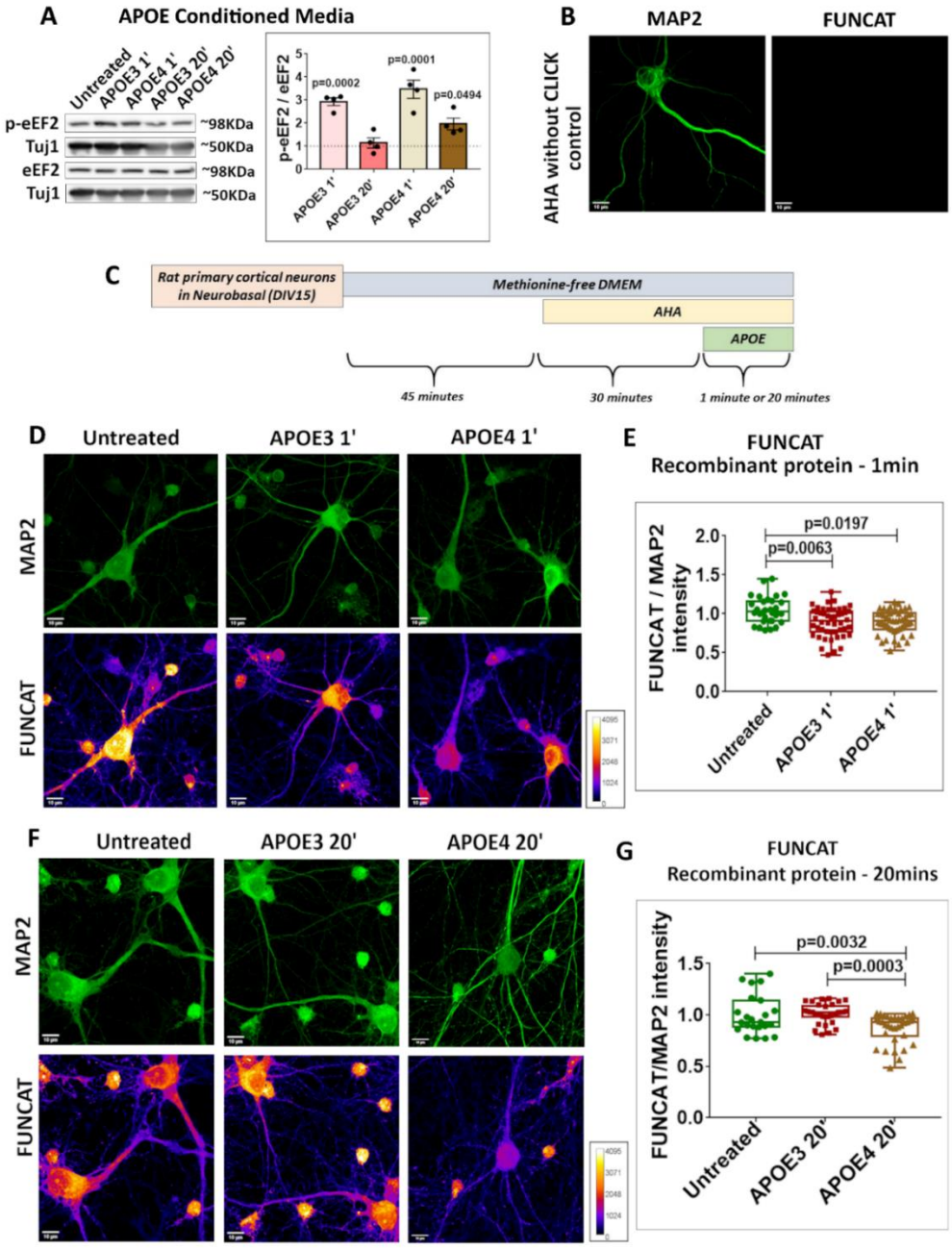

Figure 4.3 - Both APOE3 and APOE4 inhibit global protein synthesis at 1-minute, while only APOE4 is inhibitory at 20 minutes

A - Representative immunoblots showing the levels of p-eEF2, eEF2 and Tuj1 in rat primary cortical neurons after 1 minute and 20 minutes treatment with APOE3 or APOE4 iPSC conditioned media. The graph represents the ratio of p-eEF2 to eEF2 normalized to Tuj1 under different APOE conditions. Data is represented as mean +/- SEM. Dotted line indicates the untreated condition. All the APOE treatments were normalized to untreated condition. N=4. One-way ANOVA ($p<0.0001$) followed by Dunnett's multiple comparison test.

B – Validation of the FUNCAT assay. Representative images indicating MAP2 and FUNCAT fluorescent signals in rat primary cortical neurons subjected to click chemistry without AHA incorporation.

C – Experimental design for the FUNCAT assay.

D - The representative images for MAP2 and FUNCAT fluorescent signals in rat primary cortical neurons under untreated conditions or after 1 minute treatment with APOE3 / APOE4 recombinant protein (15nM) (Scale bar - 10µM).

E - The graph represents the quantification of the FUNCAT fluorescent intensity normalized to MAP2 fluorescent intensity under different APOE treatment conditions at 1-minute time point. N = 20-40 neurons from 4 independent experiments, One-way ANOVA ($p=0.0058$) followed by Tukey's multiple comparison test.

F - The representative images for MAP2 and FUNCAT fluorescent signals in rat primary cortical neurons under untreated conditions or after 20-minute treatment with APOE3 / APOE4 recombinant protein (15nM) (Scale bar - 10µM).

G - The graph represents the quantification of the FUNCAT fluorescent intensity normalized to MAP2 fluorescent intensity under different APOE treatment conditions at 20-minute time point. N = 20-40 neurons from 4 independent experiments, One-way ANOVA ($p=0.0001$) followed by Tukey's multiple comparison test.

4.4 APOE3 treated neurons recover from protein synthesis inhibition faster than APOE4 treated neurons

Previously, we observed that both APOE3 and APOE4 caused an inhibition of protein synthesis, but APOE3 treated neurons recovered to basal conditions faster than APOE4 treated neurons. In order to investigate this further, we subjected the neurons to a phase of recovery after 1-minute or 20-minute APOE treatment (Fig 4.4 A). Rat primary cortical neurons (DIV15) were treated with APOE3 or APOE4 iPSC conditioned media for 1 minute, following which APOE conditioned media was removed and they were subjected to recovery using pre-conditioned neurobasal for 5-minutes, 10-minutes and 20-minutes (Fig 4.4 A). Firstly, we observed that 1-minute treatment with APOE4 led to higher increase in eEF2 phosphorylation compared to 1-minute APOE3 treatment (Fig 4.4 B). With 5-minutes of recovery following 1-minute treatment, eEF2 phosphorylation continued to remain significantly high in APOE4 treated neurons compared to APOE3 treatment (Fig 4.4 B). However, by 10-minutes and 20-minutes of recovery, APOE4 treated neurons had recovered to the same extent as APOE3 treated

neurons (Fig 4.4 B). This clearly demonstrated that the recovery from translation inhibition was slower in APOE4 treated neurons.

Additionally, we also subjected the 20-minute APOE4 conditioned media treated neurons to a 20-minute recovery period (Fig 4.4 A and C). The phosphorylation of eEF2 reduced significantly following the 20-minute recovery indicating that the APOE4 treated neurons can recover from the translation inhibition even with 20-minute treatment if APOE is removed from the media (Fig 4.4 C). Along the same lines, we questioned what would the translation response be if the neurons were treated with APOE chronically. To answer this, we treated rat primary cortical neurons with APOE iPSC conditioned media for 24 hours (Fig 4.4 D). We observed that 24-hour APOE4 treatment caused a substantial increase in eEF2 phosphorylation compared to APOE3 or APOE KO conditions (Fig 4.4 D). Thus, chronic presence of APOE4 also caused an inhibition of protein synthesis.

Figure 4.4

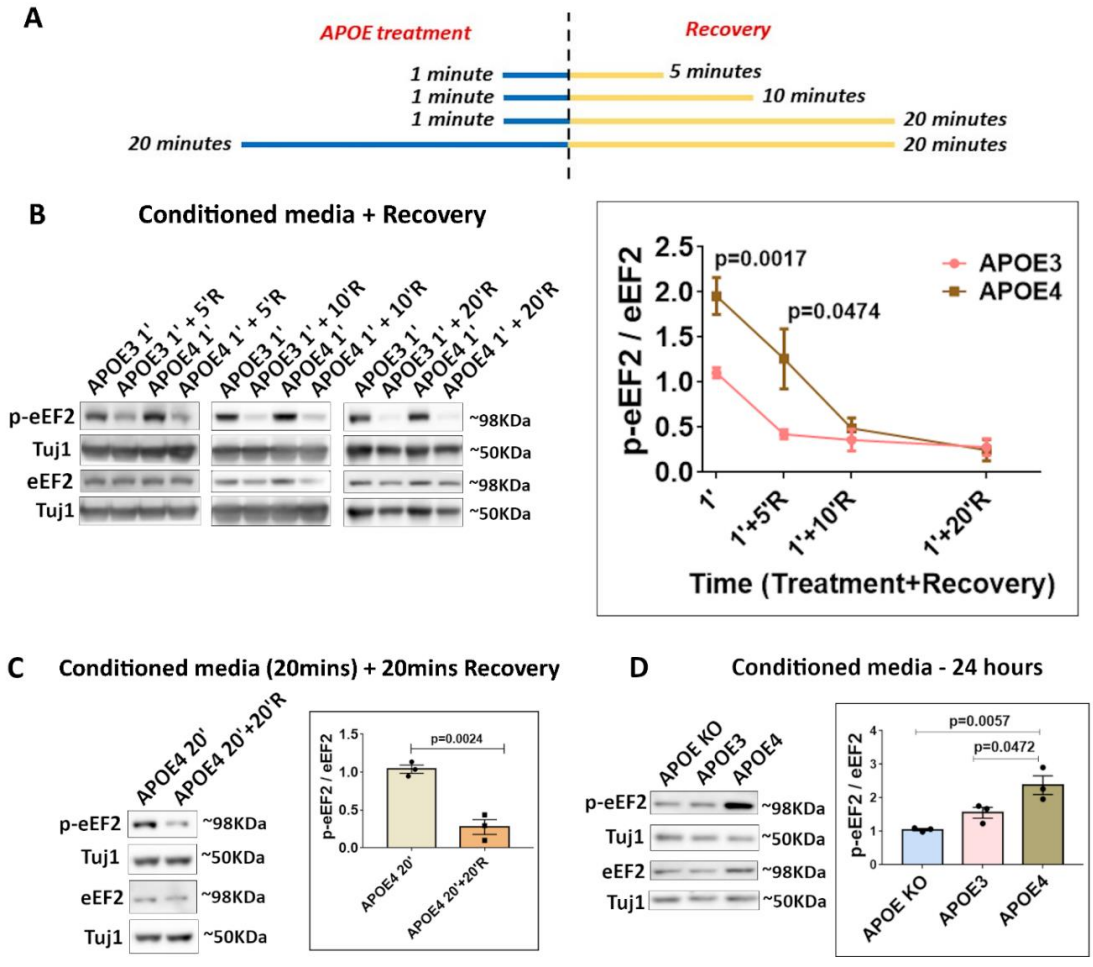

Figure 4.4 - APOE3 treated neurons recover from protein synthesis inhibition faster than APOE4 treated neurons

A – Experimental design for APOE treatment followed by recovery

B - Representative immunoblots showing the levels of p-eEF2, eEF2 and Tuj1 in rat primary cortical neurons after 1 minute treatment with APOE3 or APOE4 iPSC conditioned media followed by 5-minute, 10-minute and 20-minute recovery with pre-conditioned neurobasal media. The graph represents the ratio of p-eEF2 to eEF2 normalized to Tuj1 under different APOE conditions. The data from each recovery time point is normalized to its corresponding 1-minute APOE treated set. Data is represented as mean +/- SEM. For APOE3 1' and APOE4 1', N=8, Unpaired Student's t-test. For APOE 1' + 5'R, N=4, Unpaired Student's t-test. For APOE 1' + 10'R, N=5. For APOE 1' + 20'R, N=3.

C - Representative immunoblots showing the levels of p-eEF2, eEF2 and Tuj1 in rat primary cortical neurons after 20-minute treatment with APOE4 iPSC conditioned media followed by 20-minute recovery with pre-conditioned neurobasal media. The graph represents the ratio of p-eEF2 to eEF2 normalized to Tuj1 under different APOE conditions. Data is represented as mean +/- SEM. N=3, Unpaired Student's t-test.

D - Representative immunoblots showing the levels of p-eEF2, eEF2 and Tuj1 in rat primary cortical neurons after 24-hour treatment with APOE KO or APOE3 or APOE4 iPSC conditioned media (8-10nM). The graph represents the ratio of p-eEF2 to eEF2 normalized to Tuj1 under different APOE conditions. Data is represented as mean +/- SEM. N=3, One-way ANOVA (p=0.0068) followed by Tukey's multiple comparison test.

4.5 Summary and discussion

In this chapter, we have shown that 20-minute treatment with APOE4 conditioned media or recombinant protein causes an increase in the phosphorylation of eEF2 in rat primary cortical neurons and rat synaptoneurosomes. This leads to an inhibition of global protein synthesis which was demonstrated through FUNCAT assay as well. We ensured the robustness and relevance of our results by testing it in the human neuron system. Similar to rat neurons, we observed that APOE4 conditioned media treatment for 20 minutes caused an increase in eEF2 phosphorylation in human APOE KO neurons as well. Though neurons express very limited amounts of APOE, conditions of stress are shown to increase neuronal APOE expression[33–35]. The experiments performed in the APOE KO neuron system validated that the effect on protein synthesis was not due to changes in neuronal APOE expression, rather it was due to the signaling downstream of APOE receptors. In support of this, APOE receptor antagonist RAP was able to prevent APOE4 mediated increase in eEF2 phosphorylation in rat primary neurons and synaptoneurosomes, further strengthening the involvement of APOE-APOE receptor cascade in the protein synthesis response.

We also investigated the temporal profile of the protein synthesis response on APOE treatment. Interestingly, we found that both APOE3 and APOE4 lead to an increase in eEF2 phosphorylation at an early time point 1-minute. This was also confirmed by the FUNCAT assay where APOE3 and APOE4 treatment for 1-minute showed a reduction of global protein synthesis. However, by 20-minutes, protein synthesis had recovered to basal in APOE3 treated neurons, whereas it remained inhibited in APOE4 treated neurons. This prompted us to study the recovery from protein synthesis inhibition on

APOE treatment. We found that the recovery from translation inhibition was indeed slower in APOE4 treated neurons. Previously, studies have reported the differences in APOE isoforms with respect to the extent of activation of signaling pathways such as ERK and Akt pathways, with APOE4 isoform causing the highest activation [5,36,37]. Similarly, we observed that APOE4 isoform caused the highest phosphorylation of eEF2, even at the 1-minute time point. However, the key difference between the APOE isoforms was their distinct temporal profiles. The temporal differences in APOE mediated response are not studied extensively and our results provide novel insights to understand the basic question 'What makes APOE4 a risk factor in AD?'.

The removal of APOE from the media enabled the neurons to recover from the protein synthesis inhibition. However, the chronic and constant exposure to APOE4 for 24 hours caused a significant increase in eEF2 phosphorylation. We understand that our model system of isolated primary neurons lacks the physiological clearance APOE mechanisms provided by the astrocytes. Hence, we estimate that the effects of APOE4 on protein synthesis could be more subtle physiologically. However, unlike the neurotransmitters which are released in a localized way and cleared out very fast, we also estimate that the neurons would have a continuous and non-localized exposure to APOE. Thus, in the longer run, the slower recovery from protein synthesis inhibition combined with continuous exposure to APOE could play a major role in contributing to APOE4 mediated pathology.

4.6 References

1. Lane-Donovan, C. & Herz, J. ApoE, ApoE Receptors, and the Synapse in Alzheimer's Disease. *Trends in Endocrinology and Metabolism* **28**, 273–284 (2017).
2. Kanekiyo, T., Xu, H. & Bu, G. ApoE and Aβ in Alzheimer's disease: Accidental encounters or partners? *Neuron* **81**, 740–754 (2014).
3. Kim, J., Basak, J. M. & Holtzman, D. M. The Role of Apolipoprotein E in Alzheimer's Disease. *Neuron* **63**, 287–303 (2009).
4. Liu, C. C., Kanekiyo, T., Xu, H. & Bu, G. Apolipoprotein e and Alzheimer disease: Risk, mechanisms and therapy. *Nature Reviews Neurology* vol. 9 (2013).
5. Huang, Y. W. A., Zhou, B., Wernig, M. & Südhof, T. C. ApoE2, ApoE3, and ApoE4 Differentially Stimulate APP Transcription and Aβ Secretion. *Cell* **168**, 427-441.e21 (2017).
6. Lin, Y. T. *et al.* APOE4 Causes Widespread Molecular and Cellular Alterations Associated with Alzheimer's Disease Phenotypes in Human iPSC-Derived Brain Cell Types. *Neuron* **98**, 1141-1154.e7 (2018).
7. Small, B. J., Rosnick, C. B., Fratiglioni, L. & Bäckman, L. Apolipoprotein E and cognitive performance: A meta-analysis. *Psychology and Aging* **19**, (2004).
8. Wisdom, N. M., Callahan, J. L. & Hawkins, K. A. The effects of apolipoprotein E on non-impaired cognitive functioning: A meta-analysis. *Neurobiology of Aging* **32**, (2011).
9. de Jager, P. L. *et al.* A genome-wide scan for common variants affecting the rate of age-related cognitive decline. *Neurobiology of Aging* **33**, (2012).

10. Reas, E. T. *et al.* Effects of APOE on cognitive aging in community-dwelling older adults. *Neuropsychology* **33**, (2019).

11. Albrecht, M. A. *et al.* Longitudinal cognitive decline in the AIBL cohort: The role of APOE ε4 status. *Neuropsychologia* **75**, (2015).

12. Rodriguez, G. A., Burns, M. P., Weeber, E. J. & Rebeck, G. W. Young APOE4 targeted replacement mice exhibit poor spatial learning and memory, with reduced dendritic spine density in the medial entorhinal cortex. *Learning and Memory* **20**, (2013).

13. Liu, D. S. *et al.* APOE4 enhances age-dependent decline in cognitive function by down-regulating an NMDA receptor pathway in EFAD-Tg mice. *Molecular Neurodegeneration* **10**, 1–17 (2015).

14. Sen, A., Alkon, D. L. & Nelson, T. J. Apolipoprotein E3 (ApoE3) but not ApoE4 protects against synaptic loss through increased expression of protein kinase C?? *Journal of Biological Chemistry* **287**, 15947–15958 (2012).

15. Wang, C. *et al.* Human apoE4-targeted replacement mice display synaptic deficits in the absence of neuropathology. *Neurobiology of Disease* **18**, 390–398 (2005).

16. Dumanis, S. B. *et al.* ApoE4 Decreases Spine Density and Dendritic Complexity in Cortical Neurons In Vivo. *Journal of Neuroscience* **29**, 15317–15322 (2009).

17. Teter, B. *et al.* Defective neuronal sprouting by human apolipoprotein E4 is a gain-of-negative function. *Journal of Neuroscience Research* **68**, (2002).

18. Veinbergs, I., Everson, A., Sagara, Y. & Masliah, E. Neurotoxic effects of apolipoprotein E4 are mediated via dysregulation of calcium homeostasis. *Journal of Neuroscience Research* **67**, (2002).

19. Yong, S. M., Lim, M. L., Low, C. M. & Wong, B. S. Reduced neuronal signaling in the ageing apolipoprotein-E4 targeted replacement female mice. *Scientific Reports* **4**, (2014).

20. Nathan, B. P. *et al.* Differential effects of apolipoproteins E3 and E4 on neuronal growth in vitro. *Science* **264**, (1994).

21. Dumanis, S. B. *et al.* ApoE4 decreases spine density and dendritic complexity in cortical neurons in vivo. *Journal of Neuroscience* **29**, (2009).

22. Yong, S. M., Lim, M. L., Low, C. M. & Wong, B. S. Reduced neuronal signaling in the ageing apolipoprotein-E4 targeted replacement female mice. *Scientific Reports* **4**, 1–9 (2014).

23. Hernández-Ortega, K., Garcia-Esparcia, P., Gil, L., Lucas, J. J. & Ferrer, I. Altered Machinery of Protein Synthesis in Alzheimer's: From the Nucleolus to the Ribosome. *Brain Pathology* **26**, 593–605 (2016).

24. Elder, M. K. *et al.* Dysregulation of the de novo proteome accompanies pathology progression in the APP/PS1 mouse model. *PrePrint* (2020).

25. Beckelman, B. C. *et al.* Dysregulation of Elongation Factor 1A Expression is Correlated with Synaptic Plasticity Impairments in Alzheimer's Disease. *Journal of Alzheimer's Disease* **54**, (2016).

26. Knight, J. R. P. *et al.* Control of translation elongation in health and disease. *DMM Disease Models and Mechanisms* vol. 13 (2020).

27. Hizli, A. A. *et al.* Phosphorylation of Eukaryotic Elongation Factor 2 (eEF2) by Cyclin A–Cyclin-Dependent Kinase 2 Regulates Its Inhibition by eEF2 Kinase. *Molecular and Cellular Biology* **33**, (2013).

28. Ovchinnikov, L. P. *et al.* Three phosphorylation sites in elongation factor 2. *FEBS Letters* **275**, (1990).

29. Price, N. T. *et al.* Identification of the phosphorylation sites in elongation factor-2 from rabbit reticulocytes. *FEBS Letters* **282**, (1991).

30. Ryazanov, A. G. & Spirin, A. S. Phosphorylation of elongation factor 2: A key mechanism regulating gene expression in vertebrates. *New Biologist* vol. 2 (1990).

31. Scheetz, A. J., Nairn, A. C. & Constantine-Paton, M. NMDA receptor-mediated control of protein synthesis at developing synapses. *Nature Neuroscience* (2000) doi:10.1038/72915.

32. Ghosh Dastidar, S. *et al.* Distinct regulation of bioenergetics and translation by group I mGluR and NMDAR. *EMBO reports* (2020) doi:10.15252/embr.201948037.

33. Pu-Ting, X. *et al.* Specific regional transcription of apolipoprotein E in human brain neurons. *American Journal of Pathology* **154**, (1999).

34. Harris, F. M. *et al.* Astroglial regulation of apolipoprotein E expression in neuronal cells: Implications for Alzheimer's disease. *Journal of Biological Chemistry* **279**, 3862–3868 (2004).

35. Xu, Q. *et al.* Profile and regulation of apolipoprotein E (ApoE) expression in the CNS in mice with targeting of green fluorescent protein gene to the ApoE locus. *Journal of Neuroscience* **26**, (2006).

36. Huang, Y. W. A., Zhou, B., Nabet, A. M., Wernig, M. & Südhof, T. C. Differential Signaling Mediated by ApoE2, ApoE3, and ApoE4 in Human Neurons Parallels Alzheimer's Disease Risk. *Journal of Neuroscience* **39**, 7408–7427 (2019).

37. Hoe, H. S., Harris, D. C. & Rebeck, G. W. Multiple pathways of apolipoprotein E signaling in primary neurons. *Journal of Neurochemistry* **93**, 145–155 (2005).

Chapter 5

Effect of APOE on NMDAR mediated translation response

5.0 Introduction

Protein synthesis is highly regulated spatially and temporally downstream of neuronal activity[1–6]. Stimulation of neurons with specific neurotransmitters or neurotrophic factors is shown to elicit distinct translation responses involving translation of specific candidate mRNAs[4,6–11]. Over the past few decades, numerous studies have demonstrated the local protein synthesis in neurons, especially at the dendrites, enabling the synapses to specifically synthesize new proteins required for long-term plasticity[2,6,12–15]. This in turn enables the synapses to independently control their strength downstream of activity, without relying on the transport of specific proteins from the soma[1,2,5,15]. Considering the dysregulation of basal protein synthesis in APOE4 treated neurons (demonstrated in Chapter 4) and the importance of activity mediated protein synthesis for synaptic plasticity, we decided to investigate the effect of APOE4 on activity mediated translation response as well.

Glutamate being the principal excitatory neurotransmitter in mammalian CNS, stimulation of glutamate receptors is critical for long term plasticity response[16,17]. The importance of activity driven protein synthesis regulation in glutamate mediated plasticity is also well understood [3,10,18]. There are 2 main types of glutamate receptors – ionotropic and metabotropic[19]. The ionotropic receptors encompass three kinds – Kainite receptor, AMPA receptors (AMPARs) and NMDA receptors (NMDARs)[19]. On the other hand, there are 8 kinds of metabotropic glutamate receptors (mGluRs – mGluR1 to mGluR8) distributed into 3 groups [19]. Among these, the translation response is well characterized for Group 1 mGluRs and NMDARs. The activation of mGluRs is known to cause a global upregulation of protein synthesis; whereas the NMDAR mediated translation response involves early phase translation inhibition followed by global translation activation[7,20–23].

We decided to focus on the effect of APOE on protein synthesis response mediated by NMDARs for two primary reasons -

1. APOE receptors (both LRP1 and ApoeR2) are shown to interact with NMDARs. APOE receptors are shown to be present at the post-synapse[24,25] and their interaction with NMDARs is shown to be mediated through the post-synaptic density protein PSD95 [24–26]. The endosomes containing the internalized APOE receptors upon APOE binding are shown to contain NMDARs as well, further supporting the interaction between the two receptors[27]. The activation of ERK signaling pathway downstream of APOE receptors is also shown have the involvement of NMDARs[28,29]. Using NMDAR antagonists is shown to block APOE mediated ERK phosphorylation to an extent similar to using APOE receptor antagonists[28,29]. Though the mechanism is not well understood, it is clear that binding of APOE to its receptor causes an activation of NMDARs as well. This

formed the basis to hypothesize that APOE could affect the translation response downstream of NMDARs.

2. NMDARs behave as co-incidence detectors of both pre-synaptic activity (release of glutamate) and post-synaptic activity (voltage change causing removal of magnesium block and induction of calcium signaling)[30]. This co-incident detection makes NMDAR dependent plasticity, particularly long-term potentiation (LTP), very crucial for associative learning and adapting to environmental stimuli[30,31]. Not surprisingly, spatial learning and memory is shown to be dependent on NMDAR-LTP[30,32,33]. The induction of LTP is shown to be dependent on protein synthesis, and also results in the regulation of protein synthesis[20,30]. NMDAR-LTP induction is shown to be affected in APOE4 mice model [34,35], which also show defects is spatial learning and memory[36]. Thus, NMDAR mediated plasticity is shown to be affected in APOE4 mice model, but the effect of APOE4 on NMDAR mediated protein synthesis remains unclear. Hence, we decided to study the effect of APOE4 on protein synthesis downstream of NMDAR stimulation.

Results

5.1 NMDAR stimulation for 5 minutes leads to global inhibition of protein synthesis accompanied with translation activation of specific candidates

Our lab has extensively studied the translation response downstream of NMDARs, particularly with 5-minute NMDA stimulation (20µM). We have previously shown that 5-minute NMDAR stimulation leads to a global inhibition of protein synthesis indicated by increase in eEF2 phosphorylation (Fig 5.1 A) [7,22]. In this background, specific set of candidate mRNAs such as PTEN and PSD95 get translationally activated (Fig 5.1 A)[7]. To begin with, I wanted to check if I can validate this previous finding in my model system. As reported earlier, 5-minute NMDAR stimulation (in neurobasal media) of rat primary cortical neurons (DIV15) caused an increase in eEF2 phosphorylation indicating translation inhibition (Fig 5.1 B). At the same time, NMDAR stimulation also caused an increase in PTEN and PSD95 protein levels in these neurons (Fig 5.1 C and D), indicating the translation activation of specific candidates.

Figure 5.1

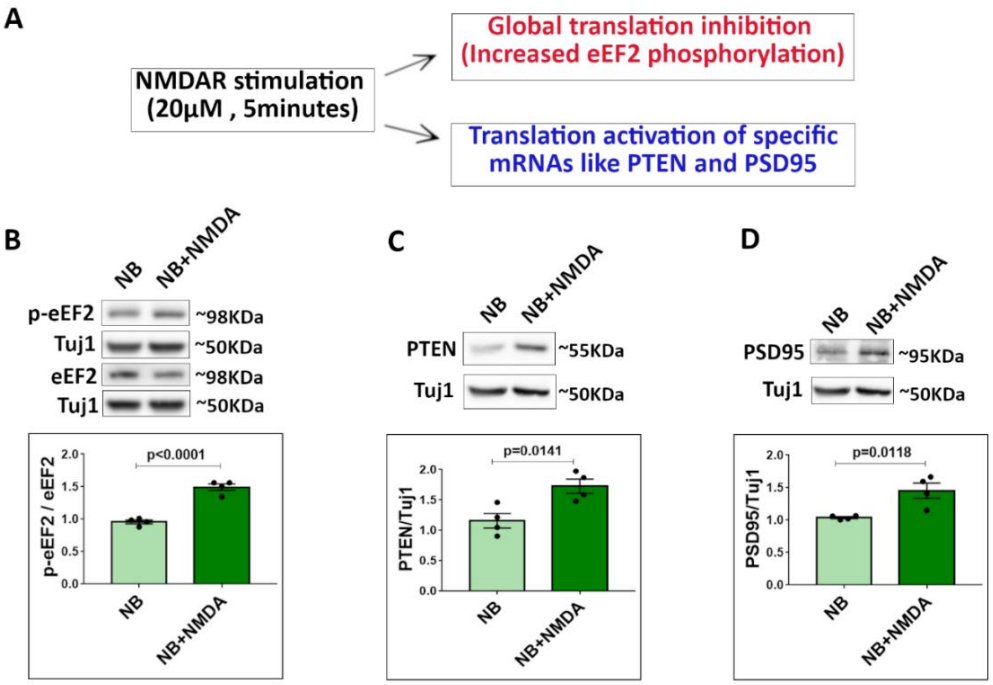

Figure 5.1 - 5-minute NMDAR stimulation leads to global inhibition of protein synthesis accompanied with translation activation of specific candidates

A – Translation response downstream of 5-minute stimulation of NMDARs in rat primary cortical neurons (DIV15) using 20µM NMDA.

B - Representative immunoblots showing the levels of p-eEF2, eEF2 and Tuj1 in rat primary cortical neurons after 5-minute NMDAR stimulation. The graph represents the ratio of p-eEF2 to eEF2 normalized to Tuj1. Data is represented as mean +/- SEM. N=4, Unpaired Student's t-test.

C - Representative immunoblots showing the levels of PTEN and Tuj1 in rat primary cortical neurons after 5-minute NMDAR stimulation. The graph represents the levels of PTEN normalized to Tuj1. Data is represented as mean +/- SEM. N=4, Unpaired Student's t-test.

D - Representative immunoblots showing the levels of PSD95 and Tuj1 in rat primary cortical neurons after 5-minute NMDAR stimulation. The graph represents the levels of PSD95 normalized to Tuj1. Data is represented as mean +/- SEM. N=4, Unpaired Student's t-test.

5.2 APOE KO conditioned media treatment does not affect NMDAR translation response

Since the translation response for 5-minute NMDAR stimulation is well-established, we decided to investigate this in APOE treated neurons. Briefly, rat primary cortical neurons (DIV15) were stimulated with NMDA during the last 5 minutes of the 20-minute APOE conditioned media treatment (Fig 5.2 A). Following the stimulation, we assessed the phosphorylation status of eEF2, PTEN and PSD95 protein levels in the neurons as readouts for NMDAR translation response (Fig 5.2 A). To confirm that the treatment with iPSC conditioned media does not affect NMDAR translation response, we stimulated (20 µM NMDA, 5 minutes) the neurons treated with APOE KO iPSC conditioned media for 20 minutes. As observed under control/ neurobasal conditions, APOE KO conditioned media treated neurons also showed an increase in eEF2 phosphorylation (Fig 5.2 B), PTEN (Fig 5.2 C) and PSD95 (Fig 5.2 D) protein levels on NMDAR stimulation. Thus, the 5-minute NMDAR translation response of global translation inhibition accompanied with translation activation of specific mRNAs was unaffected by conditioned media treatment.

Figure 5.2

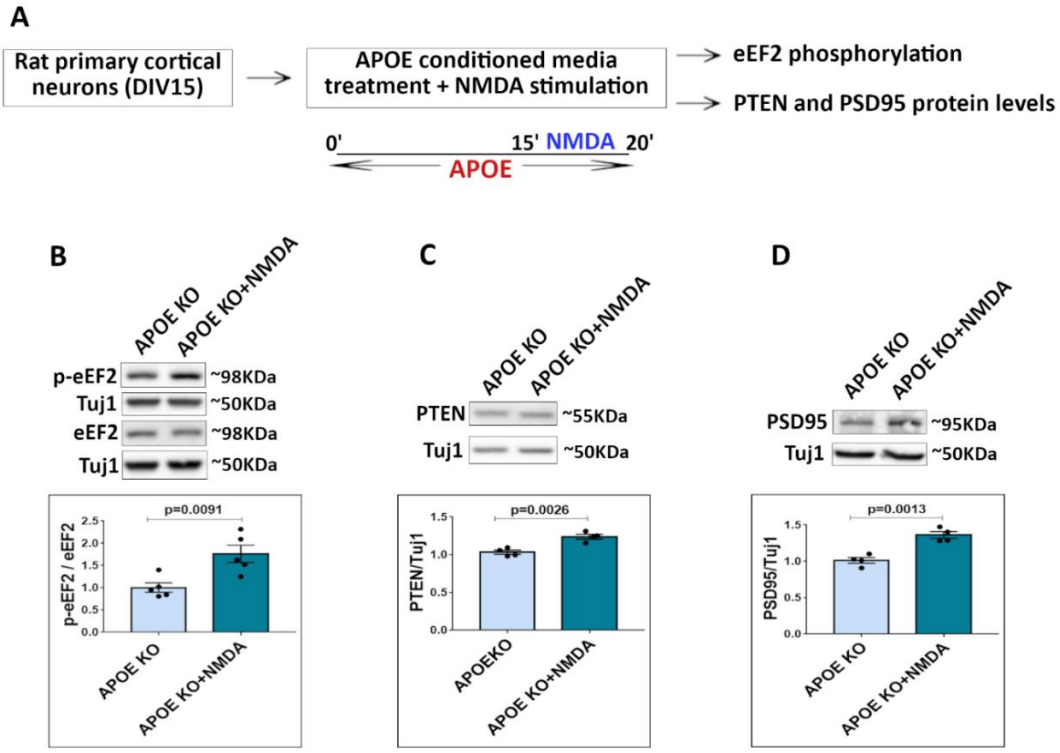

Figure 5.2 – APOE KO conditioned media treatment does not affect NMDAR translation response

A – Experiment design for NMDAR stimulation following APOE conditioned media treatment of rat primary cortical neurons

B - Representative immunoblots showing the levels of p-eEF2, eEF2 and Tuj1 in rat primary cortical neurons treated with APOE KO conditioned media for 20 minutes along with 5-minute NMDAR stimulation. The graph represents the ratio of p-eEF2 to eEF2 normalized to Tuj1. Data is represented as mean +/- SEM. N=5, Unpaired Student's t-test.

C - Representative immunoblots showing the levels of PTEN and Tuj1 in rat primary cortical neurons treated with APOE KO conditioned media for 20 minutes along with 5-minute NMDAR stimulation. The graph represents the levels of PTEN normalized to Tuj1. Data is represented as mean +/- SEM. N=5, Unpaired Student's t-test.

D - Representative immunoblots showing the levels of PSD95 and Tuj1 in rat primary cortical neurons treated with APOE KO conditioned media for 20 minutes along with 5-minute NMDAR stimulation. The graph represents the levels of PSD95 normalized to Tuj1. Data is represented as mean +/- SEM. N=5, Unpaired Student's t-test.

5.3 APOE4 affects translation inhibition on 5-minute NMDAR stimulation

Once we verified that conditioned media treatment does not affect NMDAR response, we subjected rat primary cortical neurons to NMDAR stimulation (20µM, 5 minutes) in the background of APOE3 or APOE4 iPSC conditioned media treatment for 20 minutes. Neurons treated with APOE3 conditioned media showed increased eEF2

phosphorylation (Fig 5.3 A), as observed with neurobasal and APOE KO conditioned media treatment. On the other hand, APOE4 conditioned media treatment caused an increase in eEF2 phosphorylation (Fig 5.3 A) as observed previously (Chapter 4). However, APOE4 treated neurons failed to respond to NMDAR stimulation as they did not show a further increase in eEF2 phosphorylation (Fig 5.3 A). Similar results were observed with rat cortical synaptoneurosomes as well. Synaptoneurosomes treated with recombinant APOE3 protein (15nM) for 20 minutes along with NMDAR stimulation (20µM, 5 minutes) showed an increase in eEF2 phosphorylation (Fig 5.3 B). But, APOE4 recombinant protein treated synaptoneurosomes failed to respond to NMDAR stimulation with respect to eEF2 phosphorylation and global translation inhibition (Fig 5.3 C).

We performed FUNCAT assay as well to validate the NMDAR translation response. Briefly, rat primary cortical neurons were subjected to APOE3 or APOE4 recombinant protein treatment for 20 minutes along with NMDAR stimulation (20µM) during the last 5 minutes, following which they were subjected to FUNCAT assay. As observed with eEF2 phosphorylation, NMDA stimulation following APOE3 treatment caused a decrease in FUNCAT signal compared to APOE3 treatment indicating a decrease in global protein synthesis (Fig 5.3 D and E). As observed earlier (Chapter 4), 20-minute APOE4 treatment led to a reduction of the FUNCAT signal (Fig 5.3 D and E). However, NMDAR stimulation following APOE4 treatment did not cause a change in the FUNCAT signal compared to APOE4 treated neurons (Fig 5.3 D and E), indicating that NMDAR mediated translation inhibition response was lost on APOE4 treatment.

Figure 5.3

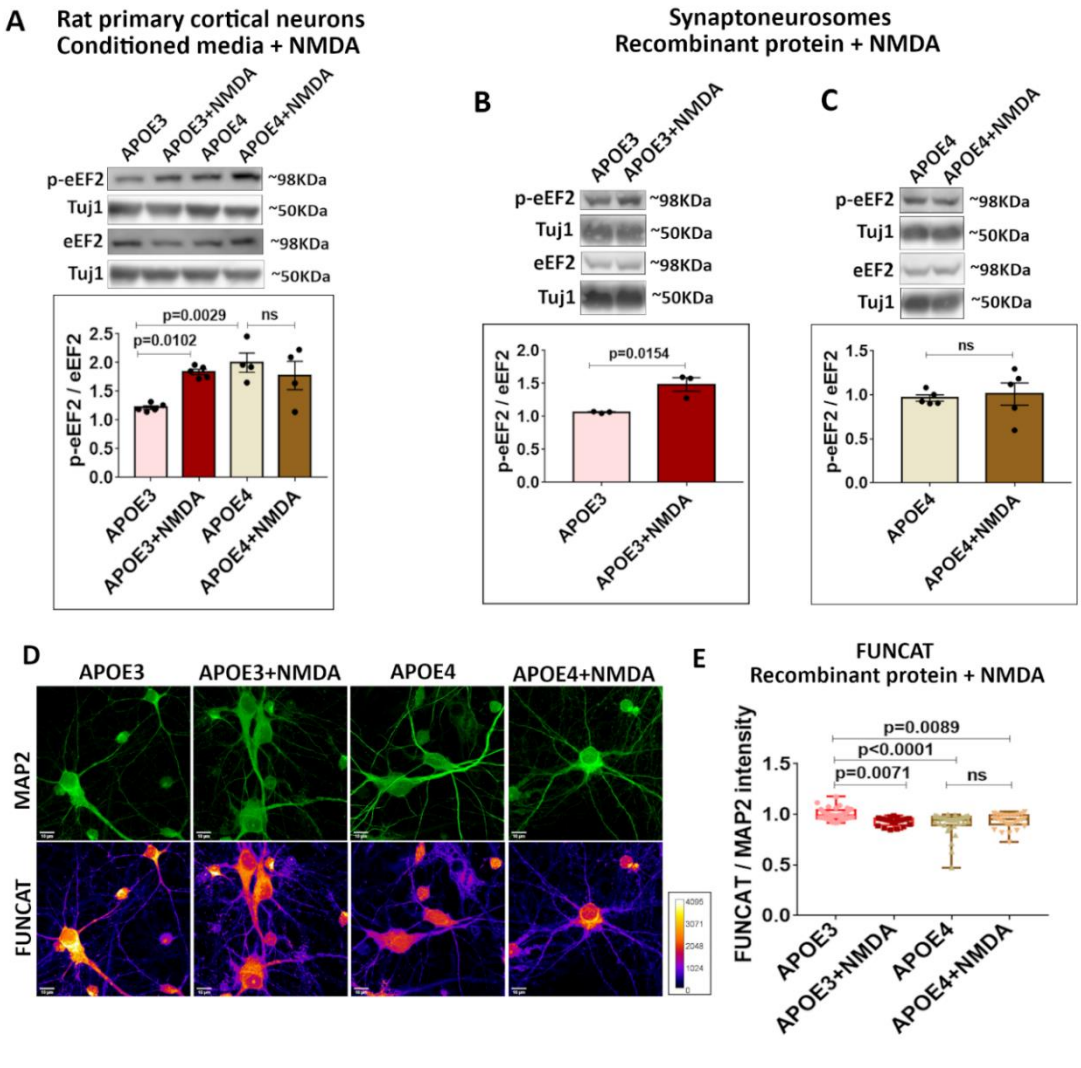

Figure 5.3 - APOE4 affects translation inhibition on 5-minute NMDAR stimulation

A - Representative immunoblots showing the levels of p-eEF2, eEF2 and Tuj1 in rat primary cortical neurons treated with APOE3 or APOE4 conditioned media for 20 minutes along with 5-minute NMDAR stimulation. The graph represents the ratio of p-eEF2 to eEF2 normalized to Tuj1. Data is represented as mean +/- SEM. N=4-5, One-way ANOVA ($p=0.0047$) followed by Dunnett's multiple comparison test.

B - Representative immunoblots showing the levels of p-eEF2, eEF2 and Tuj1 in rat cortical synaptoneurosomes treated with APOE3 recombinant protein for 20 minutes along with 5-minute NMDAR stimulation. The graph represents the ratio of p-eEF2 to eEF2 normalized to Tuj1. Data is represented as mean +/- SEM. N=3, Unpaired Student's t-test.

C - Representative immunoblots showing the levels of p-eEF2, eEF2 and Tuj1 in rat cortical synaptoneurosomes treated with APOE4 recombinant protein for 20 minutes along with 5-minute NMDAR stimulation. The graph represents the ratio of p-eEF2 to eEF2 normalized to Tuj1. Data is represented as mean +/- SEM. N=5, Unpaired Student's t-test.

D - The representative images for MAP2 and FUNCAT fluorescent signals in rat primary cortical neurons treated with APOE3 / APOE4 recombinant protein (15nM) for 20 minutes along with NMDAR stimulation for 5 minutes (Scale bar - 10µM).

E - The graph represents the quantification of the FUNCAT fluorescent intensity normalized to MAP2 fluorescent intensity under different APOE treatment conditions along with NMDAR stimulation. N = 20-40 neurons from 2 independent experiments, One-way ANOVA ($p<0.0001$) followed by Tukey's multiple comparison test.

5.4 APOE4 affects candidate specific translation activation on 5-minute NMDAR stimulation

In the previous sections, we examined only the translation inhibition response on NMDAR stimulation. Here, we further examined the NMDAR mediated translation activation of specific candidate mRNAs like PTEN and PSD95. NMDAR stimulation (20µM, 5 minutes) following APOE3 conditioned media treatment for 20 minutes led to increased levels of PTEN and PSD95 protein (Fig 5.4 A and B) in rat primary neurons. Thus, NMDAR specific translation activation was unaffected in the presence of APOE3. However, APOE4 conditioned media treatment for 20-minutes caused an increase in PTEN and PSD95 levels (Fig 5.4 A and B), mimicking the condition of APOE3+NMDA. NMDAR stimulation following APOE4 conditioned media treatment caused no further change in PTEN and PSD95 levels compared to APOE4 treated neurons (Fig 5.4 A and B). Hence, along with global translation inhibition, NMDA mediated translation activation of specific candidates was also perturbed in the presence of APOE4.

Additionally, we measured the levels of PTEN and PSD95 mRNAs on APOE conditioned media treatment with or without NMDAR stimulation. APOE KO, APOE3 and APOE4 conditioned media treated (20 minutes) neurons showed similar levels of PTEN and PSD95 mRNAs (Fig 5.4 C and D). NMDAR stimulation in the conditioned

media background did not alter the PTEN and PSD95 mRNA levels (Fig 5.4 C and D). Thus, the increase in PTEN and PSD95 protein levels observed on NMDAR stimulation (in APOE KO and APOE3 background) and APOE4 treatment were due to translation activation, and not transcriptional upregulation.

Figure 5.4

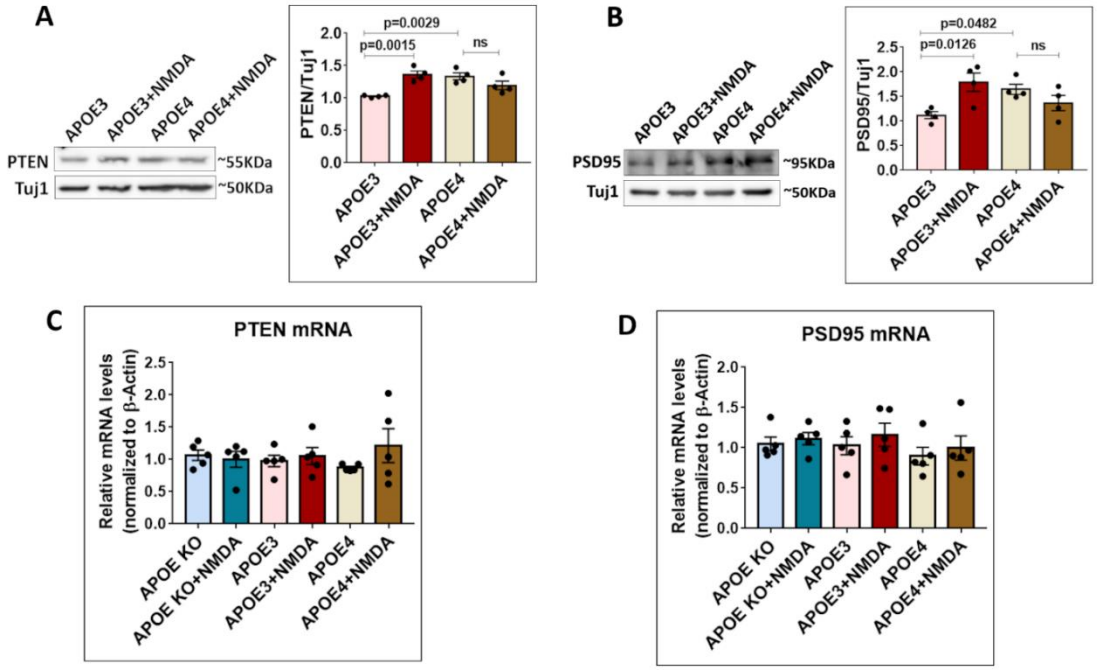

Figure 5.4 - APOE4 affects candidate specific translation activation on 5-minute NMDAR stimulation

A - Representative immunoblots showing the levels of PTEN and Tuj1 in rat primary cortical neurons treated with APOE3 or APOE4 conditioned media for 20 minutes along with 5-minute NMDAR stimulation. The graph represents the PTEN levels normalized to Tuj1. Data is represented as mean +/- SEM. N=4, One-way ANOVA (p=0.002) followed by Dunnett's multiple comparison test.

B - Representative immunoblots showing the levels of PSD95 and Tuj1 in rat primary cortical neurons treated with APOE3 or APOE4 conditioned media for 20 minutes along with 5-minute NMDAR stimulation. The graph represents the PSD95 levels normalized to Tuj1. Data is represented as mean +/- SEM. N=4, One-way ANOVA (p=0.0216) followed by Dunnett's multiple comparison test.

C - Rat primary cortical neurons were treated with APOE KO/APOE3/APOE4 conditioned media for 20 minutes along with NMDAR stimulation for 5 minutes and subjected to RT-PCR to measure the levels of PTEN mRNA. The graph indicates the copy number of PTEN mRNA normalized to copy number of β-actin mRNA under different treatment conditions. Data is represented as mean +/- SEM, N=5. One-way ANOVA (ns).

H - Rat primary cortical neurons were treated with APOE KO/APOE3/APOE4 conditioned media for 20 minutes along with NMDAR stimulation for 5 minutes and subjected to RT-PCR to measure the levels of PSD95 mRNA. The graph indicates the copy number of PSD95 mRNA normalized to copy number of β-actin mRNA under different treatment conditions. Data is represented as mean +/- SEM, N=5. One-way ANOVA (ns).

5.5 APOE4 does not mimic NMDAR translation response

While it does appear like the APOE4 treatment is mimicking 5-minute NMDA mediated translation response, it was important to consider that the APOE4 treatment was for 20 minutes while NMDAR stimulation was for 5 minutes. Hence, in order to obtain a better understanding of the NMDA mediated translation response temporally, we stimulated rat primary cortical neurons (DIV15) with NMDA (20µM) for 1 minute, 5 minutes and 20 minutes. With 1-minute stimulation of NMDARs, phosphorylation of eEF2 increased significantly compared to basal levels (Fig 5.5 A). This increase in phosphorylation of eEF2 was observed with 1-minute APOE3 and APOE4 treatment as well (Chapter 4). With 5-minute NMDAR stimulation, phosphorylation of eEF2 was still higher than basal, but lower compared to 1-minute NMDAR stimulation condition (Fig 5.5 A). Interestingly, 20 minutes of NMDAR stimulation caused a decrease in phosphorylation of eEF2 compared to basal conditions (Fig 5.5 A), indicating global translation activation (Fig 5.5 A). We performed FUNCAT assay at 1, 5 and 20-minute NMDAR stimulation time points to support the eEF2 phosphorylation data. The FUNCAT signal showed a significant decrease with 1-minute and 5-minute NMDAR stimulation compared to basal condition, indicating decreased translation (Fig 5.5 B and C). In correspondence with p-eEF2 decrease, the FUNCAT signal with 20-minute NMDAR stimulation showed a marked increase (Fig 5.5 B and C), further validating the global protein synthesis upregulation in the later phase of NMDAR translation response. Hence, at 20-minute time point, while APOE4 led to an increase in eEF2 phosphorylation and APOE3 did not alter p-eEF2 levels, NMDAR stimulation led to decrease in eEF2 phosphorylation (Fig 5.5 D). Thus, at 20-minute time point, the translation response of NMDAR stimulation, APOE3 treatment and APOE4 treatment were completely different (Fig 5.5 D).

Figure 5.5

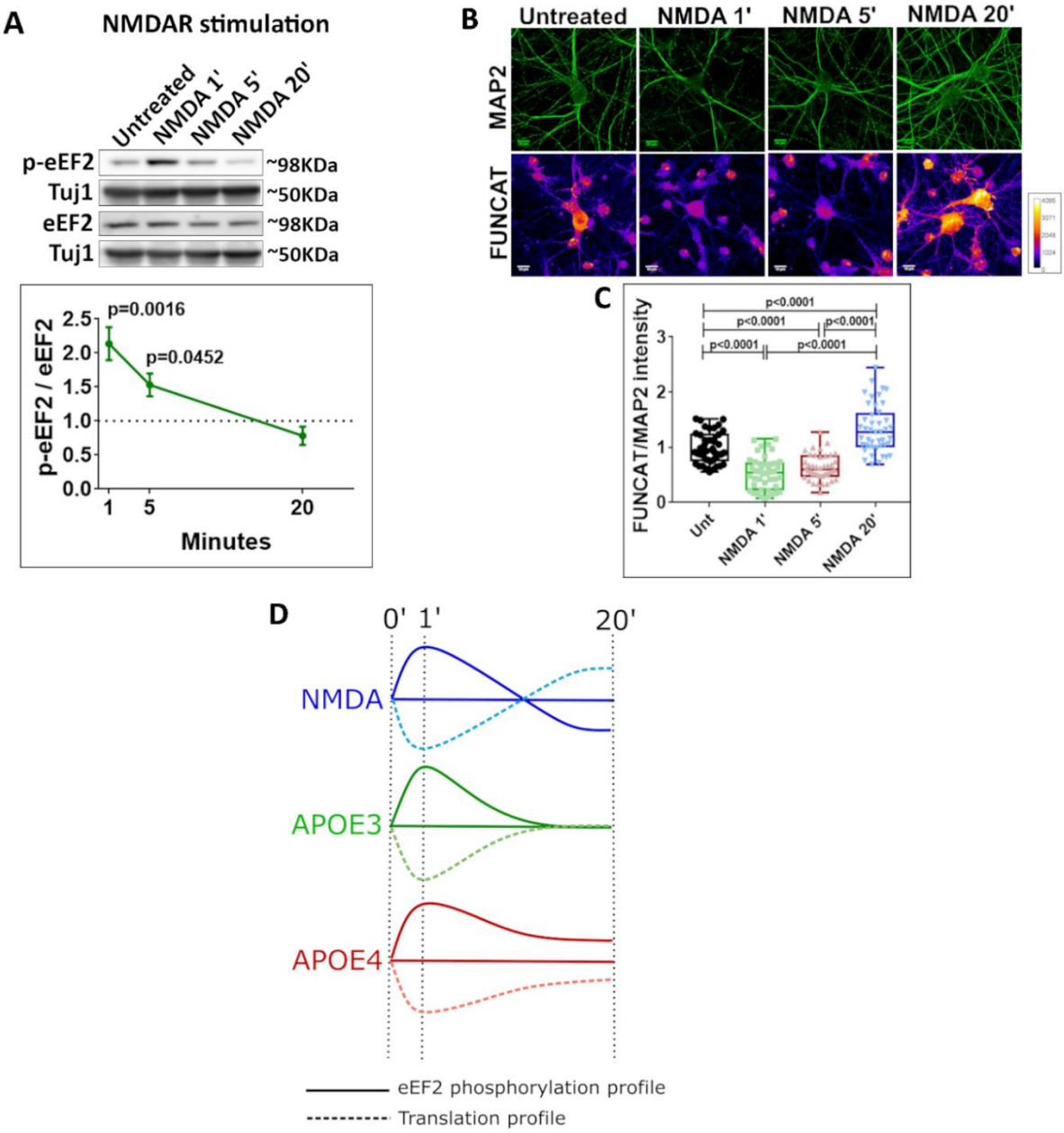

Figure 5.5 - APOE4 does not mimic NMDAR translation response

A - Representative immunoblots showing the levels of p-eEF2, eEF2 and Tuj1 in rat primary cortical neurons stimulated with NMDA (20µM) for 1 minute, 5 minutes and 20 minutes. The graph represents the ratio of p-eEF2 to eEF2 normalized to Tuj1. Data is represented as mean +/- SEM. N=3, One-way ANOVA (p=0.0015) followed by Tukey's multiple comparison test.

B - The representative images for MAP2 and FUNCAT fluorescent signals in rat primary cortical neurons stimulated with NMDA (20 µM) for 1, 5 and 20 minutes (Scale bar - 10µM).

C - The graph represents the quantification of the FUNCAT fluorescent intensity normalized to MAP2 fluorescent intensity under different NMDAR stimulation

conditions. N = 40-50 neurons from 3 independent experiments, One-way ANOVA ($p<0.0001$) followed by Tukey's multiple comparison test.

D – Model illustrating the temporal profiles of eEF2 phosphorylation and global protein synthesis on NMDAR stimulation, APOE3 treatment and APOE4 treatment.

5.6 Summary and Discussion

In this chapter, we validated the previously established 5-minute NMDAR translation response in our primary neuron system. 5-minute stimulation with NMDA (20µM) caused a global inhibition of protein synthesis as indicated by eEF2 phosphorylation and FUNCAT. In the background of global translation inhibition, specific candidate mRNAs like PTEN and PSD95 get translationally activated [7]. In the conditions of neurobasal, APOE KO conditioned media and APOE3 conditioned media/ recombinant protein treatment, the translation response to 5-minute NMDAR stimulation is conserved, with respect to global translation inhibition and candidate specific translation activation. However, in the presence of APOE4 conditioned media/ recombinant protein, the translation response to 5-minute NMDAR stimulation is perturbed. Thus, presence of APOE4 not only affects global protein synthesis, it also impairs NMDAR mediated protein synthesis. The loss of activity mediated translation with APOE4 treatment provides a potentially strong explanation for the synaptic pathologies and defects observed in APOE4 model systems.

Treatment with APOE4 for 20 minutes caused an increase in eEF2 phosphorylation, decreased protein synthesis (reduced FUNCAT signal), increase in PTEN and PSD95 levels. It appeared that APOE4 treatment mimicked the condition of APOE3 treatment + NMDA stimulation. But, the 20-minute APOE4 treatment had a similar translation response as 5-minute NMDAR stimulation. In order to understand the APOE translation response better in comparison to NMDAR translation profile, we investigated the NMDAR translation response at 1-minute and 20-minute time points as well. At 1-minute time point, NMDAR stimulation led to significant increase in eEF2 phosphorylation and translation inhibition, identical to 1-minute treatment of APOE3 and APOE4. Hence, at the earlier time point, all three translation responses were similar, implying the involvement of NMDARs in the early phase of APOE response. As discussed in the introduction, APOE binding to its receptors is shown to influence NMDAR activity due to the interaction between APOE receptors and NMDARs[25,26,37,38]. Thus, we were also prompted to investigate the involvement of NMDARs in the early phase translation inhibition caused by APOE3 and APOE4 (discussed in further chapters).

However, at 20-minute time point, NMDAR stimulation led to decrease in eEF2 phosphorylation and translation upregulation. While translation status of APOE3 treated neurons was similar to untreated conditions at 20 minutes, APOE4 treatment for 20 minutes caused an increase in eEF2 phosphorylation and translation inhibition. Though the translation profile seemed similar at 1-minute time point, it diverged over time and the later phase translation profiles of all the three conditions were completely distinct. The divergence of the translation profiles hinted that NMDARs were probably not involved in the later phase of APOE response; while there could be other distinct

components in the later phase of APOE and NMDAR responses. This brings attention to the regulation and specificity of translation response downstream of different stimuli. Hence, we also hypothesize that the candidates getting translationally activated and inhibited in these different conditions could be distinct. Techniques like high throughput sequencing could give more information on the candidates and help in identifying the specific pathways influenced under each condition. Though this an interesting future direction, our focus was towards understanding the mechanisms causing the distinct translation profiles rather than investigating the effects of it. Hence, we proceeded to further dissect out the translation profiles for NMDAR stimulation, APOE3 and APOE4 treatment with the hope to achieve more mechanistic insights into these differences.

5.7 References

1. Martin, K. C., Barad, M. & Kandel, E. R. Local protein synthesis and its role in synapse-specific plasticity. *Current Opinion in Neurobiology* vol. 10 (2000).
2. Sutton, M. A. & Schuman, E. M. Dendritic Protein Synthesis, Synaptic Plasticity, and Memory. *Cell* vol. 127 49–58 (2006).
3. Gong, R., Chang, S. P., Abbassi, N. R. & Tang, S. J. Roles of glutamate receptors and the mammalian target of rapamycin (mTOR) signaling pathway in activity-dependent dendritic protein synthesis in hippocampal neurons. *Journal of Biological Chemistry* **281**, (2006).
4. Aakalu, G., Smith, W. B., Nguyen, N., Jiang, C. & Schuman, E. M. Dynamic visualization of local protein synthesis in hippocampal neurons. *Neuron* **30**, (2001).
5. Swanger, S. A. & Bassell, G. J. Dendritic protein synthesis in the normal and diseased brain. *Neuroscience* vol. 232 (2013).
6. Casadio, A. *et al.* A transient, neuron-wide form of CREB-mediated long-term facilitation can be stabilized at specific synapses by local protein synthesis. *Cell* **99**, (1999).
7. Kute, P. M., Ramakrishna, S., Neelagandan, N., Chattarji, S. & Muddashetty, Ravi. S. NMDAR mediated translation at the synapse is regulated by MOV10 and FMRP. *Molecular Brain* **12**, 65 (2019).
8. Ravindran, S., Nalavadi, V. C. & Muddashetty, R. S. BDNF induced translation of limk1 in developing neurons regulates dendrite growth by fine-tuning cofilin1 activity. *Frontiers in Molecular Neuroscience* (2019) doi:10.3389/fnmol.2019.00064.
9. Muddashetty, R. S. *et al.* Reversible Inhibition of PSD-95 mRNA Translation by miR-125a, FMRP Phosphorylation, and mGluR Signaling. *Molecular Cell* (2011) doi:10.1016/j.molcel.2011.05.006.
10. Hsu, W. L. *et al.* Glutamate stimulates local protein synthesis in the axons of rat cortical neurons by activating α-amino-3-hydroxy-5-methyl-4-isoxazolepropionic acid (AMPA) receptors and metabotropic glutamate receptors. *Journal of Biological Chemistry* **290**, (2015).
11. David, O., Barrera, I., Gould, N., Gal-Ben-Ari, S. & Rosenblum, K. D1 Dopamine Receptor Activation Induces Neuronal eEF2 Pathway-Dependent Protein Synthesis. *Frontiers in Molecular Neuroscience* **13**, (2020).

12. Fonseca, R., Nägerl, U. V. & Bonhoeffer, T. Neuronal activity determines the protein synthesis dependence of long-term potentiation. *Nature Neuroscience* **9**, (2006).

13. Johnstone, V. P. A. & Raymond, C. R. Postsynaptic protein synthesis is required for presynaptic enhancement in persistent forms of long-term potentiation. *Frontiers in Synaptic Neuroscience* **5**, (2013).

14. Abraham, W. C. & Williams, J. M. LTP maintenance and its protein synthesis-dependence. *Neurobiology of Learning and Memory* **89**, (2008).

15. Nihonmatsu, I., Ohkawa, N., Saitoh, Y., Okubo-Suzuki, R. & Inokuchi, K. Selective targeting of mRNA and the following protein synthesis of CaMKIIα at the long-term potentiation-induced site. *Biology Open* **9**, (2020).

16. Mattson, M. P. Glutamate and neurotrophic factors in neuronal plasticity and disease. in *Annals of the New York Academy of Sciences* vol. 1144 (2008).

17. Genoux, D. & Montgomery, J. M. Glutamate receptor plasticity at excitatory synapses in the brain. in *Clinical and Experimental Pharmacology and Physiology* vol. 34 (2007).

18. Marin, P. *et al.* Glutamate-dependent phosphorylation of elongation factor-2 and inhibition of protein synthesis in neurons. *Journal of Neuroscience* **17**, (1997).

19. Traynelis, S. F. *et al.* Glutamate receptor ion channels: Structure, regulation, and function. *Pharmacological Reviews* vol. 62 (2010).

20. Hoeffer, C. A. & Klann, E. NMDA receptors and translational control. in *Biology of the NMDA Receptor* (2008). doi:10.1201/9781420044157.ch6.

21. Scheetz, A. J., Nairn, A. C. & Constantine-Paton, M. NMDA receptor-mediated control of protein synthesis at developing synapses. *Nature Neuroscience* (2000) doi:10.1038/72915.

22. Ghosh Dastidar, S. *et al.* Distinct regulation of bioenergetics and translation by group I mGluR and NMDAR. *EMBO reports* (2020) doi:10.15252/embr.201948037.

23. Muddashetty, R. S., Kelić, S., Gross, C., Xu, M. & Bassell, G. J. Dysregulated metabotropic glutamate receptor-dependent translation of AMPA receptor and postsynaptic density-95 mRNAs at synapses in a mouse model of fragile X syndrome. *Journal of Neuroscience* (2007) doi:10.1523/JNEUROSCI.0937-07.2007.

24. May, P. *et al.* Neuronal LRP1 Functionally Associates with Postsynaptic Proteins and Is Required for Normal Motor Function in Mice. *Molecular and Cellular Biology* **24**, (2004).

25. Nakajima, C. *et al.* Low density lipoprotein receptor-related protein 1 (LRP1) modulates N-methyl-D-aspartate (NMDA) receptor-dependent intracellular signaling and NMDA-induced regulation of postsynaptic protein complexes. *Journal of Biological Chemistry* **288**, 21909–21923 (2013).

26. Hoe, H. S. *et al.* Apolipoprotein E receptor 2 interactions with the N-Methyl-D-aspartate receptor. *Journal of Biological Chemistry* **281**, (2006).

27. Chen, Y., Durakoglugil, M. S., Xian, X. & Herz, J. ApoE4 reduces glutamate receptor function and synaptic plasticity by selectively impairing ApoE receptor recycling. *Proceedings of the National Academy of Sciences of the United States of America* **107**, (2010).

28. Hoe, H. S., Harris, D. C. & Rebeck, G. W. Multiple pathways of apolipoprotein E signaling in primary neurons. *Journal of Neurochemistry* **93**, (2005).

29. Ohkubo, N. *et al.* Apolipoprotein E4 Stimulates cAMP Response Element-binding Protein Transcriptional Activity through the Extracellular Signal-regulated Kinase Pathway. *Journal of Biological Chemistry* **276**, 3046–3053 (2001).

30. Lüscher, C. & Malenka, R. C. NMDA receptor-dependent long-term potentiation and long-term depression (LTP/LTD). *Cold Spring Harbor Perspectives in Biology* **4**, (2012).

31. Lisman, J. Long-term potentiation: Outstanding questions and attempted synthesis. *Philosophical Transactions of the Royal Society B: Biological Sciences* vol. 358 (2003).

32. Sanders, E. M. *et al.* Separate functional properties of NMDARs regulate distinct aspects of spatial cognition. *Learning and Memory* **25**, (2018).

33. Saucier, D. & Cain, D. P. Spatial learning without NMDA receptor-dependent long-term potentiation. *Nature* **378**, (1995).

34. Trommer, B. L. *et al.* ApoE isoform-specific effects on LTP: Blockade by oligomeric amyloid-β1-42. *Neurobiology of Disease* **18**, (2005).

35. Trommer, B. L. *et al.* ApoE isoform affects LTP in human targeted replacement mice. *NeuroReport* **15**, (2004).

36. Rodriguez, G. A., Burns, M. P., Weeber, E. J. & Rebeck, G. W. Young APOE4 targeted replacement mice exhibit poor spatial learning and memory, with reduced dendritic spine density in the medial entorhinal cortex. *Learning and Memory* **20**, (2013).

37. Hoe, H. S., Harris, D. C. & Rebeck, G. W. Multiple pathways of apolipoprotein E signaling in primary neurons. *Journal of Neurochemistry* **93**, 145–155 (2005).

38. Bacskai, B. J., Xia, M. Q., Strickland, D. K., Rebeck, G. W. & Hyman, B. T. The endocytic receptor protein LRP also mediates neuronal calcium signaling via N-methyl-D-aspartate receptors. *Proceedings of the National Academy of Sciences of the United States of America* **97**, 11551–11556 (2000).

Chapter 6

Understanding APOE mediated translation response using polysome profiling

6.0 Introduction

Translation response to NMDAR stimulation follows a distinct temporal profile. As shown in Chapter 5, APOE4 affects the translation response to 5-minute NMDAR stimulation, with respect to global translation inhibition and translation activation of specific candidate mRNAs. However, the translation profile downstream of APOE4 has different kinetics in itself. While 20-minute APOE4 treatment caused translation inhibition, 20-minute NMDAR stimulation caused global translation activation. To obtain more mechanistic insights into these differences and to obtain a better understanding of the APOE4+NMDA translation defect, we performed polysome profiling with NMDAR stimulation and APOE conditioned media treated neurons.

Polysome profiling is a technique where the cell lysates are subjected to a density-based separation on a linear sucrose gradient using ultracentrifugation [1–4]. The samples separated based on density are collected as individual fractions corresponding to mRNPs (messenger ribonucleoproteins), ribosomal subunits (40S and 60S), monosomes (80S) and polysomes. The individual fractions are probed for the distribution of different proteins and mRNAs[4–6], hence providing the translation profile of the cells. Investigating the distribution of ribosomal proteins or rRNA in the individual fractions provides insights into global translation status of the cell. Shift of ribosomes from lighter fractions (monosomes and light polysomes) towards heavier fractions (heavy polysomes) would indicate translation activation and vice versa. At the same time, it allows to probe for individual candidate mRNAs as well, without losing the sight of the global translation response downstream of specific stimulation or treatment. Another advantage of the technique is the ability to distinguish between the translationally active polysomes and stalled polysomes [6,7]. Thus, along with studying the distribution of the candidate mRNAs, it would be possible to investigate their translation status as well. Further, the mRNA or protein distribution profiles can be compared between different treatment conditions.

Careful investigation of the translation profiles and use of inhibitors for specific stages of eukaryotic translation can answer if the translation regulation is initiation or elongation mediated for specific candidates[4,8,9]. As I have explained previously in Chapters 4 and 5, the primary mode of regulation of translation elongation is through phosphorylation of eukaryotic translation elongation factor (eEF2), where increased eEF2 phosphorylation corresponds to decrease in global protein synthesis[10–12]. The primary mechanisms of inhibition of cap-dependent eukaryotic translation initiation are by phosphorylation of eIF2α and phosphorylation of 4EBP[13]. The increased phosphorylation of α-subunit of eIF2 increases its binding to its own GEF eIF2B, hence preventing the formation of the ternary complex of translation initiation. eIF2α kinases PKR, PERK, GCN2 and HRI are primarily activated downstream of different kinds of

cellular stress such as unfolded protein response, ER stress, amino-acid starvation etc., [13]. On the other hand, increased phosphorylation of the cap binding protein 4EBP drastically increases its affinity for eIF4E, hence it sequesters eIF4E and prevents the formation of eIF4F cap-binding complex [13]. The regulation of protein synthesis through eIF2α phosphorylation at initiation stage gets reflected in the earlier fractions of the polysome profile as it would prevent the formation of 80S complex; whereas the regulation at elongation stage gets reflected in the heavier polysome fractions. Hence, understanding the translation profiles and identifying the stages of translation regulation under different treatment conditions would help in recognizing the potential signaling pathways involved in the specific translation response.

Results

6.1 Grouping of polysome profiling fractions

Rat primary cortical neurons (DIV15) treated with cycloheximide were subjected to ultracentrifugation and separated on a 15% - 45% linear sucrose gradient. 11 fractions corresponding to mRNPs, ribosomal subunits (40S and 60S), monosomes (80S) and polysomes were collected from the separated gradient. As the fractions were collected, they were passed through a UV spectrophotometer, measuring the absorbance at 254nm to provide the polysome profile (Fig 6.1 A). In order to identify the actively translating polysomal pool, the rat primary cortical neurons were treated with puromycin (1 mM) performing the polysome profiling assay. Puromycin, being a t-RNA analog, gets incorporated by the actively translating polysomes and disrupts them [6,7]. The 11 fractions collected under conditions of cycloheximide and puromycin treatment were subjected to immunoblotting for the ribosomal protein RPLP0 (Fig 6.1 C). The distribution of RPLP0 was used as a proxy for the distribution of ribosomes. Upon puromycin treatment, there was a reduction of percentage of RPLP0 distributed in fractions 7-11, and they showed a shift towards the initial fractions 1-6 (Fig 6.1 B and C). Hence, the puromycin sensitive fractions 7-11 were grouped as actively translating fractions while the puromycin insensitive fractions 1-6 were grouped as non-translating fractions (Fig 6.1 D). Thus, the ratio of the percentage distribution of any mRNA or protein in fractions 7-11 by fractions 1-6 indicates the ratio of the distribution in translating pool over non-translating pool (Fig 6.1D).

Figure 6.1

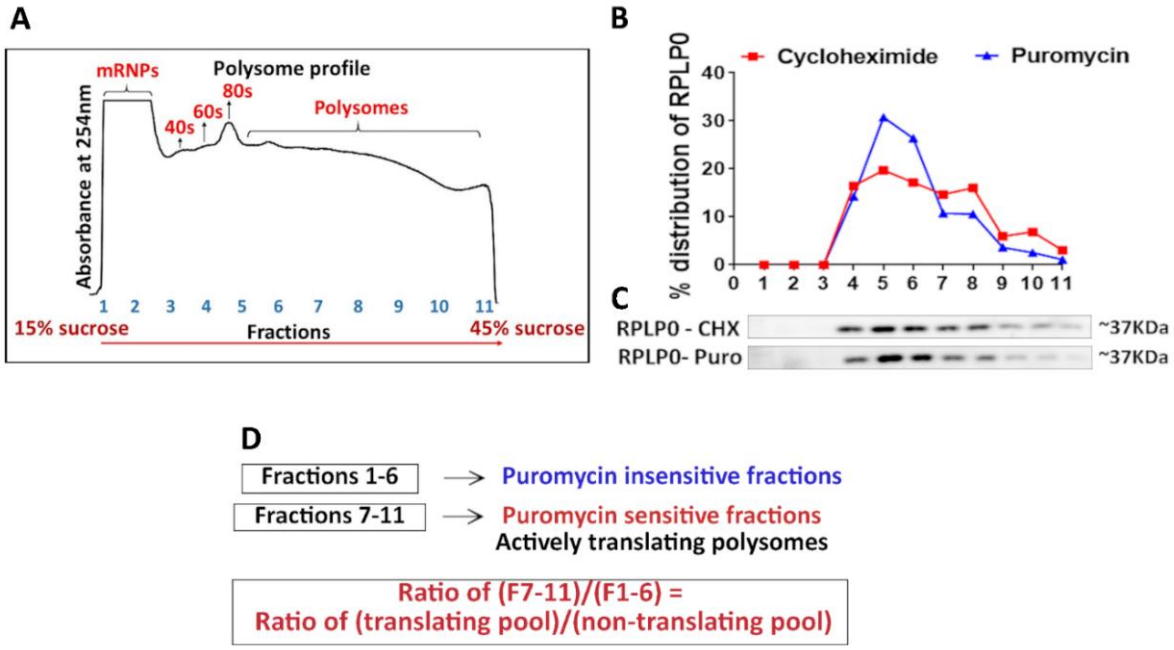

Figure 6.1 - Grouping of polysome profiling fractions

A – Absorbance profile at 254nm indicating the 11 fractions separated on a 15%-45% linear sucrose gradient. The fractions correspond to mRNPs, 40S, 60S, 80S and polysomes.

B – The percentage distribution of ribosomal protein RPLP0 in the 11 fractions on cycloheximide and puromycin treatment of rat primary cortical neurons.

C – Representative immunoblots indicating the distribution of ribosomal protein RPLP0 in the 11 fractions on cycloheximide and puromycin treatment of rat primary cortical neurons.

D – Grouping of fractions 1-6 as non-translating pool and fractions 7-11 as translating pool based on the puromycin sensitivity.

6.2 Polysome profiling validates the NMDAR translation response

Rat primary cortical neurons (DIV15) were subjected to polysome profiling after NMDAR stimulation (20µM) for 1 minute, 5 minutes and 20 minutes. The fractions collected were probed for the distribution of RPLP0 protein (Fig 6.2 A and 6.2 D). In correlation with eEF2 phosphorylation results, 5-minute NMDAR stimulation caused the shift of RPLP0 from the translating fractions 7-11 towards the non-translating pool of fractions 1-6 (Fig 6.2 B and 6.2 C). The decrease in actively translating ribosomal pool further supports the translation inhibition caused by 5-minute NMDAR stimulation. On the other hand, 20-minute NMDAR stimulation led to a shift of RLP0 towards the actively translating fractions 7-11, thus validating the translation upregulation caused by 20-minute NMDAR stimulation (Fig 6.2 E and 6.2 F). However, 1-minute NMDAR stimulation did not cause any change in the RPLP0/ribosome distribution (Fig 6.2 E and 6.2 F), while eEF2 phosphorylation response was highest at this time point. Hence, at 5-minute and 20-minute time points of NMDAR stimulation,

the shift of ribosomes observed in polysome profiling assay correlates with the eEF2 phosphorylation status, validating the early phase translation inhibition and later phase translation upregulation on NMDAR stimulation.

Figure 6.2

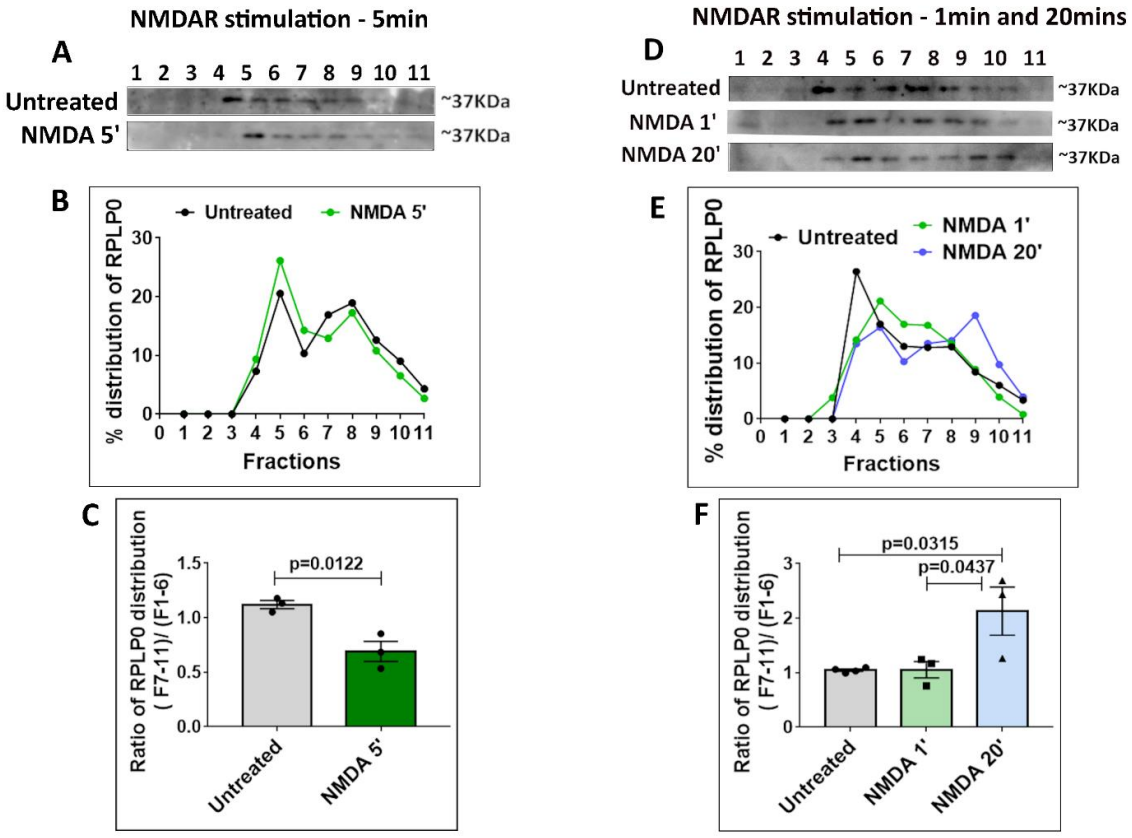

Figure 6.2 - Polysome profiling validates the NMDAR translation profile

A - Representative immunoblots indicating the distribution of ribosomal protein RPLP0 in Fractions 1-11 on 5-minute NMDAR stimulation of rat primary cortical neurons.

B - The percentage distribution of ribosomal protein RPLP0 in Fractions 1-11 on 5-minute NMDAR stimulation of rat primary cortical neurons.

C – The ratio of the percentage distribution of RPLP0 in the translating pool (F7-11) by non-translating pool (F1-6) on 5-minute NMDAR stimulation of rat primary cortical neurons. Data is represented as mean +/- SEM. N=3. Unpaired Student's t-test.

D - Representative immunoblots indicating the distribution of ribosomal protein RPLP0 in Fractions 1-11 on 1-minute and 20-minute NMDAR stimulation of rat primary cortical neurons.

E - The percentage distribution of ribosomal protein RPLP0 in Fractions 1-11 on 1-minute and 20-minute NMDAR stimulation of rat primary cortical neurons.

F - The ratio of the percentage distribution of RPLP0 in the translating pool (F7-11) by non-translating pool (F1-6) on 1-minute and 20-minute NMDAR stimulation of rat

primary cortical neurons. Data is represented as mean +/- SEM, N=3. One-way ANOVA (p=0.0248) followed by Tukey's multiple comparison test.

6.3 Polysome profiling validates the APOE mediated translation response – Global translation inhibition

In order to obtain further insights into APOE mediated translation profiles, we subjected the APOE treated neurons to the polysome profiling assay. Firstly, we performed polysome profiling with the rat primary cortical neurons (DIV15) treated with APOE3/APOE4 iPSC conditioned media for 1-minute and probed them for the distribution of RPLP0 (Fig 6.3 A). With respect to the eEF2 phosphorylation and FUNCAT assay, both APOE3 and APOE4 caused translation inhibition at 1-minute time point (Chapter 4). Accordingly, there was no difference in the percentage distribution of RPLP0 between APOE3 and APOE4 treated neurons at 1-minute time point (Fig 6.3 B and 6.3 C).

Further, we performed polysome profiling with rat primary cortical neurons (DIV15) treated with APOE3 or APOE4 iPSC conditioned media for 20 minutes along with NMDAR stimulation (20µM) during the last 5 minutes (Fig 6.3 D). As observed previously, 5-minute NMDAR stimulation in APOE3 background caused a shift of RPLP0 from translating Fractions 7-11 towards Fractions 1-6 (Fig 6.3 E and 6.3 F). 20-minute treatment with APOE4 conditioned media also caused a shift of the ribosomes from the translating pool to the non-translating pool (Fig 6.3 E and 6.3 F). Thus, in correlation with eEF2 phosphorylation and FUNCAT results, 20-minute APOE4 treatment was similar to APOE3+NMDA condition, both of which caused an inhibition of protein synthesis compared to APOE3 treatment. However, the shift of RPLP0 towards the non-translating initial fractions (especially Fraction 4) was maximum in APOE4+NMDA condition (Fig 6.3 E and 6.3 F) indicating abnormal translation response. Hence, though APOE4 treated neurons remained non-responsive to NMDAR stimulation with respect to eEF2 phosphorylation, PTEN and PSD95 protein levels, polysome profiling indicated that they show a further reduction of protein synthesis with respect to ribosomal distribution.

Figure 6.3

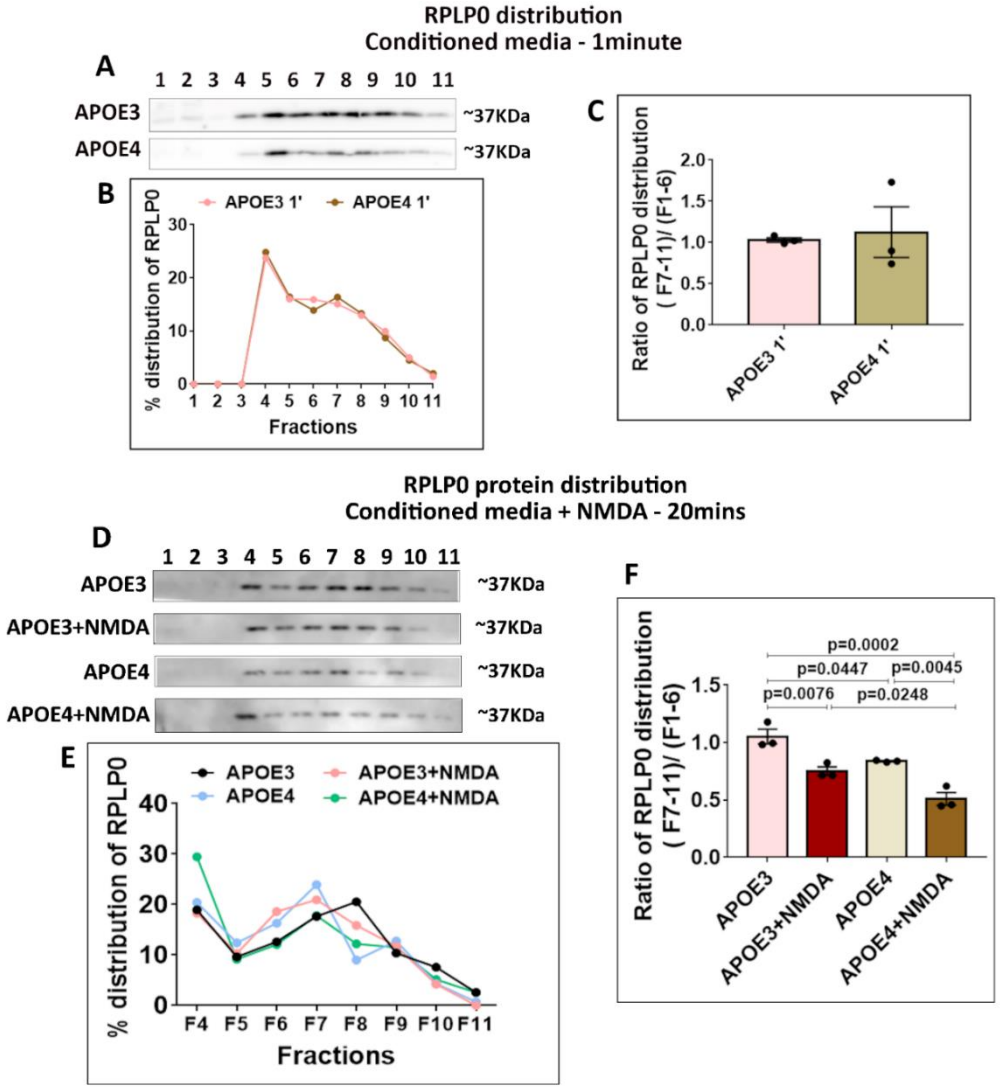

Figure 6.3 - Polysome profiling validates the APOE mediated translation response – Global translation inhibition

A - Representative immunoblots indicating the distribution of ribosomal protein RPLP0 in Fractions 1-11 on 1-minute APOE3 or APOE4 iPSC conditioned media treatment of rat primary cortical neurons.

B - The percentage distribution of ribosomal protein RPLP0 in Fractions 1-11 on 1-minute APOE3 or APOE4 iPSC conditioned media treatment of rat primary cortical neurons.

C – The ratio of the percentage distribution of RPLP0 in the translating pool (F7-11) by non-translating pool (F1-6) on 1-minute APOE3 or APOE4 iPSC conditioned media treatment of rat primary cortical neurons. Data is represented as mean +/- SEM, N=3. Unpaired Student's t-test.

D - Representative immunoblots indicating the distribution of ribosomal protein RPLP0 in Fractions 1-11 on 20-minute APOE3 or APOE4 iPSC conditioned media treatment along with 5-minute NMDAR stimulation of rat primary cortical neurons.

E - The percentage distribution of ribosomal protein RPLP0 in Fractions 4-11 on 20-minute APOE3 or APOE4 iPSC conditioned media treatment along with 5-minute NMDAR stimulation of rat primary cortical neurons.

F - The ratio of the percentage distribution of RPLP0 in the translating pool (F7-11) by non-translating pool (F1-6) on 20-minute APOE3 or APOE4 iPSC conditioned media treatment along with 5-minute NMDAR stimulation of rat primary cortical neurons. Data is represented as mean +/- SEM. N=3, One-way ANOVA (p=0.0002) followed by Tukey's multiple comparison test.

6.4 Polysome profiling validates the APOE mediated translation response – Candidate specific translation activation

As observed in the results discussed in Chapter 5, 20-minute APOE4 treatment not only led to global translation inhibition, but it also caused the translation activation of specific candidates like PTEN and PSD95, mimicking the translation response of 5-minute NMDAR stimulation. In order to investigate this further, we probed for the distribution of PTEN and PSD95 mRNAs in the polysome profiling fractions under the conditions of APOE3 or APOE4 iPSC conditioned media treatment for 20 minutes along with NMDAR stimulation (20µM, 5 minutes). 5-minute NMDAR stimulation in the background of APOE3 treatment caused a shift of PTEN and PSD95 mRNAs towards Fractions 7-11 from Fractions 1-6 (Fig 6.4 A, 6.4 B, 6.4 C, 6.4 D). This indicated that the specific translation activation of these candidates on NMDAR stimulation was intact in the presence of APOE3. 20-minute APOE4 conditioned media treatment caused a shift of these mRNAs towards the translating pool of Fractions 7-11 (Fig 6.4 A, 6.4 B, 6.4 C, 6.4 D), validating the increased protein levels of PTEN and PSD95 observed on APOE4 treatment (Chapter 5). This further corroborated the observation that 20-minute APOE4 treatment mimicked 5-minute NMDAR stimulation in APOE3 background. However, with APOE4+NMDA condition, there was no significant difference in the PTEN and PSD95 mRNAs in Fractions 7-11 compared to APOE4 treatment (Fig 6.4 A, 6.4 B, 6.4 C, 6.4 D). We used β-actin and α-tubulin mRNAs as controls as their distribution in the Fractions 1-11 did not change significantly with respect to APOE treatment or NMDAR stimulation (Fig 6.4 E, 6.4 F, 6.4 G, 6.4 H).

Figure 6.4

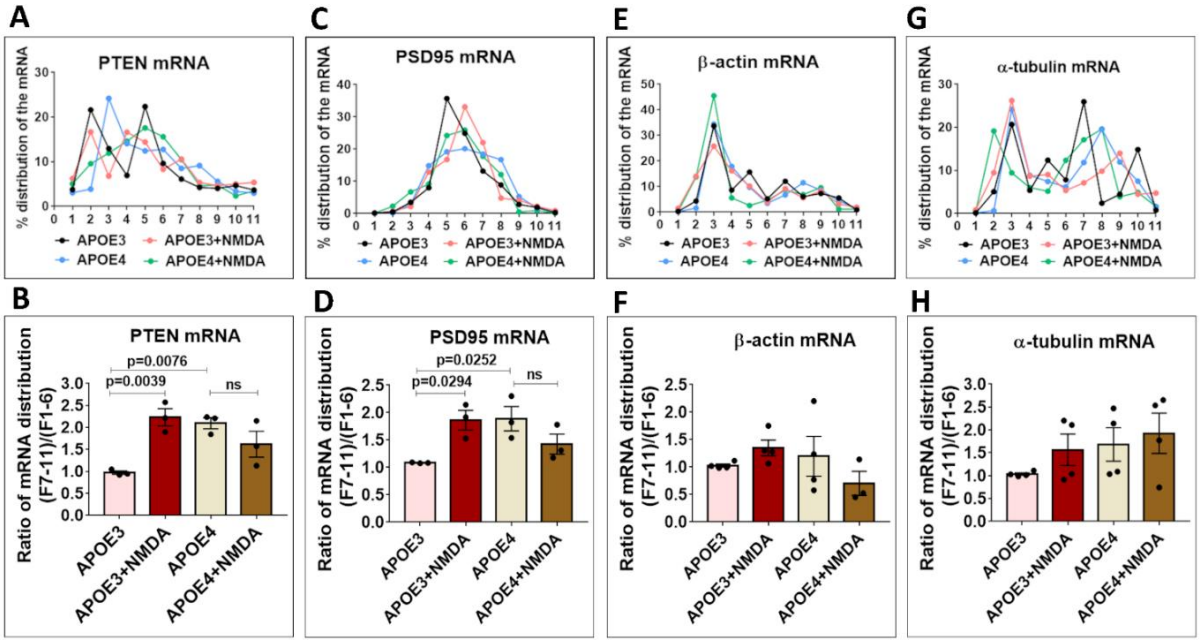

Figure 6.4 - Polysome profiling validates the APOE mediated translation response – Candidate specific translation activation

A - The percentage distribution of PTEN mRNA in Fractions 1-11 on 20-minute APOE3 or APOE4 iPSC conditioned media treatment along with 5-minute NMDAR stimulation of rat primary cortical neurons.

B - The ratio of the percentage distribution of PTEN mRNA in the translating pool (F7-11) by non-translating pool (F1-6) on 20-minute APOE3 or APOE4 iPSC conditioned media treatment along with 5-minute NMDAR stimulation of rat primary cortical neurons. Data is represented as mean +/- SEM. N=3, One-way ANOVA (p=0.006) followed by Dunnett's multiple comparison test.

C - The percentage distribution of PSD95 mRNA in Fractions 1-11 on 20-minute APOE3 or APOE4 iPSC conditioned media treatment along with 5-minute NMDAR stimulation of rat primary cortical neurons.

D - The ratio of the percentage distribution of PSD95 mRNA in the translating pool (F7-11) by non-translating pool (F1-6) on 20-minute APOE3 or APOE4 iPSC conditioned media treatment along with 5-minute NMDAR stimulation of rat primary cortical neurons. Data is represented as mean +/- SEM. N=3, One-way ANOVA (p=0.0286) followed by Dunnett's multiple comparison test

E - The percentage distribution of β-actin mRNA in Fractions 1-11 on 20-minute APOE3 or APOE4 iPSC conditioned media treatment along with 5-minute NMDAR stimulation of rat primary cortical neurons.

F - The ratio of the percentage distribution of β-actin mRNA in the translating pool (F7-11) by non-translating pool (F1-6) on 20-minute APOE3 or APOE4 iPSC conditioned

media treatment along with 5-minute NMDAR stimulation of rat primary cortical neurons. Data is represented as mean +/- SEM. N=3, One-way ANOVA (ns).

G - The percentage distribution of α-tubulin mRNA in Fractions 1-11 on 20-minute APOE3 or APOE4 iPSC conditioned media treatment along with 5-minute NMDAR stimulation of rat primary cortical neurons.

H - The ratio of the percentage distribution of α-tubulin mRNA in the translating pool (F7-11) by non-translating pool (F1-6) on 20-minute APOE3 or APOE4 iPSC conditioned media treatment along with 5-minute NMDAR stimulation of rat primary cortical neurons. Data is represented as mean +/- SEM. N=3, One-way ANOVA (ns).

6.5 NMDAR stimulation in APOE4 background causes the shift of the mRNAs to the mRNP pool

We observed that the ribosomal shift towards Fractions 1-6 was highest in APOE4+NMDA condition, indicating maximal translation inhibition (Fig 6.3). And, when we paid close attention to the mRNA distribution, it appeared that the shift of the mRNAs was particularly high in the initial fractions (Fractions 1-3) in APOE4+NMDA condition (Fig 6.4). In order to acquire a better understanding of the translation response in APOE4+NMDA condition, we reanalyzed the initial non-translating Fractions 1-6 only (Fig 6.5 A). Fractions 1-6 were grouped into two pools - Fractions 1-3 which primarily constituted the mRNPs as they did not show the signal for RPLP0 (ribosomes) and Fractions 4-6 which constituted the ribosomal subunits and monosomes (Fig 6.5 B). The ratio of the percentage distribution of the mRNAs in Fractions 1-3 over Fractions 4-6 indicated their enrichment in the mRNP pool which was devoid of ribosomes (Fig 6.5 B). Interestingly, PSD95, β-actin and α-tubulin mRNAs showed a marked enrichment in Fractions 1-3 in APOE4+NMDA condition (Fig 6.5 C, 6.5 D and 6.5 E). This seemed like a general response as both NMDAR/APOE specific candidates like PSD95 and NMDAR/APOE non-responsive control mRNAs showed the same response in APOE4+NMDA condition. To validate this further, we picked another important synaptic candidate mRNA CaMKIIα. Interestingly, CaMKIIα also showed an increase in Fractions 1-3 on APOE4+NMDA condition (Fig 6.5 F). However, PTEN mRNA did not show this trend of increase in Fractions 1-3 on APOE4+NMDA condition (Fig 6.5 G). Unlike other mRNAs, PTEN mRNA is majorly (about 75%) present in Fractions 1-6 (Fig 6.4 A) even in the unstimulated condition. This may be the reason for not observing a shift of PTEN mRNA within these pools. Thus, along with showing maximum shift of ribosomes towards the non-translating pool, NMDAR stimulation in APOE4 background also causes an increased accumulation of mRNAs in the mRNP fractions.

Figure 6.5

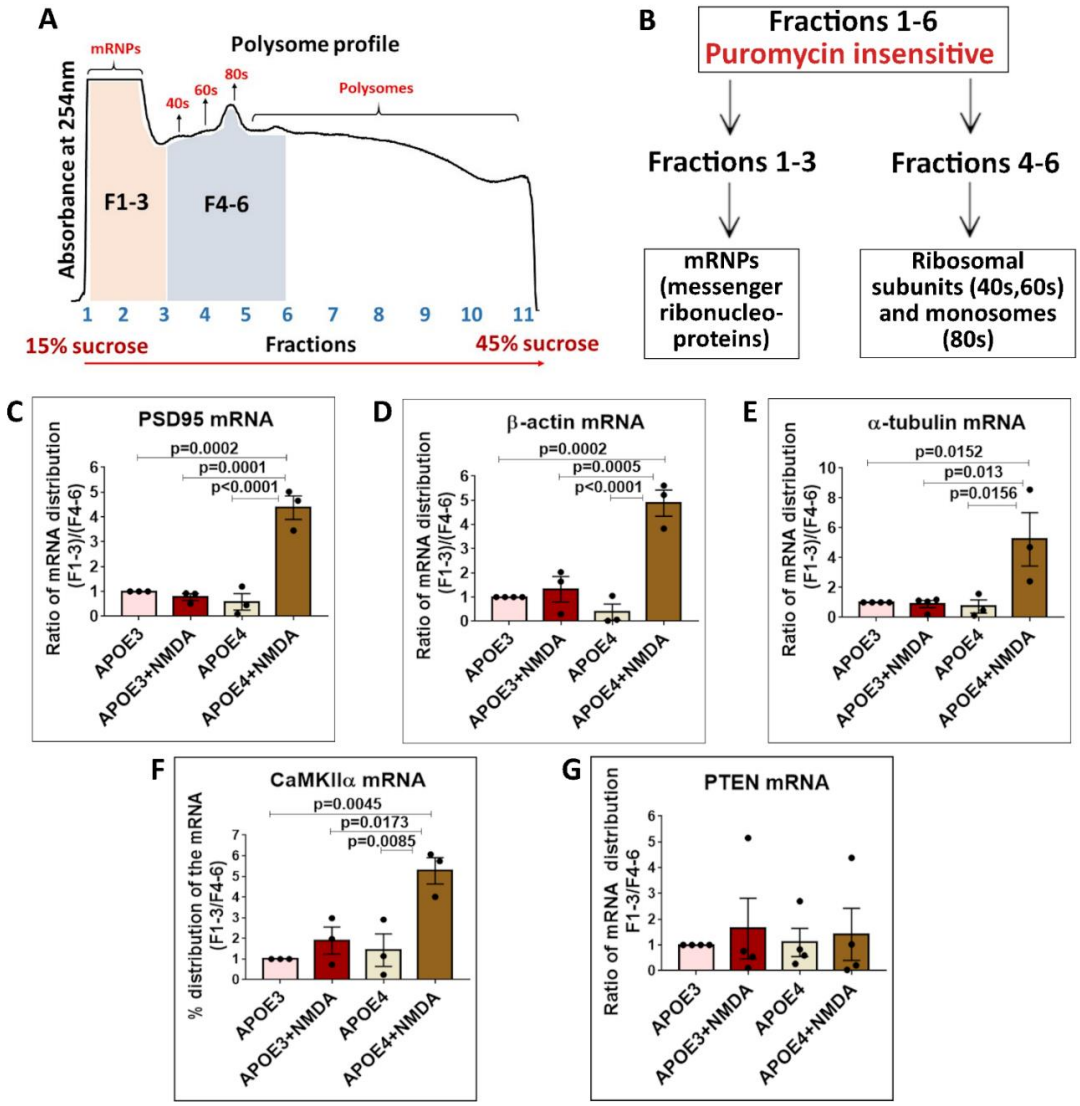

Figure 6.5 - NMDAR stimulation in APOE4 background causes the shift of the mRNAs to the mRNP pool

A - Absorbance profile at 254nm indicating the grouping of Fractions 1-6 into two pools – Fractions 1-3 (mRNPs) and Fractions 4-6 (Ribosomal subunits and monosomes)

B - Flowchart indicating the grouping of Fractions 1-6 into two pools – Fractions 1-3 (mRNPs) and Fractions 4-6 (Ribosomal subunits and monosomes). The ratio of percentage distribution of the mRNAs in Fractions 1-3 over Fractions 4-6 was considered for further analysis.

C - The ratio of the percentage distribution of PSD95 mRNA in the Fractions 1-3 (mRNPs) over Fractions 4-6 on 20-minute APOE3 or APOE4 iPSC conditioned media treatment along with 5-minute NMDAR stimulation of rat primary cortical neurons. Data is represented as mean +/- SEM. N=3, One-way ANOVA ($p<0.0001$) followed by Tukey's multiple comparison test.

D - The ratio of the percentage distribution of β-actin mRNA in the Fractions 1-3 (mRNPs) over Fractions 4-6 on 20-minute APOE3 or APOE4 iPSC conditioned media treatment along with 5-minute NMDAR stimulation of rat primary cortical neurons. Data is represented as mean +/- SEM. N=3, One-way ANOVA ($p<0.0001$) followed by Tukey's multiple comparison test.

E - The ratio of the percentage distribution of α-tubulin mRNA in the Fractions 1-3 (mRNPs) over Fractions 4-6 on 20-minute APOE3 or APOE4 iPSC conditioned media treatment along with 5-minute NMDAR stimulation of rat primary cortical neurons. Data is represented as mean +/- SEM. N=3-4, One-way ANOVA ($p=0.0079$) followed by Tukey's multiple comparison test.

F - The ratio of the percentage distribution of CaMKIIα mRNA in the Fractions 1-3 (mRNPs) over Fractions 4-6 on 20-minute APOE3 or APOE4 iPSC conditioned media treatment along with 5-minute NMDAR stimulation of rat primary cortical neurons. Data is represented as mean +/- SEM. N=3-4, One-way ANOVA ($p=0.0038$) followed by Tukey's multiple comparison test.

G - The ratio of the percentage distribution of PTEN mRNA in the Fractions 1-3 (mRNPs) over Fractions 4-6 on 20-minute APOE3 or APOE4 iPSC conditioned media treatment along with 5-minute NMDAR stimulation of rat primary cortical neurons. Data is represented as mean +/- SEM. N=4, One-way ANOVA (ns).

6.6 NMDAR stimulation in APOE4 background causes stress response

The increased accumulation of the mRNAs in the mRNP pool (fractions 1-3) indicated the translation inhibition of the mRNAs in APOE4+NMDA condition, predominantly at the stage of translation initiation. In order to understand this better, we probed the polysome fractions for the distribution of small ribosomal subunit protein RPS6 (Fig 6.6 A and 6.6 B). Fraction 3 showed the presence of RPS6 protein, while the large subunit protein RPLP0 was absent in Fraction 3. However, Fraction 4 showed the presence of both RPS6 and RPLP0. If translation was inhibited at the initiation stage, we would anticipate the increase in 43s or 48s pre-initiation complexes which would be distributed in Fractions 3 and 4. Hence, we quantified the percentage of RPS6 in Fractions 3 and 4 under different conditions. We observed that APOE4+NMDA condition showed a marked increase in the percentage of RPS6 in Fractions 3-4 (Fig 6.6 B and 6.6 C), indicating a potential increase in the pre-initiation complexes. To validate this further, we probed for the phosphorylation of eukaryotic translation initiation factor eIF2α, a well-established readout for increased stress response, under the conditions of APOE3/APOE4 iPSC conditioned media treatment along with NMDAR stimulation (Fig 6.6 D). APOE4 treatment followed by NMDAR stimulation led to a significant increase in the phosphorylation of eIF2α, which was not observed with APOE4 treatment or NMDAR stimulation in APOE3 background (Fig 6.6 D). Thus, NMDAR stimulation in APOE4 background caused a stress response phenotype by increasing the phosphorylation of eIF2α and shifting the mRNAs to the inhibitory/mRNP pool.

Figure 6.6

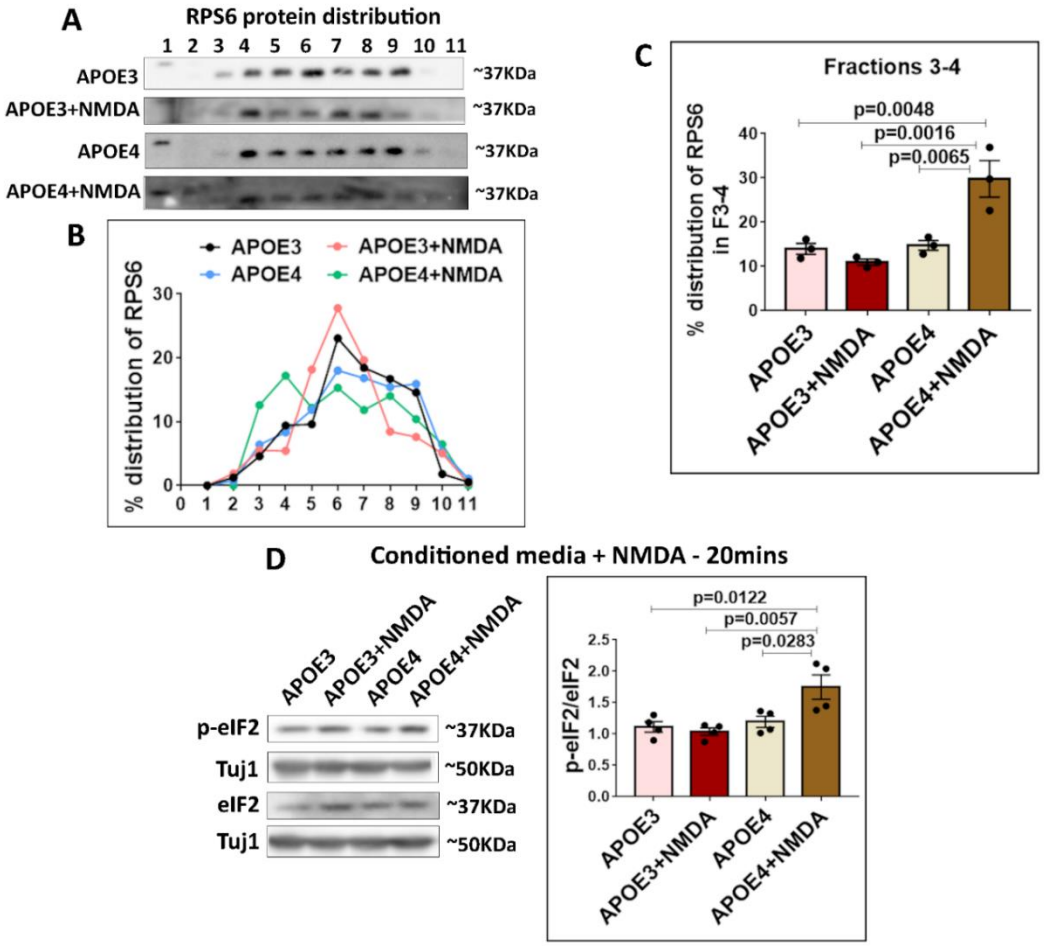

Figure 6.6 - NMDAR stimulation in APOE4 background causes stress response

A - Representative immunoblots indicating the distribution of ribosomal protein RPS6 in Fractions 1-11 on 20-minute APOE3 or APOE4 iPSC conditioned media treatment along with 5-minute NMDAR stimulation of rat primary cortical neurons.

B - The percentage distribution of ribosomal protein RPS6 in Fractions 1-11 on 20-minute APOE3 or APOE4 iPSC conditioned media treatment along with 5-minute NMDAR stimulation of rat primary cortical neurons.

C - The percentage distribution of RPS6 in Fractions 3-4 on 20-minute APOE3 or APOE4 iPSC conditioned media treatment along with 5-minute NMDAR stimulation of rat primary cortical neurons. Data is represented as mean +/- SEM. N=3, One-way ANOVA (p=0.0015) followed by Tukey's multiple comparison test.

D - Representative immunoblots showing the levels of p-eIF2, eIF2 and Tuj1 in rat primary cortical neurons on 20-minute APOE3 or APOE4 iPSC conditioned media treatment along with 5-minute NMDAR stimulation. The graph represents the ratio of p-eIF2 to eIF2 normalized to Tuj1. Data is represented as mean +/- SEM. N=4, One-way ANOVA (p=0.0047) followed by Tukey's multiple comparison test.

6.7 Summary and Discussion

In this chapter, we use polysome profiling as a technique to validate and provide more insights into the translation profiles on NMDAR stimulation and APOE treatment. Firstly, we validated the translation profile for NMDAR stimulation. 1-minute NMDAR stimulation caused the highest increase in eEF2 phosphorylation (Chapter 5); however, this was not reflected in the polysome profiling assay as we did not observe any change in the ribosomal distribution. We hypothesize that, though eEF2 is phosphorylated, it would probably take longer for the shift in ribosomes to transpire. However, with 5-minute NMDAR stimulation (where eEF2 phosphorylation is lower than 1-minute NMDAR stimulation but higher than untreated) the reduction of ribosomes in the actively translating fractions was clearly evident. This further points out towards the idea that the changes in eEF2 phosphorylation precede the changes in the ribosomal distributions. At 20-minute time point of NMDAR stimulation, the marked ribosomal shift towards the actively translating pool confirms the robust translation activation of late phase NMDAR stimulation. Thus, we were able to illustrate the use of polysome profiling and ribosomal distributions to study global translation profiles.

The ribosomal distribution was similar between 1-minute APOE3 and APOE4 conditioned media treatment. This correlates with the eEF2 phosphorylation and FUNCAT results indicating that both APOE3 and APOE4 cause translation inhibition at 1-minute. However, with 20-minute APOE4 treatment, the ribosomes decreased in the translating pool compared to APOE3 treatment, affirming the translation inhibition caused by APOE4 treatment. 5-minute NMDAR stimulation in APOE3 background showed the normal NMDAR response of decreased ribosomes in the translating pool. Interestingly, 5-minute NMDAR stimulation in APOE4 background showed the maximum reduction of ribosomes in the translating fractions, though the eEF2 phosphorylation remained similar to APOE4 treatment alone. This indicated that there were additional mechanisms contributing to the translation inhibition in APOE4+NMDA condition and prompted us to probe for translation initiation as well. The results from eIF2 phosphorylation confirmed that the inhibition of translation initiation occurred in APOE4+NMDA condition only. Hence, the ribosomal distributions/ polysome profiling was a sensitive tool that helped in identifying that NMDAR stimulation indeed had an effect in APOE4 background as well. While APOE4 treatment and NMDAR stimulation in APOE3 background caused inhibition of translation elongation, NMDAR stimulation in APOE4 background led to inhibition of translation initiation and elongation.

Another advantage of polysome profiling was that we could probe for the polysomal distribution of individual candidate mRNAs and understand their translation profiles in the background of the global translation status. Accordingly, we were able to show the translation activation or shift of PTEN and PSD95 mRNAs into the actively translating pool on NMDAR stimulation in APOE3 background, which corresponds to the increased protein levels as well (Chapter 5). Treatment with APOE4 for 20 minutes brings out the same response as APOE3+NMDA. But, on NMDAR stimulation in APOE4 background, the protein levels of PTEN and PSD95 remained similar to APOE4 treatment, and the mRNA distribution in the translating pool also did not change significantly. However, when we analyzed the non-translating pool alone by re-

grouping fractions 1-6, we were able to capture a distinct phenomenon where the mRNAs showed a dramatic increase in the first three fractions corresponding to the mRNP pool. This was observed for mRNAs which were non-targets of NMDAR stimulation as well, indicating that it was an abnormal response. Hence, polysome profiling became an important tool to identify the shift of mRNAs towards the translation inhibitory mRNP complexes with APOE4+NMDA condition.

The increased eIF2 phosphorylation and shift of mRNAs towards the mRNP fractions in APOE4+NMDA condition directed towards the stress response phenotype. This demonstrated that the physiological synaptic stimulation could generate a stress response in the background of a treatment which mimics the physiological stimulation. The translation initiation inhibition in APOE4+NMDA background was further supported by the increased accumulation of RPS6 in Fractions 3-4 which potentially represent the 43S and 48S pre-initiation complexes. This also opens up an interesting arena for future studies to identify the signaling pathways/ kinases responsible for the activation of eIF2 phosphorylation in APOE4+NMDA condition only. Thus, as explained in the introduction, the use of polysome profiling provided greater sensitivity and helped us in dissecting out the mechanistic details of translation inhibition in different conditions, especially that of APOE4+NMDA. In summary, though APOE4 causes translation elongation inhibition, NMDAR stimulation in APOE4 background causes inhibition of translation initiation and elongation leading to stress response.

6.8 References

1. Pringle, E. S., McCormick, C. & Cheng, Z. Polysome Profiling Analysis of mRNA and Associated Proteins Engaged in Translation. *Current Protocols in Molecular Biology* **125**, (2019).
2. Zhang, S. *et al.* Insights Into Translatomics in the Nervous System. *Frontiers in Genetics* vol. 11 (2020).
3. Zhao, J., Qin, B., Nikolay, R., Spahn, C. M. T. & Zhang, G. Translatomics: The global view of translation. *International Journal of Molecular Sciences* vol. 20 (2019).
4. Esposito, A. M. *et al.* Eukaryotic polyribosome profile analysis. *Journal of Visualized Experiments* (2010) doi:10.3791/1948.
5. Muddashetty, R. S. *et al.* Reversible Inhibition of PSD-95 mRNA Translation by miR-125a, FMRP Phosphorylation, and mGluR Signaling. *Molecular Cell* (2011) doi:10.1016/j.molcel.2011.05.006.
6. Kute, P. M., Ramakrishna, S., Neelagandan, N., Chattarji, S. & Muddashetty, Ravi. S. NMDAR mediated translation at the synapse is regulated by MOV10 and FMRP. *Molecular Brain* **12**, 65 (2019).
7. Aviner, R. The science of puromycin: From studies of ribosome function to applications in biotechnology. *Computational and Structural Biotechnology Journal* vol. 18 (2020).
8. Tscherne, J. S. & Pestka, S. Inhibition of protein synthesis in intact HeLa cells. *ANTIMICROB.AGENTS CHEMOTHER.* **8**, (1975).

9. Coudert, L., Adjibade, P. & Mazroui, R. Analysis of translation initiation during stress conditions by polysome profiling. *Journal of Visualized Experiments* (2014) doi:10.3791/51164.

10. Knight, J. R. P. *et al.* Control of translation elongation in health and disease. *DMM Disease Models and Mechanisms* vol. 13 (2020).

11. Ryazanov, A. G. & Spirin, A. S. Phosphorylation of elongation factor 2: A key mechanism regulating gene expression in vertebrates. *New Biologist* vol. 2 (1990).

12. Kaul, G., Pattan, G. & Rafeequi, T. Eukaryotic elongation factor-2 (eEF2): Its regulation and peptide chain elongation. *Cell Biochemistry and Function* **29**, (2011).

13. Sonenberg, N. & Hinnebusch, A. G. Regulation of Translation Initiation in Eukaryotes: Mechanisms and Biological Targets. *Cell* vol. 136 (2009).

Chapter 7

The role of calcium in APOE mediated translation response

7.0 Introduction

In the previous chapters, we observed that both APOE3 and APOE4 inhibit protein synthesis at an early time point (1-minute) similar to NMDAR stimulation. However, only APOE4 affects the translation response to NMDAR stimulation. In order to obtain more mechanistic insights about the differences in the translation responses, we decided to study the calcium profiles under these conditions.

Calcium is an important secondary messenger, especially downstream of synaptic stimulations. Stimulation of ionotropic NMDARs or metabotropic mGluRs have distinct calcium profiles which determine their downstream signaling [1–3]. NMDA receptors are ionotropic glutamate receptors which have a high permeability for calcium along with sodium and potassium [2]. Stimulation of NMDARs leads to a robust increase in intracellular calcium contributed by different sources – NMDA receptors, L-Type Voltage Gated Calcium Channels (L-VGCCs), and internal calcium stores [3–8]. The activation of the different sources of calcium upon NMDAR stimulation is spatially and sequentially regulated [3,6,8,9]. NMDARs lead to the first burst of calcium which further activates L-VGCCs, followed by internal stores through calcium-induced calcium release (CICR)[4,6–8]. Previous studies have outlined the contribution of calcium in causing the inhibitory phase of NMDAR translation response through activation of eEF2 kinase [10,11]. eEF2 kinase is a calcium-calmodulin dependent kinase III which is known to get activated upon elevated calcium levels, particularly downstream of NMDARs[12]. However, the role of calcium in the later phase translation activation upon NMDAR stimulation is less explored.

Another example of the specific calcium signature downstream of synaptic activity is with respect to stimulation of metabotropic glutamate receptors (mGluRs). While NMDARs are shown to activate both external and internal sources of calcium, mGluR stimulation primary involves internal calcium sources. The activation of Group 1 mGluRs is coupled to the G-Protein Coupled Receptor (GPCR) pathway leading to the generation of Inositol-3-Phosphate (IP3) and Diacylglycerol (DAG) through the cleavage mediated by PLC[13]. IP3 causes the release of calcium from the ER stores by binding to IP3 receptors. mGluR activation is also shown to cause influx of extracellular calcium through L-VGCCs in the later stages[14]. Thus, the calcium signature and its regulation downstream of mGluR stimulation is also highly distinct and specific.

Therefore, we speculated if the distinct translation response downstream of APOE isoforms was also linked to calcium. Another important reason to study calcium was that APOE has been reported to cause an influx of calcium in neurons through the activation of NMDARs [15–19]. Hence, the increased eEF2 phosphorylation upon APOE treatment could potentially be linked to calcium influx through NMDARs. Thus, putting together these 3 points (1. APOE causes calcium influx in neurons through NMDARs; 2. NMDAR stimulation causes distinct calcium profile through sequential activation of

different sources and 3. Early phase translation inhibition on NMDAR stimulation is calcium-dependent), we thought that calcium could be an interesting link to understand APOE and NMDA translation profiles. Hence, we investigated the calcium signatures and sources involved in APOE treatment and their contribution to the translation response.

Results

7.1 NMDA and APOE mediated translation response is calcium dependent

To begin with, we investigated the role of calcium in NMDAR dependent translation response. We stimulated rat primary cortical neurons with NMDA (20 µM) in ACSF with or without calcium (Fig 7.1 A). When the neurons were stimulated with NMDA in the presence of calcium, the translation response was similar to previous observation. The eEF2 phosphorylation increased at 1-minute and 5-minute time points, indicating a phase of translation inhibition (Fig 7.1 A). At 20-minute, eEF2 phosphorylation showed a significant reduction compared to the earlier time points indicating a phase of translation activation (Fig 7.1 A). In the absence of external calcium (calcium-free ACSF), the eEF2 phosphorylation did not change on NMDAR stimulation at 1, 5 or 20-minute time points compared to basal condition (Fig 7.1 A). Thus, the presence of extracellular calcium was critical for the NMDAR response, both with respect to early translation inhibition and later phase of translation activation.

As reported earlier, the neurons treated with APOE4 recombinant protein for 20 minutes in the presence of extracellular calcium showed an increase in eEF2 phosphorylation compared to APOE3 treated neurons (Fig 7.1 C). However, APOE4 mediated increase in eEF2 phosphorylation was completely abolished in the absence of calcium (Fig 7.1 C). Untreated or APOE3 treated neurons in calcium-free ACSF did not show any change in eEF2 phosphorylation (Fig 7.1 B and 7.1 C). Thus, the APOE4 mediated translation inhibition was also dependent on extracellular calcium.

As a control, we wanted to verify that the changes in eEF2 phosphorylation were not due to the changes in the levels of eEF2 kinase (eEF2K) and phosphatase (PP2A). Previously, there have been reports showing that APOE4 causes a transcriptional downregulation of the regulatory subunit of PP2A [20]. However, in our model system and APOE treatment paradigm (conditioned media for 20 minutes), we did not observe any changes in the mRNA levels of eEF2 kinase (Fig 7.1 D) and PP2A regulatory subunit (Fig 7.1 E). Thus, the changes in eEF2 phosphorylation were not mediated by transcriptional changes of the kinase or phosphatase.

Figure 7.1

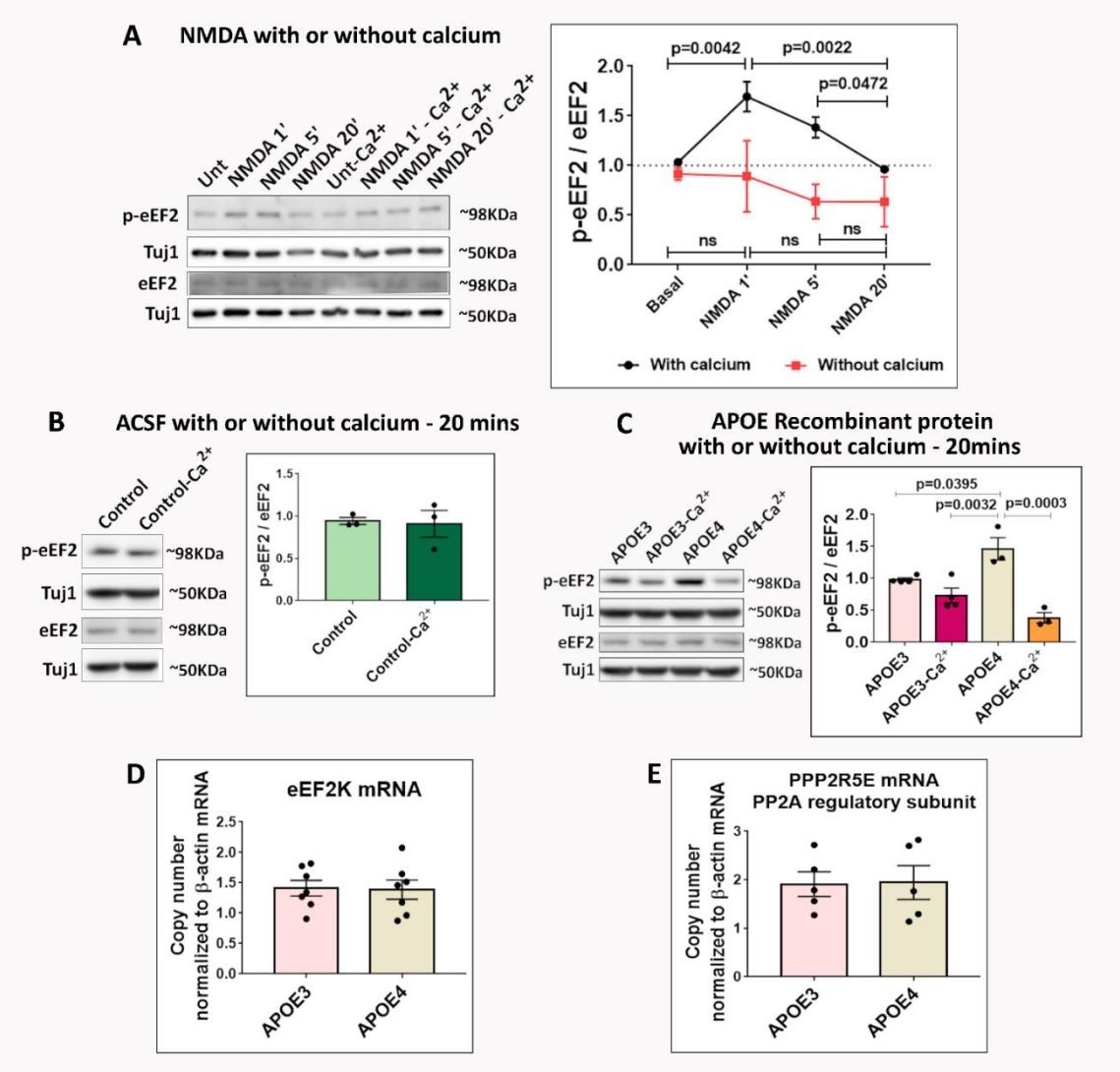

Figure 7.1 – NMDA and APOE mediated translation response is calcium dependent

A - Representative immunoblots showing the levels of p-eEF2, eEF2 and Tuj1 in rat primary cortical neurons stimulated with NMDA for 1-minute, 5-minute and 20-minutes in the presence or absence of extracellular calcium. The graph represents the ratio of p-eEF2 to eEF2 normalized to Tuj1. Data is represented as mean +/- SEM. N=3. For data points with calcium, One-way ANOVA (p=0.0017) followed by Tukey's multiple comparison test. For data points without calcium, One-way ANOVA (ns – non-significant).

B - Representative immunoblots showing the levels of p-eEF2, eEF2 and Tuj1 in rat primary cortical neurons in the presence or absence of extracellular calcium. The graph represents the ratio of p-eEF2 to eEF2 normalized to Tuj1. Data is represented as mean +/- SEM. N=3, Unpaired Student's t-test.

C - Representative immunoblots showing the levels of p-eEF2, eEF2 and Tuj1 in rat primary cortical neurons treated with APOE3 or APOE4 conditioned media for 20 minutes in the presence or absence of extracellular calcium. The graph represents the

ratio of p-eEF2 to eEF2 normalized to Tuj1. Data is represented as mean +/- SEM. N=3-4, One-way ANOVA (p=0.0004) followed by Tukey's multiple comparison test.

D – Rat primary cortical neurons were treated with APOE3/APOE4 conditioned media for 20 minutes and subjected to RT-PCR to measure the levels of eEF2 kinase mRNA. The graph indicates the copy number of eEF2K mRNA normalized to copy number of β-actin mRNA. Data is represented as mean +/- SEM, N=7. Unpaired Student's t-test (ns).

E – Rat primary cortical neurons were treated with APOE3/APOE4 conditioned media for 20 minutes and subjected to RT-PCR to measure the levels of PP2A regulatory subunit PPP2R5E mRNA. The graph indicates the copy number of PPP2R5E mRNA normalized to copy number of β-actin mRNA. Data is represented as mean +/- SEM, N=5. Unpaired Student's t-test (ns).

7.2 NMDAR stimulation and APOE treatment involves distinct calcium signatures and sources

In the previous section, we showed that NMDA and APOE mediated translation response was calcium dependent. NMDAR stimulation is known to cause influx of calcium through NMDA receptors which eventually activates L-type Voltage Gated Calcium Channels (L-VGCCs) [3,7]. The activation of L-VGCCs is known to sustain the influx of calcium in neurons. Similarly, APOE is known to cause calcium influx in neurons through NMDARs [15–19], but the involvement of L-VGCCs is not clear. We investigated the contribution of these two sources in NMDA and APOE calcium responses by performing calcium imaging with Fluo-4AM dye.

As reported previously, stimulation with NMDA caused a rapid and robust influx of calcium in neurons (Fig 7.2 A), which specifically gets blocked upon pre-incubation with NMDAR antagonist MK801 (Fig 7.2 A). NMDAR stimulation in the presence of L-VGCC antagonist Nifedipine did not block the initial influx of calcium; however, the sustained increase in calcium was blocked (Fig 7.2 A). This establishes the temporal pattern of the different calcium sources involved in NMDAR response. The initial entry of calcium into the neurons occurs through NMDARs, which further activates L-VGCC and sustains the increased levels of calcium.

Next, we investigated the calcium profiles upon APOE treatment. Addition of APOE3 recombinant protein caused a short burst of calcium into the neurons (Fig 7.2 B). The pre-treatment with MK801 completely blocked the calcium entry indicating that NMDARs were one of the major sources of calcium influx upon APOE3 treatment (Fig 7.2 B). Interestingly, pre-incubation with Nifedipine had no effect on APOE3 mediated calcium response indicating that L-VGCCs had no role (Fig 7.2 B). Thus, NMDARs were the primary source of calcium influx upon APOE3 treatment. On the other hand, addition of APOE4 recombinant protein caused a robust influx of calcium in the neurons (Fig 7.2 C). Pre-incubation with MK801 prevented the APOE4 mediated calcium influx showing that NMDARs were the primary source of calcium entry (Fig 7.2 C). Pre-incubation with Nifedipine did not block the influx of calcium, though it prevented the sustenance of calcium levels (Fig 7.2 C); thus, showing that L-VGCCs were activated upon APOE4 addition and contributed to the later phase of calcium response. Hence,

APOE4 calcium response also involved two sources – NMDARs which initiated the calcium entry and L-VGCCs which sustained the calcium influx.

Figure 7.2

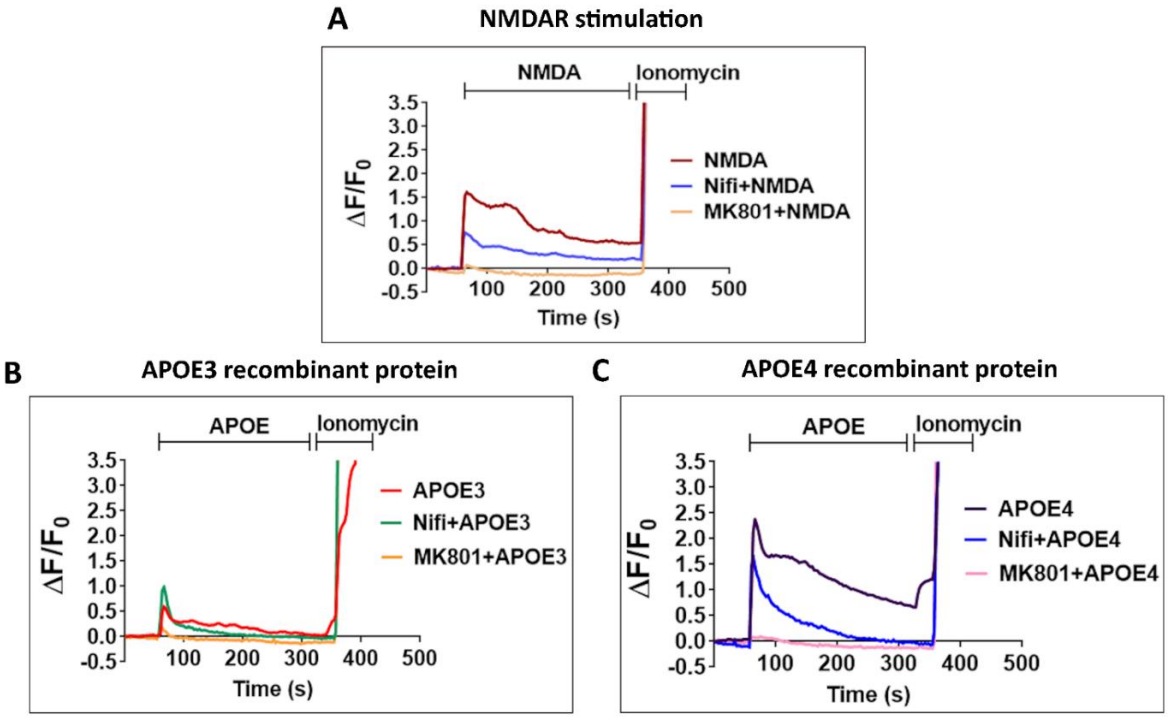

Figure 7.2 – The distinct calcium signatures and sources upon NMDAR stimulation and APOE treatment

Rat primary cortical neurons (DIV15) were subjected to calcium imaging for 7 minutes using Fluo-4AM dye. The graphs represent the time trace for the change in the fluorescence (Delta F/ F0) at a given time point compared with initial fluorescence (F0) under the following conditions –

A - NMDAR stimulation (20 µM), nifedipine (50 µM) pre-treatment followed by NMDAR stimulation (20 µM), and MK801 (25 µM) pre-treatment followed by NMDAR stimulation (20mM).

B - APOE3 treatment (15 nM), nifedipine (50 µM) pre-treatment followed by APOE3 addition (15 nM), and MK801 (25 µM) pre-treatment followed by APOE3 addition (15 nM).

C – APOE4 treatment (15 nM), nifedipine (50 µM) pre-treatment followed by APOE4 addition (15 nM), and MK801 (25 µM) pre-treatment followed by APOE4 addition (15 nM).

7.3 APOE4 causes a higher and sustained influx of calcium compared to APOE3

Next, we quantified the calcium responses (change in the Fluo-4AM intensities) at 1-minute and 2-minutes after the addition of APOE. At both the time points, the extent of the calcium influx caused by APOE4 in the neurons was significantly higher than APOE3 (Fig 7.3 A and Fig 7.3 E). The influx of calcium caused by APOE3 and APOE3 in the presence of Nifedipine (Nifi+APOE3) was not significantly different at 1-minute

and 2-minute time points (Fig 7.3 B and Fig 7.3 F). However, in the presence of MK801, APOE3 mediated calcium influx was significantly lower at both the time points (Fig 7.3 B and Fig 7.3 F), thus validating that NMDARs were the primary source of calcium entry on APOE3 treatment. With APOE4 addition, only MK801 significantly reduced the calcium influx at both 1-minute and 2-minute time points (Fig 7.3 C and Fig 7.3 G). Nifedipine pre-incubation significantly reduced the calcium levels on APOE4 addition at 2-minute time point only (Fig 7.3 C), whereas it did not affect the calcium influx at 1-minute time point compared to APOE4 treatment (Fig 7.3 G). Thus, NMDARs were the primary source of calcium influx on APOE4 addition as well. L-VGCCs contribute to the sustenance of calcium, hence affecting the calcium response at 2-minute time point rather than 1-minute. Another interesting observation was that, at both 1-minute and 2-minute time points, the calcium influx caused by NMDARs in APOE4 condition (Nifedipine+APOE4 condition) was significantly higher than APOE3 and Nifedipine+APOE3 (Fig 7.3 D and Fig 7.3 H). Thus, the initial NMDAR component of the calcium was also higher in case of APOE4 addition as compared to APOE3 (Fig 7.3 D and Fig 7.3 H). Finally, we measured the calcium levels in neurons subjected to chronic exposure of APOE4 for 24 hours. APOE4 recombinant protein (Fig 7.3 I) or APOE4 conditioned media (Fig 7.3 J) treatment for 24 hours led to a significant increase in resting calcium levels.

Figure 7.3

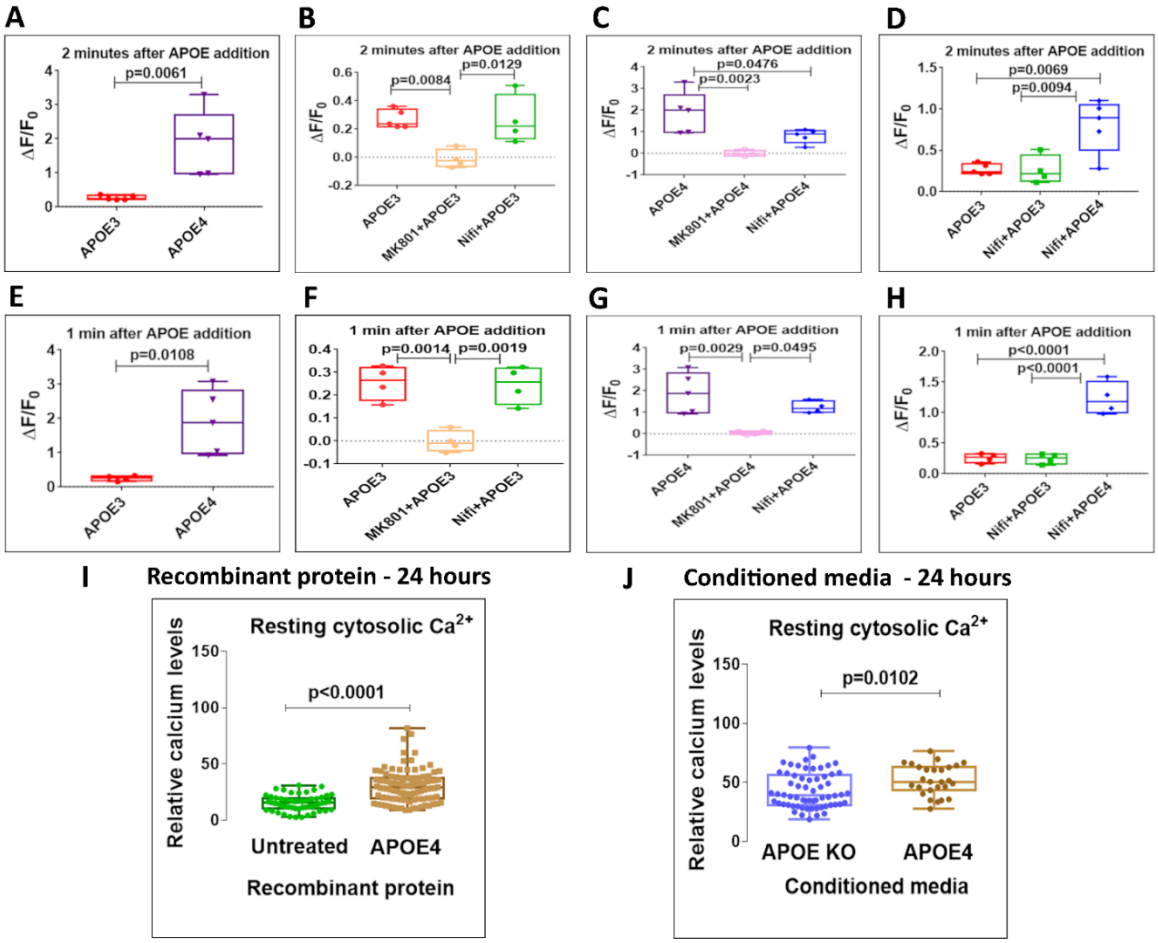

Figure 7.3 – APOE4 causes a higher and sustained influx of calcium compared to APOE3

A-D - Box plots representing the quantification of the change in Flou4-AM fluorescence (ΔF/F0) after 2 min of APOE addition. N=4–5 experiments, each experiment has the average value of 40–50 neurons.

A - Unpaired Student's t test; B - One-way ANOVA ($p = 0.0058$) followed by Tukey's multiple comparison test; C - One-way ANOVA ($p = 0.0029$) followed by Tukey's multiple comparison test; D - One-way ANOVA ($p = 0.0038$) followed by Tukey's multiple comparison test.

E-H - Box plots representing the quantification of the change in Flou4-AM fluorescence (ΔF/F0) after 1 min of APOE addition. N=4–5 experiments, each experiment has the average value of 40–50 neurons.

E - Unpaired Student's t test; F - One-way ANOVA ($p=0.0008$) followed by Tukey's multiple comparison test; G - One-way ANOVA ($p = 0.0038$) followed by Tukey's multiple comparison test; H - One-way ANOVA ($p<0.0001$) followed by Tukey's multiple comparison test.

I - The graph shows the resting cytosolic calcium measured in rat primary cortical neurons (DIV15) were treated with APOE4 recombinant protein (15 nM) for 24 h and subjected to calcium imaging using Fluo8-AM. N=50–60 neurons from 3 independent experiments, Kolmogorov–Smirnov test.

J - The graph shows the resting cytosolic calcium measured in rat primary cortical neurons (DIV15) were treated with APOE KO or APOE4 (10–15 nM) conditioned media for 24 h and subjected to calcium imaging using Fluo8-AM. N=50–60 neurons from 3 independent experiments, Kolmogorov–Smirnov test.

7.4 NMDAR and L-VGCC inhibitors affect APOE mediated increase in eEF2 phosphorylation

NMDARs were the primary initiating source of calcium influx on APOE addition. Correspondingly, pre-treatment with MK801 was able to prevent both APOE3 and APOE4 mediated increase in eEF2 phosphorylation at 1-minute time point (Fig 7.4 A), while MK801 incubation had no effect on eEF2 phosphorylation in the absence of APOE conditioned media (Fig 7.4 A). L-VGCCs did not prevent the APOE mediated calcium influx, whereas they helped in the sustenance of APOE4 calcium at later time points. Accordingly, Nifedipine did not block the APOE mediated increase in eEF2 phosphorylation at 1-minute (Fig 7.4 B). Nifedipine alone did not have an effect on eEF2 phosphorylation in the absence of APOE (Fig 7.4 B). However, Nifedipine successfully prevented the APOE4 mediated increase in eEF2 phosphorylation at 20 minutes (Fig 7.4 C); while it had no effect on eEF2 phosphorylation in APOE3 condition (Fig 7.4 C). As a control, we validated that either of the drugs MK801 or Nifedipine did not have an effect on eEF2 phosphorylation in the presence of APOE KO conditioned media (Fig 7.4 D and Fig 7.4 E).

Figure 7.4

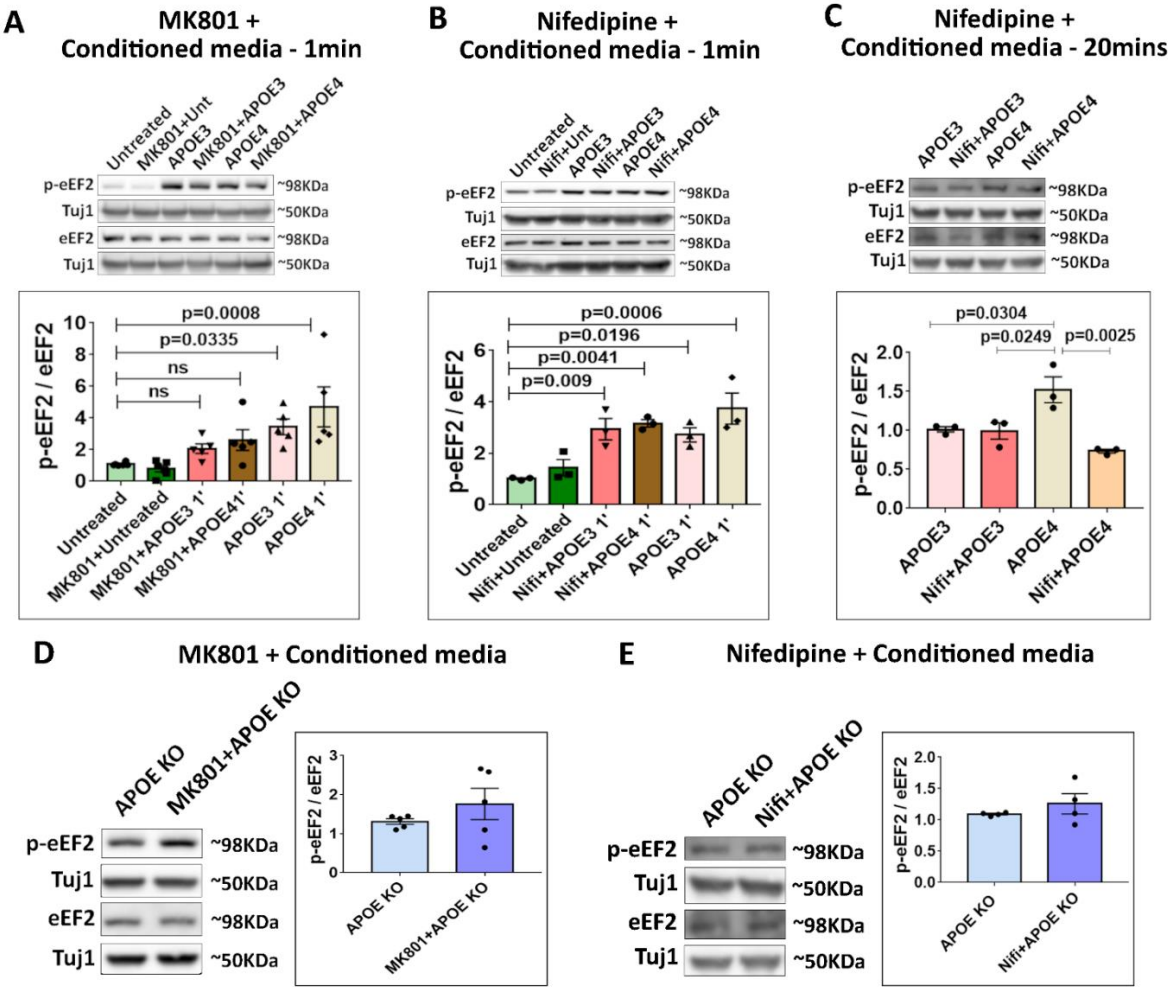

Figure 7.4 – NMDAR and L-VGCC inhibitors affect APOE mediated increase in eEF2 phosphorylation

A - Representative immunoblots showing the levels of p-eEF2, eEF2 and Tuj1 in rat primary cortical neurons on 1-minute APOE3 or APOE4 iPSC conditioned media treatment along with MK801 (25 µM) pre-incubation. The graph represents the ratio of p-eEF2 to eEF2 normalized to Tuj1. Data is represented as mean +/- SEM, N = 5, One-way ANOVA (p = 0.0006) followed by Dunnett's multiple comparison test.

B - Representative immunoblots showing the levels of p-eEF2, eEF2 and Tuj1 in rat primary cortical neurons on 1-minute APOE3 or APOE4 iPSC conditioned media treatment along with Nifedipine (50 µM) pre-incubation. The graph represents the ratio of p-eEF2 to eEF2 normalized to Tuj1. Data is represented as mean +/- SEM, N=3, One-way ANOVA (p = 0.001) followed by Dunnett's multiple comparison test.

C - Representative immunoblots showing the levels of p-eEF2, eEF2 and Tuj1 in rat primary cortical neurons on 20-minute APOE3 or APOE4 iPSC conditioned media treatment along with Nifedipine (50 µM) pre-incubation. The graph represents the ratio of p-eEF2 to eEF2 normalized to Tuj1. Data is represented as mean +/- SEM, N=3, One-way ANOVA (p = 0.0036) followed by Tukey's multiple comparison test.

D - Representative immunoblots showing the levels of p-eEF2, eEF2 and Tuj1 in rat primary cortical neurons on 1-minute APOE KO iPSC conditioned media treatment along with MK801 (25 µM) pre-incubation. The graph represents the ratio of p-eEF2 to eEF2 normalized to Tuj1. Data is represented as mean +/- SEM, N = 5, Unpaired Student's t-test (ns).

E - Representative immunoblots showing the levels of p-eEF2, eEF2 and Tuj1 in rat primary cortical neurons on 20-minute APOE KO iPSC conditioned media treatment along with Nifedipine (50 µM) pre-incubation. The graph represents the ratio of p-eEF2 to eEF2 normalized to Tuj1. Data is represented as mean +/- SEM, N=4, Unpaired Student's t-test (ns).

7.5 NMDAR and L-VGCC inhibitors affect APOE mediated inhibition of protein synthesis

We used the FUNCAT assay to directly measure the protein synthesis response in the presence of calcium channel blockers MK801 and Nifedipine. In line with the eEF2 phosphorylation and calcium results, MK801 was able to prevent the APOE3 (Fig 7.5 A and Fig 7.5 B) and APOE4 (Fig 7.5 C and Fig 7.5 D) mediated translation inhibition at 1-minute. MK801 incubation alone in the absence of APOE had no effect on protein synthesis (Fig 7.5 B and Fig 7.5 D). Similarly, at the later time point of 20 minutes, Nifedipine completely blocked the APOE4 mediated translation inhibition (Fig 7.5 E and Fig 7.5 F); whereas Nifedipine had no effect on protein synthesis in APOE3 background (Fig 7.5 E and Fig 7.5 F). Thus, MK801 prevented the APOE4 mediated translation inhibition at the early time point and Nifedipine blocked it at the later time point.

Figure 7.5

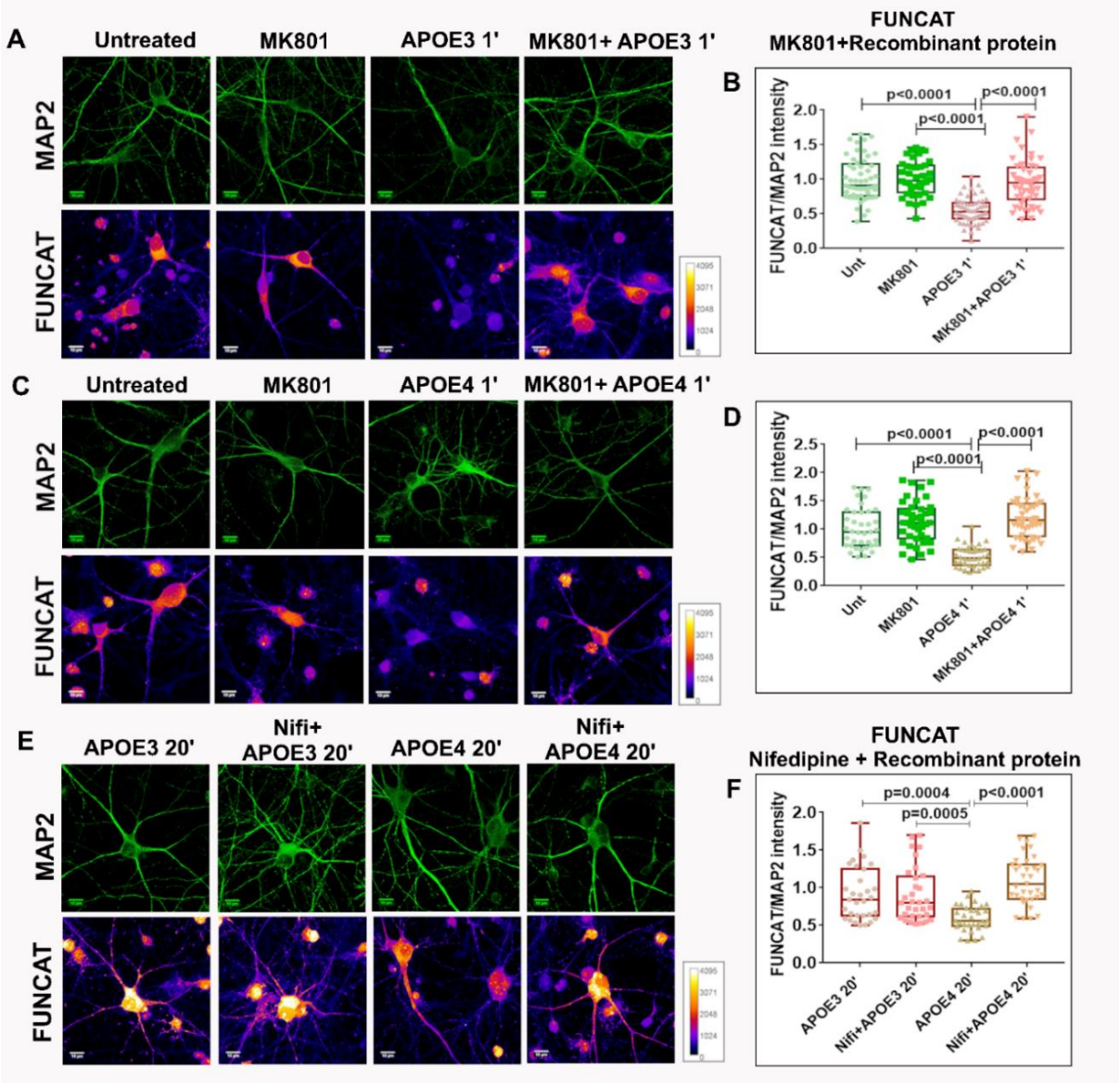

Figure 7.5 – NMDAR and L-VGCC inhibitors affect APOE mediated inhibition of protein synthesis

A - The representative images for MAP2 and FUNCAT fluorescent signals in rat primary cortical neurons treated with APOE3 recombinant protein (15 nM) for 1-minute along with MK801 pre-incubation (25 µM) (Scale bar - 10µM).

B - The graph represents the quantification of the FUNCAT fluorescent intensity normalized to MAP2 fluorescent intensity under different APOE3 and MK801 treatment conditions at 1-minute time point. Each data point represents an individual neuron. N=40–50 neurons from 4 independent experiments, One-way ANOVA ($p<0.0001$) followed by Tukey's multiple comparison test.

C - The representative images for MAP2 and FUNCAT fluorescent signals in rat primary cortical neurons treated with APOE4 recombinant protein (15 nM) for 1-minute along with MK801 pre-incubation (25 µM) (Scale bar - 10µM).

D - The graph represents the quantification of the FUNCAT fluorescent intensity normalized to MAP2 fluorescent intensity under different APOE4 and MK801 treatment conditions at 1-minute time point. Each data point represents an individual neuron. N=40–50 neurons from 4 independent experiments, One-way ANOVA ($p<0.0001$) followed by Tukey's multiple comparison test.

E - The representative images for MAP2 and FUNCAT fluorescent signals in rat primary cortical neurons treated with APOE3 or APOE4 recombinant protein (15 nM) for 20 minutes along with MK801 pre-incubation (50 µM) (Scale bar - 10µM).

F - The graph represents the quantification of the FUNCAT fluorescent intensity normalized to MAP2 fluorescent intensity under different APOE and Nifedipine treatment conditions at 20-minute time point. Each data point represents an individual neuron. N=20–30 neurons from 4 independent experiments, One-way ANOVA ($p<0.0001$) followed by Tukey's multiple comparison test.

7.6 mGluR activation reduces the eEF2 phosphorylation on NMDAR stimulation and APOE4 treatment

Both APOE4 treatment and NMDAR stimulation caused the influx of calcium through NMDA receptors and L-VGCCs. Yet, only NMDAR stimulation caused translation activation at 20 minutes; whereas eEF2 phosphorylation remained elevated with 20-minutes APOE4 treatment. Thus, we hypothesized that NMDAR stimulation could involve different components which trigger the dephosphorylation of eEF2 and activate protein synthesis. The rise of cellular calcium on NMDAR stimulation is contributed by 3 sources in a sequential manner – NMDA receptors, L-VGCCs and calcium release from ER[7]. We tested if the calcium release from internal stores could have a role in the phase of translation activation.

It is well-established that mGluR stimulation causes release of calcium from internal stores through IP3 receptors. Hence, we used mGluR agonist DHPG to trigger internal calcium release and checked its effect on eEF2 phosphorylation. To begin with, we added DHPG during the translation inhibition phase of NMDAR stimulation to check if it can dephosphorylate eEF2 and activate translation. The phosphorylation of eEF2 was maximum at 1-minute and remained high till 5 minutes on NMDAR stimulation (Fig 7.6 A). Thus, we used a 5-minute NMDAR stimulation paradigm where we added DHPG during the last 4 minutes (Fig 7.6 A). The idea was that if DHPG can actively dephosphorylate eEF2, then p-eEF2 levels with NMDA+DHPG for 5 minutes would be lower than 5-minute NMDA stimulation alone. Interestingly, we found that the addition of DHPG could bring down the phosphorylation of eEF2 even in the presence of NMDA (Fig 7.6 A). This suggested that release of calcium from internal stores could potentially cause the translation activation.

Further, we tried the same experiment with APOE treatment. Since phosphorylation of eEF2 was maximum at 1-minute and continued to remain high till 20 minutes in the

case of APOE4, we checked if the presence of DHPG along with APOE4 can reduce the eEF2 phosphorylation by 20 minutes. So, in the course of 20-minute APOE treatment, we added DHPG during the last 19 minutes (Fig 7.6 C). We observed that addition of DHPG was able to reduce eEF2 phosphorylation in the presence of APOE4 as well (Fig 7.6 D). Thus, we hypothesize that calcium release from internal stores could be the factor which distinguishes the NMDAR and APOE4 translation profiles.

Figure 7.6

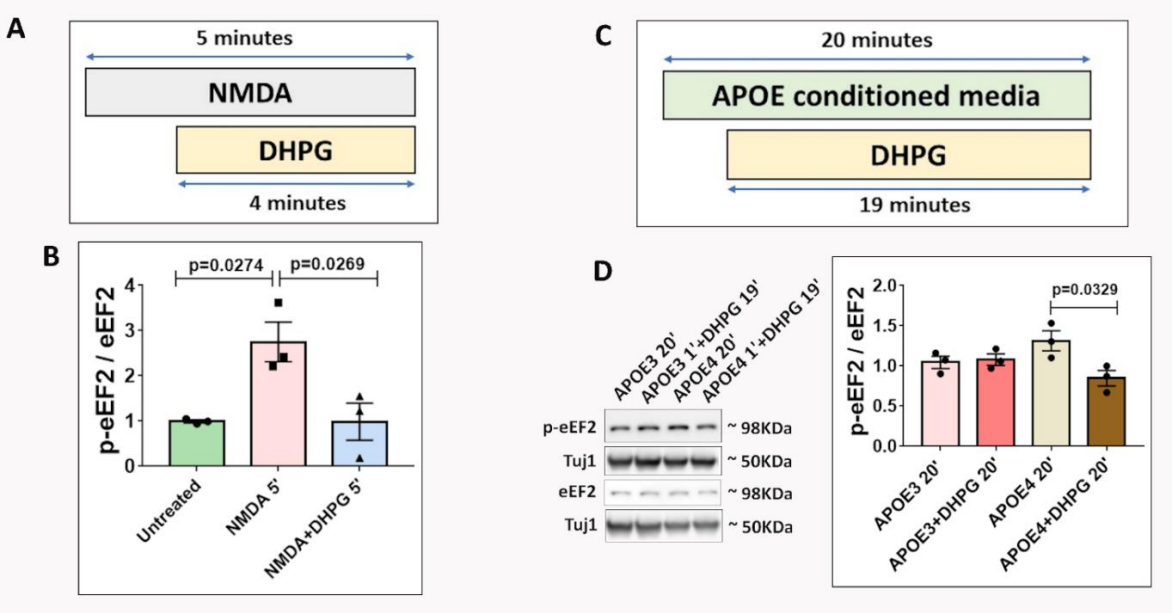

Figure 7.6 – mGluR activation reduces the eEF2 phosphorylation on NMDAR stimulation and APOE4 treatment

A – Schematic representing the NMDAR stimulation and mGluR activation paradigm in rat primary cortical neurons

B – Representative immunoblots showing the levels of p-eEF2, eEF2 and Tuj1 in rat primary cortical neurons on NMDAR stimulation (20µM, 1 minute) or NMDAR stimulation followed by DHPG addition (20µM NMDA 1', 50µM DHPG 4'). The graph represents the ratio of p-eEF2 to eEF2 normalized to Tuj1. Data is represented as mean +/- SEM, N=4, One-way ANOVA (p=0.0005) followed by Tukey's multiple comparison test.

C – Schematic representing the APOE treatment and mGluR activation paradigm in rat primary cortical neurons

D – Representative immunoblots showing the levels of p-eEF2, eEF2 and Tuj1 in rat primary cortical neurons on APOE conditioned media treatment (20') with or without DHPG stimulation (50µM, 19'). The graph represents the ratio of p-eEF2 to eEF2 normalized to Tuj1. Data is represented as mean +/- SEM, N=3, One-way ANOVA (p=0.0485) followed by Tukey's multiple comparison test.

7.7 Summary and Discussion

In this chapter, we explore the link between protein synthesis and calcium homeostasis to explain the translation responses upon NMDAR stimulation and APOE treatment. To begin with, we establish that calcium is required to elicit the NMDAR mediated protein synthesis response, both with respect to early phase translation inhibition and later phase translation activation. Further, we show that the APOE4 mediated translation inhibition is also dependent on extracellular calcium. We studied the calcium traces upon NMDAR stimulation and APOE treatment; and identified the sources of calcium influx as well. NMDAR stimulation involved the influx of calcium through NMDA receptors, followed by activation of L-VGCCs. APOE3 treatment caused a short burst of calcium through NMDA receptors, without the involvement of L-VGCCs. APOE4 treatment led to a robust increase in calcium levels caused by the activation of NMDA receptors and L-VGCCs. Accordingly, we were able to block the APOE3 and APOE4 mediated eEF2 phosphorylation and translation inhibition at early time (1-minute) using NMDAR antagonist MK801. L-VGCC antagonist Nifedipine blocked the APOE4 mediated eEF2 phosphorylation and translation inhibition at later time point (20-minutes). Thus, the highlight of this chapter was the demonstration of how different calcium signatures and sources regulate protein synthesis.

Interestingly, both NMDAR stimulation and APOE4 treatment led to the influx of calcium through NMDA receptors and L-VGCCs. Yet, the translation response at 20-minute NMDAR stimulation (translation activation) and 20-minute APOE4 exposure (translation inhibition) were different. Hence, we hypothesized that the translation activation on NMDAR stimulation probably involved an additional component. The stimulation of NMDARs leading to L-VGCC activation is reported to initiate CICR from the ER stores[7]. Hence, the intracellular calcium increase downstream of NMDAR activation is contributed by calcium from external sources (NMDARs and L-VGCCs) followed by calcium from internal sources (ER stores), likely to occur in distinct phases which are temporally and spatially separated. We hypothesized that these distinct calcium sources could be coupled to the distinct translation phases observed on NMDAR activation. Along the lines of this hypothesis, we questioned if the release of calcium from internal sources could be the key difference between the APOE4 and NMDAR stimulation. And, we questioned if the release of calcium from internal stores could have a role in the phase of translation activation. Additional support to was provided to this idea from the studies which show that stimulation of Group 1 metabotropic glutamate receptors using DHPG leads to the release of calcium from internal stores and causes global translation activation [11,13,14].

Thus, broadly, the influx of calcium from external sources (NMDARs and L-VGCCs) caused the inhibition of translation, through calcium dependent activation of eEF2 kinase and eEF2 phosphorylation. We hypothesize that the calcium release from internal stores could cause the activation of translation, potentially through activation of phosphatases leading to decreased eEF2 phosphorylation. Interestingly, in case of NMDAR stimulation, the phase of translation activation is also triggered by calcium influx from external sources, as NMDAR stimulation for 20 minutes in the absence of calcium fails to cause protein synthesis activation (Fig 7.1 A). This highlights the sequential regulation of calcium on NMDAR stimulation - calcium release from internal

stores is triggered by the initial calcium influx from external sources [3,7]. As reported previously, L-VGCCs behave like the switches which trigger the calcium release from ER [7]. The activation of CICR is shown to have a feedback inhibition on the calcium entry through L-VGCCs and NMDARs[7]. Hence, we hypothesize that in case of APOE4, the release of calcium from internal stores is blocked; either due to the failure of L-VGCCs to trigger CICR or due to defective CICR. To address few aspects of our hypothesis, we performed preliminary experiments with mGluR agonist DHPG which is shown to release calcium from internal stores through IP3 receptors. The addition of DHPG was able to decrease the phosphorylation of eEF2 during the translation inhibition phase of NMDAR stimulation (5-minute) and APOE4 treatment (20-minute). Hence, we think that the internal calcium stores are the critical component of NMDAR protein synthesis response which is defective in case of APOE4. And, we propose this as an interesting future direction to take this work forward.

Another interesting question that arises is that why was L-VGCC activated by APOE4 only, and not APOE3. One of the possible explanations is that the initial calcium influx through NMDARs is significantly higher in case of APOE4 compared to APOE3. Hence, APOE4 might cause a higher depolarization required for the activation of L-VGCCs. The other possibility is that APOE4 binding to its cognate receptor could activate some signaling pathways which directly regulate L-VGCCs. Another critical point we note is that MK801 completely blocked the APOE4 mediated calcium influx and showed a recovery of translation inhibition. However, eEF2 phosphorylation still showed a trend of increase (though not statistically significant) in the presence of MK801 in APOE4 treated neurons. Hence, though NMDAR mediated calcium seems to be the primary initiating cause, we cannot rule out the possibility that other signaling pathways and calcium independent mechanisms could be involved in APOE4 mediated increase in eEF2 phosphorylation. Finally, another unexplained aspect is the mechanism through which APOE activates NMDARs. We have previously shown that the effect of APOE on protein synthesis is mediated through APOE receptors (Chapter 4). Though the influence of APOE receptor-associated signaling on NMDARs has been studied [21], the exact mechanism behind APOE mediated calcium influx through NMDARs is yet to be understood. Another possible mechanism of APOE mediated NMDAR activation could be through the production of Aβ. APOE4 has been shown to cause an increase in Aβ production [22,23] and Aβ is shown to directly activate NMDARs[24]. This could be another interesting future direction to take the work forward.

7.8 References

1. Papadia, S. & Hardingham, G. E. The Dichotomy of NMDA Receptor Signaling. *The Neuroscientist* **13**, (2007).

2. Lau, C. G. *et al.* Regulation of NMDA receptor Ca2+ signalling and synaptic plasticity. *Biochemical Society Transactions* **37**, (2009).

3. Higley, M. J. & Sabatini, B. L. Calcium signaling in dendritic spines. *Cold Spring Harbor Perspectives in Biology* **4**, (2012).

4. Emptage, N., Bliss, T. V. P. & Fine, A. Single synaptic events evoke NMDA receptor-mediated release of calcium from internal stores in hippocampal dendritic spines. *Neuron* **22**, (1999).

5. Griffith, T., Tsaneva-Atanasova, K. & Mellor, J. R. Control of Ca2+ Influx and Calmodulin Activation by SK-Channels in Dendritic Spines. *PLoS Computational Biology* **12**, (2016).

6. Lee, K. F. H., Soares, C., Thivierge, J. P. & Béïque, J. C. Correlated Synaptic Inputs Drive Dendritic Calcium Amplification and Cooperative Plasticity during Clustered Synapse Development. *Neuron* **89**, (2016).

7. Dittmer, P. J., Wild, A. R., Dell'Acqua, M. L. & Sather, W. A. STIM1 Ca2+ Sensor Control of L-type Ca2+-Channel-Dependent Dendritic Spine Structural Plasticity and Nuclear Signaling. *Cell Reports* **19**, 321–334 (2017).

8. Hiester, B. G. *et al.* L-Type Voltage-Gated Ca2+ Channels Regulate Synaptic-Activity-Triggered Recycling Endosome Fusion in Neuronal Dendrites. *Cell Reports* **21**, (2017).

9. Rajadhyaksha, A. *et al.* L-type Ca2+ channels are essential for glutamate-mediated CREB phosphorylation and c-fos gene expression in striatal neurons. *Journal of Neuroscience* **19**, (1999).

10. Scheetz, A. J., Nairn, A. C. & Constantine-Paton, M. NMDA receptor-mediated control of protein synthesis at developing synapses. *Nature Neuroscience* (2000) doi:10.1038/72915.

11. Ghosh Dastidar, S. *et al.* Distinct regulation of bioenergetics and translation by group I mGluR and NMDAR. *EMBO reports* (2020) doi:10.15252/embr.201948037.

12. Heise, C. *et al.* Elongation factor-2 phosphorylation in dendrites and the regulation of dendritic mRNA translation in neurons. *Frontiers in Cellular Neuroscience* vol. 8 (2014).

13. Wang, H. & Zhuo, M. Group I metabotropic glutamate receptor-mediated gene transcription and implications for synaptic plasticity and diseases. *Frontiers in Pharmacology* **3 NOV**, (2012).

14. Mao, L. & Wang, J. Q. Group I metabotropic glutamate receptor-mediated calcium signalling and immediate early gene expression in cultured rat striatal neurons. *European Journal of Neuroscience* **17**, 741–750 (2003).

15. Tolar, M. *et al.* Truncated apolipoprotein E (ApoE) causes increased intracellular calcium and may mediate ApoE neurotoxicity. *Journal of Neuroscience* **19**, (1999).

16. Veinbergs, I., Everson, A., Sagara, Y. & Masliah, E. Neurotoxic effects of apolipoprotein E4 are mediated via dysregulation of calcium homeostasis. *Journal of Neuroscience Research* **67**, (2002).

17. Qiu, Z., Crutcher, K. A., Hyman, B. T. & Rebeck, G. W. apoE isoforms affect neuronal N-methyl-D-aspartate calcium responses and toxicity via receptor-mediated processes. *Neuroscience* **122**, 291–303 (2003).

18. Hoe, H. S., Harris, D. C. & Rebeck, G. W. Multiple pathways of apolipoprotein E signaling in primary neurons. *Journal of Neurochemistry* **93**, (2005).

19. Xu, D. & Peng, Y. Apolipoprotein E 4 triggers multiple pathway-mediated Ca2+ overload, causes CaMK II phosphorylation abnormity and aggravates oxidative stress caused cerebral cortical neuron damage. *European review for medical and pharmacological sciences* **21**, (2017).

20. Theendakara, V., Bredesen, D. E. & Rao, R. v. Downregulation of protein phosphatase 2A by apolipoprotein E: Implications for Alzheimer's disease. *Molecular and Cellular Neuroscience* **83**, (2017).

21. Lane-Donovan, C. & Herz, J. ApoE, ApoE Receptors, and the Synapse in Alzheimer's Disease. *Trends in Endocrinology and Metabolism* **28**, 273–284 (2017).

22. Huang, Y. W. A., Zhou, B., Wernig, M. & Südhof, T. C. ApoE2, ApoE3, and ApoE4 Differentially Stimulate APP Transcription and Aβ Secretion. *Cell* **168**, 427-441.e21 (2017).

23. Lin, Y. T. *et al.* APOE4 Causes Widespread Molecular and Cellular Alterations Associated with Alzheimer's Disease Phenotypes in Human iPSC-Derived Brain Cell Types. *Neuron* **98**, 1141-1154.e7 (2018).

24. Texidó, L., Martín-Satué, M., Alberdi, E., Solsona, C. & Matute, C. Amyloid β peptide oligomers directly activate NMDA receptors. *Cell Calcium* **49**, (2011).

Chapter 8

Concluding remarks

8.0 Highlights

- APOE4 causes a global inhibition of protein synthesis through sustained phosphorylation of eEF2 for 20 minutes.
- The increase in eEF2 phosphorylation is mediated by sustained influx of calcium through NMDAR and L-VGCC activation.
- Hence, the NMDA mediated translation response is perturbed in APOE4 treated neurons, potentially causing a stress-related phenotype through eIF2α phosphorylation.
- APOE3 causes an initial inhibition of global translation which recovers to basal levels by 20 minutes, thus not altering the NMDA mediated translation response.
- APOE3 causes a short burst of calcium through NMDARs only, without the involvement of L-VGCCs, thus leading to an acute increase in eEF2 phosphorylation.
- Hence, different calcium signatures and sources lead to distinct temporal profiles of translation.

8.1 Summary

The primary finding of my work is that APOE4, a well-established risk factor for Alzheimer's disease affects global protein synthesis in neurons. We observe that the different APOE isoforms APOE3 (not a risk factor for AD) and APOE4 (risk factor for AD) generate distinct protein synthesis profiles. APOE3 leads to a transient inhibition of global protein synthesis which eventually recovers to basal levels. However, APOE4 causes a larger and sustained inhibition of global protein synthesis which fails to recover to basal levels in 20-minute period. We show that the inhibition of protein synthesis is mediated by the increase in the phosphorylation of eukaryotic translation elongation factor eEF2.

The protein synthesis downstream of NMDAR stimulation has a distinct temporal profile with early phase translation inhibition and late phase translation activation. Though the initial translation response upon APOE3 and APOE4 treatment appears to mimic the early phase NMDAR translation inhibition, the protein synthesis profiles at the later phase is distinct. While NMDAR stimulation causes translation activation at 20-minute time point, APOE4 treatment causes translation inhibition and protein synthesis recovers to basal levels under APOE3 treatment. As a result of the distinct temporal profiles of translation, the neurons retain their physiological response to NMDAR stimulation in the background of APOE3 treatment. However, in the presence

of APOE4, the translation response to NMDAR stimulation is perturbed. Interestingly, the phosphorylation of eIF2α increases only in the condition of APOE4 treatment along with NMDAR stimulation, implying the involvement of stress response to a physiological stimulus.

Finally, the distinct profiles of protein synthesis are closely linked to calcium influx signatures. The stimulation of NMDARs causes an influx of calcium through NMDARs and L-VGCCs. APOE3 treatment causes a short burst of calcium influx through activation of NMDARs alone. However, APOE4 causes a larger and sustained influx of calcium through sequential activation of NMDARs followed by L-VGCCs. The sustained increase of calcium in the neurons on APOE4 treatment leads to the steady increase in eEF2 phosphorylation as well, thus causing an inhibition of global protein synthesis in APOE4 background. Thus, in summary, we propose the following model –

Figure 8

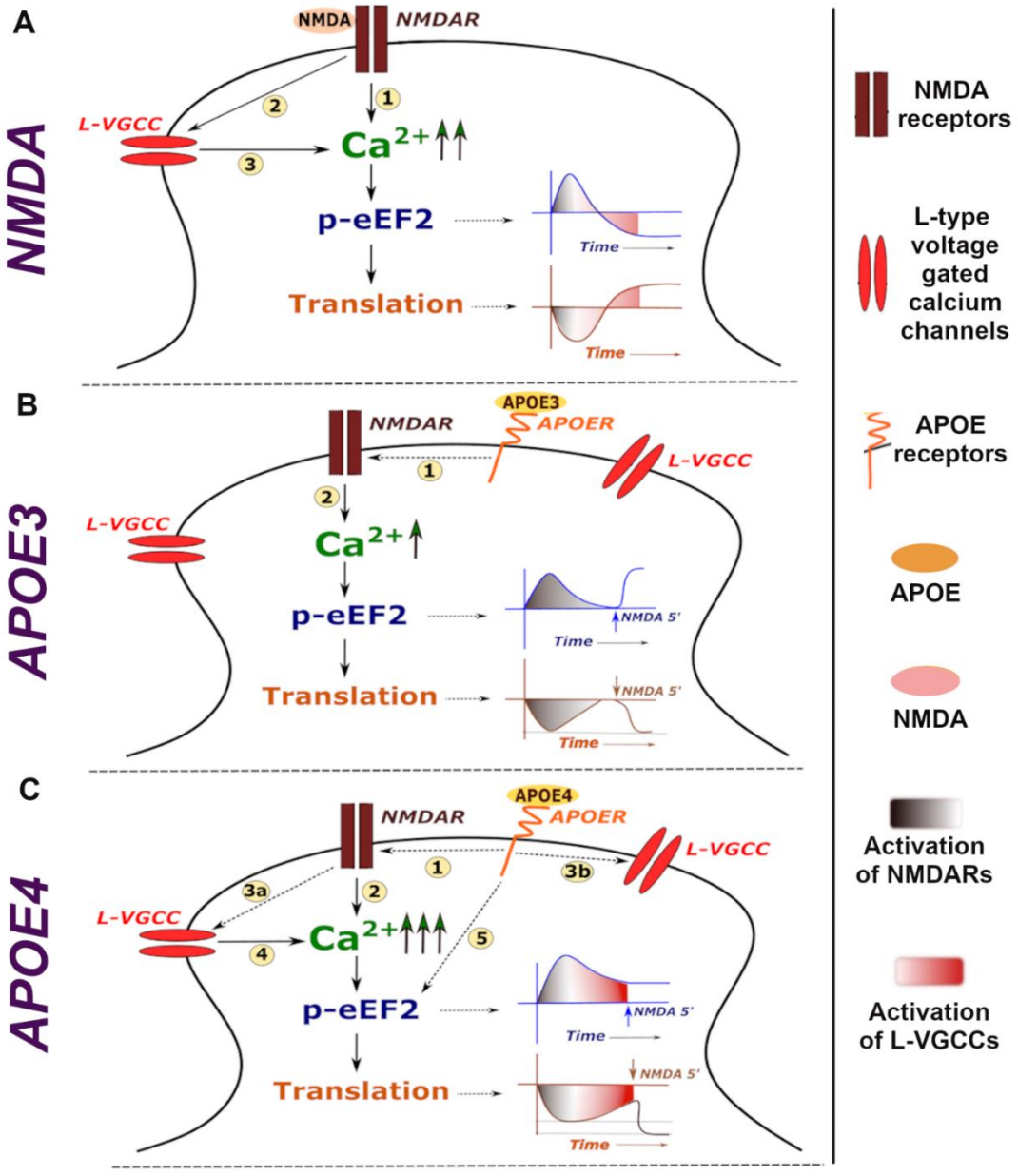

Figure 8 - Model illustrating calcium signature and corresponding protein synthesis regulation downstream of NMDAR stimulation and APOE treatment

A - Stimulation of NMDA receptors lead to influx of calcium through NMDARs (1) which activates L-VGCCs (2). The influx of calcium through L-VGCCs further helps in sustaining the calcium levels on NMDAR stimulation (3). The calcium through NMDARs and L-VGCCs generates a specific temporal profile of eEF2 phosphorylation, causing an initial inhibition of global protein synthesis followed by translation activation in a later phase.

B - Exposure to APOE3 activates NMDARs through an unknown mechanism (1), leading to a short burst of calcium through it (2). This leads to an acute increase in eEF2 phosphorylation, primarily contributed by calcium influx through NMDARs, which recovers to basal levels. Global translation also follows a similar temporal profile of initial decrease followed by recovery. Hence, the NMDA activity mediated translation response is unaffected in APOE3 treated neurons.

C - Exposure to APOE4 activates NMDARs through an unknown mechanism (1), causing higher influx of calcium through NMDARs (2) than APOE3 condition. The higher calcium influx through NMDARs could lead to L-VGCC activation in APOE4 condition (3a). Besides, APOE4 binding to APOE receptors could also directly regulate the sustained activation of L-VGCCs (3b). Overall, the L-VGCC activation under APOE4 treatment condition contributes to the huge and sustained increase in calcium levels (4). This leads to the sustained increase in eEF2 phosphorylation as well as global translation inhibition. There could also be a possibility of APOE4 activating signalling cascades which further contribute to the sustained increase in eEF2 phosphorylation (5). Hence, the NMDA activity mediated response is perturbed, potentially causing a stress-response phenotype in APOE4 treated neurons.

8.2 Future perspectives

There are numerous avenues that the project opens, and it can be taken forward in multiple ways. One of the ways is to investigate the upstream mechanisms which govern the APOE mediated protein synthesis response. The mechanism by which NMDARs are activated upon APOE binding to its cognate receptors is unknown. Understanding the signaling pathways downstream of APOE receptors which could modulate NMDARs would be the first way to take it forward. Additionally, if APOE4 directly regulates L-VGCCs or eEF2 phosphorylation is another aspect which can be investigated. The other direction to take the study forward would be investigating downstream of the APOE protein synthesis response. One of the possibilities would be to check the candidates which are getting translationally affected upon NMDAR, APOE3 and APOE4 treatment at different time points. Ribosome profiling can be performed at early and late time points under different treatment conditions to validate if the candidates are similar or different, and what cellular processes they regulate. Additionally, the effect of APOE4 mediated protein synthesis inhibition upon synaptic plasticity can be studied. The levels of different pre- and post-synaptic protein can be investigated in the presence of APOE4. It would be ideal if our important findings, especially with regards to the effect of APOE4 on protein synthesis, can be replicated

in vivo in APOE4 mice model. Further studies could be performed in animal models of APOE4 to investigate the readouts of synaptic morphology, number, and plasticity to connect it to the protein synthesis phenotype.

The role of Aβ in APOE4 mediated protein synthesis is unexplored. Since APOE4 is known to increase the levels of APP and Aβ, the contribution of these to the protein synthesis response can be studied. One of the most interesting take homes from the study is the role of calcium in regulating protein synthesis response. Though we studied the role of external calcium sources like NMDARs and L-VGCCs, we did not investigate the role of internal calcium sources such as Endoplasmic Reticulum and mitochondria. The contribution of ER calcium release to the protein synthesis response, both in the context of basal condition and APOE4 treatment, would be important to completely understand the regulation by calcium. Additionally, we focused on L-VGCCs only in our current work, however the role of other different types of VGCCs (such as N, T, R-type) could also be investigated. Further, we studied the effect of APOE on the activity paradigm of NMDAR stimulation only. However, it is known that protein synthesis is important for other synaptic responses as well, such as mGluR stimulation, BDNF treatment or NGF treatment. Hence, the effect of APOE downstream of other stimulation paradigms can also be investigated to get a better picture of the impact of APOE on synaptic translation.

Finally, the role of calcium in regulation of protein synthesis could be an interesting topic to explore further. This study focuses on the temporal regulation of protein synthesis by the sequential activation of different calcium sources. But the different calcium sources are also spatially segregated. For example, NMDARs are present at the post-synapse; VGCCs are at the synapses, dendritic shafts as well as cell bodies. ER calcium source would be mostly in the dendritic/axonal shafts and cell bodies, but lesser at the synapse heads. Hence, along with the temporal aspect, the spatial regulation of calcium could be important factor influencing translation. Considering a) the local regulation of translation at the synapses and b) calcium being an important local secondary messenger at the synapses, the role of calcium as one of the modes of translation regulation (similar to microRNAs or RBPs) would be worth investigating in the future.

References - For Chapter 1 (Introduction)

1. Hardy, J. A Hundred Years of Alzheimer's Disease Research. *Neuron* vol. 52 (2006).

2. Stelzmann, R. A., Norman Schnitzlein, H. & Reed Murtagh, F. An english translation of alzheimer's 1907 paper, "über eine eigenartige erkankung der hirnrinde." *Clinical Anatomy* **8**, (1995).

3. Tomlinson, B. E., Blessed, G. & Roth, M. Observations on the brains of non-demented old people. *Journal of the Neurological Sciences* **7**, (1968).

4. Blessed, G., Tomlinson, B. E. & Roth, M. The association between quantitative measures of dementia and of senile change in the cerebral grey matter of elderly subjects. *The British journal of psychiatry : the journal of mental science* **114**, (1968).

5. Tomlinson, B. E., Blessed, G. & Roth, M. Observations on the brains of demented old people. *Journal of the Neurological Sciences* **11**, (1970).

6. TERRY, R. D., GONATAS, N. K. & WEISS, M. ULTRASTRUCTURAL STUDIES IN ALZHEIMER'S PRESENILE DEMENTIA. *The American journal of pathology* **44**, (1964).

7. Masters, C. L. *et al.* Amyloid plaque core protein in Alzheimer disease and Down syndrome. *Proceedings of the National Academy of Sciences of the United States of America* **82**, (1985).

8. Goldgaber, D., Lerman, M. I., McBride, O. W., Saffiotti, U. & Gajdusek, D. C. Characterization and chromosomal localization of a cDNA encoding brain amyloid of Alzheimer's disease. *Science* **235**, (1987).

9. Kang, J. *et al.* The precursor of Alzheimer's disease amyloid A4 protein resembles a cell-surface receptor. *Nature* **325**, (1987).

10. van Camp, G. *et al.* Identification of chromosome 21 DNA polymorphisms for genetic studies in Alzheimer's disease and Down syndrome. *Human Genetics* **87**, (1991).

11. Goate, A. M. *et al.* PREDISPOSING LOCUS FOR ALZHEIMER'S DISEASE ON CHROMOSOME 21. *The Lancet* **333**, (1989).

12. Murrell, J., Farlow, M., Ghetti, B. & Benson, M. D. A mutation in the amyloid precursor protein associated with hereditary Alzheimer's disease. *Science* **254**, (1991).

13. Mullan, M. *et al.* Clinical comparison of Alzheimer's disease in pedigrees with the codon 717 Val→Ile mutation in the amyloid precursor protein gene. *Neurobiology of Aging* **14**, (1993).

14. Mullan, M. *et al.* A pathogenic mutation for probable Alzheimer's disease in the APP gene at the N–terminus of β–amyloid. *Nature Genetics* **1**, (1992).

15. Hendriks, L. *et al.* Presenile dementia and cerebral haemorrhage linked to a mutation at codon 692 of the β–amyloid precursor protein gene. *Nature Genetics* **1**, (1992).

16. Goate, A. *et al.* Segregation of a missense mutation in the amyloid precursor protein gene with familial Alzheimer's disease. *Nature* **349**, (1991).

17. Chartier-Harlin, M. C. *et al.* Early-onset Alzheimer's disease caused by mutations at codon 717 of the β-amyloid precursor protein gene. *Nature* **353**, (1991).

18. Crook, R. *et al.* A variant of Alzheimer's disease with spastic paraparesis and unusual plaques due to deletion of exon 9 of presenilin 1. *Nature Medicine* **4**, (1998).

19. Levy-Lahad, E. *et al.* Candidate gene for the chromosome 1 familial Alzheimer's disease locus. *Science* **269**, (1995).

20. Rogaev, E. I. *et al.* Familial Alzheimer's disease in kindreds with missense mutations in a gene on chromosome 1 related to the Alzheimer's disease type 3 gene. *Nature* **376**, (1995).

21. Levy-Lahad, E. *et al.* A familial Alzheimer's disease locus on chromosome I. *Science* **269**, (1995).

22. Sherrington, R. *et al.* Cloning of a gene bearing missense mutations in early-onset familial Alzheimer's disease. *Nature* **375**, (1995).

23. Schellenberg, G. D. *et al.* Genetic linkage evidence for a familial Alzheimer's disease locus on chromosome 14. *Science* **258**, (1992).

24. Kidd, M. Paired helical filaments in electron microscopy of Alzheimer's Disease. *Nature* **197**, (1963).

25. Nukina, N. & Ihara, Y. One of the antigenic determinants of paired helical filaments is related to tau protein. *Journal of Biochemistry* **99**, (1986).

26. Goedert, M., Wischik, C. M., Crowther, R. A., Walker, J. E. & Klug, A. Cloning and sequencing of the cDNA encoding a core protein of the paired helical filament of Alzheimer disease: Identification as the microtubule-associated protein tau. *Proceedings of the National Academy of Sciences of the United States of America* **85**, (1988).

27. Kosik, K. S., Joachim, C. L. & Selkoe, D. J. Microtubule-associated protein tau (τ) is a major antigenic component of paired helical filaments in Alzheimer disease. *Proceedings of the National Academy of Sciences of the United States of America* **83**, (1986).

28. Wood, J. G., Mirra, S. S., Pollock, N. J. & Binder, L. I. Neurofibrillary tangles of Alzheimer disease share antigenic determinants with the axonal microtubule-associated protein tau (τ). *Proceedings of the National Academy of Sciences of the United States of America* **83**, (1986).

29. Hasegawa, M. *et al.* Protein sequence and mass spectrometric analyses of tau in the Alzheimer's disease brain. *Journal of Biological Chemistry* **267**, (1992).

30. Brion, J. P. *et al.* Tau in Alzheimer neurofibrillary tangles. N- and C-terminal regions are differentially associated with paired helical filaments and the location of a putative abnormal phosphorylation site. *Biochemical Journal* **273**, (1991).

31. Ihara, Y., Nukina, N., Miura, R. & Ogawara, M. Phosphorylated tau protein is integrated into paired helical filaments in alzheimer's disease. *Journal of Biochemistry* **99**, (1986).

32. Grundke-Iqbal, I. *et al.* Abnormal phosphorylation of the microtubule-associated protein tau (tau) in Alzheimer cytoskeletal pathology. *Proceedings of the National Academy of Sciences of the United States of America* **83**, (1986).

33. Lee, V. M. Y., Balin, B. J., Otvos, L. & Trojanowski, J. Q. A68: A major subunit of paired helical filaments and derivatized forms of normal tau. *Science* **251**, (1991).

34. Alonso, A. D., Grundke-Iqbal, I., Barra, H. S. & Iqbal, K. Abnormal phosphorylation of tau and the mechanism of Alzheimer neurofibrillary degeneration: sequestration of microtubule-

associated proteins 1 and 2 and the disassembly of microtubules by the abnormal tau. *PNAS* (1997) doi:10.1073/pnas.94.1.298.

35. Alonso, A. D. C., Zaidi, T., Novak, M., Grundke-Iqbal, I. & Iqbal, K. Hyperphosphorylation induces self-assembly of τ into tangles of paired helical filaments/straight filaments. *Proceedings of the National Academy of Sciences of the United States of America* **98**, (2001).

36. Augustinack, J. C., Schneider, A., Mandelkow, E. M. & Hyman, B. T. Specific tau phosphorylation sites correlate with severity of neuronal cytopathology in Alzheimer's disease. *Acta Neuropathologica* **103**, (2002).

37. Zhang, Y., Thompson, R., Zhang, H. & Xu, H. APP processing in Alzheimer's disease. *Molecular Brain* **4**, 3 (2011).

38. Zheng, H. & Koo, E. H. The amyloid precursor protein: Beyond amyloid. *Molecular Neurodegeneration* **1**, 1–12 (2006).

39. de Strooper, B., Iwatsubo, T. & Wolfe, M. S. Presenilins and γ-secretase: Structure, function, and role in Alzheimer disease. *Cold Spring Harbor Perspectives in Medicine* **2**, (2012).

40. Xu, X. γ-Secretase catalyzes sequential cleavages of the AβPP transmembrane domain. *Journal of Alzheimer's Disease* vol. 16 (2009).

41. Hunter, S. & Brayne, C. Understanding the roles of mutations in the amyloid precursor protein in Alzheimer disease. *Molecular Psychiatry* vol. 23 (2018).

42. Jarrett, J. T., Berger, E. P. & Lansbury, P. T. The Carboxy Terminus of the β Amyloid Protein Is Critical for the Seeding of Amyloid Formation: Implications for the Pathogenesis of Alzheimer's Disease. *Biochemistry* **32**, (1993).

43. Younkin, S. G. The role of Aβ42 in Alzheimer's disease. in *Journal of Physiology Paris* vol. 92 (1998).

44. Kelleher, R. J. & Shen, J. Presenilin-1 mutations and Alzheimer's disease. *Proceedings of the National Academy of Sciences of the United States of America* vol. 114 (2017).

45. Li, N. *et al.* Effect of presenilin mutations on APP cleavage; Insights into the pathogenesis of FAD. *Frontiers in Aging Neuroscience* **8**, (2016).

46. Cline, E. N., Bicca, M. A., Viola, K. L. & Klein, W. L. The Amyloid-β Oligomer Hypothesis: Beginning of the Third Decade. *Journal of Alzheimer's Disease* vol. 64 (2018).

47. Gouras, G. K., Almeida, C. G. & Takahashi, R. H. Intraneuronal Aβ accumulation and origin of plaques in Alzheimer's disease. *Neurobiology of Aging* **26**, 1235–1244 (2005).

48. LaFerla, F. M., Green, K. N. & Oddo, S. Intracellular amyloid-β in Alzheimer's disease. *Nature Reviews Neuroscience* **8**, 499–509 (2007).

49. Atwood, C. S. *et al.* Amyloid-β: A chameleon walking in two worlds: A review of the trophic and toxic properties of amyloid-β. *Brain Research Reviews* **43**, 1–16 (2003).

50. Moreira, P. I., Carvalho, C., Zhu, X., Smith, M. A. & Perry, G. Mitochondrial dysfunction is a trigger of Alzheimer's disease pathophysiology. *Biochimica et Biophysica Acta - Molecular Basis of Disease* **1802**, 2–10 (2010).

51. Gordon, B. A. *et al.* Spatial patterns of neuroimaging biomarker change in individuals from families with autosomal dominant Alzheimer's disease: a longitudinal study. *The Lancet Neurology* **17**, (2018).

52. Croteau, E. *et al.* A cross-sectional comparison of brain glucose and ketone metabolism in cognitively healthy older adults, mild cognitive impairment and early Alzheimer's disease. *Experimental Gerontology* **107**, (2018).

53. Kapogiannis, D. & Mattson, M. P. Disrupted energy metabolism and neuronal circuit dysfunction in cognitive impairment and Alzheimer's disease. *The Lancet Neurology* vol. 10 (2011).

54. Szablewski, L. Glucose Transporters in Brain: In Health and in Alzheimer's Disease. *Journal of Alzheimer's Disease* vol. 55 (2017).

55. Wang, W., Zhao, F., Ma, X., Perry, G. & Zhu, X. Mitochondria dysfunction in the pathogenesis of Alzheimer's disease: Recent advances. *Molecular Neurodegeneration* vol. 15 (2020).

56. Bubber, P., Haroutunian, V., Fisch, G., Blass, J. P. & Gibson, G. E. Mitochondrial abnormalities in Alzheimer brain: Mechanistic implications. *Annals of Neurology* **57**, (2005).

57. Adav, S. S., Park, J. E. & Sze, S. K. Quantitative profiling brain proteomes revealed mitochondrial dysfunction in Alzheimer's disease. *Molecular Brain* **12**, (2019).

58. Minjarez, B. *et al.* Identification of proteins that are differentially expressed in brains with Alzheimer's disease using iTRAQ labeling and tandem mass spectrometry. *Journal of Proteomics* **139**, (2016).

59. Sorrentino, V. *et al.* Enhancing mitochondrial proteostasis reduces amyloid-β proteotoxicity. *Nature* **552**, (2017).

60. Manczak, M., Park, B. S., Jung, Y. & Reddy, P. H. Differential Expression of Oxidative Phosphorylation Genes in Patients with Alzheimer's Disease: Implications for Early Mitochondrial Dysfunction and Oxidative Damage. *NeuroMolecular Medicine* **5**, (2004).

61. Mastroeni, D. *et al.* Nuclear but not mitochondrial-encoded oxidative phosphorylation genes are altered in aging, mild cognitive impairment, and Alzheimer's disease. *Alzheimer's and Dementia* **13**, (2017).

62. Brooks, W. M. *et al.* Gene expression profiles of metabolic enzyme transcripts in Alzheimer's disease. *Brain Research* **1127**, (2007).

63. Liang, W. S. *et al.* Alzheimer's disease is associated with reduced expression of energy metabolism genes in posterior cingulate neurons. *Proceedings of the National Academy of Sciences of the United States of America* **105**, (2008).

64. Zhang, L. *et al.* Potential hippocampal genes and pathways involved in Alzheimer's disease: A bioinformatic analysis. *Genetics and Molecular Research* **14**, (2015).

65. Parker, W. D., Parks, J., Filley, C. M. & Kleinschmidt-Demasters, B. K. Electron transport chain defects in alzheimer's disease brain. *Neurology* **44**, (1994).

66. Zhang, C., Rissman, R. A. & Feng, J. Characterization of ATP alternations in an Alzheimer's disease transgenic mouse model. *Journal of Alzheimer's Disease* **44**, (2015).

67. Cha, M. Y. *et al.* Mitochondrial ATP synthase activity is impaired by suppressed O-GlcNAcylation in Alzheimer's disease. *Human Molecular Genetics* **24**, (2015).

68. Butterfield, D. A. & Halliwell, B. Oxidative stress, dysfunctional glucose metabolism and Alzheimer disease. *Nature Reviews Neuroscience* vol. 20 (2019).

69. Zhu, X. *et al.* Hydroxynonenal-generated crosslinking fluorophore accumulation in Alzheimer disease reveals a dichotomy of protein turnover. *Free Radical Biology and Medicine* **52**, (2012).

70. Nunomura, A. *et al.* The earliest stage of cognitive impairment in transition from normal aging to alzheimer disease is marked by prominent RNA oxidation in vulnerable neurons. *Journal of Neuropathology and Experimental Neurology* **71**, (2012).

71. Kong, Q. & Lin, C. L. G. Oxidative damage to RNA: Mechanisms, consequences, and diseases. *Cellular and Molecular Life Sciences* (2010) doi:10.1007/s00018-010-0277-y.

72. Nunomura, A. *et al.* Oxidative damage is the earliest event in Alzheimer disease. *Journal of Neuropathology and Experimental Neurology* **60**, 759–767 (2001).

73. Tramutola, A., Lanzillotta, C., Perluigi, M. & Butterfield, D. A. Oxidative stress, protein modification and Alzheimer disease. *Brain Research Bulletin* vol. 133 (2017).

74. Wang, J., Xiong, S., Xie, C., Markesbery, W. R. & Lovell, M. A. Increased oxidative damage in nuclear and mitochondrial DNA in Alzheimer's disease. *Journal of Neurochemistry* **93**, (2005).

75. Mecocci, P., MacGarvey, U. & Beal, M. F. Oxidative damage to mitochondrial DNA is increased in Alzheimer's disease. *Annals of Neurology* **36**, (1994).

76. Wang, X. *et al.* Impaired balance of mitochondrial fission and fusion in Alzheimer's disease. *Journal of Neuroscience* **29**, (2009).

77. Wang, X. *et al.* Amyloid-β overproduction causes abnormal mitochondrial dynamics via differential modulation of mitochondrial fission/fusion proteins. *Proceedings of the National Academy of Sciences of the United States of America* **105**, (2008).

78. Cho, D.-H. *et al.* S-Nitrosylation of Drp1 Mediates β-Amyloid-Related Mitochondrial Fission and Neuronal Injury. *Science* **324**, (2009).

79. Manczak, M., Calkins, M. J. & Reddy, P. H. Impaired mitochondrial dynamics and abnormal interaction of amyloid beta with mitochondrial protein Drp1 in neurons from patients with Alzheimer's disease: Implications for neuronal damage. *Human Molecular Genetics* **20**, (2011).

80. Kerr, J. S. *et al.* Mitophagy and Alzheimer's Disease: Cellular and Molecular Mechanisms. *Trends in Neurosciences* vol. 40 (2017).

81. Sheng, M., Sabatini, B. L. & Su, T. C. Synapses and Alzheimer ' s Disease. *Cold Spring Harb Perspect Biol* (2012) doi:10.3390/nu9070670.

82. Shankar, G. M. & Walsh, D. M. Alzheimer's disease: Synaptic dysfunction and Aβ. *Molecular Neurodegeneration* **4**, (2009).

83. Selkoe, D. J. Alzheimer ' s Disease Is a Synaptic Failure Author (s): Dennis J . Selkoe. *Science* **298**, 789–791 (2002).

84. DeKosky, S. T. & Scheff, S. W. Synapse loss in frontal cortex biopsies in Alzheimer's disease: Correlation with cognitive severity. *Annals of Neurology* **27**, (1990).

85. Terry, R. D. *et al.* Physical basis of cognitive alterations in alzheimer's disease: Synapse loss is the major correlate of cognitive impairment. *Annals of Neurology* **30**, (1991).

86. Scheff, S. W., Price, D. A., Schmitt, F. A. & Mufson, E. J. Hippocampal synaptic loss in early Alzheimer's disease and mild cognitive impairment. *Neurobiology of Aging* **27**, (2006).

87. Scheff, S. W., Price, D. A., Schmitt, F. A., Dekosky, S. T. & Mufson, E. J. Synaptic alterations in CA1 in mild Alzheimer disease and mild cognitive impairment. *Neurology* **68**, (2007).

88. Masliah, E. *et al.* Altered expression of synaptic proteins occurs early during progression of Alzheimer's disease. *Neurology* **56**, (2001).

89. Davies, C. A., Mann, D. M. A., Sumpter, P. Q. & Yates, P. O. A quantitative morphometric analysis of the neuronal and synaptic content of the frontal and temporal cortex in patients with Alzheimer's disease. *Journal of the Neurological Sciences* **78**, (1987).

90. Reddy, P. H. *et al.* Differential loss of synaptic proteins in Alzheimer's disease: Implications for synaptic dysfunction. *Journal of Alzheimer's Disease* **7**, 103–117 (2005).

91. Knobloch, M. & Mansuy, I. M. Dendritic spine loss and synaptic alterations in Alzheimer's disease. *Molecular Neurobiology* **37**, 73–82 (2008).

92. Wei, W. *et al.* Amyloid beta from axons and dendrites reduces local spine number and plasticity. *Nature Neuroscience* **13**, (2010).

93. Haass, C. & Selkoe, D. J. Soluble protein oligomers in neurodegeneration: Lessons from the Alzheimer's amyloid β-peptide. *Nature Reviews Molecular Cell Biology* vol. 8 (2007).

94. Klyubin, I. *et al.* Amyloid β protein immunotherapy neutralizes Aβ oligomers that disrupt synaptic plasticity in vivo. *Nature Medicine* **11**, (2005).

95. Townsend, M., Shankar, G. M., Mehta, T., Walsh, D. M. & Selkoe, D. J. Effects of secreted oligomers of amyloid β-protein on hippocampal synaptic plasticity: A potent role for trimers. *Journal of Physiology* **572**, (2006).

96. Walsh, D. M. *et al.* Naturally secreted oligomers of amyloid β protein potently inhibit hippocampal long-term potentiation in vivo. *Nature* **416**, (2002).

97. Wang, Y. & Mandelkow, E. Tau in physiology and pathology. *Nature Reviews Neuroscience* **17**, 5–21 (2016).

98. Malenka, R. C. & Bear, M. F. LTP and LTD: An embarrassment of riches. *Neuron* vol. 44 (2004).

99. Freir, D. B., Holscher, C. & Herron, C. E. Blockade of long-term potentiation by β-amyloid peptides in the CA1 region of the rat hippocampus in vivo. *Journal of Neurophysiology* **85**, (2001).

100. Lambert, M. P. *et al.* Diffusible, nonfibrillar ligands derived from Aβ1-42 are potent central nervous system neurotoxins. *Proceedings of the National Academy of Sciences of the United States of America* **95**, (1998).

101. Chapman, P. F. *et al.* Impaired synaptic plasticity and learning in aged amyloid precursor protein transgenic mice. *Nature Neuroscience* **2**, (1999).

102. Cullen, W. K., Suh, Y. H., Anwyl, R. & Rowan, M. J. Block of LTP in rat hippocampus in vivo by β-amyloid precursor protein fragments. *NeuroReport* **8**, (1997).

103. Cleary, J. P. *et al.* Natural oligomers of the amyloid-β protein specifically disrupt cognitive function. *Nature Neuroscience* **8**, (2005).

104. Hsieh, H. *et al.* AMPAR Removal Underlies Aβ-Induced Synaptic Depression and Dendritic Spine Loss. *Neuron* **52**, (2006).

105. Shankar, G. M. *et al.* Natural oligomers of the Alzheimer amyloid-β protein induce reversible synapse loss by modulating an NMDA-type glutamate receptor-dependent signaling pathway. *Journal of Neuroscience* **27**, (2007).

106. Shankar, G. M. *et al.* Amyloid-beta protein dimers isloated directly from Alzheimer brain impair synaptic plasticity and memory. *Nature medicine* **14**, 837–842 (2008).

107. de Felice, F. G. *et al.* Aβ oligomers induce neuronal oxidative stress through an N-methyl-D-aspartate receptor-dependent mechanism that is blocked by the Alzheimer drug memantine. *Journal of Biological Chemistry* **282**, (2007).

108. Decker, H. *et al.* N-Methyl-d-aspartate receptors are required for synaptic targeting of Alzheimer's toxic amyloid-β peptide oligomers. *Journal of Neurochemistry* **115**, (2010).

109. Dineley, K. T., Hogan, D., Zhang, W. R. & Taglialatela, G. Acute inhibition of calcineurin restores associative learning and memory in Tg2576 APP transgenic mice. *Neurobiology of Learning and Memory* **88**, (2007).

110. Wu, H. Y. *et al.* Amyloid β induces the morphological neurodegenerative triad of spine loss, dendritic simplification, and neuritic dystrophies through calcineurin activation. *Journal of Neuroscience* **30**, (2010).

111. Liu, J., Chang, L., Song, Y., Li, H. & Wu, Y. The role of NMDA receptors in Alzheimer's disease. *Frontiers in Neuroscience* vol. 13 (2019).

112. Li, S. *et al.* Soluble Oligomers of Amyloid β Protein Facilitate Hippocampal Long-Term Depression by Disrupting Neuronal Glutamate Uptake. *Neuron* **62**, (2009).

113. Findley, C. A., Bartke, A., Hascup, K. N. & Hascup, E. R. Amyloid Beta-Related Alterations to Glutamate Signaling Dynamics During Alzheimer's Disease Progression. *ASN Neuro* vol. 11 (2019).

114. Renner, M. *et al.* Deleterious Effects of Amyloid β Oligomers Acting as an Extracellular Scaffold for mGluR5. *Neuron* **66**, (2010).

115. Um, J. W. *et al.* Metabotropic Glutamate Receptor 5 Is a Coreceptor for Alzheimer Aβ Oligomer Bound to Cellular Prion Protein. *Neuron* **79**, 887–902 (2013).

116. Wang, H. Y. *et al.* β-Amyloid1-42 binds to α7 nicotinic acetylcholine receptor with high affinity. Implications for Alzheimer's disease pathology. *Journal of Biological Chemistry* **275**, (2000).

117. Uddin, M. S. *et al.* Autophagy and Alzheimer's disease: From molecular mechanisms to therapeutic implications. *Frontiers in Aging Neuroscience* vol. 10 (2018).

118. Yang, D. S. *et al.* Reversal of autophagy dysfunction in the TgCRND8 mouse model of Alzheimer's disease ameliorates amyloid pathologies and memory deficits. *Brain* **134**, 258–277 (2011).

119. Baloyannis, S. J. Golgi apparatus and protein trafficking in Alzheimer's disease. in *Journal of Alzheimer's Disease* vol. 42 (2014).

120. Meraz-Ríos, M. A., Toral-Rios, D., Franco-Bocanegra, D., Villeda-Hernández, J. & Campos-Peña, V. Inflammatory process in Alzheimer's Disease. *Frontiers in Integrative Neuroscience* (2013) doi:10.3389/fnint.2013.00059.

121. Fakhoury, M. Microglia and astrocytes in Alzheimer's disease: implications for therapy. *Current Neuropharmacology* **15**, (2017).

122. Solito, E. & Sastre, M. Microglia function in Alzheimer's disease. *Frontiers in Pharmacology* **3 FEB**, (2012).

123. Cunningham, C., Wilcockson, D. C., Campion, S., Lunnon, K. & Perry, V. H. Central and systemic endotoxin challenges exacerbate the local inflammatory response and increase neuronal death during chronic neurodegeneration. *Journal of Neuroscience* **25**, (2005).

124. Holmes, C. *et al.* Systemic infection, interleukin 1β, and cognitive decline in Alzheimer's disease. *Journal of Neurology Neurosurgery and Psychiatry* **74**, (2003).

125. Richard, K. L., Filali, M., Préfontaine, P. & Rivest, S. Toll-like receptor 2 acts as a natural innate immune receptor to clear amyloid β1-42 and delay the cognitive decline in a mouse model of Alzheimer's disease. *Journal of Neuroscience* **28**, (2008).

126. Reed-Geaghan, E. G., Savage, J. C., Hise, A. G. & Landreth, G. E. CD14 and toll-like receptors 2 and 4 are required for fibrillar Aβ-stimulated microglial activation. *Journal of Neuroscience* **29**, (2009).

127. Lee, C. Y. D. & Landreth, G. E. The role of microglia in amyloid clearance from the AD brain. *Journal of Neural Transmission* vol. 117 (2010).

128. Bamberger, M. E., Harris, M. E., McDonald, D. R., Husemann, J. & Landreth, G. E. A cell surface receptor complex for fibrillar β-amyloid mediates microglial activation. *Journal of Neuroscience* **23**, (2003).

129. Sajja, V. S. S. S., Hlavac, N. & VandeVord, P. J. Role of glia in memory deficits following traumatic brain injury: Biomarkers of glia dysfunction. *Frontiers in Integrative Neuroscience* vol. 10 (2016).

130. Combs, C. K., Colleen Karlo, J., Kao, S. C. & Landreth, G. E. β-amyloid stimulation of microglia anti monocytes results in TNFα-dependent expression of inducible nitric oxide synthase and neuronal apoptosis. *Journal of Neuroscience* **21**, (2001).

131. Krabbe, G. *et al.* Functional Impairment of Microglia Coincides with Beta-Amyloid Deposition in Mice with Alzheimer-Like Pathology. *PLoS ONE* **8**, (2013).

132. Wyss-Coray, T. & Rogers, J. Inflammation in Alzheimer disease-A brief review of the basic science and clinical literature. *Cold Spring Harbor Perspectives in Medicine* **2**, (2012).

133. el Khoury, J. *et al.* Ccr2 deficiency impairs microglial accumulation and accelerates progression of Alzheimer-like disease. *Nature Medicine* **13**, (2007).

134. Ries, M. & Sastre, M. Mechanisms of Aβ clearance and degradation by glial cells. *Frontiers in Aging Neuroscience* **8**, 1–9 (2016).

135. González-Reyes, R. E., Nava-Mesa, M. O., Vargas-Sánchez, K., Ariza-Salamanca, D. & Mora-Muñoz, L. Involvement of astrocytes in Alzheimer's disease from a neuroinflammatory and oxidative stress perspective. *Frontiers in Molecular Neuroscience* vol. 10 (2017).

136. Toivari, E., Manninen, T., Nahata, A. K., Jalonen, T. O. & Linne, M. L. Effects of transmitters and amyloid-beta peptide on calcium signals in rat cortical astrocytes: Fura-2AM measurements and stochastic model simulations. *PLoS ONE* **6**, (2011).

137. Alberdi, E. *et al.* Ca2+-dependent endoplasmic reticulum stress correlates with astrogliosis in oligomeric amyloid β-treated astrocytes and in a model of Alzheimer's disease. *Aging Cell* **12**, (2013).

138. Haughey, N. J. & Mattson, M. P. Alzheimer's amyloid β-peptide enhances ATP/Gap junction-mediated calcium-wave propagation in astrocytes. *NeuroMolecular Medicine* **3**, (2003).

139. Lim, D. *et al.* Amyloid beta deregulates astroglial mGluR5-mediated calcium signaling via calcineurin and Nf-kB. *GLIA* **61**, (2013).

140. Ronco, V. *et al.* Differential deregulation of astrocytic calcium signalling by amyloid-β, TNFα, IL-1β and LPS. *Cell Calcium* **55**, (2014).

141. Grolla, A. A. *et al.* Aβ leads to Ca2+ signaling alterations and transcriptional changes in glial cells. *Neurobiology of Aging* **34**, (2013).

142. Lee, L., Kosuri, P. & Arancio, O. Picomolar amyloid-β peptides enhance spontaneous astrocyte calcium transients. *Journal of Alzheimer's Disease* **38**, (2014).

143. Xiu, J., Nordberg, A., Zhang, J. T. & Guan, Z. Z. Expression of nicotinic receptors on primary cultures of rat astrocytes and up-regulation of the α7, α4 and β2 subunits in response to nanomolar concentrations of the β-amyloid peptide1-42. *Neurochemistry International* **47**, (2005).

144. Delekate, A. *et al.* Metabotropic P2Y1 receptor signalling mediates astrocytic hyperactivity in vivo in an Alzheimer's disease mouse model. *Nature Communications* **5**, (2014).

145. Vincent, A. J., Gasperini, R., Foa, L. & Small, D. H. Astrocytes in Alzheimer's disease: Emerging roles in calcium dysregulation and synaptic plasticity. *Journal of Alzheimer's Disease* vol. 22 (2010).

146. Matos, M. *et al.* Astrocytic adenosine A2A receptors control the amyloid-β peptide-induced decrease of glutamate uptake. *Journal of Alzheimer's Disease* **31**, (2012).

147. Bali, J., Gheinani, A. H., Zurbriggen, S. & Rajendran, L. Role of genes linked to sporadic Alzheimer's disease risk in the production of β-amyloid peptides. *Proceedings of the National Academy of Sciences of the United States of America* **109**, (2012).

148. Wolfe, C. M., Fitz, N. F., Nam, K. N., Lefterov, I. & Koldamova, R. The role of APOE and TREM2 in Alzheimer ′ s disease—Current understanding and perspectives. *International Journal of Molecular Sciences* vol. 20 (2019).

149. Liu, C. C., Kanekiyo, T., Xu, H. & Bu, G. Apolipoprotein e and Alzheimer disease: Risk, mechanisms and therapy. *Nature Reviews Neurology* vol. 9 (2013).

150. Carmona, S. *et al.* The role of TREM2 in Alzheimer's disease and other neurodegenerative disorders. *The Lancet Neurology* vol. 17 (2018).

151. Hatters, D. M., Peters-Libeu, C. A. & Weisgraber, K. H. Apolipoprotein E structure: insights into function. *Trends in Biochemical Sciences* vol. 31 (2006).

152. Kanekiyo, T., Xu, H. & Bu, G. ApoE and Aβ in Alzheimer's disease: Accidental encounters or partners? *Neuron* **81**, 740–754 (2014).

153. Lane-Donovan, C. & Herz, J. ApoE, ApoE Receptors, and the Synapse in Alzheimer's Disease. *Trends in Endocrinology and Metabolism* **28**, 273–284 (2017).

154. Mahley, R. W. & Rall, S. C. A <scp>POLIPOPROTEIN</scp> E: Far More Than a Lipid Transport Protein. *Annual Review of Genomics and Human Genetics* (2000) doi:10.1146/annurev.genom.1.1.507.

155. Bu, G. Apolipoprotein e and its receptors in Alzheimer's disease: Pathways, pathogenesis and therapy. *Nature Reviews Neuroscience* vol. 10 (2009).

156. Bu, G., Geuze, H. J., Strous, G. J. & Schwartz, A. L. 39 kDa receptor-associated protein is an ER resident protein and molecular chaperone far LDL receptor-related protein. *EMBO Journal* **14**, (1995).

157. Herz, J., Goldstein, J. L., Strickland, D. K., Ho, Y. K. & Brown, M. S. 39-kDa protein modulates binding of ligands to low density lipoprotein receptor-related protein/α2-macroglobulin receptor. *Journal of Biological Chemistry* **266**, (1991).

158. Willnow, T. E. *et al.* RAP, a specialized chaperone, prevents ligand-induced ER retention and degradation of LDL receptor-related endocytic receptors. *EMBO Journal* **15**, (1996).

159. Hoe, H. S., Harris, D. C. & Rebeck, G. W. Multiple pathways of apolipoprotein E signaling in primary neurons. *Journal of Neurochemistry* **93**, (2005).

160. Huang, Y. W. A., Zhou, B., Wernig, M. & Südhof, T. C. ApoE2, ApoE3, and ApoE4 Differentially Stimulate APP Transcription and Aβ Secretion. *Cell* (2017) doi:10.1016/j.cell.2016.12.044.

161. Huang, Y. W. A., Zhou, B., Nabet, A. M., Wernig, M. & Südhof, T. C. Differential Signaling Mediated by ApoE2, ApoE3, and ApoE4 in Human Neurons Parallels Alzheimer's Disease Risk. *Journal of Neuroscience* **39**, 7408–7427 (2019).

162. Ohkubo, N. *et al.* Apolipoprotein E4 Stimulates cAMP Response Element-binding Protein Transcriptional Activity through the Extracellular Signal-regulated Kinase Pathway. *Journal of Biological Chemistry* **276**, 3046–3053 (2001).

163. Nakajima, C. *et al.* Low density lipoprotein receptor-related protein 1 (LRP1) modulates N-methyl-D-aspartate (NMDA) receptor-dependent intracellular signaling and NMDA-induced regulation of postsynaptic protein complexes. *Journal of Biological Chemistry* **288**, (2013).

164. Qiu, Z., Crutcher, K. A., Hyman, B. T. & Rebeck, G. W. apoE isoforms affect neuronal N-methyl-D-aspartate calcium responses and toxicity via receptor-mediated processes. *Neuroscience* **122**, 291–303 (2003).

165. Bacskai, B. J., Xia, M. Q., Strickland, D. K., Rebeck, G. W. & Hyman, B. T. The endocytic receptor protein LRP also mediates neuronal calcium signaling via N-methyl-D-aspartate receptors. *Proceedings of the National Academy of Sciences of the United States of America* **97**, (2000).

166. Hoe, H. S. *et al.* Apolipoprotein E receptor 2 interactions with the N-Methyl-D-aspartate receptor. *Journal of Biological Chemistry* **281**, (2006).

167. Chen, Y., Durakoglugil, M. S., Xian, X. & Herz, J. ApoE4 reduces glutamate receptor function and synaptic plasticity by selectively impairing ApoE receptor recycling. *Proceedings of the National Academy of Sciences of the United States of America* **107**, (2010).

168. Namba, Y., Tomonaga, M., Kawasaki, H., Otomo, E. & Ikeda, K. Apolipoprotein E immunoreactivity in cerebral amyloid deposits and neurofibrillary tangles in Alzheimer's disease and kuru plaque amyloid in Creutzfeldt-Jakob disease. *Brain Research* **541**, (1991).

169. Strittmatter, W. J. *et al.* Binding of human apolipoprotein E to synthetic amyloid β peptide: Isoform-specific effects and implications for late-onset Alzheimer disease. *Proceedings of the National Academy of Sciences of the United States of America* **90**, (1993).

170. LaDu, M. J. *et al.* Purification of apolipoprotein E attenuates isoform-specific binding to β-amyloid. *Journal of Biological Chemistry* **270**, (1995).

171. Jiang, Q. *et al.* ApoE Promotes the Proteolytic Degradation of Aβ. *Neuron* **58**, (2008).

172. Li, J. *et al.* Differential regulation of amyloid-β endocytic trafficking and lysosomal degradation by apolipoprotein E isoforms. *Journal of Biological Chemistry* **287**, (2012).

173. Baitsch, D. *et al.* Apolipoprotein e induces antiinflammatory phenotype in macrophages. *Arteriosclerosis, Thrombosis, and Vascular Biology* **31**, (2011).

174. Cudaback, E., Li, X., Montine, K. S., Montine, T. J. & Keene, C. D. Apolipoprotein E isoform-dependent microglia migration. *The FASEB Journal* **25**, (2011).

175. Zhu, Y. *et al.* APOE genotype alters glial activation and loss of synaptic markers in mice. *GLIA* **60**, (2012).

176. Deane, R. *et al.* LRP/amyloid β-peptide interaction mediates differential brain efflux of Aβ isoforms. *Neuron* **43**, (2004).

177. Bell, R. D. *et al.* Transport pathways for clearance of human Alzheimer's amyloid β-peptide and apolipoproteins E and J in the mouse central nervous system. *Journal of Cerebral Blood Flow and Metabolism* **27**, (2007).

178. Deane, R. *et al.* apoE isoform-specific disruption of amyloid β peptide clearance from mouse brain. *Journal of Clinical Investigation* **118**, (2008).

179. Bell, R. D. *et al.* Apolipoprotein e controls cerebrovascular integrity via cyclophilin A. *Nature* **485**, (2012).

180. Nishitsuji, K., Hosono, T., Nakamura, T., Bu, G. & Michikawa, M. Apolipoprotein E regulates the integrity of tight junctions in an isoform-dependent manner in an in vitro blood-brain barrier model. *Journal of Biological Chemistry* **286**, (2011).

181. Cerf, E., Gustot, A., Goormaghtigh, E., Ruysschaert, J.-M. & Raussens, V. High ability of apolipoprotein E4 to stabilize amyloid-β peptide oligomers, the pathological entities responsible for Alzheimer's disease. *The FASEB Journal* **25**, (2011).

182. Hashimoto, T. *et al.* Apolipoprotein e, especially apolipoprotein E4, increases the oligomerization of amyloid β peptide. *Journal of Neuroscience* **32**, (2012).

183. Huang, Y. W. A., Zhou, B., Wernig, M. & Südhof, T. C. ApoE2, ApoE3, and ApoE4 Differentially Stimulate APP Transcription and Aβ Secretion. *Cell* **168**, 427-441.e21 (2017).

184. Lin, Y. T. *et al.* APOE4 Causes Widespread Molecular and Cellular Alterations Associated with Alzheimer's Disease Phenotypes in Human iPSC-Derived Brain Cell Types. *Neuron* **98**, 1141-1154.e7 (2018).

185. Wu, L., Zhang, X. & Zhao, L. Human apoe isoforms differentially modulate brain glucose and ketone body metabolism: Implications for Alzheimer's disease risk reduction and early intervention. *Journal of Neuroscience* **38**, (2018).

186. Reiman, E. M. *et al.* Functional brain abnormalities in young adults at genetic risk for late-onset Alzheimer's dementia. *Proceedings of the National Academy of Sciences of the United States of America* **101**, (2004).

187. Reiman, E. M. *et al.* Correlations between apolipoprotein E ε4 gene dose and brain-imaging measurements of regional hypometabolism. *Proceedings of the National Academy of Sciences of the United States of America* **102**, (2005).

188. Valla, J. *et al.* Reduced posterior cingulate mitochondrial activity in expired young adult carriers of the APOE ε4 Allele, the major late-onset Alzheimer's susceptibility gene. *Journal of Alzheimer's Disease* **22**, (2010).

189. Perkins, M. *et al.* Altered Energy Metabolism Pathways in the Posterior Cingulate in Young Adult Apolipoprotein e ϵ 4 Carriers. *Journal of Alzheimer's Disease* **53**, (2016).

190. Chen, H. K. *et al.* Apolipoprotein E4 domain interaction mediates detrimental effects on mitochondria and is a potential therapeutic target for alzheimer disease. *Journal of Biological Chemistry* **286**, (2011).

191. Simonovitch, S., Schmukler, E., Masliah, E., Pinkas-Kramarski, R. & Michaelson, D. M. The Effects of APOE4 on Mitochondrial Dynamics and Proteins in vivo. *Journal of Alzheimer's Disease* **70**, (2019).

192. Schmukler, E. *et al.* Altered mitochondrial dynamics and function in APOE4-expressing astrocytes. *Cell Death and Disease* **11**, (2020).

193. Nakamura, T., Watanabe, A., Fujino, T., Hosono, T. & Michikawa, M. Apolipoprotein E4 (1-272) fragment is associated with mitochondrial proteins and affects mitochondrial function in neuronal cells. *Molecular Neurodegeneration* **4**, (2009).

194. Liang, T. *et al.* ApoE4 (Δ272–299) induces mitochondrial-associated membrane formation and mitochondrial impairment by enhancing GRP75-modulated mitochondrial calcium overload in neuron. *Cell and Bioscience* **11**, (2021).

195. Plassman, B. L. *et al.* Apolipoprotein E ε4 allele and hippocampal volume in twins with normal cognition. *Neurology* **48**, (1997).

196. M.G., D. *et al.* Memory complaints and APOE-epsilon4 accelerate cognitive decline in cognitively normal elderly. *Neurology* **57**, (2001).

197. Reas, E. T. *et al.* Effects of APOE on cognitive aging in community-dwelling older adults. *Neuropsychology* **33**, (2019).

198. de Jager, P. L. *et al.* A genome-wide scan for common variants affecting the rate of age-related cognitive decline. *Neurobiology of Aging* **33**, (2012).

199. Wisdom, N. M., Callahan, J. L. & Hawkins, K. A. The effects of apolipoprotein E on non-impaired cognitive functioning: A meta-analysis. *Neurobiology of Aging* **32**, (2011).

200. Small, B. J., Rosnick, C. B., Fratiglioni, L. & Bäckman, L. Apolipoprotein E and cognitive performance: A meta-analysis. *Psychology and Aging* **19**, (2004).

201. Rodriguez, G. A., Burns, M. P., Weeber, E. J. & Rebeck, G. W. Young APOE4 targeted replacement mice exhibit poor spatial learning and memory, with reduced dendritic spine density in the medial entorhinal cortex. *Learning and Memory* **20**, (2013).

202. Yong, S. M., Lim, M. L., Low, C. M. & Wong, B. S. Reduced neuronal signaling in the ageing apolipoprotein-E4 targeted replacement female mice. *Scientific Reports* **4**, (2014).

203. Teter, B. *et al.* Defective neuronal sprouting by human apolipoprotein E4 is a gain-of-negative function. *Journal of Neuroscience Research* **68**, (2002).

204. Nathan, B. P. *et al.* Differential effects of apolipoproteins E3 and E4 on neuronal growth in vitro. *Science* **264**, (1994).

205. Dumanis, S. B. *et al.* ApoE4 decreases spine density and dendritic complexity in cortical neurons in vivo. *Journal of Neuroscience* **29**, (2009).

206. Trommer, B. L. *et al.* ApoE isoform affects LTP in human targeted replacement mice. *NeuroReport* **15**, (2004).

207. Trommer, B. L. *et al.* ApoE isoform-specific effects on LTP: Blockade by oligomeric amyloid-β1-42. *Neurobiology of Disease* **18**, (2005).

208. Korwek, K. M., Trotter, J. H., Ladu, M. J., Sullivan, P. M. & Weeber, E. J. Apoe isoform-dependent changes in hippocampal synaptic function. *Molecular Neurodegeneration* **4**, 1–18 (2009).

209. Sheng, Z., Prorok, M., Brown, B. E. & Castellino, F. J. N-methyl-d-aspartate receptor inhibition by an apolipoprotein E-derived peptide relies on low-density lipoprotein receptor-associated protein. *Neuropharmacology* **55**, (2008).

210. Veinbergs, I., Everson, A., Sagara, Y. & Masliah, E. Neurotoxic effects of apolipoprotein E4 are mediated via dysregulation of calcium homeostasis. *Journal of Neuroscience Research* **67**, (2002).

211. Tolar, M. *et al.* Truncated apolipoprotein E (ApoE) causes increased intracellular calcium and may mediate ApoE neurotoxicity. *Journal of Neuroscience* **19**, (1999).

212. Xu, D. & Peng, Y. Apolipoprotein E 4 triggers multiple pathway-mediated Ca2+ overload, causes CaMK II phosphorylation abnormity and aggravates oxidative stress caused cerebral cortical neuron damage. *European review for medical and pharmacological sciences* **21**, (2017).

213. Kelleher, R. J., Govindarajan, A. & Tonegawa, S. Translational regulatory mechanisms in persistent forms of synaptic plasticity. *Neuron* vol. 44 (2004).

214. Sutton, M. A. & Schuman, E. M. Dendritic Protein Synthesis, Synaptic Plasticity, and Memory. *Cell* (2006) doi:10.1016/j.cell.2006.09.014.

215. Rosenberg, T. *et al.* The roles of protein expression in synaptic plasticity and memory consolidation. *Frontiers in Molecular Neuroscience* vol. 7 (2014).

216. Bramham, C. R. & Wells, D. G. Dendritic mRNA: Transport, translation and function. *Nature Reviews Neuroscience* vol. 8 (2007).

217. Cefaliello, C. *et al.* Deregulated Local Protein Synthesis in the Brain Synaptosomes of a Mouse Model for Alzheimer's Disease. *Molecular Neurobiology* **57**, (2020).

218. Elder, M. K. *et al.* Age-dependent shift in the de novo proteome accompanies pathogenesis in an Alzheimer's disease mouse model. *Communications Biology* **4**, 823 (2021).

219. Meier, S. *et al.* Pathological Tau Promotes Neuronal Damage by Impairing Ribosomal Function and Decreasing Protein Synthesis. *Journal of Neuroscience* **36**, 1001–1007 (2016).

220. Evans, H. T., Benetatos, J., van Roijen, M., Bodea, L. & Götz, J. Decreased synthesis of ribosomal proteins in tauopathy revealed by non-canonical amino acid labelling. *The EMBO Journal* **38**, (2019).

221. Koren, S. A. *et al.* Tau drives translational selectivity by interacting with ribosomal proteins. *Acta Neuropathologica* **137**, (2019).

222. Radford, H., Moreno, J. A., Verity, N., Halliday, M. & Mallucci, G. R. PERK inhibition prevents tau-mediated neurodegeneration in a mouse model of frontotemporal dementia. *Acta Neuropathologica* **130**, (2015).

223. Moreno, J. A. *et al.* Oral treatment targeting the unfolded protein response prevents neurodegeneration and clinical disease in prion-infected mice. *Science Translational Medicine* **5**, (2013).

224. Ma, T. *et al.* Dysregulation of the mTOR pathway mediates impairment of synaptic plasticity in a mouse model of Alzheimer's disease. *PLoS ONE* **5**, (2010).

225. Yang, W. *et al.* Repression of the eIF2α kinase PERK alleviates mGluR-LTD impairments in a mouse model of Alzheimer's disease. *Neurobiology of Aging* **41**, (2016).

226. Ahmad, F. *et al.* Reactive Oxygen Species-Mediated Loss of Synaptic Akt1 Signaling Leads to Deficient Activity-Dependent Protein Translation Early in Alzheimer's Disease. *Antioxidants and Redox Signaling* **27**, (2017).

227. Ding, Q. Ribosome Dysfunction Is an Early Event in Alzheimer's Disease. *Journal of Neuroscience* **25**, 9171–9175 (2005).

228. Ding, Q., Markesbery, W. R., Cecarini, V. & Keller, J. N. Decreased RNA, and increased RNA oxidation, in ribosomes from early Alzheimer's disease. *Neurochemical Research* **31**, 705–710 (2006).

229. Hernández-Ortega, K., Garcia-Esparcia, P., Gil, L., Lucas, J. J. & Ferrer, I. Altered Machinery of Protein Synthesis in Alzheimer's: From the Nucleolus to the Ribosome. *Brain Pathology* **26**, 593–605 (2016).

230. Beckelman, B. C. *et al.* Dysregulation of Elongation Factor 1A Expression is Correlated with Synaptic Plasticity Impairments in Alzheimer's Disease. *Journal of Alzheimer's Disease* **54**, (2016).

231. An, W. L. *et al.* Up-regulation of phosphorylated/activated p70 S6 kinase and its relationship to neurofibrillary pathology in Alzheimer's disease. *American Journal of Pathology* **163**, (2003).

232. Li, X. *et al.* Phosphorylated eukaryotic translation factor 4E is elevated in Alzheimer brain. *NeuroReport* **15**, (2004).

233. Wek, R. C. Role of eIF2α kinases in translational control and adaptation to cellular stress. *Cold Spring Harbor Perspectives in Biology* **10**, (2018).

234. Oliveira, M. M. & Klann, E. eIF2-dependent translation initiation: Memory consolidation and disruption in Alzheimer's disease. *Seminars in Cell and Developmental Biology* (2021) doi:10.1016/j.semcdb.2021.07.009.

235. Smith, H. L. & Mallucci, G. R. The unfolded protein response: Mechanisms and therapy of neurodegeneration. *Brain* **139**, (2016).

236. Ohno, M. Roles of eIF2α kinases in the pathogenesis of Alzheimer's disease. *Frontiers in Molecular Neuroscience* vol. 7 (2014).

237. Chang, R. C. C., Wong, A. K. Y., Ng, H. K. & Hugon, J. Phosphorylation of eukaryotic initiation factor-2α (eIF2α) is associated with neuronal degeneration in Alzheimer's disease. *NeuroReport* **13**, (2002).

238. Lourenco, M. v. *et al.* TNF-α mediates PKR-dependent memory impairment and brain IRS-1 inhibition induced by Alzheimer's β-amyloid oligomers in mice and monkeys. *Cell Metabolism* **18**, (2013).

239. Ma, T. *et al.* Suppression of eIF2α kinases alleviates AD-related synaptic plasticity and spatial memory deficits Tao. *Nature Neuroscience* **16**, (2013).

240. Oliveira, M. M. *et al.* Correction of eIF2-dependent defects in brain protein synthesis, synaptic plasticity, and memory in mouse models of Alzheimer's disease. *Science Signaling* **14**, (2021).

241. Freeman, O. J. & Mallucci, G. R. The UPR and synaptic dysfunction in neurodegeneration. *Brain Research* vol. 1648 (2016).

242. O'Connor, T. *et al.* Phosphorylation of the Translation Initiation Factor eIF2α Increases BACE1 Levels and Promotes Amyloidogenesis. *Neuron* **60**, (2008).

243. Knight, J. R. P. *et al.* Control of translation elongation in health and disease. *DMM Disease Models and Mechanisms* vol. 13 (2020).

244. Ghosh Dastidar, S. *et al.* Distinct regulation of bioenergetics and translation by group I mGluR and NMDAR. *EMBO reports* (2020) doi:10.15252/embr.201948037.

245. Scheetz, A. J., Nairn, A. C. & Constantine-Paton, M. NMDA receptor-mediated control of protein synthesis at developing synapses. *Nature Neuroscience* (2000) doi:10.1038/72915.

246. Ma, T. *et al.* Inhibition of AMP-activated protein kinase signaling alleviates impairments in hippocampal synaptic plasticity induced by amyloid β. *Journal of Neuroscience* **34**, (2014).

247. Jan, A. *et al.* eEF2K inhibition blocks Aβ42 neurotoxicity by promoting an NRF2 antioxidant response. *Acta Neuropathologica* **133**, (2017).

248. Beckelman, B. C. *et al.* Genetic reduction of eEF2 kinase alleviates pathophysiology in Alzheimer's disease model mice. *Journal of Clinical Investigation* **129**, (2019).